PURIFICATION AND CHARACTERIZATION OF GOAT PANCREAS THIOL PROTEINASE INHIBITOR

ABSTRACT

OF THE

THESIS

SUBMITTED FOR THE AWARD OF THE DEGREE OF

Doctor of Philosophy

IN

BIOCHEMISTRY

BY

MEDHA PRIYADARSHINI

DEPARTMENT OF BIOCHEMISTRY
FACULTY OF LIFE SCIENCES
ALIGARH MUSLIM UNIVERSITY
ALIGARH (INDIA)

2009

ABSTRACT

Thiol proteinases synonymous with cysteine proteinases comprise a group of proteolytic enzymes which are widely distributed among living organisms. They play very important role in the intracellular proteolysis such as catabolism of proteins and peptides, development and function of the immune system and tumor, cell invasion. It implies that their regulation is important otherwise it will cause uncontrolled proteolysis and tissue damage. ***In principle, cystatins provide this regulation.***

Cystatins are widespread, naturally occurring tight binding reversible inhibitors of cysteine proteinases found either within the cytosol or secreted from the cells [Kopitar-Jerala, 2006]. The diverse group of thiol proteinase inhibitors comprises the cystatin superfamily, divided into three main groups depending on the presence of single or multiple 'cystatin domains', presence or absence of a signal sequence, carbohydrate content and sulphydryl groups. **Family I- the stefins** are cytosolic, 100-residue single chain proteins with no disulphide bonds or carbohydrates, **Family II- the cystatins** are mainly extracellular, 120 residue single chain proteins with two disulphide bonds but no carbohydrates and **Family III- the kininogens** are multidomain, blood plasma glycoproteins [Turk et al., 2008]. The importance of cystatins is underlined by the pathological conditions that arise upon loss or mutations of cystatin genes/function [Turk et al., 2008; Cox, 2009].

RESULTS OBTAINED IN THE STUDY ARE SUMMARIZED AS FOLLOWS:

Chapter 1

A 44 kDa thiol proteinase inhibitor (PTPI) has been purified and characterized from goat pancreas in terms of its biochemical and biophysical properties. Purification was achieved by a four step procedure involving alkaline treatment (pH 11.0), acetone fractionation, ammonium sulphate precipitation (20-80%) and gel filtration chromatography on Spehacryl S 100 HR column. The preparation was found homogenous on the basis of charge and molecular weight. The inhibitor was obtained with 20.4% yield and 500 fold purity. Pancreatic thiol proteinase inhibitor (PTPI) was found to have two subunits linked by non covalent interactions as determined by SDS-PAGE under reducing as well as non reducing conditions. The stokes radius,

diffusion and sedimentation coefficients of PTPI were 27.3Å, 7.87 x 10^{-7} cm^2 sec^{-1} and 3.83 s, respectively. It was stable in pH range 3-10 and upto 70°C. It possessed 2.32% carbohydrate content and no disulphide bonds. PTPI was immunogenic and induced antibody formation in rabbits. However, it exhibited no immunogenic identity with cystatins isolated from goat lung and brain.

The purified inhibitor inhibited papain and ficin very efficiently and to slightly lesser extent bromelain but failed to inhibit bovine trypsin, chymotrypsin and pepsin. The respective Ki values obtained for papain, ficin and bromelain were 5.88, 9.02 and 22.28 *nM. Association rate constant and hence the affinity of the inhibitor for* proteinases was in the following order: papain (1.49 x 10^4 $M^{-1}s^{-1}$) > ficin (1.39 x 10^4 $M^{-1}s^{-1}$) > bromelain (5.94 x 10^3 $M^{-1}s^{-1}$). The K_{-1} values obtained for papain, ficin and bromelain were 8.76 x 10^{-5}, 3.35 x 10^{-4} and 1.32 x 10^{-4} s^{-1}, respectively. The calculated half-life values of enzyme-inhibitor complex for papain, ficin and bromelain were 7.91 x 10^3, 5.51 x 10^3, and 5.23 x 10^3 s and the IC50 values were, 0.08, 0.078 and 0.154 μM, respectively for the three proteinases; again reinforcing greater affinity of the inhibitor for papaya proteinase.

The partial amino acid sequence analysis of the heavier subunit revealed that PTPI has highest sequence homology with bovine parotid and skin cystatin C. The glycine residue is present at 11^{th} position rather than at conserved position 9 which has also been reported for human placental cystatin and human stefin A structure. The hydropathy plot of first 24 amino acid residues suggested that most amino acids of this stretch might be in hydrophobic core of the protein.

Secondary structural composition of the inhibitor showed presence of 17.18% α helical content. The binding of PTPI to activated papain was accompanied by pronounced changes in the far ultraviolet circular dichroism, ultraviolet absorption and fluorescence emission spectra. These changes were compatible with perturbations of the environment of aromatic residues in one or both the proteins of the complex arising from a conformational change.

The absence of disulphide bonds is a unique character of type 1 cystatin family members. Molecular masses of type 1 and 2 cystatin families range in 11 kDa to 13 kDa [Turk and Bode, 1991]. Presence of carbohydrates is however limited only to kininogens, with few exceptions found for members of type 2 cystatin family. PTPI is devoid of any disulphide linkage, has high molecular mass (44 kDa) and bears sequence similarities to both stefins and cystatins. Studies on kinetics of inhibition as

well as on biophysical interaction of PTPI with thiol proteinases shows that it bears resemblances with other members of type 2 cystatin family. Based on above parameters PTPI can be regarded as a variant of type 1 and type 2 cystatin families. This is not unusual as there is growing list of proteins found to possess some of cystatin superfamily structural and functional motifs, but bearing substantial differences causing them to be classified as variants of cystatin superfamily.

Chapter 2

Equilibrium studies of guanidine hydrochloride (GdnHCl) and urea induced unfolding of PTPI were also performed by monitoring the inhibitor activity, intrinsic fluorescence, circular dichroism (CD) and 1-anilino-naphthalene-8-sulphonate binding.

A sigmoidal dependence of inhibitory activity on GdnHCl concentration was observed. 65% inactivation occurred at 4 M GdnHCl, beyond this concentration PTPI was almost completely inactivated. The fluorescence emission spectrum of PTPI suffered a 15 nm red shift in wavelength of maximum emission (λ_{max}) (from 335 nm for native protein to 350 nm at higher concentrations of GdnHCl) with quenching of fluorescence intensity, suggesting the unfolding of PTPI. Secondary structure analysis of PTPI revealed minute effects on mean residue ellipticity ($MRE_{222\ nm}$) till 1 M GdnHCl. However, complete loss of signal was observed at higher concentrations of the denaturant. Midpoint of transition, Cm, deduced from normalized transition curves of activity, λ_{max}, and $MRE_{222\ nm}$ data was 3.2 M GdnHCl. Further, a shift in Cm was observed with PTPI concentration. Changes in molecular properties of PTPI such as inhibitory activity, $MRE_{222\ nm}$ and λ_{max} with increasing GdnHCl concentration revealed a monophasic sigmoidal dependence with coincidental profiles, characteristic of cooperative unfolding, suggesting a two state model for denaturation of the inhibitor.

In urea, unfolding pathway differed from that observed in GdnHCl. Almost complete inactivation was observed beyond 6 M urea. A gradual increase in λ_{max} occurred with increasing urea concentration. It red shifted to 350 nm at 8 M urea indicating that treatment of PTPI with high concentrations of urea leads to unfolding of the inhibitor. A sigmoidal behaviour of decrease in $MRE_{222\ nm}$ with increasing urea concentration was observed, with complete loss of signal noticeable above 5 M urea. The Cm value deduced from normalized transition curves for activity and $MRE_{222\ nm}$ was 3.6 M. No

dependence of Cm on concentration of the inhibitor was obtained. The Cm value determined from λ_{max} curve was 4 M. The non coincidence of transition curves in urea denaturation as measured by probes sensitive to different levels of protein structure, are consistent with a mechanism involving intermediate state. However, intermediates are not clearly observed.

The denaturation by both GdnHCl and urea was only partially reversible, with retrieval of only 10% of the native activity on extensive dilution only in case of GdnHCl denaturation. Also at all denaturant concentrations the inhibitor refolded to a species having significantly different spectroscopic properties from native PTPI.

Urea is known to be about half as effective as GdnHCl in inducing protein unfolding and dissociation, suggestive of a 2-fold rule. The results of the present study show that PTPI is an exception to this 2-fold rule. The Cm for urea unfolding was 3.6 M (4 M from λ_{max} curve) and that for GdnHCl was 3.2 M, pointing to significant contributions of both hydrophobic and electrostatic interactions in maintenance of active site and/or dimeric nature of the inhibitor.

Chapter 3

Partially or totally unfolded states that are occasionally populated in vivo after biosynthesis on the ribosome, stress conditions or mutation and are favoured by changes on pH, ionic strength and mutations are most susceptible to initiate aggregation [Soldi et al., 2005].

We reasoned that aggregation and fibrillation of PTPI may also require the protein to access partially denatured states and thus explored existence of non native intermediates under experimentally imposed acidic conditions. PTPI was subjected to denaturation over a pH range of 1.0-7.0 and the conformational changes induced were studied by circular dichroism and intrinsic and extrinsic fluorescence.

Till pH 5.0 no change in λ_{max} of emission was observed. A decrease in pH to 3.0 caused a 10 nm blue shift. Further lowering of pH to 2.0 was accompanied by a 2 nm red shift followed by a 3 nm red shift again at pH 1.0. ANS binding was initiated at pH 3.0 (with a blue shift in λ_{max} of ANS emission to 490 nm) and reached a maximum at pH 1.0. Secondary structure analysis revealed ~40% loss at pH 3.0 but at pH 1.0 there was gain in secondary structure content (of ~34%). Conclusively, PTPI at pH 3.0 existed as partially unfolded intermediate having ~60% residual secondary structure but almost completely altered tertiary structure. PTPI at pH 1.0 exhibits

more of a molten globule like features having native like secondary structure contents and enhanced ability to bind ANS, however with tertiary contacts quite similar to native PTPI.

The organic solvent 2, 2, 2-trifluoroethanol (TFE) is known to stabilize the partially unfolded proteins [Rashid et al., 2006b] and has been extensively employed for amyloid fibril induction in various proteins [Zerovnik et al., 2007]. From a range of concentrations used, in the present study 10% TFE induced native like secondary structure in pH 3.0 state of PTPI. Similar results were also obtained for PTPI at pH 1.0 and 2.0.

Based on these results six solvent conditions were chosen to study amyloid fibril formation in PTPI. The inhibitor was incubated at pH 1.0, 2.0, 3.0 and at these three pH in presence of 10% (v/v) TFE. Two standard procedures were used to follow amyloid growth in above samples, Thioflavin T (ThT) fluorescence assay and transmission electron microscopy (TEM).

Enhancement of ThT fluorescence was observed only after 55 days of incubation of PTPI at pH 2.0. Contrastingly at pH 3.0, enhancement was noticed within 5 days of incubation. Results obtained for PTPI incubated at pH 1.0 were quite similar to those obtained for pH 3.0 sample. The results revealed that amyloid type aggregates from PTPI form under acidic conditions and more readily at pH 3.0 and 1.0 than at pH 2.0.

In the presence of TFE, amyloid growth was accelerated, for the sample at pH 2.0 several fold enhancement in ThT fluorescence intensity was observed within 30 days of incubation. Similarly at pH 3.0, a profound increment was observed without any distinct lag phase. The characteristics of fibrillation at pH 1.0 were in similitude with sample at pH 3.0. Controls at each condition did not show any ThT binding.

On subjection to transmission electron microscopy (TEM), after 15 days of incubation sharp fibrils were seen in pH 3.0 sample (in the presence of 10% (v/v) TFE) and peculiar foliage like pattern was observed for pH 1.0 sample (in the presence of 10% (v/v) TFE). The sample incubated at pH 2.0 (in the presence of 10% (v/v) TFE) also gave fibrils but after one month of incubation.

Divalent metal ions (Zn^{2+} and Cu^{2+}) effectuated a concentration dependent decline in ThT fluorescence of preformed fibrils at pH 3.0 suggesting deaggregation of the fibrils. When added prior to the initiation of fibrillation of PTPI (at pH 3.0, with 10% (v/v) TFE) 50 μM Cu^{2+} and 10 μM Zn^{2+} prevented any amyloid aggregation.

These results corroborate with generic hypothesis of amyloid fibrillation proteins,

outline the conditions necessary for PTPI fibrillation and point towards the strong influence of solvent conditions on fibril morphology. Use of divalent metal ions against amyloid formation is also suggested.

Chapter 4

In this chapter effect of reactive species on purified goat pancreatic thiol proteinase inhibitor has been evaluated.

Riboflavin sensitized photodynamic modifications of PTPI lead to inactivation of its antiproteolytic activity and formation of aggregated products (at higher riboflavin concentrations). A continued disappearance of inhibitory activity towards papain was observed with increasing concentration of riboflavin and varying time periods of incubation reaching a maximum value of 83% (loss in activity). Sodium azide (a known singlet oxygen quencher) and potassium iodide (quencher of flavin triplet state) suppressed the activity loss as well as aggregation. Mannitol and thiourea failed to show any such protective effect. Natural antioxidants, curcumin (Cur), caffeic acid (CA) and quercetin (QE) diminished the riboflavin exerted damage which was evident by following observations, activity of treated PTPI was enhanced, aggregation was inhibited and tryptophan fluorescence retrieved back. Curcumin, however, provided only partial moderation.

Hypochlorous acid and to lesser extent hydrogen peroxide destroyed the antiproteolytic potential of PTPI. HOCl even at low concentrations significantly decreased the functional integrity of the inhibitor (90% loss in activity). High concentrations of H_2O_2 also partially diminished proteinase inhibitory capacity of PTPI by a mechanism involving almost no contribution from hydroxyl radicals (sodium benzoate and thiourea afforded no protection and mannitol only to small extent). Structural analyses revealed fragmentation of PTPI upon HOCl exposure. H_2O_2 also caused loss in band intensity and appearance of some higher mobility material. λ_{max} suffered a red shift of 15 nm in the presence of H_2O_2. Diminution of the inflicted damage was observed on treatment with Cur, CA, QE, with former two being more effective than QE. There was subjugation of PTPI activity loss, fragmentation and changes in intrinsic fluorescence pattern in presence of bioflavonoids.

The effect of nitric oxide on structure and function of PTPI was also studied. There was a concentration dependent loss in activity. The λ_{max} red shifted to 350 nm (from 335 nm for native PTPI) in the presence of NO. On the whole the inhibitor was

severely compromised functionally (72% loss in activity) and structurally. The three natural antioxidants, Cur, CA and QE negated the loss in tryptophan fluorescence and PTPI inhibitory activity. Maximum protection was offered by Cur and CA.

The results evinced the susceptibility of PTPI to aforementioned reactive species and the modifications induced included altered molecular weight (aggregation or fragmentation) and fluorescence characteristics and loss of inhibitory function. Also, Cur, CA and QE provided protection against the oxidative and nitrosative damage.

Chapter 5

Experiments were conducted to investigate the effects of sodium valproate, glimepiride, metformin hydrochloride and synthetic insulin on the structure and function of the inhibitor.

Sodium valproate and glimepiride caused dose dependent loss of PTPI's inhibitory activity with almost 80% loss precipitating at 10 μM sodium valproate and 40 μM glimepiride concentrations. Drug interaction induced structural changes in PTPI were monitored by intrinsic fluorescence and UV vis spectrophotometric analyses. Complex changes were noticed in the fluorescence properties of PTPI indicating alteration in the environment of the aromatic amino acid residues induced on interaction with drugs. The difference spectra also showed profound changes suggesting involvement of tryptophan, tyrosine and phenylalanine residues in complexation. Secondary structural analysis of insulin-PTPI complexes revealed increase in ellipticity at 222 nm suggesting enhancement of native stability of the inhibitor. Metformin hydrochloride complexation caused only mild effects.

The results implicate the loss of thiol proteinase inhibitor function in drug induced pancreatitis by sodium valproate. They also provide a platform for understanding the non responsiveness to antidiabetic drugs after a prolonged period and clues to enhance the insulin potency.

Maintenance of appropriate equilibrium between free cysteine proteinases and their complexes with inhibitors is imperative for proper function of all living systems/tissues. This equilibrium in pancreas is critical for pancreatitis onset and its severity, diabetes and cancer [van Acker et al., 2002; Thrower et al., 2006; Rivenbark and Coleman, 2009]. ***The studies are worthy of future research with regards to interaction of PTPI with pancreatic cathepsins and its role in pancreatic (patho) physiology.***

PURIFICATION AND CHARACTERIZATION OF GOAT PANCREAS THIOL PROTEINASE INHIBITOR

THESIS

SUBMITTED FOR THE AWARD OF THE DEGREE OF

Doctor of Philosophy

IN

BIOCHEMISTRY

BY

MEDHA PRIYADARSHINI

DEPARTMENT OF BIOCHEMISTRY
FACULTY OF LIFE SCIENCES
ALIGARH MUSLIM UNIVERSITY
ALIGARH (INDIA)

2009

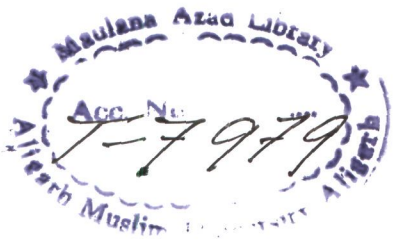

For

Mommy & Papa

The God like

godsend

To

Bhashi, the best of all the pals, sisters and guides

&

Bhaiya, the aegis

And

Primed by my friends: the extended self

University Exchange Nos.
0571-2700920, 2700916
Ext, (INT)Office - 3720
Chairman's Chamber - 3721
Ext. (0571) 2700741
Fax. No. (0571) 2706002

DEPARTMENT OF BIOCHEMISTRY
FACULTY OF LIFE SCIENCES
ALIGARH MUSLIM UNIVERSITY
ALIGARH-202002 (INDIA)

Ref. No..... *Dated* 15.10.09

Certificate

This is to certify that the work entitled ***"Purification and Characterization of Goat Pancreas Thiol Proteinase Inhibitor"*** embodied in this thesis is an original work done by **Ms. Medha Priyadarshini** under my supervision and is suitable for the award of Ph. D. degree in Biochemistry.

(Prof. Bilqees Bano)

O God send out thy light and thy truth; let them lead me.
The Old Testament, Psalm-43.3

Acknowledgement

I never knew I had been surrounded by an ocean of goodness. The experience has been of a seed; carried by the wind or water, unsolicited, unawares; far and near, for growth and survival. I have not a single name to spare, yet there are special ones: the hormone (-ic) catapults steadying my projectile and camouflaging my being; deceiving the storms.

I am indebted to ***Prof. Bilqees Bano****, my supervisor, for her proficient guidance, conscientious scrutiny, abounding encouragement and congenial assistance. In times of my tryst with destiny, she stood beside me as a motherly figure and was source of hope, affection, care and advice. Nothing but her help, faith and continuing support has salvaged me from darkness.*

Special thanks are due ex-chairman ***Prof. S. M. Hadi****, for unobtrusive benefaction of all necessary facilities.*

I register my sincere thanks to honourable chairman, ***Prof. A. N. K. Yusufi****, for his inexplicable concern, unprecedented help and unconditional beneficence that microvilli-ed my capacity to fight back.*

I remain profoundly grateful to ***Prof. M. Saleemuddin*** *for the magnanimity shown.*

I am also thankful to all my teachers, ***Prof. Masood Ahmed****,* ***Prof. Naheed Banu****,* ***Prof. Qayyuum Hussain****,* ***Prof. Riaz Mahmood****,* ***Prof. Imrana Naseem****,* ***Dr. M. Tabish****,* ***Dr. Farah Khan****, and* ***Dr. Aabgeena Naeem*** *for their concern and unabated encouragement.*

I am heartily thankful to ***Fahim Sir*** *for his encyclopaedic advices, eternal jollity and incessant concern.*

I exuberantly acknowledge the help offered by ***Prof. Arunima Lal*** *(Dept. of Chemistry, AMU),* ***Dr. R. H. Khan*** *(Interdisciplinary Biotech. Unit, AMU) and* ***Prof. T. P. Singh*** *in conducting various experiments in their respective labs.*

I am most grateful to ***Dr. Moied Ahmad*** *(Dept. of Anaesthesiology, JNMCH, AMU) for his divine help that negated the tsunamic calamities.*

I was fortunate enough to have most wonderful seniors around comforting my stay in the lab. I have had the benefit of special advice from ***Dr. Sameena****,* ***Dr. Sonish****,* ***Dr. Amjad****,* ***Dr. Suhail****,* ***Dr. Kashif****,* ***Dr. Riffat****,* ***Dr. Asfar****,* ***Yasha di****,* ***Shamila aapa*** *and* ***Irfa aapa****.*

Kaleem bhai *over-showered me with his brotherly care and guidance.* ***Fouzia aapa*** *gave the strokes of brilliance wherever the canvas had faded.* ***Sadia aapa*** *has been a morale booster and a great companion throughout.* ***Ayesha aapa*** *with her crispness endured all the molten globules and her care besought relaxation.*

Showket bhaiya *and* ***Irum aapa*** *with their genuine concern and soothing affection emboldened my spirit. I wish to mention* ***Amy aapa****, who has been my companion in*

*many anxious, sometimes convivial and always protracted discussions. **Deeba aapa** had been a depot of love and especially of the labware.*

*Sabika, Toshi, Mahreen and Nish neutralized the savour of gloom that then seasoned my life. Words are scarce to express my thankfulness to **Aarti, Farah, Deepti,** for their excellent comradeship and **Rukhsana** and **Humaira** for their lovely gestures. **Benz** always lended a patient ear to all my problems, bore long gaps in a two way communication and had been there whenever I needed help.*

*I thank **Jeelani** for being there at the commencement of zero hour of test and for being www.ncbi.nlm.nih.gov.*

*Besides I am most grateful to **Dr. Vibhanshu, Dr. Sandeep, Dr. Anupriya, Dr. Aiman** and **Dr. Subuhi** for being a constellation of goodness. And other magnificent human beings, **Sarmad, Sheeba, Sara, Uzma, Luv, Ashraf, Haseeb, Ashreeb, Shafqat, Maryam,** and umpteen people here and there for keeping the circuit complete.*

Nabeela deserves a special mention for her ease, suavity and sisterly affection. The only thing that drove me crazy was her cleanliness fever and workaholic nature.

*Faisal always lended a helping hand whenever required. I thank all my young colleagues, **Fahad, Zoheb, Nida, Shakeel, Shoa, Shireen, Hussain, Taqi, Iftekhar, Sandesh, Amit, Bilal,** and others for the general bloom they provide to the lab and for the courtesies.*

Shahnawaz has supported me unfailingly with a true interest. At each step he had been there, sometimes like an analyst, sometimes like a critique but always like a friend. I bet this thesis would have had half of its pages without his help. His 'badiya hey' magically transformed worst into good.

*There is one person who can render a helping hand to unspoken: **Shams**. His support has been like a sky protecting from the meteoric damage.*

***Aatif** with his exuberant persona and readiness to help never made me feel the need of a younger bro.*

***Aaliya** is a living parable of care and compassion. She nestled me enumerable times protecting me from the caustic environ around. Tsee chukh asal koor and beene.*

*Along with providing a strong sense of support and bearing with me the ICU (onic) emotional insults, **Wasim,** had always been just one phone call away. He essentially gouged the unnecessary ifs and buts. Most importantly he provided distilled water (distilling the uncertainties) and has been Sigma Aldrich that never demanded any emoluments. All the electrphoretograms owe their being to him. With great endurance he taught me to run gel for the first time. Thought of completion of this work without his help is inconceivable.*

*I acknowledge, **Anju di** and **Jijaji** for being indispensable part of this thesis. **Priya** for her alarming chirpiness, depressing inquisitiveness and for being a combo pack of movie magic and lays chat street gossip, making my life resonant.*

*Also, **Ajay Mama** for being 'mumma', mis spelt. **Neha Bhabhi** for being eucalypt of faith. Only both of you have revived me from rigor mortis.*

*My recently discovered best friend **Papa** for being a mountain of strength and protection and a fountain of care and affection. It would not have been what it is without you. For being the best of all the fathers.*

Mommy I don't know how I have done this in your vital absence. Your faith, will, love and believe have been the victuals for the weaning emotional me. Your warrior like spirit to rebel against the times had been my sole strength, my lamppost. I have felt you, always, near me, walking with me on the stony paths as they have been. I need you. Be by my side always.

Even infinite thanks can't pay back Bhaiya. He only instilled in me the confidence to fight back, or I would have fled the field long ago.

I find it strange to thank my soul, Bhashi. She oughts to be what she is.

I thank Goldy (my typist) for providing an effortlessly readable manuscript of the thesis and Raju Bhaiya for his 'on call mobile' service that rubbed off undesired punctuations.

The biochemistry office staff and lab attendants are thanked for their timely help.

I also thank the Council of Scientific and Industrial Research for providing necessary financial assistance as a junior as well as senior research fellow.

Throughout the pressures and ardour of this work I have realized that to sustain, harmony with nature's will is a must.....

We are the clouds that veil the midnight moon;
How restlessly they speed, and gleam, and quiver,
Streaking the darkness radiantly!--yet soon
Night closes round, and they are lost forever:

Or like forgotten lyres, whose dissonant strings
Give various response to each varying blast,
To whose frail frame no second motion brings
One mood or modulation like the last.

We rest.--A dream has power to poison sleep;
We rise.--One wandering thought pollutes the day;
We feel, conceive or reason, laugh or weep;
Embrace fond foe, or cast our cares away:

It is the same!--For, be it joy or sorrow,
The path of its departure still is free:
Man's yesterday may ne'er be like his morrow;
Nought may endure but Mutability.

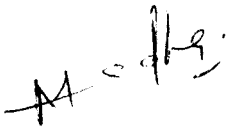

(Medha Priyadarshini)

CONTENTS

Section No.		Page No.
LIST OF ABBREVIATIONS		i
LIST OF FIGURES		ii-vi
LIST OF TABLES		vii
ABSTRACT		viii-xiv
[I]	**INTRODUCTION**	**1-51**
1.1	General	1
1.2	Discovery of the cystatin superfamily	3
1.3	Classification of the cystatin superfamily	4
1.4	General properties of the cystatin superfamily	7
1.5	Evolution	13
1.6	Structure of cystatins	15
1.7	Inhibition of proteinases	19
1.8	Biological aspects and pathophysiology of cystatins	26
1.9	Pancreas	29
1.10	Protein unfolding studies	31
1.11	Amyloid fibril formation	33
1.12	Reactive species mediated protein damage	37
1.13	Drug-protein interaction: effect of pancreatitis causing and antidiabetic agents	45
1.14	**Scope of the thesis**	**49**
[II]	**MATERIALS AND METHODS**	**52-72**
(A)	**MATERIALS**	**52**
(B)	**METHODS**	**53-72**
2.1	Purification of thiol proteinase inhibitor from goat pancreas	53
2.2	Colorimetric analyses	54
2.3	Slab Gel Electrophoresis	56
2.4	Molecular Weight Determination	57
2.5	Immunological Procedures	58
2.6	Kinetics of Inhibition	59
2.7	N-terminal Analysis	61
2.8	Spectral Analysis	62
2.9	Denaturing action of guanidine hydrochloride and urea towards pancreatic thiol proteinase inhibitor	63
2.10	In vitro study of fibrillation of PTPI	64
2.11	Modification of goat pancreatic thiol proteinase inhibitor by reactive species	67

2.12 Drug-PTPI interaction: Effect of pancreatitis causing and antidiabetic agents 71
2.13 Statistical analyses 72

[III] **RESULTS AND DISCUSSION**

CHAPTER 1 **PURIFICATION AND CHARACTERIZATION OF GOAT PANCREATIC THIOL PROTEINASE INHIBITOR (PTPI)** **73-106**

3.1 **RESULTS** **73-98**

3.1.1 Purification of the inhibitor 73
3.1.2 Gel filtration 73
3.1.3 Homogeneity of the purified inhibitor 73
3.1.4 Reducing and non-reducing PAGE 77
3.1.5 Properties of the purified pancreatic thiol proteinase inhibitor 77
3.1.6 Immunological properties 82
3.1.7 Kinetic properties of PTPI 85
3.1.8 N-terminal analysis 93
3.1.9 Spectral analyses 93

➢ **DISCUSSION** **99-106**

CHAPTER 2 **DENATURING ACTION OF GUANIDINE HYDROCHLORIDE AND UREA TOWARDS PANCREATIC THIOL PROTEINASE INHIBITOR** **107-127**

3.2 **RESULTS** **107-123**

3.2.1 Changes in molecular properties of PTPI associated with GdnHCl induced unfolding 107
3.2.2 Changes in molecular properties of PTPI associated with urea induced unfolding 113
3.2.3 ANS fluorescence 120
3.2.4 Renaturation of PTPI after GdnHCl and urea induced unfolding 121

➢ **DISCUSSION** **124-127**

CHAPTER 3 **IN VITRO FIBRILLATION OF PANCREATIC THIOL PROTEINASE INHIBITOR** **128-149**

3.3 **RESULTS** **128-144**

3.3.1 Acid denaturation of PTPI 128
3.3.2 Effect of 2, 2, 2-Trifluoroethanol (TFE) on acidic pH induced state of PTPI 132
3.3.3 Optimal pH and TFE concentration to induce PTPI amyloid fibril growth 134

3.3.4	Amyloid type aggregation/fibrillation of PTPI monitored by ThT fluorescence	136
3.3.5	TEM images	137
3.3.6	Effect of divalent metal ions, Cu2+ and Zn2+ on PTPI fibrillation	137

➢ DISCUSSION **145-149**

CHAPTER 4 **MODIFICATION OF PANCREATIC THIOL PROTEINASE INHIBITOR BY REACTIVE SPECIES** **150-178**

3.4 **RESULTS** **150-171**

3.4.1A	Interaction of PTPI with photosensitized riboflavin	150
3.4.1B	Protective effect of bioflavonoids, Curcumin (Cur), Caffeic acid (CA) and Quercetin (QE) against photodynamic modifications of PTPI	156
3.4.2A	Interaction of PTPI with hydrogen peroxide (H_2O_2)	156
3.4.2B	Protective effect of curcumin (Cur), caffeic acid (CA) and quercetin (QE) against H_2O_2 mediated modifications of PTPI	161
3.4.3A	Interaction of PTPI with hypochlorous acid (HOCl)	161
3.4.3B	Protective effect of curcumin (Cur), caffeic acid (CA) and quercetin (QE) against HOCl mediated modifications of PTPI	162
3.4.4A	Interaction of PTPI with Nitric Oxide (NO)	166
3.4.4B	Protective effect of curcumin (Cur), caffeic acid (CA) and quercetin (QE) against NO mediated modifications of PTPI	169

➢ **DISCUSSION** **172-178**

CHAPTER 5 **DRUG-PTPI INTERACTION: EFFECT OF PANCREATITIS CAUSING AND ANTIDIABETIC AGENTS** **179-194**

3.5 **RESULTS** **179-189**

3.5.1	Interaction of PTPI with sodium valproate	179
3.5.2	Interaction of PTPI with glimepiride	181
3.5.3	Interaction of PTPI with metformin hydrochloride	184
3.5.4	Interaction of PTPI with insulin	187

➢ **DISCUSSION** **190-194**

[IV] CONCLUSION 195

[V] BIBLIOGRAPHY 196-221

[VI] BIOGRAPHY i-iii

LIST OF ABBREVIATIONS

ANS	1-anilinonaphthalene-8-sulphonic acid
CA	Caffeic Acid
CD	Circular dichroism
CP (s)	Cysteine proteinase (s)
CPI	Cysteine proteinase inhibitor
Cur	Curcumin
DTNB	Dithionitrobenzoic acid
EDTA	Ethylene diamine tetra acetic acid
ELISA	Enzyme linked immunosorbent assay
g	Gram
GdnHCl	Guanidine hydrochloride
Glc	Glucose
h	Hour (s)
HOCl	Hypochlorous acid
KI	Potassium iodide
kDa	kilo Dalton
mdeg	Millidegree
µg	Microgram
µl	Microlitre
µM	Micromolar
min	Minute (s)
M	Molar
mg	Milligram
ml	Millilitre
mM	Millimolar
Mr	Molecular mass
MW	Molecular weight
nm	Nanometer
OD	Optical density
PAGE	Polyacrylamide gel electrophoresis
PTPI	Pancreatic Thiol Proteinase Inhibitor
PVDF	Polyvinyl idene difluoride
QE	Quercetin
ROS/ RNS	Reactive Oxygen Species/ Reactive Nitrogen Species
rpm	Revolutions per minute
RT	Room Temperature
SDS	Sodium dodecyl sulphate
SEM	Standard Error of Mean
SNP	Sodium Nitroprusside
TCA	Trichloroacetic acid
TEM	Transmission Electron Microscopy
TEMED	Tetraethylmethyl ethylene diamine
TFE	Trifluoroethanol
ThT	Thioflavin T
TPI	Thiol Proteinase Inhibitor
v/v	Volume by volume
VPA	Valproic acid / sodium valproate
βME	Beta mercapto ehatnaol
λ_{max}	Wavelength of maximum emission

LIST OF FIGURES

Figure No.		Page No.
INTRODUCTION		
1	A diagrammatic representation of the chain structures of proteins in the cystatin superfamily	5
2	Fold of cystatin C	6
3	Evolution of cystatin superfamily	16
4	(A) Three dimensional structure of stefin A (B) Three dimensional structure of stefin B	18
5	Scheme of the proposed model for the interaction of chicken egg white cystatin and papain	23
6	Three dimensional structure of the complex formed between human stefin B and papain	24
7	Anatomy of pancreas	30
8	Properties of amyloid polymerization	36
9	A schematic diagram of the conversion of nitric oxide (NO) to other nitrogen oxides	41
10	Chemical structures of A) Curcumin B) Quercetin C) Caffeic acid	46
11	Chemical structures of A) Valporic acid B) Metformin hydrochloride C) Glimepiride	48
CHAPTER 1		
12	Gel filtration chromatography on Sephacryl S-100 HR	75
13	Gel electrophoresis of PTPI during various stages of purification	76
14	SDS Polyacrylamide gel electrophoresis of purified PTPI	78
15	Molecular weight estimation of purified PTPI using Sephacryl S-100 HR gel filtration chromatography	78
16	Molecular weight determination of PTPI by SDS-PAGE electrophoresis	79

17	Determination of Stokes radius of PTPI by plot of Laurent and Killander [$(\log K_{av})^{1/2}$ vs r]	81
18	Effect of pH on activity of PTPI	83
19	Effect of temperature on PTPI	83
20	Thermal stability of PTPI	84
21	Direct binding ELISA	84
22	Ouchterlony immunodiffusion	86
23	Inhibitory activity of PTPI with different proteinases	86
24	Determination of inhibition constant with (Ki) papain	87
25	Determination of inhibition constant (Ki) with ficin	87
26	Determination of inhibition constant (Ki) with bromelain	88
27	Determination of dissociation rate constant (K_{-1}) with papain	91
28	Determination of dissociation rate constant (K_{-1}) with ficin	91
29	Determination of dissociation rate constant (K_{-1}) with bromelain	92
30	Hydropathy plot of the N-terminal residues of heavy subunit of PTPI	95
31	UV-Absorption difference spectra measured for PTPI-papain complex	97
32	Fluorescence spectra of PTPI alone and PTPI in complex with papain	97
33	Far UV-CD spectra of native PTPI	98
34	Far UV-CD Spectra of PTPI in complex with papain	98

CHAPTER 2

35	Effect of increasing GdnHCl concentration on activity of PTPI	108
36	Intrinsic fluorescence analysis of PTPI on interaction with various concentrations of GdnHCl	110
37	Secondary structure analysis of PTPI in the presence of GdnHCl	112
38	Changes in functional and structural properties of PTPI in the presence of GdnHCl	114
39	Effect of increasing urea concentration on activity of PTPI	115

40 Intrinsic fluorescence analysis of PTPI on interaction with various concentrations of urea 117

41 Secondary structure analysis of PTPI in the presence of urea 118

42 Changes in functional and structural properties of PTPI in presence of urea 119

43 ANS fluorescence of PTPI at various concentrations of GdnHCl and urea 122

44 Schematic diagram of GdnHCl- and urea- induced unfolding of PTPI 125

CHAPTER 3

45 pH dependence of intrinsic and ANS fluorescence properties of PTPI 130

46 pH dependence of mean residue ellipticity (MRE) of PTPI at 222 nm 131

47 Effect of TFE on PTPI at pH 3.0 133

48 Fluorescence spectra of ANS bound to PTPI under different conditions 135

49 PTPI fibrillation at pH 2.0
(a) Fluorescence emission spectra of Thioflavin T (ThT) dye in the presence of PTPI at pH 2.0
(b) Time course of fibril growth of PTPI followed by ThT fluorescence at 485 nm at pH 2.0 and in presence of 10% (v/v) TFE 138

50 PTPI finrillation at pH 3.0
(a) Fluorescence emission spectra of Thioflavin T (ThT) dye in the presence of PTPI at pH 3.0
(b) Time course of fibril growth of PTPI followed by ThT fluorescence at 485 nm at pH 3.0 and in presence of 10% (v/v) TFE 139

51 Electron micrograph of PTPI incubated under native conditions 140

52 Electron micrographs showing amyloid aggregation of PTPI incubated at pH 1.0 140

53 Electron micrographs showing amyloid aggregation of PTPI incubated at pH 2.0 141

54 Electron micrograph showing amyloid aggregation of PTPI incubated at pH 3.0 142

55 Inhibition of fibrillation of PTPI by Cu^{2+} and Zn^{2+} as probed by ThT fluorescence 144

56 Scheme for mechanism of PTPI aggregation 147

CHAPTER 4

57 Effect of scavengers on riboflavin mediated inactivation of PTPI 152

58 PAGE of native and riboflavin treated PTPI 154

59 PAGE of PTPI exposed to riboflavin in presence of various scavengers 154

60 Intrinsic fluorescence analysis of PTPI treated with different concentrations of riboflavin 155

61 Effect of scavengers on H_2O_2 mediated inactivation of PTPI 159

62 PAGE of native and H_2O_2 treated PTPI 159

63 PAGE of PTPI exposed to H_2O_2 in presence of various scavengers 160

64 Intrinsic fluorescence analysis of PTPI treated with different concentrations of H_2O_2 160

65 Effect of scavengers on HOCl mediated inactivation of PTPI 164

66 PAGE of native and HOCl treated PTPI 164

67 PAGE of PTPI exposed to HOCl in presence of various scavengers 165

68 Intrinsic fluorescence analysis of PTPI treated with different concentrations of HOCl 165

69 Intrinsic fluorescence analysis of PTPI treated with HOCl in presence of natural antioxidants 167

70 PAGE of native and SNP treated PTPI 170

71 Intrinsic fluorescence analysis of PTPI treated with different concentrations of SNP 170

72 Effect of natural antioxidants on SNP mediated inactivation of PTPI 171

73 Intrinsic fluorescence analysis of PTPI treated with SNP in presence of natural antioxidants 171

CHAPTER 5

74 Effect of Sodium valproate complexation on activity of PTPI 180

75 Intrinsic fluorescence analysis of PTPI on interaction with various concentrations of Sodium valproate (VPA) 180

76 UV-Absorption difference spectra measured for PTPI-VPA complexes 182

77 Effect of glimepiride complexation on activity of PTPI 183

78 Intrinsic fluorescence analysis of PTPI on interaction with various concentrations of glimepiride 183

79 UV-Absorption difference spectra measured for PTPI-glimepiride complexes 185

80 Effect of metformin hydrochloride complexation on activity of PTPI 186

81 Intrinsic fluorescence analysis of PTPI on interaction with various concentrations of metformin hydrochloride 186

82 Intrinsic fluorescence analysis of PTPI on interaction with various concentrations of insulin 188

83 Absorption spectra of PTPI-insulin complexes 188

84 Far UV-CD Spectra of PTPI in complex with insulin 189

LIST OF TABLES

Table No.		Page No.
INTRODUCTION		
1	CPIs from some mammalian and non mammalian sources	14
2	Equilibrium constants for dissociation (Ki) of complexes between human cystatins and chicken cystatin with lysosomal cysteine proteases (human cathepsins, papain and cruzipain)	21
3	Conserved amino-acid residues in binding segments of human cystatins	22
4	Important physiological functions that involve free radicals or their derivatives	40
5	Nitrogen oxides that have been implicated in the biological sequel of nitric oxide formation	40
CHAPTER 1		
6	Results of a typical purification of goat pancreatic thiol proteinase inhibitor	74
7	Kinetic constants obtained on interaction of PTPI with proteinases – papain, ficin and bromelain	90
8	N-terminal amino acid sequence of PTPI: A comparison	94
CHAPTER 2		
9	Fluorescence emission maxima and papain inhibitory activity during refolding of PTPI at various time intervals after 50 fold dilution of denatured samples	123
CHAPTER 4		
10	Loss of antiproteolytic activity of PTPI on treatment with photoilluminated riboflavin as a function of (A) concentration of riboflavin and (B) time of incubation	151
11	Retention of tryptophan fluorescence in the presence of different scavengers and antioxidants	155
12	Loss of antiproteolytic activity of PTPI on treatment with H_2O_2 as a function of (A) concentration of H_2O_2 and (B) time of incubation	158
13	Loss of antiproteolytic activity of PTPI on treatment with HOCl as a function of concentration of HOCl	163
14	Loss of antiproteolytic activity of PTPI on treatment with SNP as a function of (A) concentration of SNP and (B) time of incubation	168

Abstract

ABSTRACT

Thiol proteinases synonymous with cysteine proteinases comprise a group of proteolytic enzymes which are widely distributed among living organisms. They play very important role in the intracellular proteolysis such as catabolism of proteins and peptides, development and function of the immune system and tumor, cell invasion. It implies that their regulation is important otherwise it will cause uncontrolled proteolysis and tissue damage. ***In principle, cystatins provide this regulation.***

Cystatins are widespread, naturally occurring tight binding reversible inhibitors of cysteine proteinases found either within the cytosol or secreted from the cells [Kopitar-Jerala, 2006]. The diverse group of thiol proteinase inhibitors comprises the cystatin superfamily, divided into three main groups depending on the presence of single or multiple 'cystatin domains', presence or absence of a signal sequence, carbohydrate content and sulphydryl groups. **Family I- the stefins** are cytosolic, 100-residue single chain proteins with no disulphide bonds or carbohydrates, **Family II- the cystatins** are mainly extracellular, 120 residue single chain proteins with two disulphide bonds but no carbohydrates and **Family III- the kininogens** are multidomain, blood plasma glycoproteins [Turk et al., 2008]. The importance of cystatins is underlined by the pathological conditions that arise upon loss or mutations of cystatin genes/function [Turk et al., 2008; Cox, 2009].

RESULTS OBTAINED IN THE STUDY ARE SUMMARIZED AS FOLLOWS:

Chapter 1

A 44 kDa thiol proteinase inhibitor (PTPI) has been purified and characterized from goat pancreas in terms of its biochemical and biophysical properties. Purification was achieved by a four step procedure involving alkaline treatment (pH 11.0), acetone fractionation, ammonium sulphate precipitation (20-80%) and gel filtration chromatography on Spehacryl S 100 HR column. The preparation was found homogenous on the basis of charge and molecular weight. The inhibitor was obtained with 20.4% yield and 500 fold purity. Pancreatic thiol proteinase inhibitor (PTPI) was found to have two subunits linked by non covalent interactions as determined by SDS-PAGE under reducing as well as non reducing conditions. The stokes radius,

diffusion and sedimentation coefficients of PTPI were 27.3Å, 7.87 x 10^{-7} cm^2 sec^{-1} and 3.83 s, respectively. It was stable in pH range 3-10 and upto 70°C. It possessed 2.32% carbohydrate content and no disulphide bonds. PTPI was immunogenic and induced antibody formation in rabbits. However, it exhibited no immunogenic identity with cystatins isolated from goat lung and brain.

The purified inhibitor inhibited papain and ficin very efficiently and to slightly lesser extent bromelain but failed to inhibit bovine trypsin, chymotrypsin and pepsin. The respective Ki values obtained for papain, ficin and bromelain were 5.88, 9.02 and 22.28 nM. Association rate constant and hence the affinity of the inhibitor for proteinases was in the following order: papain (1.49 x 10^4 $M^{-1}s^{-1}$) > ficin (1.39 x 10^4 $M^{-1}s^{-1}$) > bromelain (5.94 x 10^3 $M^{-1}s^{-1}$). The K_{-1} values obtained for papain, ficin and bromelain were 8.76 x 10^{-5}, 3.35 x 10^{-4} and 1.32 x 10^{-4} s^{-1}, respectively. The calculated half-life values of enzyme-inhibitor complex for papain, ficin and bromelain were 7.91 x 10^3, 5.51 x 10^3, and 5.23 x 10^3 s and the IC50 values were, 0.08, 0.078 and 0.154 μM, respectively for the three proteinases; again reinforcing greater affinity of the inhibitor for papaya proteinase.

The partial amino acid sequence analysis of the heavier subunit revealed that PTPI has highest sequence homology with bovine parotid and skin cystatin C. The glycine residue is present at 11^{th} position rather than at conserved position 9 which has also been reported for human placental cystatin and human stefin A structure. The hydropathy plot of first 24 amino acid residues suggested that most amino acids of this stretch might be in hydrophobic core of the protein.

Secondary structural composition of the inhibitor showed presence of 17.18% α helical content. The binding of PTPI to activated papain was accompanied by pronounced changes in the far ultraviolet circular dichroism, ultraviolet absorption and fluorescence emission spectra. These changes were compatible with perturbations of the environment of aromatic residues in one or both the proteins of the complex arising from a conformational change.

The absence of disulphide bonds is a unique character of type 1 cystatin family members. Molecular masses of type 1 and 2 cystatin families range in 11 kDa to 13 kDa [Turk and Bode, 1991]. Presence of carbohydrates is however limited only to kininogens, with few exceptions found for members of type 2 cystatin family. PTPI is devoid of any disulphide linkage, has high molecular mass (44 kDa) and bears sequence similarities to both stefins and cystatins. Studies on kinetics of inhibition as

well as on biophysical interaction of PTPI with thiol proteinases shows that it bears resemblances with other members of type 2 cystatin family. Based on above parameters PTPI can be regarded as a variant of type 1 and type 2 cystatin families. This is not unusual as there is growing list of proteins found to possess some of cystatin superfamily structural and functional motifs, but bearing substantial differences causing them to be classified as variants of cystatin superfamily.

Chapter 2

Equilibrium studies of guanidine hydrochloride (GdnHCl) and urea induced unfolding of PTPI were also performed by monitoring the inhibitor activity, intrinsic fluorescence, circular dichroism (CD) and 1-anilino-naphthalene-8-sulphonate binding.

A sigmoidal dependence of inhibitory activity on GdnHCl concentration was observed. 65% inactivation occurred at 4 M GdnHCl, beyond this concentration PTPI was almost completely inactivated. The fluorescence emission spectrum of PTPI suffered a 15 nm red shift in wavelength of maximum emission (λ_{max}) (from 335 nm for native protein to 350 nm at higher concentrations of GdnHCl) with quenching of fluorescence intensity, suggesting the unfolding of PTPI. Secondary structure analysis of PTPI revealed minute effects on mean residue ellipticity ($MRE_{222\ nm}$) till 1 M GdnHCl. However, complete loss of signal was observed at higher concentrations of the denaturant. Midpoint of transition, Cm, deduced from normalized transition curves of activity, λ_{max}, and $MRE_{222\ nm}$ data was 3.2 M GdnHCl. Further, a shift in Cm was observed with PTPI concentration. Changes in molecular properties of PTPI such as inhibitory activity, $MRE_{222\ nm}$ and λ_{max} with increasing GdnHCl concentration revealed a monophasic sigmoidal dependence with coincidental profiles, characteristic of cooperative unfolding, suggesting a two state model for denaturation of the inhibitor.

In urea, unfolding pathway differed from that observed in GdnHCl. Almost complete inactivation was observed beyond 6 M urea. A gradual increase in λ_{max} occurred with increasing urea concentration. It red shifted to 350 nm at 8 M urea indicating that treatment of PTPI with high concentrations of urea leads to unfolding of the inhibitor. A sigmoidal behaviour of decrease in $MRE_{222\ nm}$ with increasing urea concentration was observed, with complete loss of signal noticeable above 5 M urea. The Cm value deduced from normalized transition curves for activity and $MRE_{222\ nm}$ was 3.6 M. No

dependence of Cm on concentration of the inhibitor was obtained. The Cm value determined from λ_{max} curve was 4 M. The non coincidence of transition curves in urea denaturation as measured by probes sensitive to different levels of protein structure, are consistent with a mechanism involving intermediate state. However, intermediates are not clearly observed.

The denaturation by both GdnHCl and urea was only partially reversible, with retrieval of only 10% of the native activity on extensive dilution only in case of GdnHCl denaturation. Also at all denaturant concentrations the inhibitor refolded to a species having significantly different spectroscopic properties from native PTPI.

Urea is known to be about half as effective as GdnHCl in inducing protein unfolding and dissociation, suggestive of a 2-fold rule. The results of the present study show that PTPI is an exception to this 2-fold rule. The Cm for urea unfolding was 3.6 M (4 M from λ_{max} curve) and that for GdnHCl was 3.2 M, pointing to significant contributions of both hydrophobic and electrostatic interactions in maintenance of active site and/or dimeric nature of the inhibitor.

Chapter 3

Partially or totally unfolded states that are occasionally populated in vivo after biosynthesis on the ribosome, stress conditions or mutation and are favoured by changes on pH, ionic strength and mutations are most susceptible to initiate aggregation [Soldi et al., 2005].

We reasoned that aggregation and fibrillation of PTPI may also require the protein to access partially denatured states and thus explored existence of non native intermediates under experimentally imposed acidic conditions. PTPI was subjected to denaturation over a pH range of 1.0-7.0 and the conformational changes induced were studied by circular dichroism and intrinsic and extrinsic fluorescence.

Till pH 5.0 no change in λ_{max} of emission was observed. A decrease in pH to 3.0 caused a 10 nm blue shift. Further lowering of pH to 2.0 was accompanied by a 2 nm red shift followed by a 3 nm red shift again at pH 1.0. ANS binding was initiated at pH 3.0 (with a blue shift in λ_{max} of ANS emission to 490 nm) and reached a maximum at pH 1.0. Secondary structure analysis revealed ~40% loss at pH 3.0 but at pH 1.0 there was gain in secondary structure content (of ~34%). Conclusively, PTPI at pH 3.0 existed as partially unfolded intermediate having ~60% residual secondary structure but almost completely altered tertiary structure. PTPI at pH 1.0 exhibits

more of a molten globule like features having native like secondary structure contents and enhanced ability to bind ANS, however with tertiary contacts quite similar to native PTPI.

The organic solvent 2, 2, 2-trifluoroethanol (TFE) is known to stabilize the partially unfolded proteins [Rashid et al., 2006b] and has been extensively employed for amyloid fibril induction in various proteins [Zerovnik et al., 2007]. From a range of concentrations used, in the present study 10% TFE induced native like secondary structure in pH 3.0 state of PTPI. Similar results were also obtained for PTPI at pH 1.0 and 2.0.

Based on these results six solvent conditions were chosen to study amyloid fibril formation in PTPI. The inhibitor was incubated at pH 1.0, 2.0, 3.0 and at these three pH in presence of 10% (v/v) TFE. Two standard procedures were used to follow amyloid growth in above samples, Thioflavin T (ThT) fluorescence assay and transmission electron microscopy (TEM).

Enhancement of ThT fluorescence was observed only after 55 days of incubation of PTPI at pH 2.0. Contrastingly at pH 3.0, enhancement was noticed within 5 days of incubation. Results obtained for PTPI incubated at pH 1.0 were quite similar to those obtained for pH 3.0 sample. The results revealed that amyloid type aggregates from PTPI form under acidic conditions and more readily at pH 3.0 and 1.0 than at pH 2.0.

In the presence of TFE, amyloid growth was accelerated, for the sample at pH 2.0 several fold enhancement in ThT fluorescence intensity was observed within 30 days of incubation. Similarly at pH 3.0, a profound increment was observed without any distinct lag phase. The characteristics of fibrillation at pH 1.0 were in similitude with sample at pH 3.0. Controls at each condition did not show any ThT binding.

On subjection to transmission electron microscopy (TEM), after 15 days of incubation sharp fibrils were seen in pH 3.0 sample (in the presence of 10% (v/v) TFE) and peculiar foliage like pattern was observed for pH 1.0 sample (in the presence of 10% (v/v) TFE). The sample incubated at pH 2.0 (in the presence of 10% (v/v) TFE) also gave fibrils but after one month of incubation.

Divalent metal ions (Zn^{2+} and Cu^{2+}) effectuated a concentration dependent decline in ThT fluorescence of preformed fibrils at pH 3.0 suggesting deaggregation of the fibrils. When added prior to the initiation of fibrillation of PTPI (at pH 3.0, with 10% (v/v) TFE) 50 μM Cu^{2+} and 10 μM Zn^{2+} prevented any amyloid aggregation.

These results corroborate with generic hypothesis of amyloid fibrillation proteins,

outline the conditions necessary for PTPI fibrillation and point towards the strong influence of solvent conditions on fibril morphology. Use of divalent metal ions against amyloid formation is also suggested.

Chapter 4

In this chapter effect of reactive species on purified goat pancreatic thiol proteinase inhibitor has been evaluated.

Riboflavin sensitized photodynamic modifications of PTPI lead to inactivation of its antiproteolytic activity and formation of aggregated products (at higher riboflavin concentrations). A continued disappearance of inhibitory activity towards papain was observed with increasing concentration of riboflavin and varying time periods of incubation reaching a maximum value of 83% (loss in activity). Sodium azide (a known singlet oxygen quencher) and potassium iodide (quencher of flavin triplet state) suppressed the activity loss as well as aggregation. Mannitol and thiourea failed to show any such protective effect. Natural antioxidants, curcumin (Cur), caffeic acid (CA) and quercetin (QE) diminished the riboflavin exerted damage which was evident by following observations, activity of treated PTPI was enhanced, aggregation was inhibited and tryptophan fluorescence retrieved back. Curcumin, however, provided only partial moderation.

Hypochlorous acid and to lesser extent hydrogen peroxide destroyed the antiproteolytic potential of PTPI. HOCl even at low concentrations significantly decreased the functional integrity of the inhibitor (90% loss in activity). High concentrations of H_2O_2 also partially diminished proteinase inhibitory capacity of PTPI by a mechanism involving almost no contribution from hydroxyl radicals (sodium benzoate and thiourea afforded no protection and mannitol only to small extent). Structural analyses revealed fragmentation of PTPI upon HOCl exposure. H_2O_2 also caused loss in band intensity and appearance of some higher mobility material. λ_{max} suffered a red shift of 15 nm in the presence of H_2O_2. Diminution of the inflicted damage was observed on treatment with Cur, CA, QE, with former two being more effective than QE. There was subjugation of PTPI activity loss, fragmentation and changes in intrinsic fluorescence pattern in presence of bioflavonoids.

The effect of nitric oxide on structure and function of PTPI was also studied. There was a concentration dependent loss in activity. The λ_{max} red shifted to 350 nm (from 335 nm for native PTPI) in the presence of NO. On the whole the inhibitor was

severely compromised functionally (72% loss in activity) and structurally. The three natural antioxidants, Cur, CA and QE negated the loss in tryptophan fluorescence and PTPI inhibitory activity. Maximum protection was offered by Cur and CA.

The results evinced the susceptibility of PTPI to aforementioned reactive species and the modifications induced included altered molecular weight (aggregation or fragmentation) and fluorescence characteristics and loss of inhibitory function. Also, Cur, CA and QE provided protection against the oxidative and nitrosative damage.

Chapter 5

Experiments were conducted to investigate the effects of sodium valproate, glimepiride, metformin hydrochloride and synthetic insulin on the structure and function of the inhibitor.

Sodium valproate and glimepiride caused dose dependent loss of PTPI's inhibitory activity with almost 80% loss precipitating at 10 μM sodium valproate and 40 μM glimepiride concentrations. Drug interaction induced structural changes in PTPI were monitored by intrinsic fluorescence and UV vis spectrophotometric analyses. Complex changes were noticed in the fluorescence properties of PTPI indicating alteration in the environment of the aromatic amino acid residues induced on interaction with drugs. The difference spectra also showed profound changes suggesting involvement of tryptophan, tyrosine and phenylalanine residues in complexation. Secondary structural analysis of insulin-PTPI complexes revealed increase in ellipticity at 222 nm suggesting enhancement of native stability of the inhibitor. Metformin hydrochloride complexation caused only mild effects.

The results implicate the loss of thiol proteinase inhibitor function in drug induced pancreatitis by sodium valproate. They also provide a platform for understanding the non responsiveness to antidiabetic drugs after a prolonged period and clues to enhance the insulin potency.

Maintenance of appropriate equilibrium between free cysteine proteinases and their complexes with inhibitors is imperative for proper function of all living systems/tissues. This equilibrium in pancreas is critical for pancreatitis onset and its severity, diabetes and cancer [van Acker et al., 2002; Thrower et al., 2006; Rivenbark and Coleman, 2009]. ***The studies are worthy of future research with regards to interaction of PTPI with pancreatic cathepsins and its role in pancreatic (patho) physiology.***

Introduction

[I] INTRODUCTION

1.1 GENERAL

Proteolytic enzymes, also known as proteases/peptidases, are enzymes that catalyze the breakdown of proteins by hydrolysis of peptide bonds. Proteinases are essential for the survival of all kinds of organisms, and are encoded by approximately 2% of all genes [Rawlings et al., 2004b]. Proteases are customarily classified as exopeptidases when they hydrolyze only the N- or C- terminal bonds in proteins and endopeptidases (proteinases) when they hydrolyze internal peptide bonds. However, proteases and proteinases are synonymously used in literature. Based on the catalytic mechanism, there are four types of proteases, serine, cysteine, threonine or aspartic proteases and metallo proteases. There is a recent report on glutamic proteases, being the only subtype not found in mammals so far. The primary role of proteinases was long considered to be protein degradation relevant to food digestion and intracellular protein turnover [Barrett et al., 2004]. However, now it is known that proteinases are involved in control of large number of key physiological processes such as cell-cycle progression, cell proliferation and cell death, DNA replication, tissue remodelling, haemostasis (coagulation), wound healing and immune response [Turk, 2006].

Cysteine proteinases (CPs) are the proteins with molecular mass about 21-30 kDa, showing the highest hydrolytic activity at pH 4-6.5. CPs are present in all living organisms. They are synthesized in a precursor form in order to prevent unwanted proteolysis and later subjected to cotranslational and posttranslational modifications to convert them into catalytically active mature enzymes [Turk et al., 2000]. Till now, 21 families of CPs have been discovered, almost half of them in viruses and rest of them in bacteria, protozoa, fungi, plants and mammals [Barrett et al., 2004; Barrett et al., 2001]. The first clearly recognized and extensively investigated cysteine proteinase is papain isolated from the latex of plant *Carica papaya*. Mammalian CPs are divided into 4 main groups namely;

1. Lysosomal cathepsins
2. Caspases
3. Calpains
4. Legumains

Cathepsins comprise an important section of the papain family of CPs, sharing similar amino acid sequences and folds. There are eleven human cathepsins known at the sequence level [Turk et al., 2001; Rossi et al., 2004]. Out of which seven viz.

cathepsins B, H, L, C, O, F and X are ubiquitous, such that they have a broad tissue distribution, but they may be involved in more specialized processes [Turk et al., 2000; Buhling et al., 2000]. Cathepsins K, V and S are more tissue specific with cathepsin K expressed in osteoclasts only, cathepsin V in thymus and testis, and cathepsin S in spleen and lung [Turk et al., 2000; Buhling et al., 2000]. Recently, cathepsin K was found to be expressed by breast carcinoma cell, mature macrophages, and multinucleate giant cells adjacent to amyloid deposits in brain [Punturieri et al., 2000; Zaidi et al., 2001; Rocken et al., 2001]. Cathepsins are all relatively small monomeric proteins with molecular mass (Mr) in the range of 24-35 kDa, with exception of cathepsin C, which is an oligomeric enzyme with Mr around 200 kDa [Turk et al., 2002]. All mature cathepsins are glycosylated at usually one or more glycosylation sites except cathepsin S. Human cathepsins play very important role in intracellular protein turnover in lysosomes, processing and activation of other proteins including proteinases, antigen processing and presentation and in bone remodelling. However, their specific and individual functions are often associated with their restricted tissue localization [Brix et al., 2008]. Lysosomal CPs have been found to be critical for rheumatoid arthritis, osteoarthritis and osteoporosis [Vasiljeva et al., 2007], neurological disorders [Nakanishi, 2003], pancreatitis [van Acker et al., 2002], cancer [Keppler, 2006; Gocheva and Joyce, 2007], cardiovascular diseases [Lutgens et al., 2007], etc. Cathepsins also participate in apoptosis, although there role is still not clear [Stoka et al., 2005; Turk and Stoka, 2007]. In some pathological conditions like ischemia, hypervitaminosis and exposure to UV radiations lysosomal enzymes are released in extracellular space and produce extensive damage to the extracellular matrix.

Calpains and Caspases are cytoplasmic thiol proteinases. Calpains participate in many intracellular processes like turnover of cytoskeletal proteins, cell differentiation and regulation of signal peptides. They require Ca^{2+} for activation. They are ubiquitously distributed and have been implicated in acute neurological disorders, Alzheimer's disease, muscular dystrophy and gastric cancer [Huang and Wang, 2001]. Caspases are cysteine dependent aspartate specific proteinases. They are involved in cytokine maturation, apoptosis signalling and mediation [Goyal, 2001].

Legumains are cysteine-dependent asparagine endopeptidases. They are involved in MHC class II–restricted antigen presentation [Manoury et al., 1998] and local

negative regulation of osteoclasts formation and activity [Choi et al., 1994].

REGULATION OF LYSOSOMAL THIOL PROTEINASE ACTIVITY

Despite their life-giving functions, the enormous hydrolytic potential of cathepsins can be damaging in living systems and needs to be kept strictly under control. Failures in biological mechanisms controlling proteinase activities result in many diseases such as neurodegeneration, cardiovascular diseases, osteoporosis, arthritis and cancer. Cells have evolved several distinct mechanisms for the regulation of excessive CP activity via proper gene transcription, maintenance of the rate of proteinase synthesis and degradation and most importantly the interaction of CPs with the proteins that inhibit them, viz. cysteine proteinase inhibitors or thiol proteinase inhibitors (CPIs or TPIs) or more commonly cystatins.

The cystatin superfamily comprises a large group of the cystatin domain containing proteins present in wide variety of organisms including humans. Cystatin inhibitory activity is vital for the regulation of normal physiological processes by limiting the potentially inappropriate activity of their target proteinases, cathepsins, mammalian legumain and some calpains [Alvarez-Fernandez et al., 1999; Crawford, 1987].

1.2 DISCOVERY OF THE CYSTATIN SUPERFAMILY

Hayashi et al., [1960] for the first time reported the presence of a factor capable of inhibiting the clotting activity of a thiol proteinase in mammalian system. The first isolated and partially characterized protein inhibitor of CPs was from chicken egg white and was shown to inhibit papain, ficin [Fossum and Whitaker, 1968; Sen and Whitaker, 1973] and cathepsins B and C [Keilova and Tomasek, 1975]. Later for the same protein term cystatin was proposed because of its unique property of arresting the activity of CPs [Barrett, 1981]. The first intracellular protein inhibitor of papain, cathepsin B and H was isolated and partially characterized from pig leucocytes and spleen [Kopitar et al., 1978]. The determined amino acid sequences of chicken cystatin [Turk et al., 1983; Schwabe et al., 1984] and human stefin (stefin A) from the cytosol of polymorphonuclear granulocytes [Machleidt et al., 1983] confirmed structural differences between these two homologous proteins. At the same time, inhibitors of CPs were isolated from sera of patients suffering from autoimmune diseases [Turk et al., 1983] and based on its sequence homology with chicken cystatin the name human cystatin was proposed [Brzin et al., 1984], soon renamed to human

cystatin C (HCC) [Barrett et al., 1984]. Sequences of bovine and human kininogens were determined [Nawa et al., 1983; Muller-Esterl et al., 1985a]. And concept of cystatin "superfamily" emerged precipitated by an observation that multiple cystatin-like sequences were present in kininogens and that stefins were related to both cystatins and repeats of kininogens [Ohkubo et al., 1984]. This data and First International Symposium on Cysteine Proteinases and their Inhibitors (Portoroz, Yugoslavia (now Slovenia) September 1985, organized by V. Turk) were crucial for nomenclature and classification of the cystatin superfamily [Barrett et al., 1986].

1.3 CLASSIFICATION OF THE CYSTATIN SUPERFAMILY

The first classification of the cystatin superfamily into three families was based on at least 50% sequence identity, inhibition of their target enzymes and presence or absence of disulphide bonds [Barrett et al., 1986]. Three distinct families of the protein inhibitors comprise: **family 1** or **the stefin family**, **family 2** or **the cystatin family** and **family 3** or **the kininogen family**. The first two families are single domain inhibitors whereas the kininogens are composed of three domains, two being inhibitory [Fig. 1]. A typical cystatin domain was defined to be an approximately 100-amino acids polypeptide that folds into a five stranded β-sheet, which partially wraps around a central α-helix [Fig. 2] [Bode et al., 1988]. Later, the term 'type' was introduced and the mammalian cystatins were divided into types 1, 2 and 3 [Rawlings and Barrett, 1990]. However, an increasing number of cystatins from various sources introduced new subdivision of the cystatins into four families [Rawlings and Barrett, 1990], the fourth family consisting of non-inhibitory homologues of two cystatin-like domains, such as human α_2 SH-glycoprotein (feutin) and histidine-rich glycoprotein [Brown and Dziegielewska, 1997]. The cystatin superfamily also comprises of phytocystatins. According to recently proposed classification of peptidase inhibitors into families and clans [Rawlings et al., 2004a] cystatins are assigned to family I25 which consists of three subfamilies, I25A (stefins), I25B (cystatins), I25C (are mostly not proteinase inhibitors).

Fig. 1 A diagrammatic representation of the chain structures of proteins in the cystatin superfamily

The stefins are single chain proteins without disulphide linkages. The cystatins are also single chain but possess two disulphide bonds. The structure indicated for the kininogens is that of L- and T-kininogen; H-kininogens have a longer carboxyl terminal extension. There is an additional disulphide link from segment 1 to the kinin segment. The symbol marks potential sites for the attachment of the carbohydrate side chains.

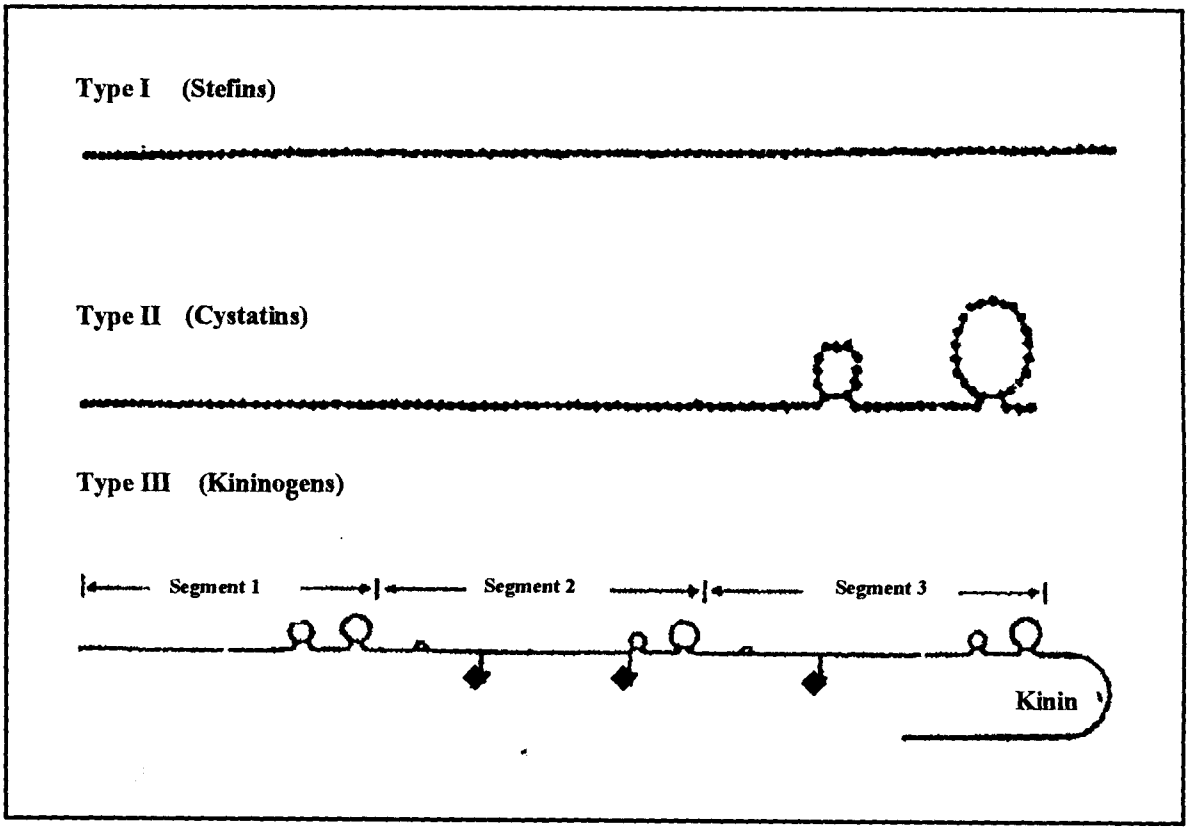
Type I (Stefins)
Type II (Cystatins)
Type III (Kininogens)
Segment 1
Segment 2
Segment 3
Kinin

Fig. 2 Fold of cystatin C

Cystatin C chain trace is shown in green in orientation which positions the N-terminal "elephant trunk" and the first and the second hairpin loops to the bottom from left to right [Adapted from Bode et al. 1988, EMBO J, 2593-2599].

1.4 GENERAL PROPERTIES OF CYSTATIN SUPERFAMILY

TYPE 1 CYSTATINS (STEFINS)

The protein inhibitors belonging to stefin family are acidic single chain proteins lacking disulphide bonds and carbohydrates, composed of ~100 amino acid residues with Mr of 11 kDa. They are primarily intracellular cytoplasmic proteins of many cell types, although they have been found in extracellular fluids as well [Abrahamson et al., 1986]. In mammals, including human, rat, bovine, mouse and porcine, two members of the stefin family, stefin A (cystatin A or α) and stefin B (cystatin B or β) have been identified [Turk et al., 1997; Barrett et al., 1986]. In addition stefin C was discovered in bovine thymus as the first tryptophan containing stefin with a prolonged N-terminus [Turk et al., 1993] and stefin D in pigs [Lenarcic et al., 1996]. Atleast three different stefin A variants are encoded within the mouse genome [Tsui et al., 1993].The type 1 cystatins belong to the subfamily I25A [Rawlings et al., 2004a].

Cystatin A

It is an inhibitor of cathepsin B in human skin discovered by Fraki [1976]. Later on Jarvinen [1978] studied it as 'acid cysteine proteinase inhibitor' (ACPI) because of its acidic pI at 4.7-5.0. Brzin et al. [1983] purified an inhibitor from blood leucocytes, and named it as "stefin'. The amino acid sequence was determined by Machleidt et al. [1983]. Green et al. [1984] characterized same type of CPI from human liver and latter renamed it as cystatin A. Cystatin A occurs in multiple isoelectric forms with predominantly acidic pI values in the range 4.5-5.0 [Hopsu-Havu et al., 1983a]. Rinnie et al. [1978] detected cystatin A in extracts of squamous epithelia from oesophagus. It was also found in dendritic reticulum cells of the lymph nodes [Rinnie et al., 1983], seminal plasma [Minakata and Asano, 1985], saliva, bovine skin [Turk et al., 1995] and in a number of epidermoid carcinomas [Rinnie et al., 1984].

Cystatin α is assumed to be a species variant of cystatin A found in rats. This protein was characterized by Jarvinen [1976] as a specific inhibitor of CP from rat skin having Mr of 13 kDa. Cystatin α is generally found on the epidermal layer [Jarvinen et al., 1978] and various other squamous epithelia [Rinnie et al., 1978]. Human stefin A is expressed at high levels in skin and presumably controls cysteine proteinases in the skin. Some cathepsins play a crucial role in the antigen presentation process indicating that the interactions between stefin A and cathepsins contribute to

the species dependent diversity of the endosomal compartments which participate in the immune response [Mihelic et al., 2006].

Cystatin B

Cystatin B was detected as an inhibitor of cathepsin B and H in human tissues by Lenney et al. [1979]. It has been purified from human spleen and liver [Jarvinen and Rinnie, 1982; Green et al., 1984]. Cystatin B is relatively basic protein with pI values of 6.25 and 6.35 for its two forms [Green et al., 1984]. It forms dimer [Green et al., 1984] which shows no inhibitory activity. With ubiquitous distribution it appears to be general inhibitor in the cytoplasm. **Cystatin β** a species variant of cystatin B was isolated from rat liver [Finkelstadt, 1957; Lenney, 1979] with pI values ranging from 5.04 to 5.6 [Kominami et al., 1981]. It has even distribution in tissues and is more abundant than cystatin α in all tissues except skin. In this it resembles cystatin B of human variant.

Stefin C

Stefin C is unique among the inhibitors from stefin family which was found in multiple forms resulting from the cleavage of Asn 5-Leu 6 bond of the inhibitor. Its MW is calculated to be 11,546 (101 amino acid residues). It was found to be acidic with pI values from 4.5 to 5.6 [Turk et al., 1993].

TYPE 2 CYSTATINS (CYSTATINS)

Cystatins typically comprise ~115 amino acids (Mr ~13-15 kDa), are largely acidic (with exception of human cystatin C) contain four conserved cysteine residues known to form two disulphide bonds [Grubb et al., 1984], usually non-glycosylated with exceptions of cystatin E/M [Ni et al., 1997; Sotirpoulou et al., 1997], cystatin F [Ni et al., 1998] and cystatin S [Esnard et al., 1990] which are glycoproteins. They are synthesized with 20-26 residues long signal peptides and are mainly extracellular, secreted proteins, occurring at relatively high concentrations in body fluids [Abrahamson et al., 1986; Kopitar-Jerala, 2006]. Similar to stefins, the cystatins contain the conserved QXVXG region in the central part of the molecule and the P-W pair in the C-terminal part of cystatins [Turk and Bode, 1991]. Chicken cystatin and HCC represent founding members of this family [Turk and Bode, 1991; Abrahamson et al., 1986]. Human type cystatins include cystatin C, D, S, SA and N with about

50% or less sequence identity [Turk and Bode, 1991; Abrahamson et al., 1986; Balbin et al., 1994]. The human type 2 cystatins are grouped in subfamily I25B of the cystatin family [Rawlings et al., 2004a].

Cystatin C

Originally cystatin C was termed as γ-trace or post-γ-globulin isolated from human cerebrospinal fluid because of its basic nature and γ electrophoretic mobility [Barrett et al., 1984; Brzin, 1984]. It was also found in the urine in renal failure patients [Butler and Flynn, 1961] and ascetic and pleural fluids [Hochwald and Thornbecke, 1962]. Cystatin C was also detected in saliva, normal serum [Cejka and Fleischmann, 1973] and seminal plasma [Colle et al., 1976]. Preferentially abundant in cerebrospinal fluid, seminal plasma, milk, synovial fluid, urine, and blood plasma [Abrahamson et al., 1986] cystatin C has also been detected intracellularly in brain cortical nerves [Lofberg et al., 1981], normal and neoplastic neuroendocrine cells in the adrenal medulla [Lofberg et al., 1982], thyroid [Lofberg et al., 1983] and pituitary [Lofberg et al., 1983; Moller et al., 1985].

Cystatin D

Cystatin D a member of human cystatin multigene family and was cloned from a genomic library using cystatin C cDNA probe [Freije et al., 1991]. The inhibitor consists of 122 amino acids residues (Mr 13,885). The deduced amino acid composition includes a putative signal peptide and has 51-55% homology with either cystatin C or secretory gland cystatins S, SA and SN. It is a relatively neutral protein with pI in the range of 6.8- 7.0 [Freije et al., 1991]. It is expressed in parotid glands, saliva and tears [Balbin et al., 1994]. This tissue restricted expression is in marked contrast with a wider distribution of all other family 2 cystatins.

Cystatin S

Human saliva contains several low MW acidic proteins which include CPIs [Isemura et al., 1984b].The first salivary inhibitor purified and sequenced was SAP-I (salivary acid protein) by Isemura et al. [1984a], which was renamed as 'cystatin S'. It contains no phosphate, in contrast to other salivary proteins. This inhibitor has also been isolated from human submaxillary, submandibular and sublingual glands and found to be present in the serous cells of the parotid and submaxillary glands [Isemura et al.,

1984b]. The protein has also been found in tears, serum, urine, bile, pancreas and bronchus [Isemura et al., 1986].

Variants of cystatin S

Several molecular variants of cystatin S have been studied by Isemura et al [1986] which differ in their N-terminal sequence and pI values. Differences in pI values resulted from phosphorylation of residues Ser3 and Ser1 in salivary cystatin [Isemura et al., 1991]. **Cystatin SN:** Originally known as cystatin SV or SA-1 [Abrahamson et al., 1986]. The protein consists of 121 amino acid residues (Mr 14,316). The pI values are in the range of 6.6-6.8. **Cystatin SA** consists of 122 amino acid residues (Mr 14,351) having acidic pI value of 4-6 [Isemura et al., 1991]. Cystatin SA isolated from saliva had N-terminal residue Glu [Isemura et al., 1986].

Cystatin E

Human cystatin E from amniotic fluid and fetal skin epithelial cell was identified and recombinant cystatin E isolated [Ni et al., 1997]. Human cystatin M is expressed by normal mammary cells and a variety of human tissues [Sotirpoulou et al., 1997]. Both proteins are identical and were renamed as cystatin E/M (MEROPS, the peptidase database). Recently, the expression of cystatin M/E was found to be restricted to the epidermis [Cheng et al., 2006] and is most probably identical to cystatin E/M.

Cystatin F

Cystatin F (leukocystatin) (MW 14,543) is primarily found in peripheral blood cells, T cells, spleen, dendritic cells and selectively, in hematopoietic cells [Ni et al., 1998; Halfon et al., 1998]. Cystatin F has an additional disulphide bridge, thus stabilizing the N-terminal part of the molecule [Ni et al., 1998]. It is the only cystatin synthesized and secreted as an inactive disulphide-linked dimeric precursor which becomes active following reduction to monomeric from [Schuttelkopf et al., 2006].

TYPE 3 CYSTATINS (KININOGENS)

Kininogens, the precursors of kinin, are large multifunctional glycoproteins in mammalian plasma and other secretions. Three different types of kininogens have been identified: high molecular weight kininogen (HK), low molecular weight

kininogen (LK) and T-kininogen an acute phase protein found only in rats [DeLa Cadena and Colman, 1991; Muller-Esterl, 1987]. Human HK and LK are single-chain proteins each composed of an N-terminal heavy chain, the kinin segment and a C-terminal light chain. The light and heavy chains are interconnected by disulphide bridges. The heavy chains and kinin segments of both kininogens have identical amino acid sequences while the light chains are different [DeLa Cadena and Colman, 1991; Salvesen et al., 1986a]. The heavy chain is composed of three cystatin domains [Fig. 1], D1-D3 [Salvesen et al., 1986a] with only D2 and D3 possessing papain inhibitory and D2 possessing calpain inhibitory activities. An inhibitory fragment, identical to the third domain of human kininogen, was isolated from human placenta and is inactivated by the lysosomal aspartic proteinase cathepsin D. Similarly HCC was also inactivated, suggesting a role for cathepsin D in regulating cysteine cathespin activity [Lenarcic et al., 1991]. Both inhibitory domains of LK and HK are grouped in subfamily I25B of the cystatin superfamily [Rawlings et al., 2004a].

Other type 2 cystatins

There are a number of other cystatins or cystatin related proteins, which are structurally related to cystatins with no inhibitory activity against papain like enzymes [Turk and Turk, 2008]. CRES (Cystatin Related Epididymal Spermatogenic) protein [Sutton et al., 1999], testatin (expression restricted to mouse pre-Sartoli cells) [Tohonen et al., 1998], cystatin SC and cystatin TE-1 (expressed in testis and epididymis, respectively) [Li et al., 2002], and several other genes were found expressed specifically in the male reproductive tract [Hamil et al., 2002; Xiang et al., 2005; Shoemaker et al., 2000], indicating the existence of a new subgroup in the type two cystatins [Cornwall et al., 2003; Sutton-Walsh et al., 2006]. These CREStatins show homology to cystatins, with the exception of the two hairpin loops responsible for the cysteine proteinase inhibition. Their role could be regulation of proteolysis in the reproductive tract as well as protection against invading pathogens, as shown by cystatin 11 [Hamil et al., 2002]. The CRES protein tend to form oligomers [Horsten et al., 2007], similar to cystatin C [Janowski et al., 2001; Wahlbom et al., 2007] and stefin B [Zerovnik et al., 2002a; Jenko-Kokalj et al., 2007]. Another type 2 cystatin, cystatin 10, expressed in cartilage, localized in prehypertrophic and hypertrophic chondrocytes is known to be an inducer of chondrocyte maturation followed by apoptosis [Koshizuka et al., 2003]. A novel cystatin type 2 protein namely CLM

expressed widely in normal tissue playing role in hematopoietic differentiation or inflammation, different from CRES was characterized by Sun and coworkers [2003].

NEW MEMBERS OF THE CYSTATIN SUPERFAMILY

The feutins and **histidine-rich glycoproteins (HRG)** comprise fourth family of cystatins. The feutin family consists of two tandem cystatin domains. Bovine feutin was first characterized by Pedersen in 1944, and its relation to cystatin superfamily described in 1988 [Elzanowski et al., 1988]. Human feutin (α_2-HS glycoprotein) was confirmed in 1987 [Dziegielewska et al., 1987; 1990; Dziegielewska and Brown, 1995]. Since then, protein and/or cDNA sequences have been reported for human, cow, pig, rat, mouse, Habu snake, feutins [Brown and Dziegielewska, 1997]. Almost all the feutin sequences contain 12 cysteine residues, showing homology to the cystatins and cystatin domains in kininogens [Dziegielewska and Brown, 1995]. HRG has been characterized in the plasma of man, mouse, rabbit, cow and pig [Leung, 1993], sharing good sequence homology with human and bovine HMW kininogen [Koide et al., 1986]. A large number of proteins have been discovered recently, which possess cystatin domains e.g. latexin [Aagaard et al., 2005]. However, feutin, HRG and latexin all seem to lack CPI activity.

Thyropins constitute a new family of papain-like CP inhibitors [Lenarcic and Bevec, 1998], classified as family I31 [Rawlings et al., 2004a]. The p41 invariant chain (Ii)-fragment of the MHC class II-Ii complex 104, 105 and equistatin from the sea anemone [Lenarcic et al., 1997] are best characterized members of this family. Thyropins show inhibitory activity against CPs and also towards aspartic and metalloproteinases [Mihelic and Turk, 2007; Lenarcic and Turk, 1999]. **Tick cystatins**: **Syalostatin L** [Kotsyfakis et al., 2006] and **syalostatin L2** [Kotsyfakis et al., 2007] have been characterized from salivary glands of the tick *Ixodes scapularis*. Both show 75% sequence identity and inhibit cathepsin L with a Ki of 4.7 nM and cathepsin V with Ki of 57 nM. **Staphostatins** are specific inhibitors of staphylococcal CPs. Three members of this family have been described-staphostatins A and B from *Staphylococcus aureus* and staphostatin A from *Staphylococcus epidermidis* [Filipek et al., 2003]. **Clitocybin** is a new type of CPI from a mushroom appearing to be related to fungal lectins and hence a new family of CPIs is suggested for them called mycocypins [Brzin et al., 2000]. **Chagasin** is a cysteine proteinase inhibitor from

Trypanozoma cruzi inhibiting both cruzipain and papain, but has no homology with cystatins [Monteiro et al., 2001].

Phytocystatins: In plants, inhibitors of CPs are known as phytocystatins. They contain the QXVXG region of type 2 cystatins, but also resemble stefins in the absence of disulphide bonds [Arai et al., 2002], providing a transitional link between type 1 and type 2 cystatins. There are numerous phytocystatins expressed and characterized on the protein level from corn [Abe et al., 1992], rice [Chen et al., 1992], soyabean [Lalitha et al., 2005], sugarcane [Oliva et al., 2004] and others. C-terminal extended phytocystatins were found as bifunctional inhibitors of papain and legumain [Martinez et al., 2007]. In addition, a "multicystatin" containing two cystatin like domains were isolated from cowpea leaves [Diop et al., 2004], tomato leaves [Wu and Haard, 2000]. Also there are certain plant proteins like monellin which lack the CPI activity but have a cystatin like three dimensional structure [Grzonka et al., 2001]. Phytocystatins and other inhibitors are important for plant defence response to insect predation, may act to resist infection by some nematodes [Koiwa et al., 1997], play a crucial role in response to various conditions [Diop et al., 2004; Brzin and Kidric, 1995] and show great potential tools for genetically engineered resistance of crop plants against pests [Aguiar et al., 2006].

Variant cystatins

Divergent cystatins showing significant homology to stefins, cystatins and kininogens have been expressed/purified and characterized from venom of African puff adder *(Bitis arietans)* [Evans and Barrett, 1987]; from perilymph of flesh fly larvae [Suzuki and Natori, 1985]; from *Drosophila melanogaster* [Delbridge and Kelly, 1990]. Some of the mammalian and non mammalian sources from where CPIs have been isolated are summarized in Table 1.

1.5 EVOLUTION

The first two proposed evolutionary dendrograms for CPIs were made based on a small number of members of the cystatin superfamily [Muller-Esterl et al., 1985b; Salvesen et al., 1986b]. The new proposed evolutionary dendrograms followed the evolution of the proteins of the cystatin superfamily along four lineages, with special

TABLE 1: CPIs FROM SOME MAMMALIAN AND NON MAMMALIAN SOURCES

Source	Tissue	Reference
Beef	Spleen	Brzin et al., 1982
Bovine	Brain	Aghajanyan et al., 1988
	Hoof	Tsushima et al., 1996
	Colostrums	Hirado et al., 1985
Dog	Colostrum	Poulik et al., 1981
	Parotid gland & Kidney	Sekine and Poulik, 1982
Horse show crab	Hemocytes	Aggarwal et al., 1996
Human	Liver	Green et al., 1984
	Spleen	Jarvinen and Rinnie, 1982
	Placenta	Rashid et al., 2006a
Rabbit	Liver	Pontremoli et al., 1983
	Skin	
Rat	Brain	Kopitar et al., 1983
Ixodes scapularis	Salivary gland	Kotsyfakis et al., 2006 & 2007
Staphylococcus aureus & epidermidis	-	Filipek et al., 2003
Trypanosoma cruzi	-	Monteiro et al., 2001
Fasciola hepatica	-	Khaznadji et al., 2005
Goat	Kidney	Zehra et al., 2005
	Brain	Sumbul & Bano, 2006
	Lung	Khan & Bano, 2009a
	Pancreas	Priyadarshini & Bano, 2009
Spirometra erinacei	-	Chung & Yang, 2008
Yellow croaker	Spleen	Li et al., 2009

attention that duplication of cystatin like segments has played important contribution to the understanding of the evolution of cystatins. According to the scheme of Muller-Esterl et al. [1985b] constructed on the basis of sequence homology, the diversity of CPIs has evolved from two ancestral building blocks 'A' and 'B'. The stefin progenitor represents the whole superfamily comprising a single 'A' unit. Cystatin acquired a second element B, possibly by gene fusion, thus forming 'AB' unit. Gene triplication of the archetype inhibitor generated the kininogen heavy chain which contains 3 cystatin like copies $(AB)_3$. The proposed evolutionary pathway also contained a 'missing link', a two cystatin domain protein that evolved from the cystatins by duplication, with two candidates for such a protein: feutin and HRG. This scheme however seem unlikely most importantly because neither domain in feutins/HRG is inhibitory but two domains of kininogens have inhibitory activity. If feutin/HRG were the 'missing link', then the kininogens which have evolved from the two domain protein would have to re-evolve their proteinase inhibitory activity and sequences [Brown and Dziegielewska, 1997]. Brown and Dziegielewska [1997] proposed the following scheme for cystatin superfamily evolution, with features similar to Muller-Esterl et al., [1985b] scheme but with a new missing link, a two cystatin domain protein in which both the domains were functional cysteine proteinase inhibitors. From it, the kininogens, feutins, and HRG could have evolved separately or perhaps in parallel and retained or lost their proteinase-inhibitory activity and active site sequences. This scheme [Fig. 3] draws support from the observation of conserved sequences immediately around the cysteine at the C-terminus of the feutins, HMW-kininogens and HRG, again suggesting a common origin for these three proteins. Based on this Lee et al., [2009] have recently grouped feutins, HRG and kininogens in a single family, type 3 cystatins.

1.6 STRUCTURE OF CYSTATINS

PRIMARY STRUCTURE

Most of the members of cystatin superfamily are polypeptides of 98-126 amino acid residues with Mr values in the range of 11-14 kDa. As regards to the amino acid composition of cystatins few distinctive features can be attributed to the subfamilies. Stefins are devoid of disulphide linkages (human cystatin A and rat cystatin α lack cysteine residues while human cystatin B and rat cystatin β have 1 and 2 cysteine

Fig. 3 Evolution of cystatin superfamily

A. Scheme from Muller-Esterl et al. [1985b]

B. Scheme proposed by Brown & Dziegielewska [1997]

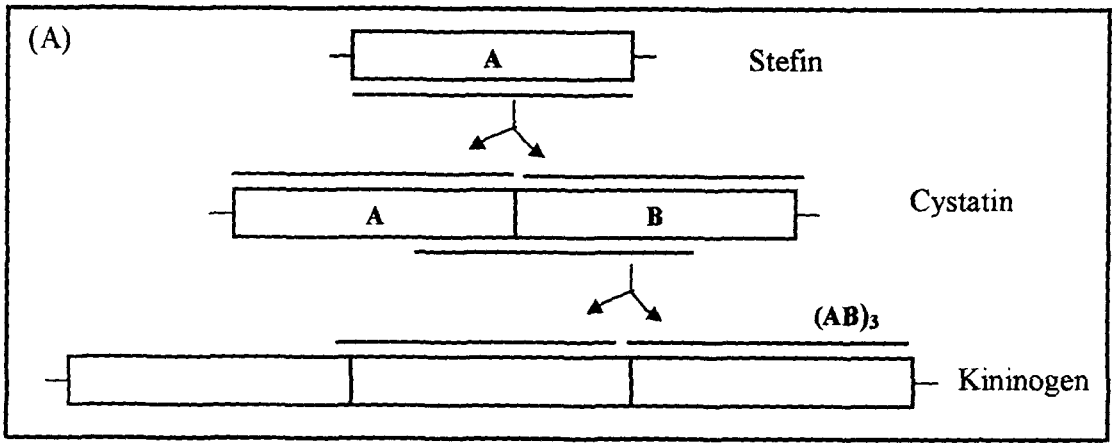
(A)
A
Stefin
A
B
Cystatin
(AB)3
Kininogen

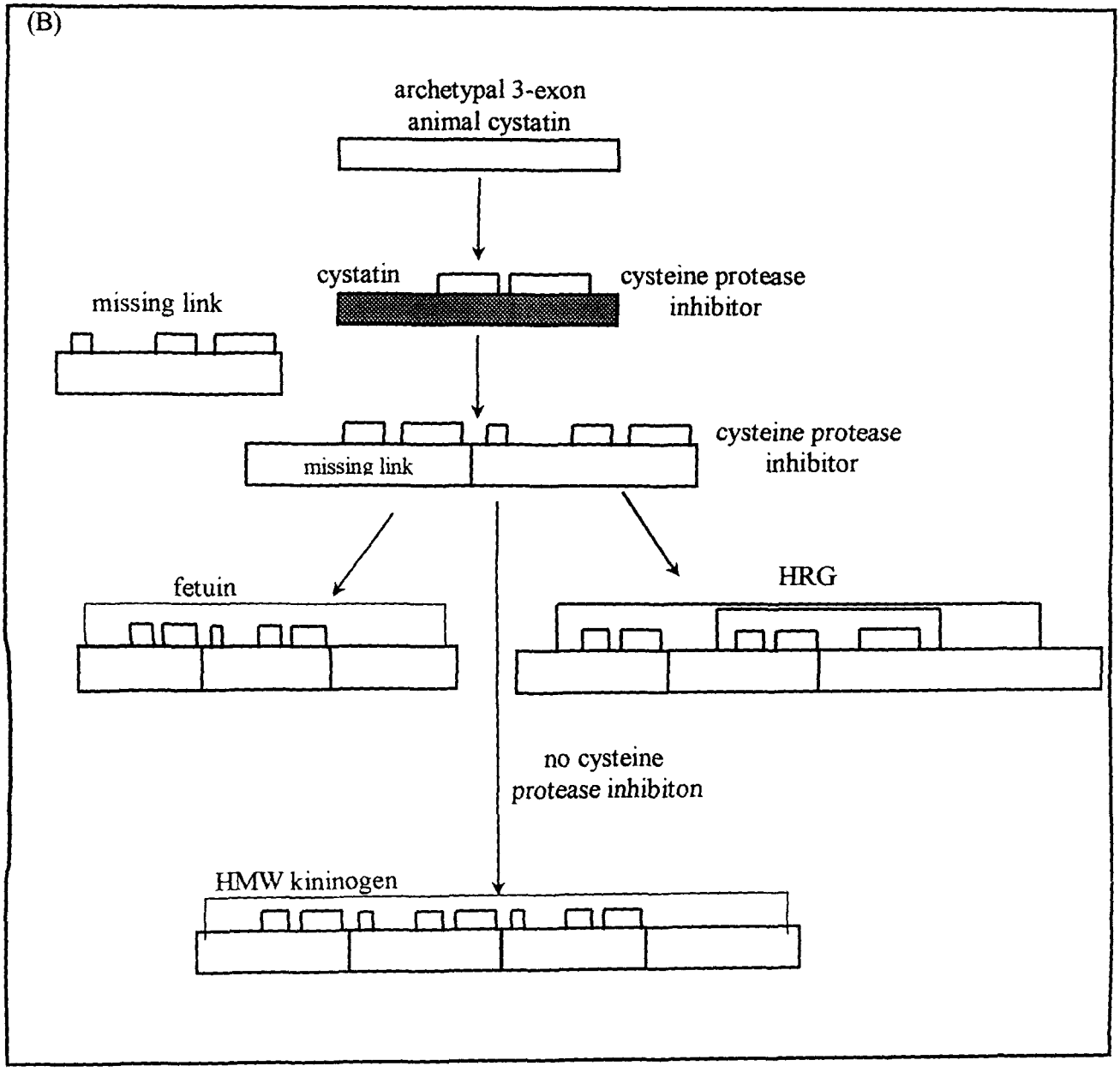
(B)
archetypal 3-exon
animal cystatin
cystatin
cysteine protease
inhibitor
missing link
missing link
cysteine protease
inhibitor
fetuin
HRG
no cysteine
protease inhibiton
HMW kininogen

residues, respectively) and tryptophan. Turk et al. [1993] however reported the presence of tryptophan in stefin C. A unique feature of stefin B is the conserved QVVAG region in the stefins of mammalian origin, with Val54 replaced by Leu54. Ni et al. [1998] reported the presence of an additional disulphide bridge in cystatin F, for stabilizing the N-terminal part of the molecule in addition to the presence of second tryptophan residue, along with the conserved Trp 106, characteristic of type 2 cystatins. The alignment of sequences of cystatins reveals common features, significant to the structure and activity of the proteins. Four residues are common to all the sequences of cystatins and inhibitory kininogen segments: Gly9, Gln53, Val55 and Gly57. These residues are considered to be of functional importance since they are absent from the non-inhibitory segment D1 of kininogens. Another six conserved residues are Val47, Val55, Ala56, Tyr60, Cys71 and Tyr100. The segment Gln53 to Gly57 is the most highly conserved region.

SECONDARY STRUCTURE

The crystalline form of chicken cystatin reported by Bode et al. [1988] revealed a new fold, the cystatin fold which is, a five stranded anti-parallel β-sheet wrapped around the central N-terminal helix [Fig. 2]. This fold has been shown to exist in HCC, chicken cystatin, cystatin D, as well as in family 1 cystatins A and B [Martin et al., 1994; 1995; Alvarez-Fernandez et al., 2005; Stubbs et al., 1990]. An appending segment of partial α-helical geometry is present in chicken cystatin [Saxena and Tayyab, 1997], but absent in HCC [Bode et al., 1988]. Tryptophan was found only in the second hairpin loop of cystatins [Bode et al., 1988]. A unique feature was observed in crystal structure of cystatin F in its dimeric 'off' state. The two monomers interacted in a fashion not seen before for cystatins or cystatin like proteins, crucially dependent on an unusual intermolecular disulphide bridge. The core sugars for one of the two N-linked glycosylation sites for cystatin F are well ordered and probably their conformation and interactions with the protein modulate its inhibitory properties in particular its reduced affinity toward asparaginyl endopeptidase compared with other cystatins [Schuttelkopf et al., 2006].

There is considerable similarity between the structural features of stefins A and B [Fig. 4], but there are also some important differences in the regions which are fundamental to proteinase binding. The difference primarily consists of the two regions of high conformational heterogeneity in free stefin A which correspond in

Fig. 4 **(A)** Three dimensional structure of stefin A (where, A, B, C, D, E are the five antiparallel β sheets strands)

(B) Three dimensional structure of stefin B (antiparallel β sheets are in green colour and α-helix is in red colour)

(A)

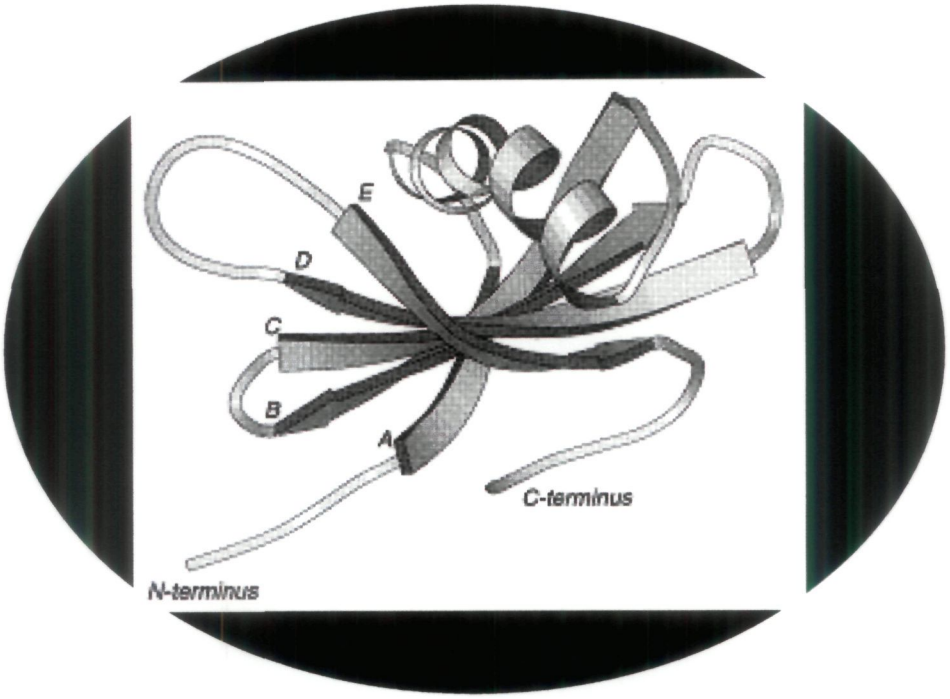

(B)

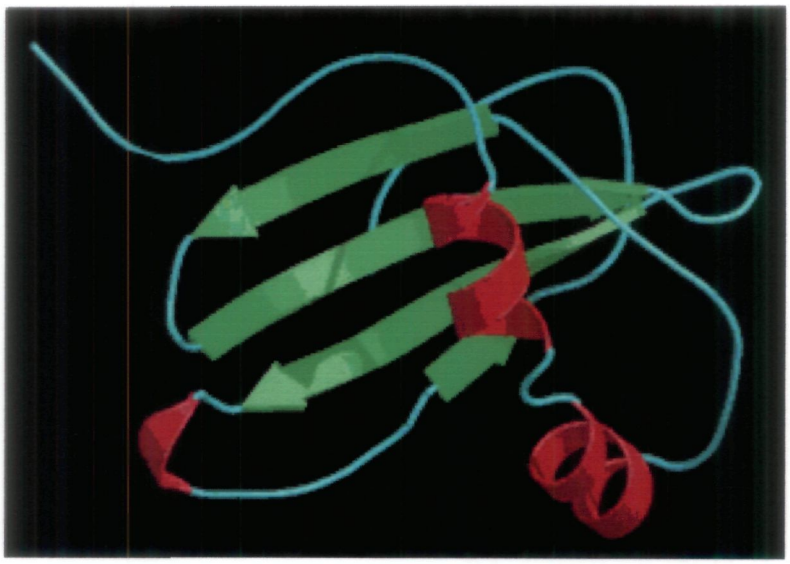

stefin B to two of the components of the tripartite wedge that docks into the active site of target proteinases. These regions which are mobile in solutions are the five N-terminal residues and the second binding loop. In the bound conformation of stefin B they form a turn and a short helix, respectively.

Circular dichroism and computer prediction of secondary structure from the sequence indicates that chicken cystatin has about 20% α-helix, 42% β-structure, 24% β-turn and 12% random coil [Schawbe et al., 1984]. Recombinant human cystatin A in good comparison to cystatin A, in far UV-CD spectrum revealed ~45% β -structure and a low α -helix content (~15%) [Pol et al., 1995].

1.7 INHIBITION OF PROTEINASES

Specificity

Cystatins are highly specific for CPs except for thyropins which show inhibitory activity against aspartic and metalloproteinases [Mihelic and Turk, 2007; Lenarcic and Turk, 1999]. However there are few cystatins capable of inhibiting mammalian legumain [Alvarez-Fernandez et al., 1999] and calpains [Crawford, 1987]. To date, none of the cytoplasmic inhibitors have been tested on ubiquitin processing and recycling proteinases [Keppler, 2006]. Stefin A and B are potent inhibitors of papain, cathepsin L, S and H but have decreased activity against cathepsin B [Musil et al., 1991]. Type 2 cystatins are important endogenous inhibitors of papain like CPs including cathepsins, parasite proteinases like cruzipain and mammalian legumain [Turk et al., 2005; Turk and Bode, 1991]. HCC and chicken cystatin inhibit papain, cathepsin L and S [Abrahamson et al., 2003]. HCC shows strong inhibitory capacity for rapid binding thus neutralizing proteinase activity in an emergency inhibition [Turk et al., 2005]. It also inhibits cruzipain, suggesting its possible defensive role after infection [Stoka et al., 1995]. Cystatin F inhibits cathepsin F, K, V, S, L and H [Langerholc et al., 2005] and weakly legumain [Alvarez-Fernandez et al., 1999]. More recently it was found that the intracellular form of cystatin F, after N-terminal truncation of the first 15 residues including cysteine, inhibits cathepsin C [Hamilton et al., 2008]. Cystatin D inhibits cathepsin S, H and L but not cathepsin B or pig legumain [Alvarez-Fernandez et al., 2005]. Human cystatin E/M inhibits papain, cathepsin B, L, V and legumain [Ni et al., 1997; Sotiropoulou et al., 1997; Cheng et al., 2006; Alvarez-Fernandez et al., 1999]. Clostripain (proteinase not belonging to

papain family) is also inhibited by cystatins [Barrett et al., 1986].

Kinetic behaviour

Cystatins are the first group of protein inhibitors of CPs for which the mechanism of inhibition was investigated. All the cystatins are non-covalent, competitive, reversible, tight binding inhibitors which inhibit the target enzymes in micromolar to picomolar range [Turk et al., 1997]. They form tight equimolar complexes with CPs [Anastasi et al., 1983]. Some of the reported values of equilibrium constants for dissociation of complexes between human cystatins and lysosomal CPs are summarized in Table 2. The affinity differences can be explained by the differences in the active site regions of endo- and exopeptidases. The access of the inhibitor to the active site of exopeptidases is partially obstructed by occluding loops in cathepsin B [Musil et al., 1991], cathepsin X [Guncar et al., 2000], propeptide parts in cathepsin H [Guncar et al., 1998] and cathepsin C [Turk et al., 2001].

Reactive site and mechanism of action

It has been established that no disulphide bond is formed between the active site cysteine residue and the inhibitor because the complexes dissociated when denatured without reduction as was found in chicken cystatin [Nicklin and Barrett, 1984] and kininogens [Gounaris et al., 1984]. The complex formation is accompanied by pronounced spectroscopic changes [Bjork et al., 1989]. On the basis of cystatin domain structure, it was proposed that there are three regions crucial for interaction with proteinases: the amino terminus and two β-hairpin loops, one in the middle and one in the C-terminal segment of the protein. The first loop contains a QXVXG sequence conserved in almost all inhibitory members of cystatins, whereas the second loop contains a P-W motif, which is also highly conserved [Table 3]. Both these loops and the amino terminus forms a wedge shaped edge, which is highly complementary to the active site of the enzyme. The N-terminally truncated forms of chicken cystatin confirmed the crucial importance for the binding of the residues preceding the conserved Gly-9 residue [Machleidt et al., 1989]. The essential interactive elements of this hypothetical complex are shown in figure 5. Complex formed on interaction of stefin B with cathepsin H is shown in figure 6.

TABLE 2: EQUILIBRIUM CONSTANTS FOR DISSOCIATION (Ki) OF COMPLEXES BETWEEN HUMAN CYSTATINS AND CHICKEN CYSTATIN WITH LYSOSOMAL CYSTEINE PROTEINASES (PAPAIN, HUMAN CATHEPSINS AND CRUZIPAIN)

CPI	Ki (nM)				
Cystatin	**Papain**	**Cathepsin B**	**Cathepsin H**	**Cathepsin L**	**Cruzipain**
Stefin A	0.019	8.2	0.31	1.3	0.0072
Stefin B	0.12	73	0.58	0.23	0.060
Cystatin C	0.00001	0.27	0.28	<0.005	0.014
Cystatin D	1.2	>1000	7.5	18	n.d.
Cystatin E/M	0.39	32	n.d.	n.d.	n.d.
Cystatin F	1.1	>1000	n.d.	0.31	n.d.
Cystatin S	108	n.d.	n.d.	n.d.	n.d
Cystatin SA	0.32	n.d.	n.d.	n.d.	n.d.
Cystatin SN	0.016	19	n.d.	n.d.	n.d.
Chicken cystatin	0.005	1.7	0.06	0.019	0.001
L-kininogen	0.015	600	0.72	0.017	0.041
H-kininogen	0.02	400	1.1	0.109	n.d.

n.d. (not determined), Ki values for human cystatins [Abrahamson et al., 2003], chicken cystatin [Barrett et al., 1986] and cruzipain inhibition by cystatins [Stoka et al., 1995].

Table 3: CONSERVED AMINO-ACID RESIDUES IN BINDING SEGMENTS OF HUMAN CYSTATINS [a, b]

Cystatin	N-terminus	I loop	II loop
A	MIPGG	**QVVAG**	
B	AcMMCGA	**QVVAG**	
C	RLVGG	**QIVAG**	**VPWQ**
D	TLAGG	**QIVAG**	**VPWE**
E	RMVGE	**QLVAG**	**VPWQ**
F	VKPGF	**QIVKG**	**VPWL**
S	IIPGG	**QTFGG**	**VPWE**
SA	IIEGG	**QIVGG**	**VPWE**
SN	IIPGG	**QTVGG**	**VPWE**
H-kininogen			
1-domain	*(QESQS)*	*(TVGSD)*	*(RSST)*
2-domain	DCLGC	**QVVAG**	*(DIQL)*
3-domain	ICVGC	**QVVAG**	**VPWE**
L-kininogen			
1-domain	*(QESQS)*	*(TVGSD)*	*(RSST)*
2-domain	DCLGC	**QVVAG**	*(DIQL)*
3-domain	ICVGC	**QVVAG**	**VPWE**

[a] Sequences in parenthesis correspond to the appropriate binding sequences of cystatins.
[b] Grzonka et al., 2001.

Fig. 5 Scheme of the proposed model for the interaction of chicken egg white-cystatin and papain

(Adapted from Turk and Bode, FEBS Lett 1991; 285:213-219)

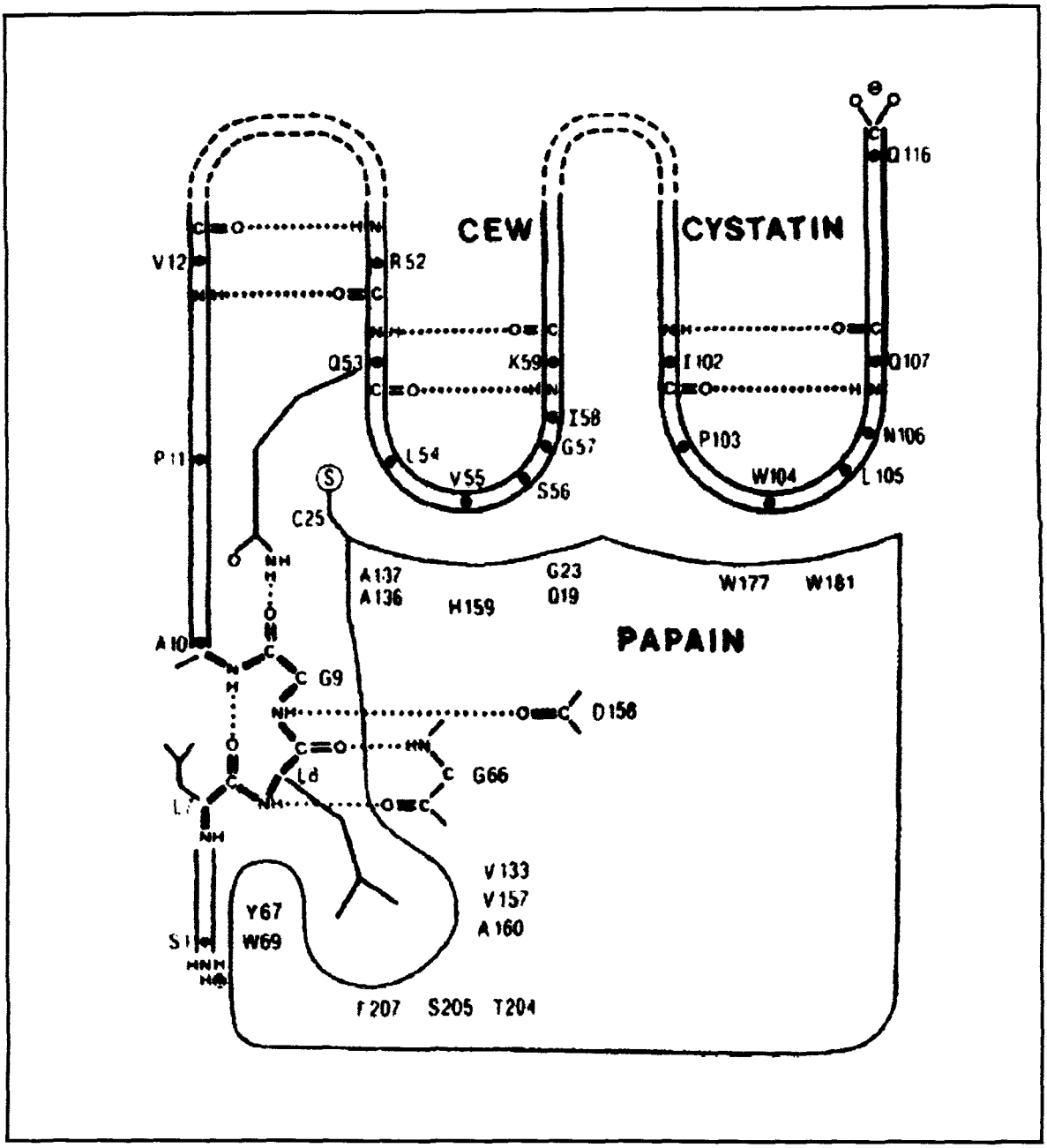
CEW
CYSTATIN
PAPAIN
V12
R52
Q53
K59
I58
G57
L54
V55
S56
P11
C25
A137
A136
H159
G23
Q19
W177
W181
A10
G9
D158
G66
Y67
W69
V133
V157
A160
F207
S205
T204
Q116
I102
Q107
P103
W106
W104
L105

Fig. 6 Three dimensional structure of the complex formed between stefin A and cathepsin H

Binding of stefin A into cathepsin H active site. Stefin A fold is shown as a green chain trace. Whereas cathepsin H fold is shown in yellow. Cathepsin H mini-chain residues are shown as red sticks which are thicker for the main chain. The mini-chain is attached to the body of cathepsin H with a disulfide shown as red yellow chain. The identified carbohydrate rings are shown in cyan. The N-terminus of stefin A displaces the C-terminus of the minichain by pushing its residues outside the binding cleft. Adopted from Turk and Turk, Acta Chim Slov 2008; 55:727-738.

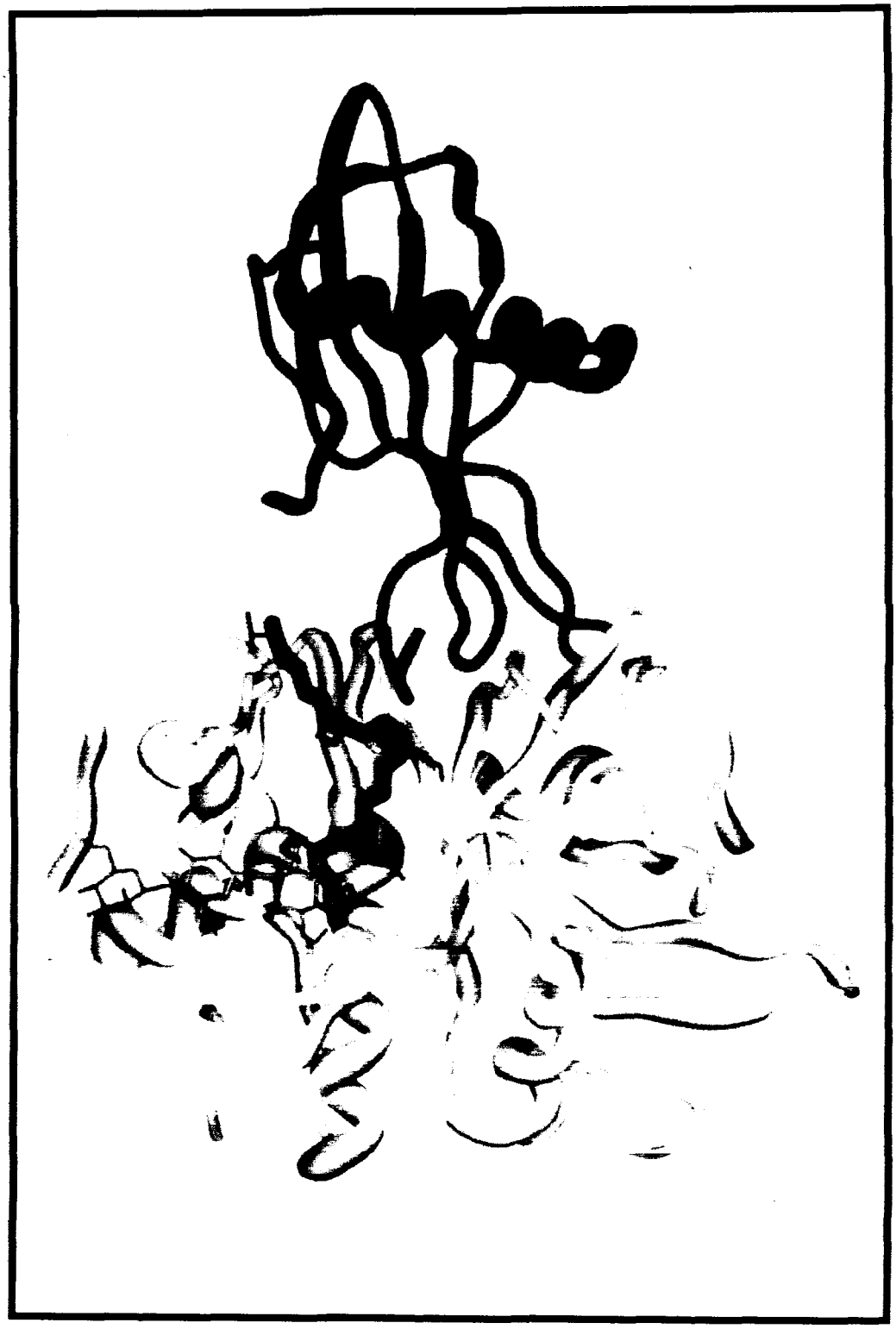

Bode et al. [1988] demonstrated that the major contribution is from the first hairpin loop containing QVVAG sequence [Turk et al., 1985]. According to the model the N-terminal segment of cystatin which is more flexible bridges over the active site Cys 25 of papain without completely burying it and additionally the side chain of Leu 8 binds to S2 subsite of papain which determines the substrate specificity of papain [Asboth et al., 1988]. This was supported by Brzin et al. [1984] who demonstrated that the truncated form of HCC starting with Leu-Val before Gly-11 (corresponding to Gly-9 of chicken cystatin) has virtually the same affinity for papain as the full length form whereas the truncated form starting with Gly-12 has been reported to show 1000 fold weaker inhibition [Abrahamson et al., 1987a]. However, Nycander and Bjork [1990] emphasized the role of Trp-104 in the inhibition of CP. According to their model, Trp-104 of cystatin interacts primarily with two Trp side chains in the active side cleft of papain, Trp 177 and Trp 181, in such a manner that the indole ring of Trp-104 stacks on the side chain of Trp 177 and the edge lies on the indole ring of Trp 181. A two step mechanism of inhibition of the lysosomal CP cathepsin B by its endogenous inhibitor cystatin C was observed by Nycander et al. [1998]. An initial weak interaction in which N-terminal of the inhibitor binds to the proteinase is followed by a conformational change. Subsequently, the occluding loop of the proteinase that partially obscures the active site is displaced by the inhibitor bringing about another conformational change. The presence of occluding loop of cathepsin B renders it much less susceptible to inhibition by cystatin than other proteinases. A similar two step binding of cystatin A to CP was suggested by Estrada and Bjork [2000].

The flexible N-terminal region of the cystatin binds independently to the target proteinases after the binding of hairpin loops. It is interesting to note that the replacement of the three N-terminal residues preceding the conserved Gly of stefin A by the corresponding 10-residues long segment of cystatin C increased the affinity of the inhibitor for cathepsin B by about 15-fold [Pavlova and Bjork, 2003], suggesting that the inhibitory potency of cystatin can be substantially improved by protein engineering. The crystal structure of human stefin A-porcine cathepsin H complex showed small distortion of the structure upon formation of the complex [Jenko et al., 2003]. In addition to the structurally derived data, the contribution of the individual residues within proteinase binding region of cystatins was additionally investigated by mutational analysis and kinetic studies performed by several different groups [Pol and Bjork, 2001; Auerswald et al., 1994; Estrada et al., 1999; Pavlova et al., 2000].

1.8 BIOLOGICAL ASPECTS AND PATHOPHYSIOLOGY OF CYSTATINS

Proteinases and their natural inhibitors may co-exist at different levels of cellular evolution. Disturbing the harmony of the normal balance of enzymatic activities of proteinases and their natural inhibitors may lead to severe biological effects.

Cystatins constitute a powerful regulatory system for endogenous CPs which are often secreted or leaked from the lysosomes of dying and diseased cells [Ekiel et al., 1997]. Besides regulation of the enormous hydrolytic potential of CPs, plethora of actions has now been ascribed to cystatins. They are known to play important roles in various pathophysiologic conditions such as sepsis [Assfalg-Machleidt et al., 1988], cancer [Cox, 2009], rheumatoid arthritis [Trabandt et al., 1991], purulent bronchiectasis [Buttle et al., 1990], multiple sclerosis [Bever and Garver, 1995], muscular dystrophy [Sohar et al., 1988], etc. which indicate that a tight enzyme regulation by cystatin is a necessity in the normal state.

Cystatins and cancer: Cathepsins involved in the degradation of extracellular matrix facilitate the growth, invasion and metastasis of tumour cells and also in tumour angiogenesis [Gocheva and Joyce, 2007; Mohamed and Sloane, 2006; Turk et al., 2004; Vasiljeva et al., 2006]. A broad spectrum of cysteine proteinase inhibitor was shown to inhibit tumour angiogenesis [Joyce et al., 2004].

Generally, cathepsin to cystatin ratio is found to be increased in most tumour types compared to normal tissues [Paraoan et al., 2009; Rivenbark and Coleman, 2009]. Elevated TPI level in various tumour types have been correlated to better prognosis like, stefin A positive breast cancer patients are less likely to develop distant metastasis [Parker et al., 2008], stefin A and B in non small cell lung cancer [Werle et al., 2006], cystatin SN is upregulated in gastric cancer [Choi et al., 2009], cystatin C [Sokol and Schiemann, 2004], cystatin M [Zhang et al., 2004], cystatin F [Utosunomiya et al., 2002], were found to be expressed in epithelial and mesenchymal tumour cells. Cystatin M is often hailed as tumour suppressor.

Stefin A and cystatin C overexpression has been shown to inhibit cancer cell invasion and metastasis [Li et al., 2005; Kopitz et al., 2005]. Cystatins may also inhibit cell migration by interfering with cell signalling pathways, by direct cathepsin and calpain inhibition [Cox, 2009]. Cathepsins B, L and S promote tumour growth in a

murine model of pancreatic tumourigenesis [Gocheva et al., 2006]. The tumour microvascular density declined by about half in pancreatic tumours in cathepsin B or cathepsin S null mice. Significant increases in apoptosis were also noted in cathepsin B, L and S null pancreatic tumours.

Cystatins and neurodegeneration: Though CPs are implicated in various pathologies of brain, there are only few studies concerning the role of cystatins in pathologies of brain. Only two genetic diseases are known in which mutations in cystatin C and stefin B are associated with disease status, **Hereditary cystatin C amyloid angiopathy (HCCAA)** the first human disorder known to be caused by deposition of cystatin C amyloid fibrils in walls of brain arteries leading to single to multiple strokes with fatal outcomes [Jensson et al., 1987]. The amyloid deposited is composed mainly of the Leu 68 Gln variant of cystatin C [Wei et al., 1998] and is associated with mutation in cystatin C gene [Palsdottir et al., 2006]. Normal cystatin C may protect pathogenesis of Alzheimer's disease by binding to soluble amyloid-β-peptide and preventing its deposition [Mi et al., 2007].

Progressive myoclonus epilepsy [EPM1] is exhibited by a group of inherited diseases characterized by myoclonic seizures, generalized epilepsy and progressive neurological degeneration caused by mutations in cystatin B gene (in the conserved QVVAG region) [Pennacchio et al., 1997; Joensuu et al., 2007].

Cystatins and cell death: Cystatins are shown to be involved in normal cell apoptosis, and most dramatically in selective tissue type for example in EPM1 [Lieuallen et al., 2001]. In fibrosarcoma cells, cystatins regulate cell death in response to TNFα [Foghsgaard et al., 2001]. An elevated cystatin C/cathepsin B ratio was found to be associated with chemoresistance in non-small cell lung carcinoma patients [Petty et al., 2006]. Intracellular cystatins normally inhibit low level lysosomal leakage. High cystatin levels are expected to be protective for general cathepsin mediated cell death.

Cystatins and immunomodulation: Cystatins have emerged as effector molecules of immunomodulation [Zavasnik-Bergant, 2008]. They can stimulate nitric oxide release from macrophages [Verdot et al., 1999]; modulate respiratory burst and phagocytosis in neutrophils [Leung-Tack et al., 1990]; and interleukin, cytokine

production in T-cells and fibroblasts [Schierack et al., 2003; Kato et al., 2002; 2004]. Most of these functions operate via putative cell surface cystatin-binding molecules or membrane domains [Kato et al., 2002]. Cystatin C has been shown to be a TGFβ receptor antagonist and TGFβ signalling pathway blocker [Sokol and Schiemann, 2004; Sokol et al., 2005]. Type 2 cystatins are also known to increase interleukin-6 expression in fibroblasts and splenocytes [Kato et al., 2000]. Cystatin C is a potent, reversible inhibitor in vitro of the human lysosomal CPs e.g., cathepsin S (Ki = 8 pM), cathepsin L (Ki = 8 pM) and cathepsin H (Ki = 220 pM). These proteinases are located all along the endocytic pathway of dendritic cell and are involved in the controlled proteolysis associated with the degradation of antigenic peptides [Pluger et al., 2002]. Cystatin F by targeting cathepsin C is known to regulate diverse immune cell effector functions [Hamilton et al., 2008].

Cystatins as antimicrobial and antiviral agents: Horse-shoe crab hemocyte cystatin has antimicrobial activity against Gram negative bacteria with IC50s against *S. typhimurium*, *E. coli* and *K. pneumoniae* in the 80-100 μg/ml range [Agarwala et al., 1996]. Both chicken and human cystatins were found to inhibit the growth of *P. gingivalis* with an IC50 of 1.1 and 1.2 fM, respectively [Blank et al., 1996]. Cystatin C is also an effective inhibitor of replication of coronavirus [Collins and Grubb, 1998]. Sialostatin L displays anti-inflammatory role and inhibits proliferation of cytotoxic T-lymphocytes [Kotsyfakis et al., 2006].

Cystatin C in clinical diagnostics: Cystatin C was the first protein to be used in clinical diagnostics. Levels of cystatin C in various body fluids is used as a barometer of disease [Shah and Bano, 2009]. Recent studies indicate that it is a better marker of glomerular filtration rate and is a stronger predictor of cardiovascular disease and mortality than serum creatinine [Fried, 2009]. Cystatin C levels can also be used to reflect the characteristics of peritoneal membrane in dialysis patients [Al-Wakeel et al., 2009]. Korolenko et al. [2008] recently found that serum cystatin C concentration can be used as one of the prognostic criteria in patients with several kinds of hemoblastoses. IL-6 levels along with that of cystatin C may be regarded as markers of increased osteoblastic activity associated to bisphosphate treatments in prostrate cancer patients with bone metastases [Tumminello et al., 2009]. Yang et al. [2009] found that its levels decrease significantly in cerebrospinal fluids of patients with

Guillain-Barre syndrome and may be involved in its pathophysiology. Cystatin B was found to be specifically over expressed in most hepatocellular carcinomas and alone or in combination with α-fetoprotein may be a useful marker for diagnosis of the diseases [Lee et al., 2008].

Role of cystatins in other diseases: Cystatins are now known to participate in neuronal differentiation [Taupin et al., 2000]. Numerous studies have demonstrated that cathepsin K, L and S are involved in elastic fibre degradation, associated with the development of different pathological conditions of cardiovascular system. Elastinolytic activities of cathepsin K, L and S can be blocked by cystatins [Novinec et al., 2007]. Equistatin is known to inhibit the growth of the red flour beetle *Triboleum castaneum* [Oppert et al., 2003], suggesting to be promising candidate for the transgenic seed technology to enhance seed resistance to storage pests. Heparin binding and cell-binding domain 5 (light chain) of H-kininogen has antibacterial acitivity against *E. coli*, *P. aeruginosa* and *Enterococcus faecalis* [Andersson et al., 2005]. Bradykinin induces dendritic cell maturation and can modulate innate or adaptive immunity [Aliberti et al., 2003; Scharfstein et al., 2007]. Cystatin C appears to be up-regulated in response to injury in the brain [Shah and Bano, 2009]. Cystatin M/E is a key molecule in a biochemical pathway that controls skin barrier formation by the regulation of both crosslinking and desquamation of stratum corneum [Zeeuwen et al., 2009]. Lower cystatin C level is also implicated in retinal degeneration in (rd1) mouse model of retinitis pigmentation [Ahuja et al., 2008]. An imbalance in cathepsin B/cystatin C level may contribute to the progression of pelvic inflammatory disease [Tsai et al., 2009]. There are many other diseases with decreased cystatin levels, such as inflammatory diseases, osteoporosis, arthritis, and diabetes as well as a number of other neurodegenerative diseases [Turk et al., 2008].

1.9 PANCREAS

Pancreas, the capital of proteolytic power, plays important role in digestion and in maintenance of glucose homeostasis in body. A soft lobulated, greyish-pink gland, 12-15 cm long (in humans), it extends nearly transversely across the posterior abdominal wall, behind stomach, from duodenum to spleen. The pancreas is composed of two separate types of glandular tissue [Fig. 7], main mass of which is exocrine, embedded in which are clusters of endocrine cells constituting pancreatic

Fig. 7 Anatomy of pancreas

Adopted from McGraw Hills Access medicine, The McGraw Hill Companies Inc., www.accessmedicine.com

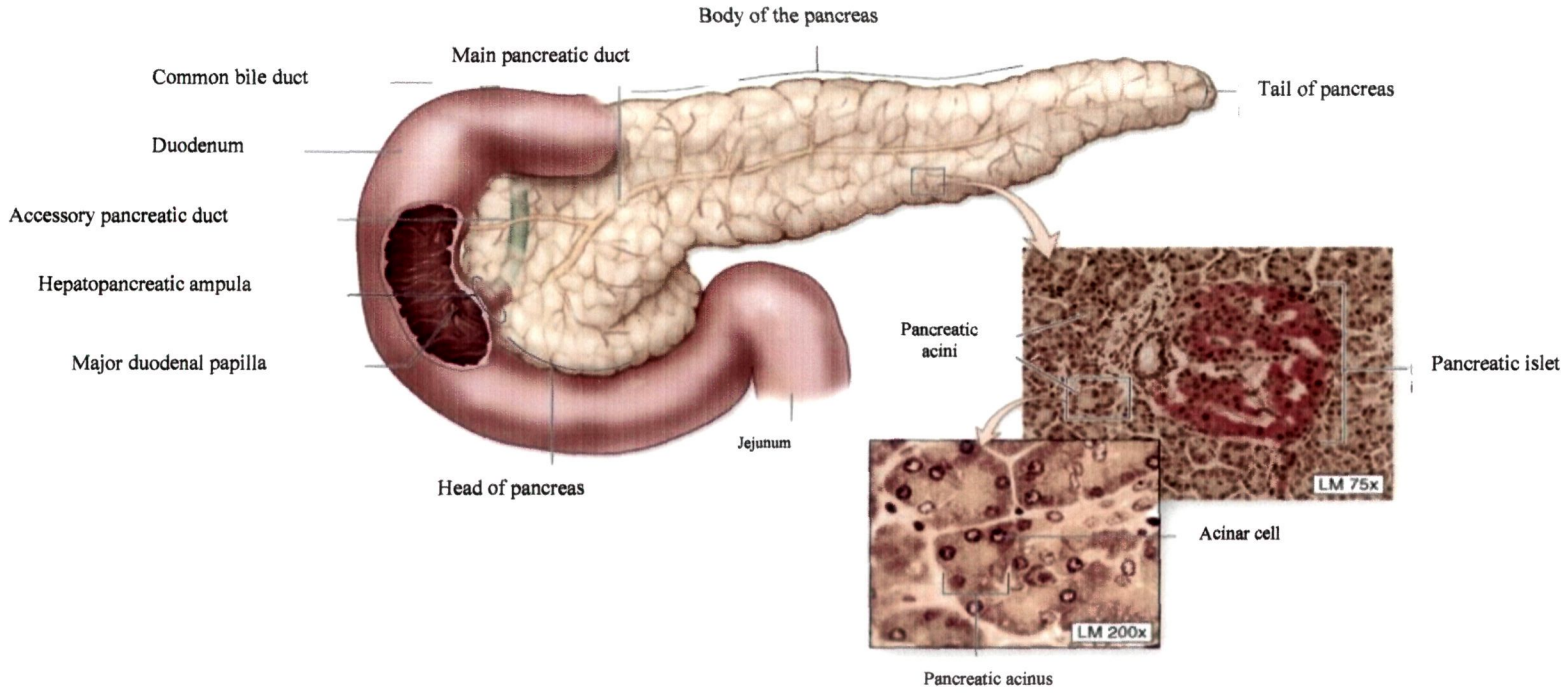
Body of the pancreas
Main pancreatic duct
Common bile duct
Duodenum
Accessory pancreatic duct
Hepatopancreatic ampula
Major duodenal papilla
Tail of pancreas
Pancreatic acini
Pancreatic islet
LM 75x
Acinar cell
LM 200x
Pancreatic acinus
Jejunum
Head of pancreas

islets. The exocrine part of pancreas is a lobulated, branched, acinar gland [Beck and Sinclair, 1971]. The acinar cells are zymogenic containing secretory granules laden with powerful enzymic constituents of pancreatic secretion. The endocrine pancreas consists of pancreatic islets (of Langerhans) spheroidal or ellipsoidal clusters or solitary or randomly embedded in the exocrine part of the pancreas [Heitz et al., 1976]. The islets contain three major types of cells, alpha [glucagon secreting; Baum et al., 1962], beta [most abundant and insulin secreting; Lacy and Davies, 1957] and delta [somatostatin secreting; Orci et al., 1975] cells. In addition, PP cell is also present in pancreas secreting hormone pancreatic polypeptide [Buffa et al., 1977].

Two major functions of the pancreas are release of insulin and glucagon in response to body glucose levels indirectly regulating protein, carbohydrate and lipid metabolism and acting as a switch between carbohydrate and lipid metabolism. Dysregulation of insulin and glucagon production causes diabetes mellitus, hyperinsulinism and hyperglycemia, respectively. Pancreatic acini secrete digestive enzymes and large volumes of sodium bicarbonate responsible for digestion of all three major food types- proteins, carbohydrates and fats. The proteolytic enzymes of the pancreatic juice are secreted in their zymogenic form.

1.10 PROTEIN UNFOLDING STUDIES

Proteins are synthesized as a linear chain of amino acids which in order to become biologically active must fold and adopt one out of an enormous number of possible conformations. This conformation referred to as native state, exists in solution as a very compact and highly ordered structure. Under physiological conditions the native (folded) and the denatured (unfolded) states of a protein are in equilibrium and the free energy change, ΔG, for the equilibrium reaction

$$\textbf{Native (N)} \rightleftharpoons \textbf{Denatured (D)}$$

is referred to as the conformational stability of a protein. The determinants of native state stability in aqueous solutions are the amino acids sequence of protein as well as the variable conditions of pH, temperature, and the concentration of salts and ligands [Alber, 1989; Pace, 1990]. Although the native conformation is essential for activity, the conformational stability is remarkably low. The native state of most naturally occurring proteins is only about 5-15 kCal/ mol more stable than its unfolded conformations [Pace, 1975]. The conformational stability of proteins (monomeric or

multimeric) can be measured by equilibrium unfolding studies using guanidine hydrochloride (GdnHCl) or urea [Pace, 1986], the two agents commonly employed as protein denaturants. Analysis of the solvent denaturant curves using these denaturants can provide measure of the conformational stability of protein [Pace, 1986; Yao and Bolen, 1995]. Protein unfolding/folding studies in GdnHCl and urea solutions have focused on the identifications of equilibrium and kinetic intermediates [Kim and Baldwin, 1990; Jaenicke, 1987]. Equilibrium denaturation studies using physical/chemical denaturants have been very useful in understanding the structure, stabilization and folding of small monomeric proteins [Tanford, 1968; Pace, 1986; 1990]. Lately, these techniques have been applied to oligomeric proteins also [Neet and Timm, 1994; Prakash et al., 2002; Akhtar et al., 2002]. Though inter- and intrasubunit reactions in oligomeric and monomeric proteins are of same physical nature, the denaturation/renaturation reactions in oligomeric proteins are more complex, usually multiphasic processes with stabilized partially folded intermediates Jaenicke and Lilie, 2000; Hornby et al., 2000], occurring either by sequential or concerted mechanisms [Jaenicke, 1987; Seckler and Jaenicke, 1992].

With dimeric (or oligomeric) proteins additional modes of stabilization are available at the quaternary structural level. A general three-state model of the equilibrium dissociation and unfolding of the dimeric protein involving native dimer (N_2), native monomer (N) or a monomeric intermediate (I) and denatured monomer (D) is described by following equation

$$\mathbf{N_2 \rightleftharpoons 2N \rightleftharpoons 2D} \quad \text{or} \quad \mathbf{N_2 \rightleftharpoons 2I \rightleftharpoons 2D}$$

Completely unfolded dimers (D_2) are not likely to exist, but evidence for partially unfolded dimeric intermediates (I_2) is reported [Blackburn and Noltmann, 1981]. The compact monomeric intermediate structure may not be identical to the conformation of the subunits in the native dimer, but some native-like secondary or tertiary folding may exist e.g. denaturation of superoxide dismutase [Mei et al., 1992], glutathione-S-transferase [Sacchetta et al., 1993], etc. Dimeric proteins can follow a 2-state transition, $\mathbf{N_2 \rightleftharpoons 2D}$, where N_2 is native dimer and D is the denatured monomer. The 2-state model implies that the native monomer (or a monomeric intermediate) does not exist at significant concentration at equilibrium i.e. the quaternary interactions are necessary for stabilization of the folded monomeric state. Two-state denaturation of dimeric proteins have been reported for Arc repressor [Milla and Sauer, 1994], SIV

protease [Grant et al., 1992], HIV protease [Grant et al., 1992], repressor of primer [Steif et al., 1993], neurotrophin-3 and neurotrophin-4/5 [Timm et al., 1994], etc.

The midpoint of thermal [Pakula and Sauer, 1989] or chemical [Bowie and Sauer, 1989b] denaturation transition can also be computed from the denaturation curves and can be used to compare 2 different proteins or a single protein behaving differently under the effects of different denaturing conditions. There are various reports available which have shown different effects of GdnHCl and urea on protein unfolding like mushroom tyrosinase which shows different behaviour towards GdnHCl, urea and SDS in terms of different transition processes for these denaturants [Park et al., 2003]. Behaviour of human placental and goat lung cystatins towards these denaturants was also found to be different in terms of midpoint of transition and presence of intermediate states [Rashid et al., 2005; Khan and Bano, 2009b].

Increasing inclination in protein folding/unfolding is due to the recognition that failure of cellular protein folding mechanisms is associated with a variety of important human disorders ranging from cystic fibrosis to Alzheimer's disease. There is a growing body of evidence indicating a critical role for partially folded protein conformers in the process of conversion of normal cellular proteins into disease causing, proteinase-resistant protein aggregates of various morphologies [Kelly, 1998; Dobson, 2004].

1.11 AMYLOID FIBRIL FORMATION

Amyloidogenesis is the aggregation of soluble proteins into structurally conserved fibers. Amyloid fibers are distinguished by their resistance to proteinase K and detergent, tinctorial properties and β-sheet rich secondary structure [Hammer et al., 2008]. Amyloid formation is a hallmark of many human diseases like Alzheimer's [Gotz et al., 2009], diabetes mellitus [Engel et al., 2008], autosomal hereditary systemic amyloidosis [De Felice, 2004], prions diseases and more than 20 different human disorders like, HCCAA, Parkinson's disease, Huntington's disease, etc. [Merlini and Bellotti, 2003]. Amyloid fibres are incredibly stable β-sheet rich structures that many proteins can form [Smith et al., 2006; Holm et al., 2007].

The ability to fibrillate is independent of the original native structure of protein [Khurana et al., 2003] and overall yield and stability of the fibrils [Hortscansky et al., 2005]. This led Dobson and coauthors to propose that amyloid-fibril formation is a generic property of proteins [Dobson, 1999; Fandrich et al., 2001]. Fibrillation

generally starts from an intermediate state, either partially unfolded or partially folded, molten globule or native like intermediate [Rochet and Lansbury, 2000]. In case of globular proteins such as cystatin C [Ekiel and Abrahamson, 1996], stefin B [Zerovnik et al., 2007], partial unfolding and in case of unfolded polypeptides such as α-synuclein [Uversky et al., 2001] and islet amyloid peptide partial folding is must. In vitro, variation of solvent conditions by changing pH or adding organic solvents can lead to partial unfolding and subsequent protein fibril formation. With unfolded polypeptides, partial folding can be obtained by lowering pH or by heating. In vivo, partial unfolding may happen as a consequence of lowered protein stability due to mutation, local change in pH in membranes, oxidative and heat stress, whereas partial folding may happen on exposure to environmental hydrophobic substances, such as pesticides [Uversky et al., 2001].

Amyloidogenic conformation and common structural traits of fibrils

Ordered fibrillar aggregates and the amyloid-fibrils can be studied at lower resolution by transmission electron microscopy (TEM), atomic force microscopy (AFM) [Goldsbury et al., 1997; Ding and Harper, 1999], cryo-electron microscopy, X-ray diffraction and solid state NMR. Common features of the fibrils are [Serpell, 2000a], β-strands (separated by 4.7 Å) running perpendicular to the long axis of the fibrils and β-sheets extending parallel to the axis. The β-strands form a β-helical twist with usual repeat at every 115 or 250 Å [Serpell, 2000a]. There are two main types of fibrils, type 2 are built from two intertwined filaments, with a diameter from 80-130 Å. Type 1 fibrils are thinner and are formed from one filament only. There are other types of fibrils for e.g., a fibril and untwisted filaments of human stefin B [Zerovnik et al., 2002a]. The fibrils generally consist of 2-6 protofilaments, each ~2-5 nm in diameter, that generally twist together to form fibrils that are typically 7-13 nm wide [Serpell et al., 2000b]. The fibrils have the ability to bind specific dyes such as thioflavin T (ThT) and congo red (CR) [Krebs et al., 2005; Klunk et al., 1999].

Kinetic basis of fibrillogenesis

Fibrillogenesis often starts with dimers as building blocks which oligomerize to tetramers, octamers etc., constituting the prefibrillar aggregates composed of fluid nuclei [Lomakin et al., 1996]. From these, protofibrils grow upto 200 nm in length and are slightly curved [Lomakin et al., 1996]. All these species accumulate in the lag

phase which is followed by an exponential growth phase in which protofibrils merge into filaments. Fully made fibrils are then made from filaments added laterally or by end to end [Aggeli et al., 2001]. Thioflavin T fluorescence is generally used to follow kinetics of fibril formation [Sabate and Saupe, 2007]. Addition of preformed fibrils (seeding) is known to speed up the process of fibrillation [Jenko et al., 2004]. These events are depicted in figure 8. Several amyloidogenic proteins form domain swapped dimers like cystatin C [Janowski et al., 2001], human stefin A [Staniforth et al., 2001], stefin B [Skerget et al., 2009]. It has been proposed that domain swapped dimers could lead to higher oligomerisation and amyloid fibrillization [Liu et al., 2001].

Fibrillogenic cystatins

Cystatins are prone to form amyloids [Morgan et al., 2008; Turk et al., 2008]. Human cystatin C is highly amyloidogenic protein. The fibril formation is also known to occur in chicken cystatin [Staniforth et al., 2001], stefin B under in vitro conditions [Zerovnik et al., 2007], stefin A [Jenko et al., 2004], latexin [Pallares et al., 2007], CRES protein [von Horsten et al., 2007]. In the case of HCC the oligomers and fibrils are formed by propagated domain swapping. This model is not compatible with stefin B, in which proline (Pro) isomerization is important in preventing steric clashing [Morgan et al., 2008]. Trans to cis isomerization of Pro 74 is involved in formation of stefin B dimers. Since this Pro is widely conserved in cystatin superfamily its isomerization can play role in amyloidogenesis [Jenko-Kokalj et al., 2007].

Protein fibrillation: connection to pathophysiology and disease

About 20 human proteins have been found in proteinaceous deposits in various conformational diseases [Zerovnik, 2002]. There is absence of any sequence or structural homology in these proteins, but a common event is thought to be a conformational change leading to lack of biological function or gain of toxic activity, and possibly formation of amyloid fibrils. Co-localization of protein aggregates with degenerating tissue and association of their presence with disease symptoms indicate the involvement of amyloid deposition in the pathogenesis of conformational diseases [Soto, 2001]. Amyloid cytotoxicity appears to be associated with prefibrillar aggregated states either because of their ability to permealize cell membranes to general ion flux [Ceru et al.; 2008; Rabzelj et al., 2008] or because the rather diffuse hydrophobic surface may catalyze unwanted reactions [Bucciantini et al., 2004].

Fig. 8 Properties of amyloid polymerization

(A) A graphic representation of amyloid fiber polymerization displaying nucleus dependent kinetics (black line). Preformed amyloid fibers can act as seeds to speed the kinetics of fiber polymerization (grey line). This process eliminates the lag phase associated with nucleus formation.

(B) Model of amyloid fiber polymerization. A build up of monomer occurs which leads to the formation of multimers and finally the amyloid fiber end product. Large arrows represent processes that are energetically favourable while small arrows represent energetically unfavourable processes.

Adopted from Hammer et al. *J Alzheimers Dis* 2008; 13:407-419.

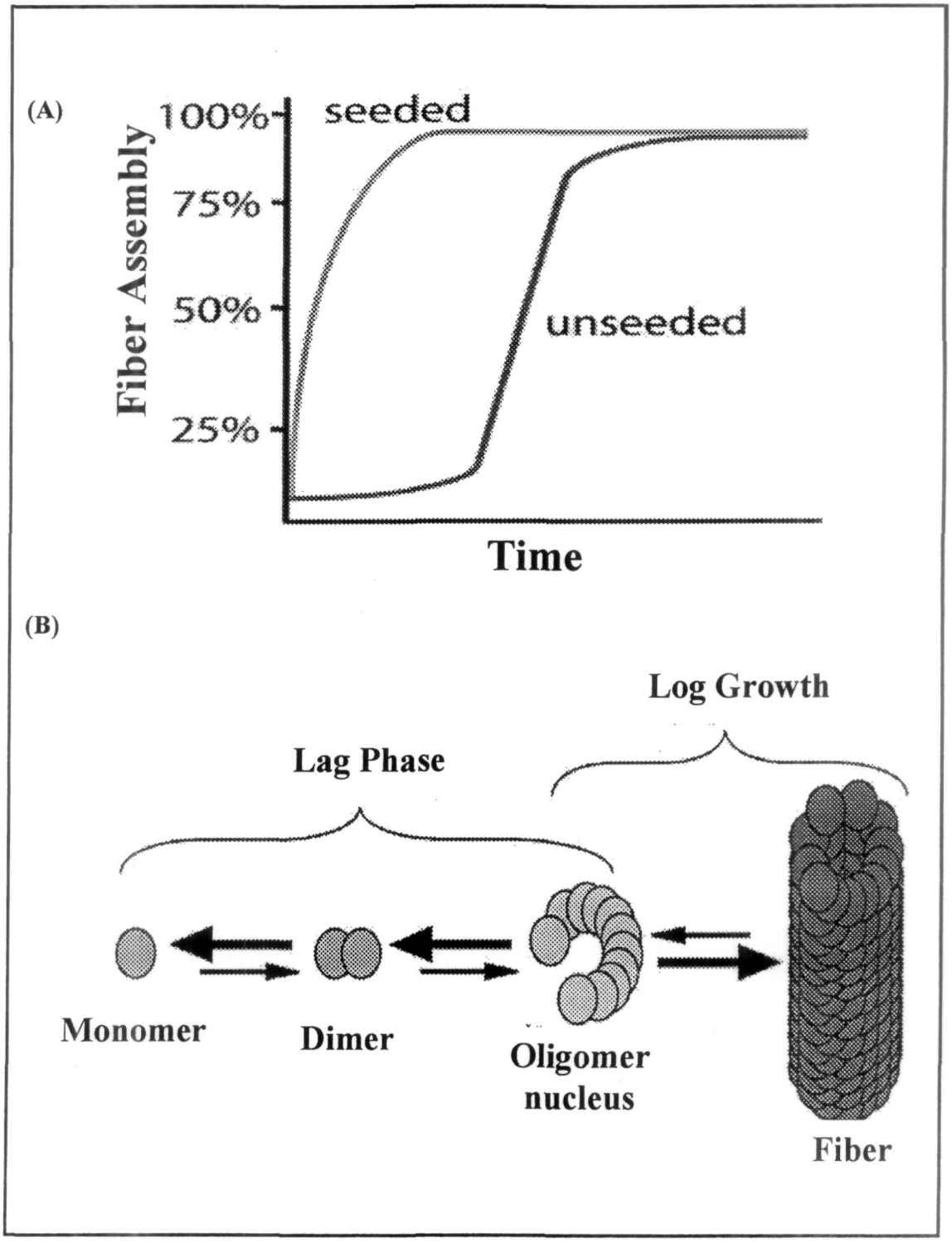
(A)
100%
75%
50%
25%
Fiber Assembly
seeded
unseeded
Time
(B)
Log Growth
Lag Phase
Monomer
Dimer
Oligomer
nucleus
Fiber

Anti-amyloidogenic and fibril destabilizing agents

A number of agents are employed with the aim to either inhibit or reverse the conformational change, or to dissolve the smaller aggregates and disassemble the amyloid fibrils. Few such approaches include 'β-sheet breakers' or 'mini-chaperones' [Soto, 2001], nicotine and melatonin [Findeis, 2000], apomorphine [Lashuel et al., 2002], various antibiotics [Zerovnik, 2002]. There are controversial reports on the inhibitory effects of metal ions on amyloid fibril formation. Recently, it was shown by Raman et al. [2005] and Zerovnik et al. [2006] that binding of Cu^{2+} and Zn^{2+} but not Fe^{3+} to amyloid-β-peptide retards amyloid fibril formation and Cu^{2+} binding to stefin B inhibits amyloid fibrillation. Contrarily, promotion of aggregation and fibrillation by presence of Cu^{2+} has been shown for prion protein [Brown et al., 1997], α-synuclein [Rasia et al., 2005], amyloid-β-protein [Atwood et al., 1998].

Recently, several natural compounds, like polyphenols, curcumin etc., have been demonstrated to remarkably inhibit the formation of fibrillar assemblies in vitro and their associated cytotoxcity [Riviere et al., 2008].

1.12 REACTIVE SPECIES MEDIATED PROTEIN DAMAGE

Radical mediated damage to proteins, initiated by electron leakage, metal-ion-dependent reactions and auto-oxidation of lipids and sugars results in production of protein hydroperoxides and aggregation or fragmentation of proteins. Damaged proteins are often functionally inactive and their unfolding is associated with enhanced susceptibility to proteinases.

Reactive species

Free radicals such as reactive oxygen (ROS) and reactive nitrogen species (RNS) are well recognised for playing a dual role as both deleterious and beneficial species [Valko et al., 2007]. Important physiological functions that involve free radicals or their derivatives are summarized in Table 4. Besides these, free radicals are also involved in ATP generation, apoptosis of effete or defective cells, production of prostaglandins and leukotrienes etc. [Devasagayam et al., 2004].

Nature has endowed cells with protective antioxidant mechanisms to neutralize and eliminate the harmful reactive species. However, oxidative stress can occur when there is a disturbance in the pro-oxidant/antioxidant systems in favour of the former

[Seis, 1985]. Overproduction of RNS is termed as nitrosative stress [Ridnour et al., 2004]. The uncontrolled oxidative stress initiates a series of harmful biochemical events associated with diverse pathological processes [Juranek and Bezek, 2005].

Reactive species are small molecules with an oxygen or nitrogen atom in their structure [Halliwell and Gutteridge, 2007]. These ROS and RNS can be free radicals with an unpaired electron [e.g. $^{\bullet}NO$ (nitric oxide radical), $O_2^{\bullet-}$ (superoxide radical) and $OH^{\bullet}$ (hydroxyl radical)] or non-radicals (e.g. H_2O_2). They can be anions [e.g. O_2^- (superoxide) and $ONOO^-$ (peroxynitrite)] or non-ions (e.g. H_2O_2, $^{\bullet}NO$, $OH^{\bullet}$).

Superoxide ($O_2^{\bullet-}$)

It is relatively innocuous, however, its reaction with other radicals like $^{\bullet}NO$ and iron clusters in some of the enzymes makes it the mother of potent reactive species collectively called as ROS. The mitochondrial respiratory chain is the most important site of $O_2^{\bullet-}$ generation [Turrens, 2003]. In biological tissues $O_2^{\bullet-}$ can be converted non-enzymically into non-radical species H_2O_2 and singlet oxygen [Steinbeck et al., 1993]. The electronic ground state of dioxygen is a triplet ($^3O_2$), having two unpaired electrons with same spin and hence a diradical, and a one-electron poor oxidant. Pairing these electrons in opposite spins give ***singlet oxygen*** **($^1O_2$)** a two electron potent oxidant. Singlet oxygen is produced in several physiological processes for e.g. by reaction of H_2O_2 and hypochlorous acid (HOCl) in neutrophils,

$$\mathbf{H_2O_2 + HOCl \longrightarrow {}^1O_2 + H_2O + HCl}$$

ROS has been implicated in etiology of various diseases [Droge, 2002; Halliwell and Gutteridge, 2007].

Riboflavin

It is an important constituent of our daily diet, present in free and conjugated forms in almost all biological tissues and fluids [Spector, 1980; Rose et al., 1986]. Flavins are known to photooxidize amino acids and effect the conformation of proteins [Joshi, 1985; Baba et al., 2004]. They are known to generate $^1O_2$, $OH^{\bullet}$, flavin triplet state, $O_2^{\bullet-}$ and H_2O_2 which can modify proteins and other biological macromolecules [Keynes et al., 2003; Cardoso et al., 2006].

Hydrogen peroxide

It is produced continuously in all cells and is often employed as a signalling molecule. Although not a free radical, it has a great physiological relevance because of its ability to penetrate biological membranes and to act like an intermediate in the production of more reactive oxygen species, namely hydroxyl radical and hypochlorous acid [Nordberg and Arner, 2001]. It does not readily oxidize most proteins, lipids or DNA but is cytotoxic at micromolar concentrations and has been implicated in number of diseased states [Pryor et al., 2006].

Nitric oxide ($^{\bullet}NO$)

It is a free radical endogenously produced in a variety of mammalian cells by both constitutive and inducible forms of nitric oxide synthase [Ghafourifar and Cadenas, 2005]. $^{\bullet}NO$ is an important mediator of a variety of diverse biochemical and physiological processes, like signal transduction, neurotransmission, smooth muscle relaxation, platelet inhibition, blood pressure modulation, immune system control, macrophage mediated cytotoxicity [Blaise et al., 2005]. Reactivity of $^{\bullet}NO$ as a free radical species is quite weak which combined with its lipophilicity allows it to be remarkably diffusible [Denicola et al., 2002]. In vivo, this diffusion is largely regulated by its reaction with haemoglobin [Liu et al., 1998]. $^{\bullet}NO$ is a mother to a family of reactive compounds, collectively called RNS [Table 5]. Their production and pathophysiological effects are represented in Fig. 9. $^{\bullet}NO$ can also react with $O_2^{\bullet-}$ to give peroxynitrite. $^{\bullet}NO_2$ can also react with $O_2^{\bullet-}$ giving peroxynitrate, a more powerful oxidant than peroxynitrite. Biological oxidations by peroxynitrate could result either directly or by its decomposition products [Pryor et al., 2006].

$$\underset{\text{(Nitrogen dioxide)}}{^{\bullet}NO_2} + \underset{\text{(Superoxide radical)}}{O_2^{\bullet-}} \longrightarrow \underset{\text{(Peroxynitrate)}}{O_2NOO^-}$$

$$\underset{\text{(Peroxynitrate)}}{O_2NOO^-} \longrightarrow \underset{\text{(Singlet oxygen)}}{^1O_2} + \underset{\text{(Nitrate)}}{NO_2^-}$$

Peroxynitrite can react with carbon dioxide generating nitrosoperoxocarboxylate (NPC), another potent protein damaging agent [Tien et al., 1999]. Overproduction of $^{\bullet}NO$ can mediate toxic effects, e.g., DNA fragmentation, cell damage and neuronal

TABLE 4: IMPORTANT PHYSIOLOGICAL FUNCTIONS THAT INVOLVE FREE RADICALS OR THEIR DERIVATIVES[a]

Type of Radical	Source of Radical	Physiological Process
Nitric oxide ($^{\bullet}NO$)	Nitric oxide synthase	Smooth muscle relaxation (control of vascular tone) and various other cGMP dependent functions
Superoxide ($O_2^{\bullet-}$) and related ROS	NAD(P)H oxidase	Control of ventilation Control of erythropoietin production and other hypoxide inducible functions *Smooth muscle relaxation* Signal transduction from various membrane receptors/enhancement of immunological functions
Superoxide ($O_2^{\bullet-}$) and related ROS	Any Source	Oxidative stress responses and the maintenance of redox homeostasis

[a]Adopted from Droge [2002].

TABLE 5: NITROGEN OXIDES IMPLICATED IN THE BIOLOGICAL SEQUEL OF NITRIC OXIDE FORMATION

Nitrogen Oxide	Common Name	Reactivity and Reaction Types	Substrates
$^{\bullet}NO$	Nitric Oxide	Weak nitrosylation	Transition metals, radicals, oxygen
NO^+	Nitrosonium	Moderate nitrosation	Thiols, amines
NO^-	Nitroxyl	Strong oxidation	Thiols, lipids, metals, oxygen, DNA
NO_2	Nitrogen Dioxide	Strong oxidation, nitration	Antioxidants, thiols, lipids
N_2O_3	Dinitrogen Trioxide	Strong nitrosation, oxidation	Thiols, amines, lipids, antioxidants
$ONOO^-$	Peroxynitrite	Strong nitration, nitrosation, oxidation	Lipids, tyrosine, phenylalanine, DNA, thiols, antioxidants
NO_2^+	Nitronium	Strong nitration	Tyrosine, amines, phenylalanine

Fig. 9 A schematic diagram of the conversion of nitric oxide (NO) to other nitrogen oxides

Hydrophilic interior of membranes will act as a lens to magnify the oxidation of NO to NO_2 or N_2O_3. The profound reactivity of these nitrogen oxides, as well as the formation of the highly cytotoxic peroxynitrite ($ONOO^-$), likely mediates cellular injury and tissue dysfunction in response to augmented NO production.

PARP (poly-ADP ribose polymerase); MMP (matrix metalloproteinase).

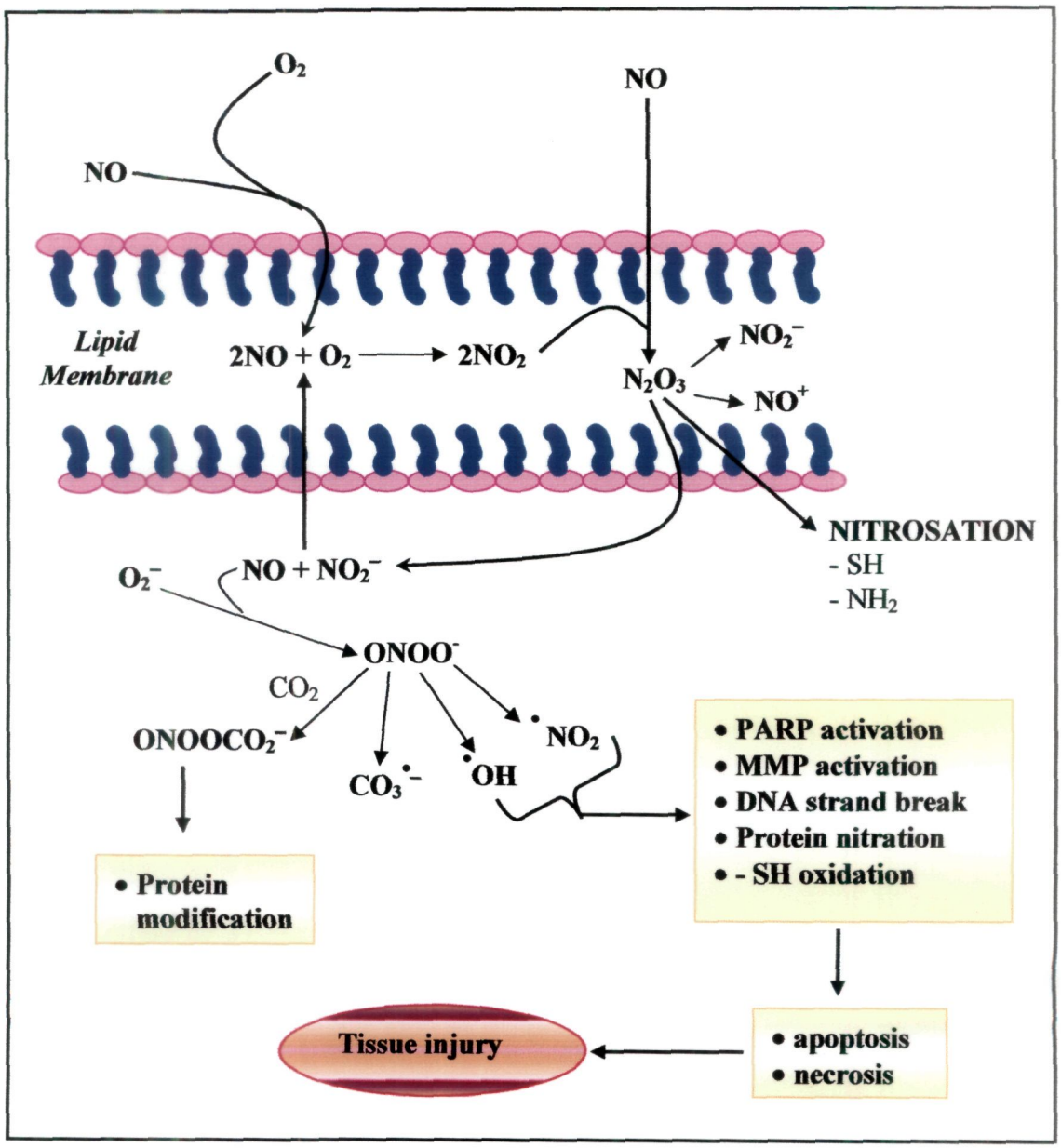
O_2
NO
NO
Lipid Membrane
$2NO + O_2 \rightarrow 2NO_2$
N_2O_3
NO_2^-
NO^+
NITROSATION
- SH
- NH_2
O_2^-
$NO + NO_2^-$
$ONOO^-$
CO_2
$ONOOCO_2^-$
$CO_3^{\bullet -}$
$^{\bullet}OH$
$^{\bullet}NO_2$
• PARP activation
• MMP activation
• DNA strand break
• Protein nitration
• - SH oxidation
• Protein modification
Tissue injury
• apoptosis
• necrosis

cell death [Dawson et al., 1992]. 'NO also shows neurotoxicity and act as pathological mediator in cerebral ischemia, epilepsy, Alzheimer's disease, Parkinson's disease and certain neurodegenerative diseases [Moncada et al., 1991] and it is also involved in toxicity associated with diabetes [Pacher et al., 2005] and pancreatitis [Chvanov et al., 2005].

Hypochlorous acid (HOCl)

One of the strongest physiological oxidants known, is produced in vivo at inflammation sites by enzymatic oxidation of chloride ions,

$$\underset{\text{(Hydrogen peroxide)}}{H_2O_2} + \underset{\text{(Chloride ion)}}{Cl^-} \xrightarrow{(MPO)} \underset{\text{(Hypochlorous acid)}}{HOCl} + \underset{\text{(Hydroxyl ion)}}{OH^-}$$

Where, MPO is enzyme myeloperoxidase.

It is estimated that between 25 and 40% of H_2O_2 generated by activated neutrophils is used to form HOCl [Babior, 2000]. An additional reaction of HOCl is with nitrite (NO_2^-) to form nitryl chloride (NO_2Cl), a reaction favoured with decreasing pH [Eiserich et al., 1998],

$$\underset{\text{(Hypochlorous acid)}}{HOCl} + \underset{\text{(Nitrite)}}{NO_2^-} + H^+ \longrightarrow \underset{\text{(Nitryl chloride)}}{NO_2Cl} + \underset{\text{(Water)}}{H_2O}$$

HOCl is a reactive chlorine species (RCS) capable of chlorinating protein tyrosine and oxidising many important biomolecules like DNA, collagen and ATPase, etc. and causing cell death [Winterbourn and Kettle, 2000; Jenner et al., 2002]. Nitryl chloride is capable of nitrating, chlorinating and dimerizing phenol compounds such as tyrosine [Eiserich et al., 1998].

Protein modification by reactive species

Free amino acids and amino acid residues in proteins are highly susceptible to oxidation by one or more reactive species (ROS/RNS/RCS) that (a) are present as pollutant in atmosphere (b) are generated as by products of normal metabolic processes and (c) are formed during exposure to X, γ, or UV radiations. Studies have shown that oxidation of proteins can lead to hydroxylation of aromatic groups and aliphatic amino acid side chains, nitration of amino acid residues, nitrosylation of sulphydryl groups, sulphoxidation of methionine residues, chlorination of aromatic

and primary amino groups, and conversion of some amino acid residues to carbonyl derivatives [Stadtman and Levine, 2003; Dean et al., 1997; Yan and Sohal, 2002; Davies et al., 1987a; 1987b; Peskin and Winterbourn, 2001]. The oxidation of proteins by reactive species can also lead to the cleavage of peptide bonds [Garrison, 1987; Uchida et al., 1990].

Exposure of proteins to free radicals causes (a) protein inactivation, e.g., of catalase and Mn superoxide dismutase by $^{\bullet}NO$ [Sigfrid et al., 2003; Castro et al., 2004], α2-macroglobulin by HOCl and H_2O_2 [Khan and Khan, 2004], goat lung cystatin by $^{\bullet}NO$ [Khan et al., 2009] and sheep plasma kininogen by ROS [Baba et al., 2004], etc. (b) protein aggregation, fragmentation or cross linking [Davies and Delsignmore, 1987; Hawkins and Davies, 1998; Chapman et al., 2003; Verzyl et al., 2000; Di Mascio et al., 2000].

Modestly oxidized proteins are usually more sensitive to proteolytic attacks by most proteinases [Davies et al., 1987b; Wolff and Dean, 1986] whereas heavily oxidized proteins have decreased susceptibility [Davies et al., 1987b] and can be a cause/consequence of certain diseased states like aging, atherosclerosis and neurodegeneration.

Vulnerability of pancreas to free radical damage

Pancreas is highly susceptible to free radical attack. Enzymatic antioxidant defence mechanisms of pancreatic β-cells are particularly weak [Cobianchi et al., 2008; Lenzen, 2008a] and can be overwhelmed by redox imbalance arising from overproduction of ROS/RNS. The consequence of this redox imbalance are lipid peroxidation, protein oxidation, DNA damage and interference of reactive species with signal transduction pathways which contribute significantly to β-cell dysfunction and death in Type 1 and Type 2 diabetes mellitus [Pacher et al., 2005; Lenzen, 2008b]. Quite similar is the case with acinar cells, mainly involved in the secretion and synthesis of digestive enzymes. There are numerous indications that ROS/RNS play a significant role in chronic and acute pancreatitis [Rau et al., 2000; Sandstrom et al., 2005; Shimizu, 2008]. Primary injury to acinar cells results in intracellular trypsinogen activation and inhibition of acinar cell secretion followed by ROS production leading to damage of biomolecules, membranes and activation of inflammatory cells which produce more ROS/RNS, responsible for acinar necrosis and amplification of the inflammation in pancreas. Furthermore, zymogen granules,

the most abundant organelle in acinar cells lack full set of scavenger characteristics of intact cells [Niederau et al., 1996] hence are liable to oxidative damage. The structural and functional impairment of these granules leads to leakage of trypsin and cell damage enhancement. Oxidative and nitrosative stress [Ischiropoulos et al., 2003; Ghafourifar et al., 1999] has been documented in pancreatic tissue by detection of ROS generation [Urunuela et al., 2002] and accumulation of products of ROS-mediated lipid peroxidation, protein oxidation and depletion of low molecular weight antioxidants [Rau et al., 2000].

Antioxidative and antinitrosative stress activities of caffeic acid, quercetin and curcumin: protection against free radicals

Knowledge about prevention of protein oxidation is cursory. Certain approaches attenuate the secondary radicals and confer cytoprotection [e.g. mesalamine against $ONOO^-$] but fail to affect the radical sinks [Sandoval et al., 1997].

Antioxidant agents of natural origin like polyphenols, flavonoids etc. have attracted special interest lately, because of their high efficacy and multifaceted health benefits [Ullah and Khan, 2008]. Several such natural components have proven to be beneficial in various disorders of pancreas like, curcumin against islet cell damage [Meghana et al., 2007; Kanitkar et al., 2008], quercetin against beta-cell damage [Kim et al., 2007; Coskun et al., 2005] and caffeic acid against pancreatic damage by free radicals [Lapidot et al., 2002].

Caffeic acid (3, 4-dihydroxycinnamic acid)

Caffeic acid (CA) [Fig. 10 (C)] is a naturally occurring phenolic compound found in many fruits, vegetables, and herbs including coffee [Gulcin, 2006]. It has antioxidant, anti-ischemia reperfusion, antithrombosis, antihypertension, antifibrosis, antivirus, antitumor and antidiabetic activities. It is known to quench superoxide and hydroxyl radicals, and RNS [Gulcin, 2006; Olmos et al., 2008; Takahama et al., 2009].

Quercetin (3, 3', 4', 5, 7-pentahydroxyflavone)

Quercetin [Fig. 10 (B)] is found bound to one or two glucose molecules (monoglycoside and diglycoside forms) as one of the most abundant dietary flavonoids in apples; black, green and buckwheat tea; onions; raspberries; redgrapes;

citrus fruits and other green leafy vegetables [Hertog and Hollman, 1996]. It has been shown in vitro to act as an antioxidant [Filipe et al., 2004], inhibit nitric oxide pathway [Mu et al., 2001], and have anti-inflammatory and anticancer activities [Wadsworth et al., 1999; Mertens-Talcott and Percival, 2005].

Quercetin and caffeic acid bear structural groups, responsible for direct scavenging of free radicals: o-dihydroxy structure in caffeic acid and in 'B' ring of quercetin and the 2, 3-double bond in conjugation with the 4-oxo function in the 'C' ring and 3- and 5-hydroxyl groups with 4- oxo function in the 'A' and 'C' rings of quercetin [Fig. 10].

Curcumin (diferuloyl methane)

Curcumin a bioflavonoid is the colouring pigment present in rhizomes of *Curcuma longa*. Curcumin has been shown to exhibit antioxidant, anti-inflammatory, antiviral, antibacterial, antifungal and anticancer activities and thus has a potential against various malignant diseases, diabetes mellitus, allergies, arthritis, Alzheimer's and other chronic illnesses [Sreejayan and Rao, 1997; Aggarwal et al., 2007; Dhillon et al., 2008]. Its polyphenolic structure with two ferulic acids linked via methylene bridge at the C atoms of the carboxyl groups [Fig. 10 (A)], double bonds in the alkene part of the molecule, hydroxyl groups of the benzene ring and central β-diketone allows it to directly scavenge free radicals like nitric oxide, ROS etc. [Sreejayan and Rao, 1997].

1.13 DRUG-PROTEIN INTERACTION: EFFECT OF PANCREATITIS CAUSING AND ANTIDIABETIC AGENTS

The binding and interaction of drugs with plasma and tissue proteins strongly affects their distribution, metabolism as well as pharmacodynamics and toxic properties. Accumulation of drug molecules at certain sites in the body causing a localized high concentration, adverse drug reactions [Wen and Ye, 1993] and ligand induced protein structure conformational changes [Takeda et al., 1988] are major problems complicating drug medical therapy. Therefore, studies analyzing the binding mechanism between proteins and drugs and the structure of resulting complexes are of particular interest. These works enable to elucidate how ligand affinity is regulated and how the protein conformation is altered upon complexation. Acute pancreatitis, an autodigestive disorder, typically presents as an acute inflammation of the pancreas.

Fig. 10 Chemical structures of A) Curcumin B) Quercetin C) Caffeic acid

(A) Curcumin

Chemical structure

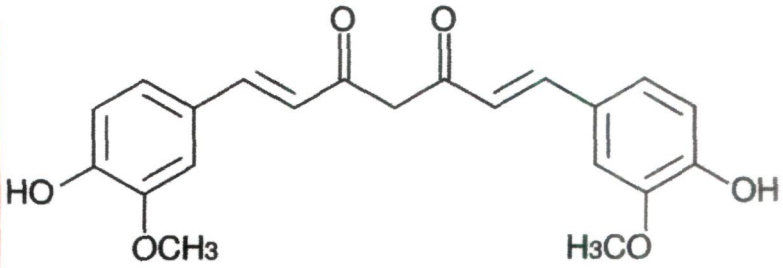

(B) Quercetin

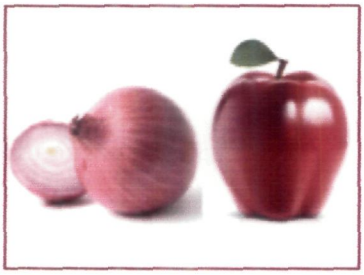

Chemical structure

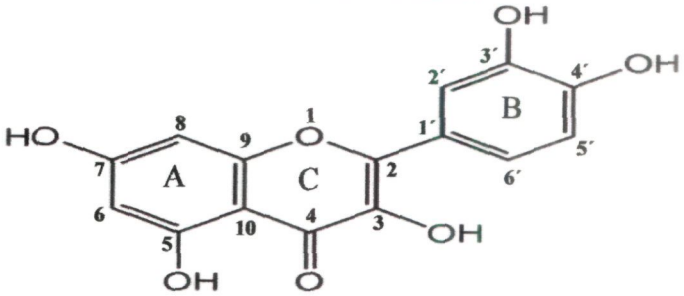

(C) Caffeic Acid

Chemical structure

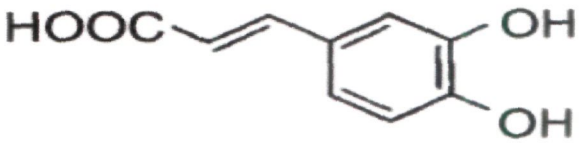

Gallstones and heavy alcohol are major causes of this condition besides hypertriglyceridemia, hyperparathyroidism, pancreatic tumors and surgery [Greenberger and Toskes, 2006]. Many frequently prescribed drugs are suspected to cause acute pancreatitis (AP), referred to as drug induced pancreatits (DIP), accounting for atleast 2-5% of reported cases of AP. Drugs commonly associated with pancreatitis belong to several classes, like antimicrobials, anti-inflammatory, antineoplastic, immunomodulating and cardiovascular agents and antiepileptic drugs (valproic acid, marketed generally as its sodium salt, sodium valproate) [Trivedi and Pitchumoni, 2005]. The mechanism of DIP is not clear. However, it may be caused by direct toxicity of drugs or by drug induced indirect mechanisms like ischemia, intravascular thrombosis and increased viscosity of pancreatic juices. One hallmark of AP is cathepsin B mediated trypsinogen activation [Halangk and Lerch, 2000] and oxidative/nitrosative stress [Shimizu, 2008]. Valproic acid has been categorised as class I medications associated with AP [Trivedi and Pitchumoni, 2005].

Valproic acid

Valproic acid (VPA, 2-propylpentanoic acid/ Sodium 2-propyl pentanoate), an 8-carbon branched chain fatty acid [Fig. 11 (A)] is an established drug for the treatment of epileptic seizures and mania in bipolar disorder [Bowden and Singh, 2005]. VPA is an emerging anticancer drug too [Kostrouchova et al., 2007]. However, it is one of most incriminate drugs causing AP besides being classified as teratogen [Norgaard et al., 2006; Gerstner et al., 2007; Werlin and Fish, 2006]. Other side effects of VPA include fatal hepatotoxicity, hyperammonemic encephalopathy and coagulation disorders [Gerstner et al., 2007]. No relationship between the occurrence of pancreatitis and duration of VPA therapy, dosage and serum level has been documented [Werlin and Fish, 2006]. Research indicates that VPA's cytotoxic activity is the result of generation of hydrogen peroxide and production of highly reactive hydroxyl radicals [Graf et al., 1998; Kawai and Arinze, 2006].

Anitdiabetic drugs may be subdivided into six groups, insulin, sulfonylureas, alphaglucosidase inhibitors, biguanides, meglitinides and thiazolidinediones. Diabetes is characterized by insufficiency in insulin secretion and/or action. Increased production of ROS/RNS is also observed in diabetes [Lenzen, 2008a; 2008b]. Since

Fig. 11 Chemical structures of A) Valporic acid B) Metformin hydrochloride C) Glimepiride

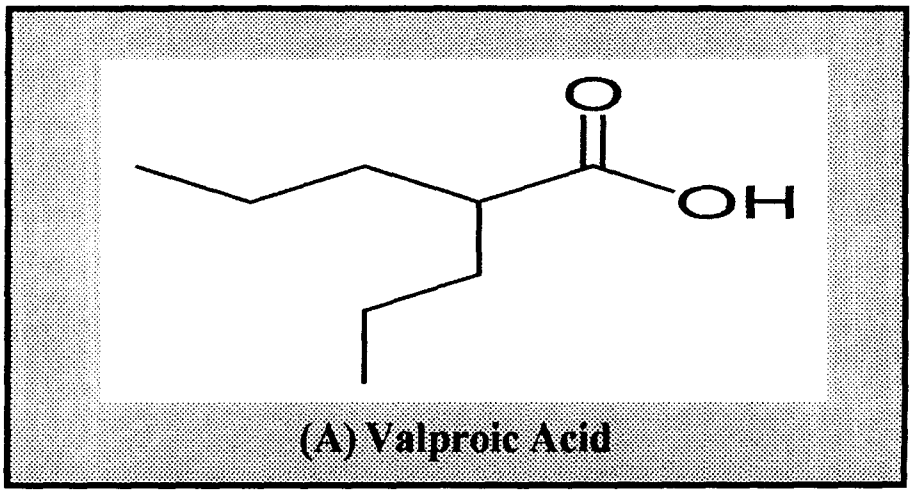

(A) Valproic Acid

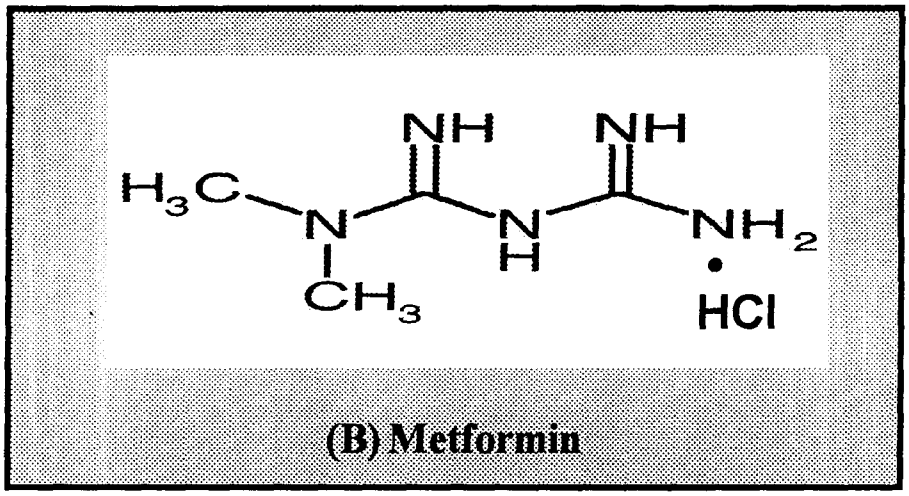

(B) Metformin

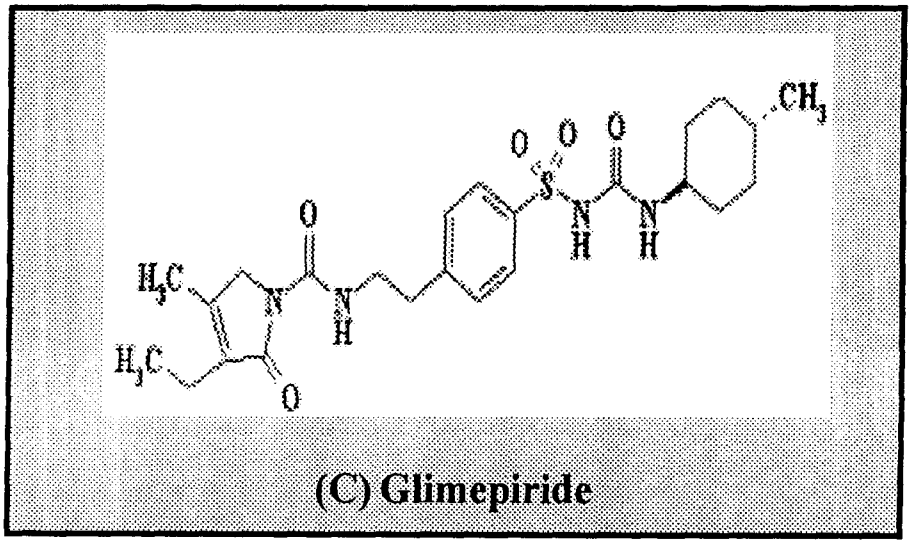

(C) Glimepiride

the introduction of insulin in the 1920s as a treatment for diabetes [Banting and Best, 1990], it is considered to be the most effective treatment.

Metformin hydrochloride

Metformin hydrochloride [N, N'-dimethylimidodicarbonimidic diamide hydrochloride, Fig. 11 B] is the only member of biguanide class of antihyperglycemics prescribed with increasing frequency for treatment of Type 2 diabetes. Its overdosage and chronic use is related to incidences of lactic acidosis.

Glimepiride

Glimepiride [Fig. 11 C] is a hypoglycemic agent of sulfonylurea class. It acts by increasing insulin secretion from pancreas and insulin sensitivity in peripheral cells. Sulfonylureas (glimepiride) cause β-cell apoptosis, produce ROS and their prolonged exposure causes disturbances in islet cell function [Sawada et al., 2008; Del Guerra et al., 2005].

1.14 SCOPE OF THE THESIS

Intracellular protein degradation occurs in two major cellular systems: lysosomal and non-lysosomal ubiquitin-proteasome systems. In the lysosomal pathway, protein degradation is a result of combined random and limited action of cathepsins. Recently, a host of functions are annexed to cathepsins, like antigen processing and presentation, bone remodelling, apoptosis mediation, etc. [Turk and Turk, 2008]. Potentially highly destructive activity of cathepsins can be regulated by their endogenous protein inhibitors, members of cystatin superfamily. A balance between proteolytic activity and proteinase inhibition is imperative to the appropriate functioning of many biological processes. Also, TPIs have been accredited with a multitude of roles and their non- or dys- functional states have been incriminated in various pathological conditions. This has stipulated the purification and characterization of members of cystatin superfamily from varied sources, since the first report of such an inhibitor from chicken egg white [Fossum and Whitaker, 1968]. Pancreas is one of the most complex tissue of the mammalian body and also capital of proteolytic power. It functions to maintain the glucose homeostasis of the body and participates in digestion. However, regulation of pancreatic cathepsins by proteinaceous inhibitors

remains a less ventured area.

Keeping this in view, the specific objectives of the planned research included:

Chapter 1

Realizing the role of cathepsins in pancreas the importance of thiol proteinase inhibitors (TPI) in their regulation was envisaged. Isolation and partial purification of TPI from pancreas of goat was performed by gel filtration chromatography. Its detailed biochemical characterization was undertaken, which included elucidation of its molecular weight, hydrodynamic properties, pH and thermal stability, partial amino acid sequence. Its interaction with model cysteine proteinase, papain was worked out to determine its kinetic properties.

Chapter 2

To assess the conformational stability of the isolated inhibitor, equilibrium denaturation studies were conducted with classical denaturants, guanidine hydrochloride and urea employing fluorescence and CD spectroscopy.

Chapter 3

Cystatins are predisposed to form amyloids. Certain pancreatic proteins are also known to undergo fibrillation (e.g. amylin). Thus, experiments were conducted to judge the propensity of isolated TPI for fibrillation under various conditions (pH variance, presence of organic solvent, trifluoroethanol, TFE) employing Transmission electron microscopy and Thioflavin T fluorescence assay. The possibility of disintegration of preformed fibrils and inhibition of de novo fibrillation of the isolated inhibitor by divalent metal cations, Zn^{2+} and Cu^{2+}, was also studied.

Chapter 4

Proteins are most liable to free radical damage because of their abundance. Pancreas also has high proclivity of oxidative and nitrosative stress build up because of its feeble antioxidant defence. Furthermore, ROS and RNS are recognized as major culprits in pancreatitis, β-cell damage in diabetes and pancreatic stellate cell fibrosis. Thus affect of various reactive species (a) ROS (b) $^{\bullet}NO$ (c) H_2O_2 (d) HOCl, was determined on activity and structure of the isolated inhibitor by fluorescence

spectroscopy and PAGE. Natural polyphenols and flavonoids, caffeic acid, curcumin and quercetin, offering inexpensive and non-toxic modes of anti-free radical therapy were analyzed to ascertain their efficacy and efficiency in preventing ROS/ nitric oxide and hypochlorous acid induced damaged to the isolated inhibitor.

Chapter 5

Drug-protein interactions are determining factors in the therapeutic, pharmacodynamic and toxicological drug properties. Experiments were conducted to find out the effects of pancreatitis causing sodium valproate and antidiabetic agents (insulin, metformin, glimepiride) on structure and function of the purified inhibitor employing UV, Fluorescence and CD spectroscopy and PAGE.

The results of the present studies showed the presence of a 44 kDa thiol proteinase inhibitor in goat pancreas subsequently named as PTPI. It was found to be highly specific and efficient inhibitor of CPs. Its physical, kinetic and biochemical properties commensurate with the cystatin superfamily signatures. The likelihood of its being amyloidogenic was proved by transmission electron microscopy (TEM) and ThT fluorescence. PTPI was found vulnerable to ROS, nitric oxide and hypochlorous acid. However, curcumin, quercetin and caffeic acid protected the free radical inflicted structural and functional alterations. Complexation with drugs caused significant conformational and functional changes in PTPI. ***Conclusively, these results forestall the significance of PTPI in vivo, in pancreatic (patho) physiology.***

Materials & Methods

[II] MATERIALS AND METHODS

[A] MATERIALS

All chemicals used were of the finest quality commercially available and their sources are indicated against them.

Sisco Research Lab (SRL, India)

Acetic acid, Acrylamide, Ascorbic acid, n-Butanol, Casein, Coommassie brilliant blue-R250, Copper sulphate, L-cysteine, 5, 5'-Dithio-bis 2-nitrobenzoic acid (DTNB), Folin ciocalteau's phenol reagent, Glycine, Glucose, Glutathione reduced, Hydrogen peroxide, Mannitol, Methanol, N N' methylene bisacrylamide, Phenol, Potassium iodide, Sodium acetate, Sodium azide, Sodium benzoate, Sodium carbonate, Sodium chloride, Sodium hydroxide, Sodium potassium tartarate, Urea, Uric acid.

Qualigens, India

Ammonium persulphate, Ammonium sulphate, Bromophenol blue, Disodium hydrogen phosphate, Ethanol, Ethylene diamine tetra-acetic acid (EDTA), Formaldehyde, Glycerol, Isopropanol, Monosodium dihydrogen phosphate, Silver nitrate, Sodium thiosulphate, Sodium dodecyl sulphate, Sulphuric acid, TEMED, Trichloroacetic acid (TCA), Tris-(Hydroxymethyl) aminomethane, Zinc chloride.

Sigma Chemical Co., USA

Agarose, 1-Anilinonaphthalene-8- sulphonic acid (ANS), Anti-rabbit alkaline phosphatase (conjugate), Blue dextran, Bovine serum albumin, Bromelain, Caffeic acid, Catalase, Chelex medium, Chymotrypsin, Curcumin, Ficin, Griess reagent, Guanidine HCl (GdnHCl), Hypochlorous acid, 2-mercaptoethanol, Ovalbumin, Papain, Pepsin, p-nitro phenyl phosphate, PVDF membrane, Quercetin, Riboflavin, Sephacryl S 100-HR, Sodium nitrite, Sodium nitroprusside, Thioflavin T, Trifluoroethanol (TFE), Trypsin.

Genei Pvt. Ltd., Bangalore, India

Freund's complete and incomplete adjuvant, Molecular weight markers-PMW-M.

Others Sodium Valproate (Microlabs Ltd., TN, India), Glimepiride (Aventis Pharma Ltd., Goa, India), Huminsulin R (Eli Lilly & Co. (India) Pvt. Ltd. Gurgaon, Haryana), Glycomet- 850 (Metformin hydrochloride) (USV Ltd., Solan, HP, India).

[B] METHODS

2.1 PURIFICATION OF THIOL PROTEINASE INHIBITOR FROM GOAT (CAPRA HIRCUS) PANCREAS

Fresh pancreatic tissue (100 g) (obtained from local slaughter house) was homogenized in 50 mM sodium phosphate buffer (200 ml, pH 7.5) containing 0.15 M sodium chloride (NaCl), 3 mM EDTA and 2% n-butanol. After centrifugation at 5000 rpm for 15 min at 4°C in a Beckman J-21 cooling centrifuge, pellet having cell debris was discarded and the supernatant was further processed.

Alkaline treatment

The supernatant was adjusted to pH 11.0 by 3 M sodium hydroxide and incubated for 30 min at 4°C. The pH was then brought back to 7.5 with glacial acetic acid. The precipitated proteins were removed by centrifugation at 8000 rpm for 30 min at 4°C.

Acetone Fractionation

The supernatant was fractionated with equal volume acetone at 4°C with stirring, over a period of 10 min. The precipitate was removed by centrifugation (at 8000 rpm for 20 min at 4°C) and discarded. A further portion of acetone equal in volume to the first was added to the supernatant as before. The precipitate was collected by centrifugation at 11,000 rpm for 30 min at 4°C and the supernatant discarded.

Ammonium Sulphate Fractionation

The precipitate dissolved in minimum amount of 50 mM sodium phosphate buffer (pH 7.5) was fractionated between 20 and 80% ammonium sulphate saturation. The precipitated protein was procured by centrifugation at 11000 rpm for 30 min at 4°C. The precipitate was dissolved in 50 mM sodium phosphate buffer pH 7.5 and dialyzed thrice against 100 ml volumes of the same buffer containing 0.15 M NaCl.

Gel Filtration Chromatography

A Sephacryl S 100-HR column (60 x 1.7 cm) was prepared as recommended by Peterson and Sober [1962]. Preswollen gel suspended in ethanol was soaked in sufficient amount of double distilled water and washed atleast thrice. The gel fines

were removed by suspending the gel in two to four fold excess of 50 mM sodium phosphate buffer, pH 7.5 and gel was allowed to settle down. The remaining gel in the supernatant was rapidly removed by suction. A glass column mounted on a sturdy vertical support was filled to one third of its length with operating buffer in order to check leaks and flush air bubbles from the dead space. The deaerated gel slurry was poured with the help of glass rod in to the column with care. The column was left standing overnight. Flow rate was increased gradually and after accomplishing a constant flow rate higher than that required for final elution, the column was adjusted to the required flow rate. The packed column was thoroughly washed with two bed volumes of operating buffer (50 mM sodium phosphate buffer, pH 7.5). In order to check uniform packing and to determine void volume of the column, 2% (w/v) solution of blue dextran in 50 mM sodium phosphate buffer (pH 7.5) was passed through the column. The volume of the blue dextran and protein solution applied was not more than 2-3% of the total bed volume. The dialyzed sample was subjected to gel filtration chromatography on Sephacryl S-100 HR column (60 x 1.7 cm) equilibrated with 50 mM sodium phosphate buffer pH 7.5. The flow rate of the column was 15 ml/h. Fractions (5 ml) were collected and assayed for protein and thiol proteinase inhibitor (TPI) activity. Homogeneity was analyzed by 7.5% PAGE.

2.2 COLORIMETRIC ANALYSIS

Determination of Protein Concentration

Protein concentration was estimated by the method of Lowry et al. [1951]. Aliquots of protein solution were taken and final volume was made up to 1 ml with distilled water. 5 ml of alkaline copper reagent (containing one part of 1 % (w/v) copper sulphate and 2 % (w/v) sodium potassium tartarate in 1 % (w/v) sodium hydroxide and sodium carbonate) was added and after 10 min of incubation at room temperature (RT), 0.5 ml of 1 N Folin Ciocalteau's phenol reagent was added. The tubes were instantly vortexed. The colour developed was read at 660 nm after 30 min in Shimadzu UV mini-vis spectrophotometer UV-1700 against a reagent blank. A standard curve was prepared using BSA.

Carbohydrate Estimation

The procedure described by Dubois [1956] was followed. 2 ml aliquots containing

10-70 μg of protein was pipetted in to a set of test tubes and 0.05 ml of 80% phenol was added. This was followed by the addition of concentrated sulphuric acid. The tubes were allowed to stand for 10 min at 30°C. The colour intensity was measured at 490 nm for the quantification of hexose content. Glucose was used as standard.

Thiol Group Estimation

The procedure described by Ellman [1959] was followed for estimating the thiol groups of isolated inhibitor. SDS and β-mercaptoethanol induced appearance of free thiol group in TPI was followed by titration with DTNB reagent. Appropriate aliquots of 0.2 ml native, SDS and β-mercaptoethanol treated inhibitor were mixed with 0.1 ml of DTNB reagent (prepared by dissolving 40 mg DTNB in 100 ml of 0.05M Tris-EDTA buffer, pH 8.0) in a total volume of 3.1 ml. The absorbance was read after 15 min at 412 nm. Free thiol concentration was calculated from the absorbance using molar extinction coefficient (ε) of 13,600 M^{-1} cm^{-1} for the released thionitrobenzoic acid. A standard plot was prepared using L-cysteine.

Assay of Thiol Proteinase Inhibitory (Cystatin) Activity

Inhibitory assay of TPI was performed as described by Kunitz [1947]. Purified PTPI was examined for its ability to prevent thiol proteinases from digesting casein. For determination of inhibitory activity, papain was activated in presence of 0.14 M L-cysteine and 0.045 M EDTA for 10 min prior to incubation of papain-PTPI complex for 30 min at 37°C in 50 mM sodium phosphate buffer, pH 7.5. The enzyme inhibitor complex was further incubated with casein for 30 min at 37°C and the reaction was stopped by addition of 10% TCA. Acid insoluble material was removed by centrifugation at 2500 rpm for 20 min. The supernatant was analysed for acid soluble peptides with Folin's phenol reagent as described by Lowry et al. [1951]. Ficin inhibition was also assayed by similar method.

Assay of Caseinolytic activity of Bromelain

The proteolytic activity of bromelain was measured according to the method of Murachi and Neurath [1960]. The enzyme was activated at 37°C for 10 min in the presence of 0.14 M L-cysteine. Then the volume was made up to 1 ml by 50 mM sodium phosphate buffer pH 7.5. 1 ml of 0.5% casein was added and incubated for 30 min at 37°C. The reaction was stopped by addition of 1 ml of 10 % TCA. Acid

insoluble material was removed by centrifugation at 2500 rpm for 15 min. The supernatant was analysed for acid soluble peptides by Folin's phenol reagent by the method of Lowry et al. [1951].

Thermal stability

Fifty micrograms of the inhibitor was incubated in 50 mM sodium phosphate buffer (pH 7.5) at various temperatures for 30 min. These samples were rapidly cooled in ice cold water bath and checked for residual activity against fifty micrograms of papain. Fifty micrograms of the inhibitor at 90°C was also incubated for different time intervals rapidly cooled and residual inhibitory activity measured against papain.

pH stability

Fifty micrograms of the inhibitor was incubated with buffers of different pH values like 50 mM sodium phosphate buffer (pH 7.0, 8.0), 50 mM sodium acetate buffer (pH 3.0-6.0) and Tris HCl buffer (pH 9 and 10) for 30 min at 37°C. Aliquots of this mixture was used for determination of remaining % inhibitory activity as described in the section of assay of proteinase inhibitory activity.

2.3 SLAB GEL ELECTROPHORESIS

Polyacrylamide Gel Electrophoresis (PAGE)

Electrophoresis was performed by the method of Laemmli [1970] using the slab gel apparatus manufactured by Biotech, India. Concentrated stock solution of 30% acrylamide containing 0.8% N'N' methylene bis-acrylamide and 1.5 M Tris, pH 8.8, were mixed in appropriate portion to give the desired concentration of gel. It was then poured in to the mould formed by glass plates (8.5x10 cm) separated by 1.5 mm thick spacers. Bubbles and leak were avoided. A comb providing template for seven wells was inserted into the stacking gel solution before the polymerization began. Polymerization was complete in about 30 min after which the comb was removed and wells overlaid with running buffer. Routinely 7.5% and 12.5% gels were used. Samples containing 40-60 μg of protein were mixed with one fourth volume of sample buffer (62.5 mM Tris HCl pH 6.8, 10% (v/v) glycerol and 0.001% bromophenol blue). Electrophoresis was performed at 100 V in the electrophoresis buffer containing192 mM glycine and 25 mM Tris-HCl (pH 6.8) until the tracking

dye reached the bottom of the gel.

SDS Polyacrylamide Gel Electrophoresis (SDS-PAGE)

Sodium dodecyl sulphate polyacrylamide gel electrophoresis was performed by the Tris-glycine system of Laemmli [1970] using slab gel electrophoresis apparatus. Concentrated stock solution of 30% acrylamide containing 0.8% N N' methylene bisacrylamide and 1.5 M Tris, pH 8.8 were mixed in appropriate proportions to give desired percentage of gel. Protein samples were prepared in solution containing 62.5 mM Tris-HCl pH 6.8, 10% (v/v) glycerol, 2% (w/v) SDS, 5% (v/v) 2-mercaptoethanol and 0.001% (w/v) bromophenol blue. The samples were incubated at 100°C for 5 min. Electrophoresis was performed at 100 V till the tracking dye reached the bottom of the gel. Running buffer used during electrophoresis contained 1% SDS in addition to 192 mM glycine and 25 mM Tris-HCl (pH 6.8).

Staining of the Gel

Coommassie Brilliant Blue Staining

After electrophoresis was complete the protein bands were visualized by staining the gel with five gel volumes of 0.25% coommassie brilliant blue R-250 in 50% methanol and 10% acetic acid for atleast 4 h. For destaining the gels were incubated in 5% methanol and 7.5% acetic acid at RT with shaking.

Silver Staining

The gel after electrophoresis was silver stained by Blum's silver stain method [Nesterenko, 1994]. The staining was initiated by fixation for 10 min in 50% acetone, 1% trichloroacetic acid and 0.015% formaldehyde with subsequent washings. After a second fixation in 50% acetone only, the gel was pretreated with 10% sodium thiosulphate and then impregnated with 20% silver nitrate, 37% formaldehyde and 10% sodium thiosulphate for 30 s to 1 min the reaction was stopped by 1% glacial acetic acid and incubated for 15 min in 1% glycerol after rinsing with distilled water.

2.4 MOLECULAR WEIGHT DETERMINATION

The molecular weight of purified goat pancreatic thiol proteinase inhibitor (PTPI)

was determined under native and denaturing (reducing and non-reducing) conditions by gel filtration chromatography and SDS-PAGE, respectively.

Molecular weight determination by Gel Filtration Chromatography

The molecular weight of native PTPI was computed from its elution volume on a Sephacryl S 100-HR column (60 x 1.7 cm). The column was calibrated by determining the elution volume of some marker proteins- Trypsin (23 kDa), Pepsin (35 kDa), Ovalbumin (43 kDa) and BSA (66 kDa). This data was analyzed according to the theoretical treatment by the method of Andrews [1964]. The linear plot between V_e/V_o and log M was used for calculating the molecular weight of PTPI where V_e is the elution volume of the protein and V_o is the void volume of the column determined using blue dextran.

Molecular weight determination by SDS-PAGE

Molecular weight of PTPI under denaturing conditions was calculated by the procedure of Weber and Osborn [1969] using SDS-PAGE. The mobilities of marker proteins determined under identical conditions were plotted against the logarithms of molecular weight. The standard proteins used were Phosphorylase b (97.4 kDa), Bovine serum albumin (68 kDa), Ovalbumin (43 kDa), Carbonic anhydrase (29.1 kDa), Soyabean trypsin inhibitor (20.1 kDa) and Lysozyme (14 kDa). The analysis of data indicated a linear relationship between log M and relative mobility (RM) and the plot was used for calculating the molecular weight of PTPI.

2.5 IMMUNOLOGICAL PROCEDURES

Production of Antiserum

Antibodies against PTPI were raised by injecting 300 µg of the purified inhibitor in Freund's complete adjuvant subcutaneously into healthy male albino rabbits. The injection was repeated every week in Freund's incomplete adjuvant and the rabbit was bled every second week. The blood collected was allowed to coagulate at 22°C for 3 h. The antisera decomplimented at 57°C for 30 min and was stored at -20°C.

Immunodiffusion

Immunodiffusion was performed by the method of Ouchterlony [1962]. 1% agarose

in normal saline containing 2% sodium azide was poured in glass petridish and allowed to solidify at RT. Required number of wells was cut. 15 µl of suitably diluted antiserum and required amount of antigen (60 µg) were added in different wells. The reaction was allowed to proceed for 12-24 h in a moist chamber at RT.

Direct binding ELISA

The generation of antigen specific antibody was measured in the sera of PTPI immunized rabbits by the technique of direct binding ELISA (enzyme linked immunosorbent assay) as given by Voller et al. [1976]. Ninety six wells of micro-titre plate (immulon 2 HB, Dynex, USA) were coated overnight with 100 µl of antigen at 4°C. The plate was washed thrice with TBS-T buffer (Tris buffered saline Tween 20, pH 7.4, 20 mM Tris, 14.3 mM sodium chloride, 200 mg potassium chloride and 5 ml Tween 20 dissolved in 1 l of distilled water and pH adjusted to 7.4 by 1 N HCl). The unoccupied sites were saturated by incubation with 150 µg/200 ml of 1.5% milk in TBS (Tris buffered saline, pH 7.4, 20 mM tris, 150 mM sodium chloride) for 5-6 h at RT. Plates were washed twice with TBS-T. The test and control wells were then loaded with 100 µl of serially diluted serum. The plate was incubated for 2 h at RT and then overnight at 4°C. 100 µl of appropriate conjugate of anti-rabbit alkaline phosphatase (1:3000) was coated in each well and kept for 2 h at RT. After regular washing with TBS-T and distilled water, the substrate p-nitro phenyl phosphate (5 µg/100 ml of 50 mM bicarbonate buffer, pH 9.5, containing 0.02% sodium azide) was added in each well and incubated for 30-45 min. The reaction was stopped by addition of 100 µl of 3 M NaOH in each well. The absorbance of each well was monitored at 405 nm on a qualigens ELISA reader.

2.6 KINETICS OF INHIBITION

Stoichiometry of Proteinase Inhibition

Papain was used for the titration of PTPI. The inhibitory activity of TPI was assessed by its ability to inhibit caseinolytic activity of papain by the method of Kunitz [1947]. The concentration of papain was varied from 0.01-0.0 µM whereas the inhibitor concentration was fixed at 0.06 µM. Identical experiments were carried out for PTPI with other proteinases, ficin and bromelain using casein as substrate [Kunitz, 1947; Murachi and Neurath, 1960].

Inhibition constant (Ki) determination

Ki determinations were carried out by lowering the enzymes and inhibitor concentrations to obtain a non-linearity of dose-response curves. Papain, ficin and bromelain were used at a concentration of 0.06 μM to react with inhibitor in varying concentrations from 0.01 to 0.24 μM. Residual activity was measured by the method of Kunitz [1947] using casein as a substrate. Four different substrate concentrations were used 0.5 Km, 1 Km, 2 Km and 3 Km and with Km = 2.4 mM. The results were analyzed by the procedure of Krupka and Laidler [1959]. The linear equation given by Henderson [1972], is presented as follows,

$$[I]_o / 1- (V_i /V_o) = Ki \left[1+[S]_o / Km\right] V_i /V_o + [E]_o$$

Where, $[I]_o$, $[E]_o$ and $[S]_o$ are the initial concentrations of Inhibitor, Enzyme and Substrate, respectively. V_o is the velocity in absence of inhibitor and V_i is the velocity in presence of inhibitor. The plot of $[I]_o$ / 1- (V_i /V_o) against V_o /V_i is a straight line, the slope of which gives,

$$Ki\ (app) = Ki \left[1+ [S]_o / Km\right]$$

True Ki was obtained from a replot of Ki (app) against $[S]_o$.

Determination of dissociation rate constant (K_{-1})

For the dissociation rate constant, the conditions for maximal association between proteinase and inhibitor were achieved before the reaction was shifted towards dissociation by adding excess substrate which binds the entire free enzyme. Dissociation of EI complex obeys first order kinetics. Thus, integrated form of the dissociation rate equation is given by:

$$\ln \left([EI]/ [EI]_o\right) = K_{-1}\, t$$

From which half life of the complexes may be calculated by rearranging as follows:

$$t_{½} = 0.693/ K_{-1}$$

Determination of association rate constant (K_{+1})

Using the values of dissociation constant and inhibition constant derived as explained above, association rate constant, K_{+1}, was determined using the relation

$$K_{+1} = K_{-1}/ Ki$$ [Abrahamson et al., 1986]

2.7 N-TERMINAL ANALYSIS

The sequencing of 24 amino acid residues from N-terminal of larger subunit of PTPI was carried out on Shimadzu ppsq-21 Sequencer which employs Edman degradation to sequentially cleave and identify amino acids starting from amino terminus of the protein [Edman and Begg, 1967]. The highly purified protein was transferred to the PVDF membrane by western blotting before amino acid analysis.

Western Blotting

a. Buffers used: CAPS buffer- 10 x stock (100 mM, pH 11): 22.13 g of 3-[cyclohexylamino] 1-propane-sulphonic acid was dissolved in 980 ml of deionized water and titrated with 2 M NaOH (15 ml) to pH 11. Deionized water was added to make final volume to 1 l and the buffer was chilled at 4°C before use. Transfer buffer- 2 l of buffer was prepared by mixing 200 ml of 10 x stock buffer, 200 ml of methanol and 1600 ml of deionized water.

b. Procedure: The PVDF membrane and the filter paper were cut according to the gel dimensions. The PVDF membrane was made wet in 100% methanol for 30 s, then soaked in distilled water for 5 min and then placed in a dish containing blotting buffer for 15 min. The gel, filter paper and fiber pads are allowed to equilibrate in transfer buffer for 15 min to 1 h depending on the gel thickness. The transblotting sandwitch is assembled as filter pad, filter paper, PVDF, gel, filter paper and then again pad. After firmly closing the cassette it was locked properly taking care not to move the transblotting sandwitch. The cassette was placed in tank filled with transfer buffer completely. The lid was put and power supply plugged in. The blot was run at 30 V overnight. Upon completion of the run, the transblotting sandwitch was disassembled to remove the PVDF membrane for development. The membrane was rinsed with distilled water and then stained with 0.1 % coommassie blue R-250 in 10% acetic acid and 50 % methanol for the minimum time necessary to visualize the band of interest. The PVDF membrane was destained for atleast 2 h in 10% acetic acid. After destaining the PVDF membrane was rinsed in 100% methanol and then soaked in distilled water for 15 min to remove the excess acetic acid and methanol. Finally the PVDF membrane was air dried and placed in a new sterile container till used for sequencing.

Hydropathy plot

The hydropathy profiles were calculated using the mean segment approach, i.e. determining the average hydropathy within a segment length of four residues, the segment being advanced one residue at a time from the sequence of N-terminal 24 residues [Kyte and Doolittle, 1982].

2.8 SPECTRAL ANALYSES

Absorption Difference Spectra

Ultraviolet (UV) absorption difference spectra was measured for PTPI (2.66 μM) along with activated papain with a molar ratio of 1:1 at 25°C. Spectra were recorded by measuring the absorption between 200-350 nm on Cintra-10 spectrophotometer in a cuvette of 1 cm path length. Appropriate controls of the solvent buffer were run and corrections were made wherever necessary.

Fluorescence spectroscopy

Fluorescence measurements for papain, PTPI and PTPI-papain complex were performed on Shimadzu spectrofluorimeter model RF-540 equipped with data recorder DR-3. The excitation wavelength was 280 nm and the slits were set at 5 nm for excitation and 10 nm for emission. The path length was 1 cm and the emission wavelength range was 300-400 nm. The protein concentration used in the fluorescence measurements was 2 μM. Each spectrum was the average of at least three scans. Appropriate controls were run and corrections made wherever necessary.

Circular Dichroism (CD) Spectroscopy

Circular dichroism measurements were carried out on a Jasco Spectropolarimeter model J-720 using a SEKONIC–XY plotter (model SPL-430 A) with thermostatically controlled cell holder attached to a NESLAB water bath model RTE 110 with an accuracy of ± 0.10°C. The instrument was calibrated with d-10-Camphorsulphonic acid. The concentration of inhibitor for far UV-CD analysis was (1.73-1.70 μM). The path length used was 0.1cm. The spectra were recorded with a scan speed of 20 nm min^{-1} and with a response time of 4 s. The concentration of the inhibitor and papain for far UV-CD spectral analysis was 0.2 mg/ml and pathlength was 0.1 cm. Each spectrum was recorded as an average of 5 scans. The emission wavelength range was

200-250 nm. Change in secondary structure of PTPI on interaction with activated papain (activated with 0.14 M cysteine and 0.045 M EDTA) at a molar ratio of 1:1 was monitored. The α helical content of PTPI was calculated from the MRE value at 222 nm using the following equation [Chen et al., 1972]

$$\% \text{ helix} = [(MRE_{222} - 2340)/ 30300] \times 100$$

2.9 DENATURING ACTION OF GUANIDINE HYDROCHLORIDE AND UREA TOWARDS PANCREATIC THIOL PROTEINASE INHIBITOR

Assay of inhibitory activity of PTPI in the presence of GdnHCl/ urea

The inhibitory activity of PTPI under native conditions was assessed by its ability to inhibit caseinolytic activity of papain by the method of [Kunitz, 1947]. The purified inhibitor (1 μM) was incubated with increasing concentrations of GdnHCl (0.5-6 M) and urea (0.5-9 M) at 25°C for 2 h before the activity was measured. Activity of untreated PTPI was taken as 100 %.

Intrinsic fluorescence studies of PTPI in the presence of denaturants (GdnHCl and Urea)

The fluorescence was recorded in the wavelength range of 300-400 nm after exciting the protein solution at 280 nm for total protein fluorescence. The slits were set at 5 nm for excitation and emission. The path length of the sample used was 1 cm. The protein concentration was taken as 1 μM. PTPI was incubated with increasing concentration of GdnHCl (0.5-6 M) and urea (0.5-9 M) for 2 h at RT before the spectra were recorded. Appropriate controls were run and corrections were made wherever necessary. Each spectrum was an average of three scans.

Refolding was also studied by fluorescence spectroscopic and activity measurements. The refolding reaction was induced by rapidly diluting (1:50 fold) aliquots of PTPI denatured at desired GdnHCl/urea concentrations in the same buffer containing appropriate concentrations of GdnHCl/urea vigorously vortexing the solution at the same time. The spectra and activity were determined at regular time intervals till 24 h.

Extrinsic/ANS fluorescence studies of PTPI in the presence of denaturants (GdnHCl and Urea)

The binding of ANS (1-anilinonapthalene-8-sulphonic acid) to PTPI in the absence and presence of increasing concentration of GdnHCl (0.5-6 M) and urea (0.5-9 M) was studied by exciting the dye at 380 nm and the emission spectra were recorded from 400-600 nm wavelength range. The molar ratio of protein to ANS was

Far UV-CD measurements of PTPI in presence of GdnHCl and Urea

Secondary structural changes of PTPI on incubation with varying concentrations of GdnHCl (0.5-6 M) and urea (0.5-9 M) were measured at 25°C. The concentration of PTPI was 1.73-1.70 μM and the path length was 0.1 cm. Each spectrum was recorded as an average of five scans. The spectra obtained were normalized by subtracting the baseline recorded for the buffer having the same concentration of denaturants under similar conditions. Data were expressed in terms of fraction denatured (f_d), calculated from the equation [Tanford, 1968],

$$f_d = (Y - Y_n)/ (Y_d - Y_n)$$

Where Y is the observed variable parameter and Y_n and Y_d are the values of the variable characterstics of the folded and unfolded conformations. A linear extrapolation of the baselines in the pre- and posttransitional regions was used to determine the fraction of unfolded protein within the transition region by assuming a two state mechanism of unfolding.

2.10 IN VITRO STUDY OF FIBRILLATION OF PTPI

Acid Denaturation Study

PTPI was allowed to undergo acid denaturation by subjecting it to buffers of varying pH range from pH 7.0 to pH 2.0. The buffers used were 50 mM solution of glycine/HCl (pH 2.0), sodium acetate (pH 3.0-5.0) and sodium phosphate (pH 6.0-7.0). pH measurements were carried on a Metzer Optical Instruments (Pvt. Ltd., India), pH meter model 603M with a least count of 0.01 pH unit. PTPI was incubated with the respective buffer of desired pH at 25°C and allowed to equilibrate for 4 h before any spectrophotometric measurements were taken.

Spectrophotometric measurements

The fluorescence was recorded in the wavelength range of 300-400 nm after exciting the protein solution at 280 nm for total protein fluorescence. The slits were set at 5 nm for excitation and emission. The path length of the sample used in the fluorescence measurements was 1 cm. The protein concentration was taken as 1 μM. ANS binding to PTPI at varying pH was studied by exciting the dye at 380 nm and the emission spectra were recorded from 400-600 nm wavelength range with a 5 nm slit width for excitation and emission. ANS to protein molar ratio of 1:50 was used for each respective measurement. Each spectrum was an average of three scans. Far UV CD spectra of PTPI at varying pH range were also measured. The concentration of PTPI used was 1.70 μM. Rest conditions were same as those described in section 2.9.

Effect of trifluoroethanol (TFE) on acid induced state of PTPI

PTPI (1 μM) was incubated in different concentrations of TFE (0-20% v/v) in 50 mM sodium acetate buffer (pH 3.0) for 2 h before the measurements. The intrinsic and extrinsic fluorescence studies were conducted in a manner similar to that given for acid denaturation studies. Far UV-CD spectra of TFE treated PTPI were also recorded in the wavelength region of 200-250 nm. The concentration of the inhibitor used was 1.70 μM and pathlength was 0.1 cm. Each spectrum was recorded as an average of five scans. The spectra obtained were normalized by subtracting the baseline recorded for the buffer having the same concentration of TFE under similar conditions.

Binding of ANS to PTPI under above conditions was studied by exciting the dye at 380 nm and recording emission spectra from 400-600 nm. Excitation and emission slits were 5 nm. Since ANS shows emission in TFE all spectra were corrected for blanks. Similar experiments were conducted for PTPI at pH 2.0 and at 1.0.

Induction of PTPI Fibril Formation

50 μM PTPI was incubated with buffers of pH 1.0, 2.0 and 3.0 containing 0.15 M sodium chloride, 0.05% sodium azide in presence or absence of 10% TFE. Before incubation, each sample was passed through a 0.2 μm filter to remove traces of aggregated material. Fibril growth was followed in six samples: (1) PTPI at pH 1.0, (2) PTPI at pH 1.0 with 10% TFE, (3) PTPI at pH 2.0, (4) PTPI at pH 2.0 with 10%

TFE, (5) PTPI at pH 3.0, (6) PTPI at pH 3.0 with 10% TFE. 50 μM PTPI at pH 7.5 served as control.

Fibril Formation in the Presence of Divalent Metal Ions, Cu^{2+} and Zn^{2+}

To study the effects of copper and zinc on fibrillation of PTPI

Prior to induction of fibril formation, either 50 μM Cu^{2+} or 10 μM Zn^{2+} was added to the mixture (50 μM PTPI incubated with buffer of pH 3.0 containing 0.15 M sodium chloride, 0.05% sodium azide, 10% TFE). Chelating buffers were prepared using chelex medium. The protein solutions were exchanged with chelating buffer of pH 7.0 prior to fibrillation assays. Either 50 μM $CuSO_4$ or 10 μM $ZnCl_2$ dissolved in water was added to the buffers. After mixing the solutions, it gave PTPI to Cu^{2+} ratio of 1:1 and PTPI to Zn^{2+} ratio of 5:1.

Either Cu^{2+} (10-150 μM) or Zn^{2+} (2-50 μM) was added to preformed fibrils at pH 3.0.

Thioflavin T Fluorescence Measurements

The Shimadzu spectrofluorimeter model RF-540 equipped with data recorder DR-3 was used for measuring the fluorescence spectra. Excitation was at 440 nm and spectra were recorded from 455 to 600 nm. Excitation and emission slits were set at 5 nm and 10 nm, respectively. Five μl of the protein solution in which fibrils were growing were dissolved in 600 μl of the ThT buffer (pH 7.5, 25 mM phosphate buffer, 0.15 M NaCl, 20 μM ThT) just before the measurements. At regular time intervals aliquots of the protein samples were withdrawn to perform ThT assay.

Electron Microscopy

A 3 μl sample of protein solution was placed and dried for 5 min on formwar coated carbon grids. After excess fluids were micropipetted from the grid surface, the grid was washed with water and stained with 0.3% aqueous uranyl acetate. Excess stain was removed and the samples were dried at RT. The samples were analyzed at 10 kV in a JEM 1010 transmission electron microscope. Images were captured with an AMT digital camera system (AMT, Chazy, NY).

2.11 MODIFICATION OF PANCREATIC THIOL PROTEINASE INHIBITOR BY REACTIVE SPECIES

REACTION OF PHOTOSENSITIZED RIBOFLAVIN WITH PTPI

PTPI (1 μM) was photoilluminated with increasing concentration of riboflavin (5-50 μM) in a final volume of 1000 μl at RT for 30 min. Riboflavin was freshly prepared at 2 mM concentration in 50 mM sodium phosphate buffer (pH 7.5). PTPI (1 μM) was also photoilluminated for different time intervals (0-60 min) with 40 μM riboflavin in a final reaction volume of 1000 μl at RT. For light incubations tubes were set at a distance of 1 cm from 40-watt cool fluorescent lamp. The light intensity was 0.768 milliwatt at a distance of 1 cm measured by a Model 351 A-Powermeter. The treated protein samples were subjected fluorescence measurements, assay of thiol proteinase inhibitory activity and PAGE (as described later).

Effect of scavengers and natural antioxidants on riboflavin induced modifications of PTPI

To validate the type of free radical involved in riboflavin induced PTPI modification different scavengers were used. PTPI (1 μM) was photoilluminated in presence of 40 μM riboflavin for 60 min, in presence of 25 mM sodium azide, potassium iodide, thiourea, mannitol, uric acid and 100 mM ascorbic acid. Protective effect of natural antioxidants against riboflavin induced damage to PTPI was also studied. PTPI (1 μM) was photoilluminated with 40 μM riboflavin in presence of curcumin (100 μM), caffeic acid (350 μM) and quercetin (350 μM) for 30 min in a final reaction volume of 1000 μl. The treated protein samples were subjected to fluorescence measurements, assay of thiol proteinase inhibitory activity and PAGE (as described later).

The stock solution of curcumin and quercetin were prepared in acetone and dimethylsluphoxide, respectively. Caffeic acid was dissolved in distilled water. Preliminary experiments were conducted with a range of concentrations of curcumin, quercetin and caffeic acid against various radicals studied. Only the most effective concentration is reported in each case.

REACTION OF HYDROGEN PEROXIDE (H_2O_2) WITH PTPI

The concentration of H_2O_2 was estimated prior to experiments by the absorbance at 230 nm and $\varepsilon = 0.081\ mM^{-1}\ cm^{-1}$ [Andreae, 1955].

Treatment of PTPI with H_2O_2

PTPI (1 μM) was incubated with (1mM -500 mM) H_2O_2 in 50 mM sodium phosphate buffer (pH 7.5) in a final reaction volume of 1000 μl at RT for 30 min. PTPI (1 μM) was also incubated with 250 mM H_2O_2 for varying time intervals (0-120 min) in a final reaction volume of 1000 μl at RT. The treated protein samples were subjected to fluorescence measurements, assay of thiol proteinase inhibitory activity and PAGE (as described later).

Effect of scavengers and natural antioxidants on H_2O_2 induced modifications of PTPI

1 μM PTPI was incubated with 250 mM H_2O_2 in presence of 25 mM mannitol, thiourea, sodium benzoate, sodium azide, glucose, 100 mM ascorbic acid, 100 μg/ml catalase, 50 μM quercetin, 100 μM curcumin and 60 μM caffeic acid in a final reaction volume of 1000 μl for 30 min. The treated protein samples were subjected to fluorescence measurements, assay of thiol proteinase inhibitory activity and PAGE.

REACTION OF HYPCHLOROUS ACID (HOCL) WITH PTPI

HOCl concentration was quantified immediately before use spectrophotometrically at 290 nm (pH 12, $\varepsilon = 350\ M^{-1}\ cm^{-1}$) [Morris, 1966]. HOCl was diluted in ice-cold water [Whiteman et al., 2003] to make a stock solution of 10 mM and stored no longer than 1 min. After this time, solution was discarded and fresh HOCl (10 mM) was made. The pH values were adjusted where necessary to pH 7.4 using 1.0 M HCl or NaOH.

Treatment of PTPI with HOCl

PTPI (1 μM) was incubated with HOCl (1-50 μM) for 30 min or with 5 μM HOCl for varying time intervals (0-30 min) in 50 mM sodium phosphate buffer (pH 7.5) in a final reaction volume of 1000 μl at RT. At the end of incubation, HOCl was quenched with 100 μM reduced glutathione. The treated protein samples were subjected to

fluorescence measurements, assay of thiol proteinase inhibitory activity and PAGE (as described later).

Effect of scavengers and natural antioxidants on HOCl induced modifications of PTPI

PTPI (1 μM) was incubated with 5 μM HOCl in presence of 25 mM sodium benzoate, mannitol, glucose, 100 mM ascorbic acid, 100 μM each of quercetin, curcumin and caffeic acid, in a final reaction volume of 1000 μl. The treated protein samples were subjected to fluorescence measurements, assay of thiol proteinase inhibitory activity and PAGE (as described later).

REACTION OF PTPI WITH NITRIC OXIDE ($^{\bullet}$NO)

Nitric oxide production from sodium nitroprusside

Sodium nitroprusside (SNP) was used as nitric oxide donor. $^{\bullet}$NO generated from SNP was measured by Griess Reagent (GR) as described by Green et al. [1982] and Marcocci et al. [1994a]. 100 mM of SNP was prepared by dissolving the powder in phosphate buffer saline (PBS) pH 7.4. The reaction mixture (2 ml) containing 100 mM SNP (0.2 ml, final concentration 10 mM) and PBS (1.8 ml) was incubated at 25°C for 180 min. At 30 min intervals 1 ml aliquots were withdrawn from the incubation and diluted with 1 ml of GR. **The Griess reaction** relies on a diazotization. The GR consists of 1% sulphanilamide and 0.1% naphthylenediamine dihydrochloride in 2% H_3PO_4. Nitrite present reacts with sulphanilamide under acidic conditions. The resulting compound reacts with naphthylenediamine dihydrochloride to form an azo compound which is read at 540 nm [Marcocci et al., 1994a]. The plot between the concentration of nitrite and incubation time exhibited the best incubation time for nitrite production from SNP.

Treatment of PTPI with SNP ($^{\bullet}$NO)

PTPI (1 μM) was incubated with 0.05 mM, 1 mM and 10 mM SNP for 30 min or with 0.05 mM SNP for varying time intervals (0-180 min) in 50 mM sodium phosphate buffer (pH 7.5) in a final reaction volume of 1000 μl at RT. Following the incubation samples were subjected to fluorescence spectroscopy, assay of antiproteolytic activity and PAGE.

Effect of natural antioxidants on SNP induced modification of PTPI

1 μM PTPI was incubated with 1 mM SNP for 30 min in presence of 20 μM curcumin, 80 μM quercetin and caffeic acid, in 50 mM sodium phosphate buffer (pH 7.5) , in a final reaction volume of 1000 μl at RT. After the incubation samples were subjected to fluorescence spectroscopy, assay of antiproteolytic activity and PAGE.

FLUORESCENCE SPECTROSCOPY

Intrinsic fluorescence measurements were carried out on a Shimadzu spectrofluorimeter model RF-540 equipped with data recorder DR-3 at 25 ± 0.1°C. The fluorescence was recorded in the wavelength range 300-400 nm after exciting the protein solution at 280 nm for total protein fluorescence. The slits were set at 5 nm for excitation and emission. The pathlength of the sample was 1 cm. Appropriate controls containing the oxidants used for the treatment were run and correction made wherever necessary. Each spectrum was the average of three scans.

POLYACRYLAMIDE GEL ELECTROPHORESIS

Samples of native and oxidized PTPI were examined by non-denaturing PAGE performed in 12.5% gels as described by Laemmli [1970], using tris-glycine buffer pH 8.3. Twenty μg of protein sample was loaded in a 12.5% gel and electrophoresed. After running the gels were silver stained by the method of Nesterenko [1994]. Atleast three gels of each experiment were performed.

ANTIPROTEOLYTIC ACTIVITY OF PTPI

Functional PTPI was assessed on the basis of its ability to inhibit the caseinolytic activity of papain as described by Kunitz [1947]. Riboflavin, H_2O_2, HOCl and SNP at the maximum concentration used in these studies did not show any effect on PTPI activity assay.

2.12 DRUG-PTPI INTERACTION: EFFECT OF PANCREATITIS CAUSING AND ANTIDIABETIC AGENTS

Effect of sodium valproate (pancreatitis inducing drug) on PTPI

PTPI (2 μM) was incubated with increasing concentration of sodium valproate (2-20 μM) in 50 mM sodium phosphate buffer (pH 7.5), in a final reaction volume of 1000 μl at RT for 30 min. Sodium valproate solutions were prepared in the same buffer. Following the incubation period, samples were subjected to spectroscopic analyses, assay of antiproteolytic activity and PAGE.

EFFECT OF ANTIDIABETIC DRUGS ON PTPI

Interaction with Glimepiride

PTPI (2 μM) was treated with increasing concentration of glimepiride (2-40 μM) in 50 mM sodium phosphate buffer (pH 7.5), in a final reaction volume of 1000 μl at RT for 30 min. Glimepiride solutions were prepared in same buffer. Following the incubation period, samples were subjected to spectroscopic analyses, assay of antiproteolytic activity and PAGE.

Interaction with Metformin hydrochloride

PTPI (2 μM) was treated with increasing concentration of metformin hydrochloride (2-12 μM) in 50 mM sodium phosphate buffer (pH 7.5), in a final reaction volume of 1000 μl at RT for 30 min. Metformin hydrochloride solutions were prepared in double distilled water. Following the incubation period, samples were subjected to spectroscopic analyses, assay of antiproteolytic activity and PAGE.

Interaction with Huminsulin R

PTPI (2 μM) was incubated with varying concentrations of Huminsulin R (0.05-2 μM) in 50 mM sodium phosphate buffer (pH 7.5), in a final reaction volume of 1000 μl at RT, for 30 min. Following the incubation period, samples were subjected to spectroscopic analyses.

SPECTROSCOPIC ANALYSES

UV-visible spectroscopy

The UV vis absorption spectra were recorded on a double beam Shimadzu UV-vis spectrophotometer UV-1700 using a cuvette of 1 cm path length, in wavelength range of 190-300 nm. Each spectrum was the average of three scans.

Fluorescence Spectroscopy

The method followed for obtaining the fluorescence spectra of drug-PTPI compexes was similar to that given in section 2.11.

CD Spectroscopy

Far UV-CD measurements of PTPI with and without huminsulin R were conducted following the method similar to that reported in section 2.9.

ANTIPROTEOLYTIC ACTIVITY

Papain inhibitory activity of drug treated PTPI was assessed in a manner similar to that reported in section 2.11.

POLYACRYLAMIDE GEL ELECTROPHORESIS

Samples of native and drug treated PTPI were examined by non-denaturing PAGE performed in 7.5% gels (and 15% gels for huminsulin) as described by Laemmli [1970], using tris-glycine buffer pH 8.3. Twenty μg of protein sample was loaded in a gel and electrophoresed. After running the gels were silver stained by the method of Nesterenko [1994]. Atleast three gels of each experiment were performed.

2.13 STATISTICAL ANALYSES

Unless specified, all experiments were repeated at least four or five times to document reproducibility. Wherever applicable data are expressed as Mean ± SEM. Significance of difference in mean values were evaluated using one-way analysis of variance (ANOVA). A probability level of $p < 0.05$ was selected as indicating statistical significance.

Results & Discussion

Chapter 1

Purification and characterization of goat pancreatic thiol proteinase inhibitor

3.1 RESULTS

3.1.1 PURIFICATION OF THE INHIBITOR

In the present work, pancreatic thiol proteinase inhibitor (PTPI) has been purified from goat pancreas by the method of Priyadarshini and Bano [2009]. As detailed in the methods section, the procedure involved four steps after homogenisation, alkaline treatment (pH 11.0), acetone fractionation, ammonium sulphate precipitation (20-80%) and gel filtration chromatography on Sephacryl S 100 HR column. The progress of typical purification is summarized in Table 6. The initial homogenate contained free cathepsins, so presumably the inhibitors were entirely complexed. The alkali treatment destroyed the lysosomal cysteine proteinases liberating the inhibitors in assayable form. A large amount of inactive proteins was precipitated during the readjustment to pH 7.5, and could be removed by centrifugation. Fractionation of the soluble material with acetone decreased the total amount of protein providing a fold purification of 18.84 and a percent yield of 58.8.

3.1.2 GEL FILTRATION

The protein precipitate obtained after ammonium sulphate fractionation was dissolved in minimum amount of 50 mM sodium phosphate buffer (pH 7.5) and was dialyzed against several changes of the same buffer (also containing 0.15 M NaCl). The dialyzed protein was filtered on Whatman paper and chromatographed on Sephacryl S-100HR column (60x1.7 cm) equilibrated with 50 mM sodium phosphate buffer, pH 7.5. A single peak giving significant papain inhibition was obtained [Fig. 12]. The fractions corresponding to the peak were pooled and were used for further analyses. The procedure provided a fold purification of 498.84 (~500) and percent yield of 20.4.

3.1.3 HOMOGENEITY OF THE PURIFIED INHIBITOR

As observed in Fig.12, the inhibitor eluted as a single symmetric peak with constant specific activity suggesting a homogenous preparation. In addition, the preparation did not inhibit bovine trypsin, chymotrypsin or pepsin. Physical evidence for homogeneity was further provided by gel electrophoresis under non-denaturing conditions. The electrophoretic pattern of PTPI is shown in Fig. 13, lane e. The inhibitor moved as a single band.

TABLE 6: RESULTS OF A TYPICAL PURIFICATION OF GOAT PANCREATIC THIOL PROTEINASE INHIBITOR

Step	Volume (ml)	Total protein (mg)[a]	Total Activity (Units)[b]	Specific Activity (Units/mg protein)	Fold Purification	Percent Yield
Crude extract	200	8000	106	0.013	1	100
Alkaline treatment	100	2899	76	0.026	2	71.6
Acetone fractionation	13	254.05	62.39	0.245	18.84	58.8
Ammonium sulphate cut (20-80%)	10	147.7	54.8	0.371	28.53	51.6
Sephacryl S-100 HR Chromatography	15	3.34	21.66	6.485	498.84	20.4

[a]Protein concentration was determined by the method of Lowry et al. [1951].
[b]One unit of enzyme inhibitory activity is defined as the amount of inhibitor bringing about 0.001 change in O. D. / ml/ min.

Fig. 12 Gel filtration chromatography on Sephacryl S-100 HR

The precipitate obtained from 20 to 80% ammonium sulphate saturation (after acetone fractionation) was dissolved and dialyzed against several changes of 50 mM sodium phosphate buffer, pH 7.5 containing 0.15 M NaCl. The sample was applied on Sephacryl S-100 HR column (60 x 1.7 cm) and fractions were eluted with the same buffer at a flow rate of 15 ml h^{-1}. Fractions of 5 ml were collected and monitored by inhibition of caseinolytic activity of papain. Fractions 7, 8, 9 were pooled for further studies.

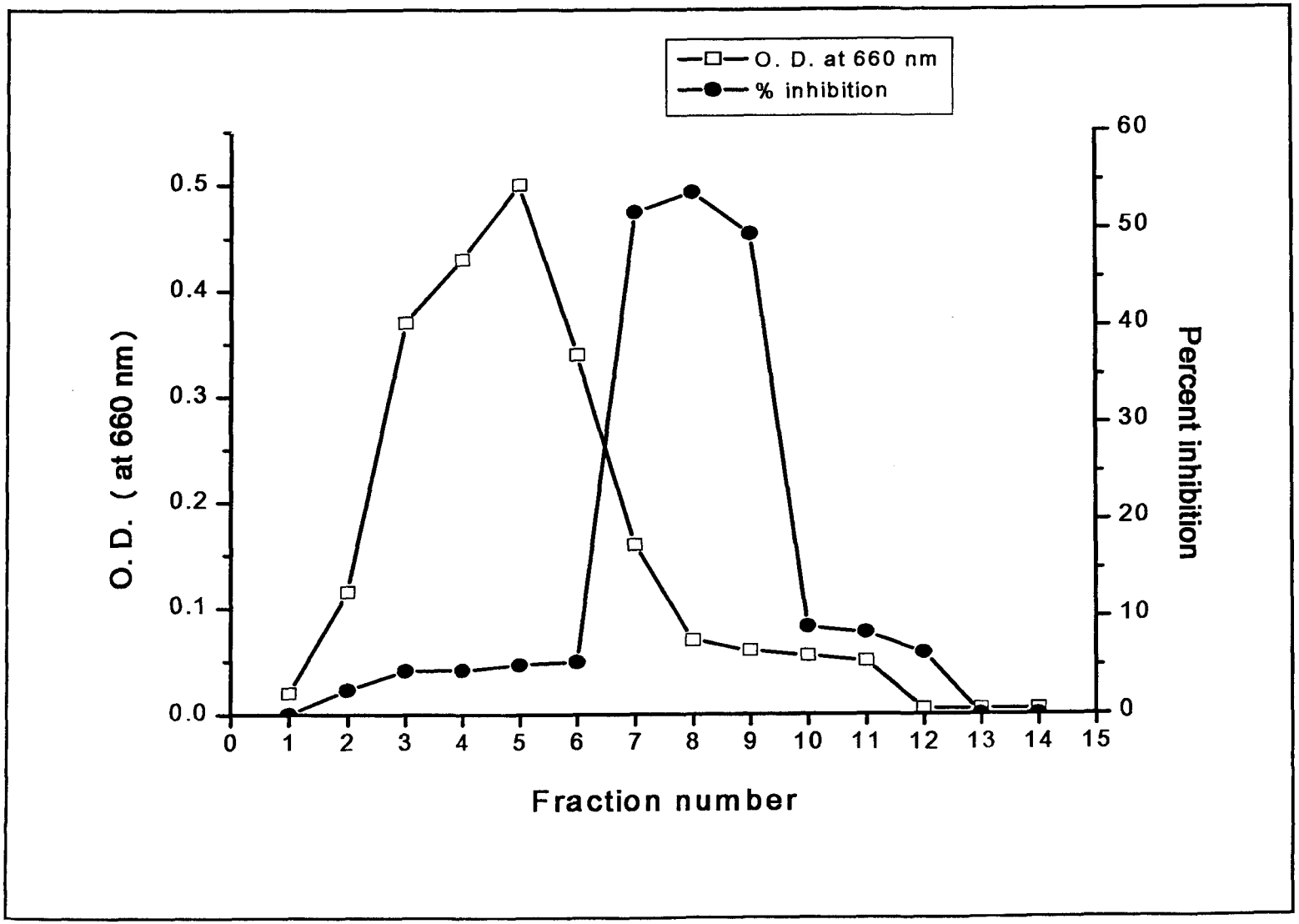
O. D. at 660 nm
% inhibition
O. D. (at 660 nm)
Percent inhibition
Fraction number
0.0
0.1
0.2
0.3
0.4
0.5
0
10
20
30
40
50
60
0 1 2 3 4 5 6 7 8 9 10 11 12 13 14 15

Fig. 13 **Gel electrophoresis of PTPI during various stages of purification**

Electrophoresis was performed on 7.5% acrylamide gel as described in methods section. Lane **a** contained 60 μg pancreas homogenate, lane **b** contained 60 μg homogenate after alkaline treatment, lane **c** is 60 μg fraction obtained after acetone treatment, lane **d** is 60 μg dialyzed fraction after ammonium sulphate fractionation, lane **e** is 60 μg pancreatic thiol proteinase inhibitor after Sephacryl S-100 gel filtration.

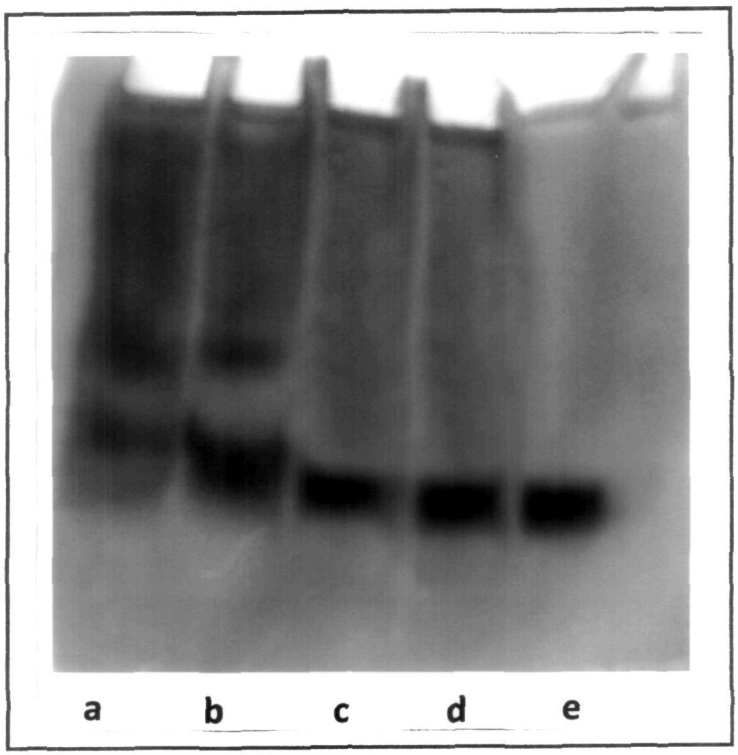
a
b
c
d
e

3.1.4 REDUCING AND NON-REDUCING PAGE

Purified PTPI was analyzed by SDS-PAGE under non-reducing (in the absence of β-mercaptoethanol) or reducing conditions (in the presence of β-mercaptoethanol). PTPI migrated as two bands with different mobilities, suggesting a double subunit structure with subunits held together by non-covalent forces [Fig.14].

3.1.5 PROPERTIES OF THE PURIFIED PANCREATIC THIOL PROTEINASE INHIBITOR

Molecular weight determination

The molecular weight of pancreatic thiol proteinase inhibitor was determined under native as well as denaturing conditions. The molecular weight of native PTPI was determined using gel filtration chromatography on Sephacryl S 100 HR. The marker proteins-Trypsin (23 kDa), Pepsin (35 kDa), Ovalbumin (43 kDa) and BSA (66 kDa) were chromatographed on the Sephacryl S 100 HR column (60 x 1.7 cm) equilibrated with 50 mM sodium phosphate buffer, pH 7.5 and their elution volume was determined. Analysis of the data indicated linear relationship between V_e/V_o and log M by the method of Andrews [1964] [Fig. 15], where V_e is the elution volume of the protein and V_o is the void volume of the column. The V_e/V_o of the native cystatin corresponds to molecular weight of 43650 (~44000) [Fig. 15].

The molecular weight of PTPI under denaturing conditions was calculated from its mobility in SDS-PAGE [Fig. 16a] by the procedure of Weber and Osborn [1969]. The mobilities of marker proteins were plotted against the logarithm of their molecular weights [Fig. 16b]. The least square analysis of the data indicated a linear relationship between log M and relative mobility (Rm). The molecular weight obtained was 43940 (~44000) (positions of two subunits corresponded to 23980 and 19960, without reduction). In the presence of βME the molecular weight was found to be 47194 (positions of two subunits corresponded to 25860 and 21334) [Fig. 16b].

Stokes radius

Stokes radius of a protein correlates well with its elution behaviour from gel filtration column. The stokes radius of PTPI was determined by its elution volume from a calibrated Sephacryl S 100 HR column (60 x 1.7 cm) equilibrated with 50 mM sodium phosphate buffer, pH 7.5 using marker proteins. The column was

Fig. 14 SDS Polyacrylamide gel electrophoresis of purified PTPI

Electrophoresis was performed on 12.5% gels as described in methods section. SDS PAGE was performed under non reducing and reducing conditions, lane a: non reducing condition (in the absence of β-mercaptoethanol), lane b: reducing conditions (in the presence of β-mercaptoethanol). Lanes a and b each contained 40μg of the inhibitor, respectively.

Fig. 15 Molecular weight estimation of purified PTPI using Sephacryl S-100 HR gel filtration chromatography

Purified PTPI was applied on a column of Sephacryl S-100 HR (60 x 1.7 cm) and eluted with 50 mM sodium phosphate buffer, pH 7.5 at a flow rate of 15 ml h^{-1}. The molecular weight markers used were, A trypsin (23 kDa); B pepsin (35 kDa); C ovalbumin (45 kDa); D bovine serum albumin (66 kDa). Arrow shows the position of PTPI elution.

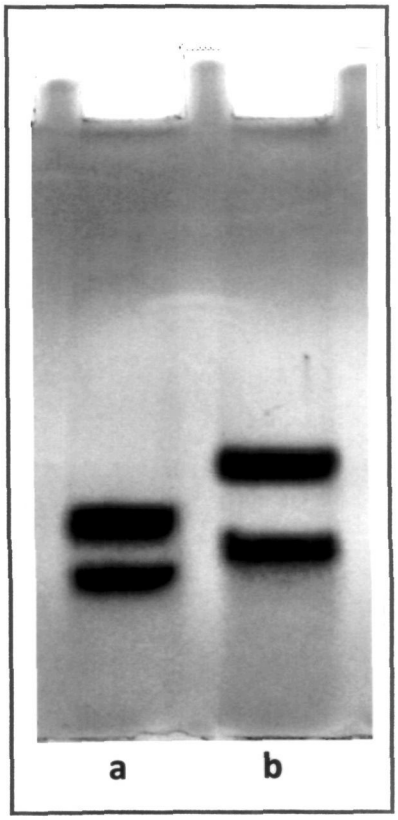
a
b

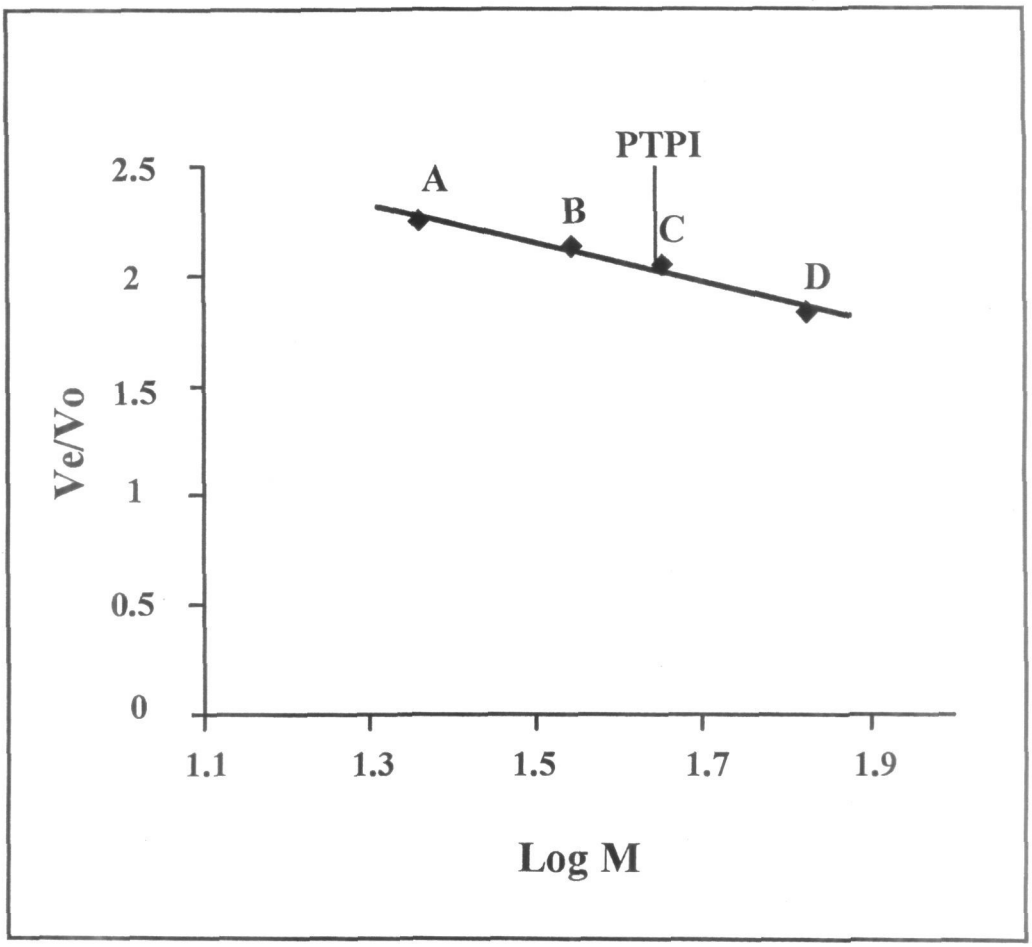
PTPI
A
B
C
D
2.5
2
1.5
1
0.5
0
Ve/Vo
1.1
1.3
1.5
1.7
1.9
Log M

Fig. 16 Molecular weight determination of PTPI by SDS-PAGE electrophoresis

(A) Electrophoresis was performed on 12.5% polyacrylamide gel. The middle gel lane contained the molecular mass standards: A, phosphorylase b (97.4 kDa); B, bovine serum albumin (68 kDa); C, ovalbumin (45 kDa); D, carbonic anhydrase (29.1 kDa); E, soyabean trypsin inhibitor (20 kDa); F, lysozyme (14.3 kDa). Lane a contained 40 μg PTPI without β-mercaptoethanol and lane b contained 40 μg of β-mercaptoethanol treated purified inhibitor.

(B) Plot of log M vs relative mobility (Rm) using least square analysis. The line indicates the positions of Subunit I and Subunit II of PTPI.

(A)

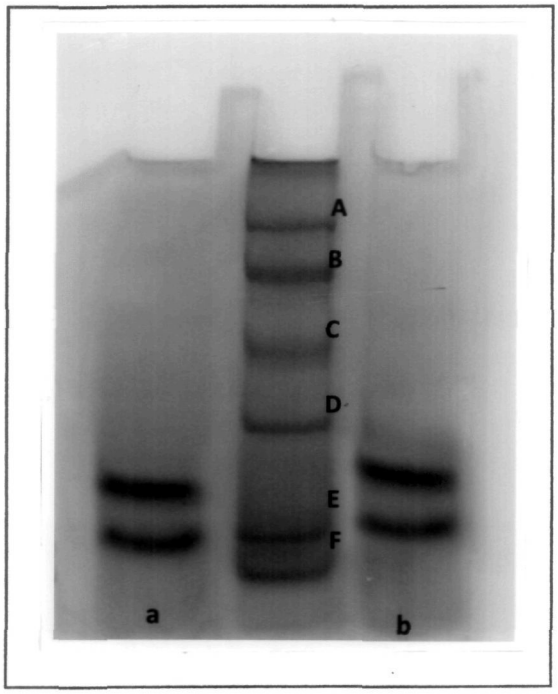
A
B
C
D
E
F
a
b

(B)

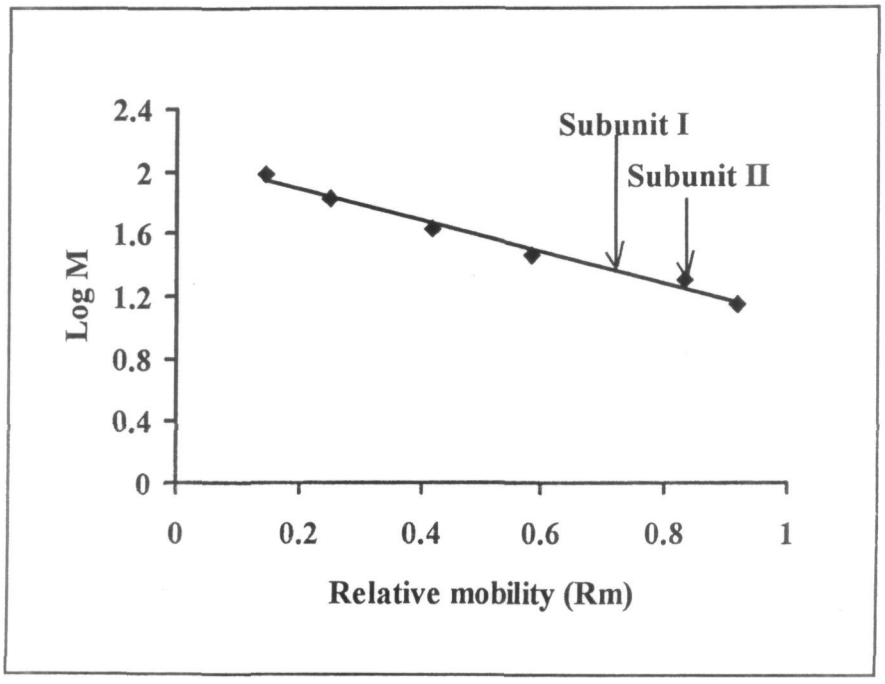
Subunit I
Subunit II
Log M
2.4
2
1.6
1.2
0.8
0.4
0
0
0.2
0.4
0.6
0.8
1
Relative mobility (Rm)

calibrated by determining the elution volume of several globular proteins with known stokes radii, such as Trypsin (20.2 Å), BSA (35.6 Å), ovalbumin (27.3 Å). The data was analyzed according to the equation,

$$K_{av} = \frac{V_e - V_o}{V_t - V_o}$$

Where, V_e= elution volume, V_o= void volume and V_t = total volume. K_{av} is the partition coefficient. The linear plot between known stokes radius and $[-\log K_{av}]^{1/2}$ of the marker proteins was used for the calculation of PTPI's stokes radius [Laurent and Killander, 1964]. As depicted in Fig. 17, the value was found to be 27.3 Å for the purified inhibitor.

Diffusion coefficient

Diffusion coefficient (D) of PTPI was found to be 7.87 x 10^{-7} cm^2 s^{-1}, computed from the value of its stokes radius by using the equation,

$$D = \frac{kT}{f} = \frac{kT}{6\pi\eta r}$$

Where k = 1.38 x 10^{-16} erg/deg is Boltzmann's constant, T is the absolute temperature and η is the coefficient of viscosity of the medium (0.01g/cm-sec for water and dilute aqueous salt solutions at 20°C). The sedimentation coefficient is given by the formula

$$S = \frac{M(1-v_2\rho)}{N_o f} = \frac{M(1-v_2\rho)}{N_o 6\pi\eta r}$$

Where M is the mass of the protein molecule in Da, N_o is the Avogadro's number, 6.023 x 10^{23}, v_2 is the partial specific volume of the protein (0.73 g/cm^3), and ρ is the density of the solvent (1.0 g/cm^3 for water). The ratio of S_{max}/S can be used to interpret the shape of the protein. In the hydrodynamic parameter S_{max}/S, S_{max} is the maximum possible sedimentation coefficient for a protein of the given mass, corresponding to a sphere of the minimum diameter, to contain mass of protein, with no water of hydration. The ratio of S_{max}/S is the same as f/f_{min}, where f is the actual frictional coefficient of the hydrated protein and f_{min} is the frictional coefficient of unhydrated minimal sphere [Tanford, 1961]. The sedimentation coefficient of PTPI was found to be 3.83 s. The S_{max}/S ratio of PTPI is 1.2.

Fig. 17 Determination of Stokes radius of PTPI by plot of Laurent and Killander [$(\log K_{av})^{1/2}$ vs r]

Marker proteins and the purified cystatin were subjected to gel filtration on Sephacryl S-100 HR (60 x 1.7 cm). The K_{av} values were computed from the elution volume of marker proteins. Stokes radii of the marker proteins were: A trypsin (20.2 Å); B ovalbumin (27.3Å); C bovine serum albumin (35.6 Å). Arrow shows the stokes radius of purified inhibitor. The experimental conditions were same as in Fig. 1.

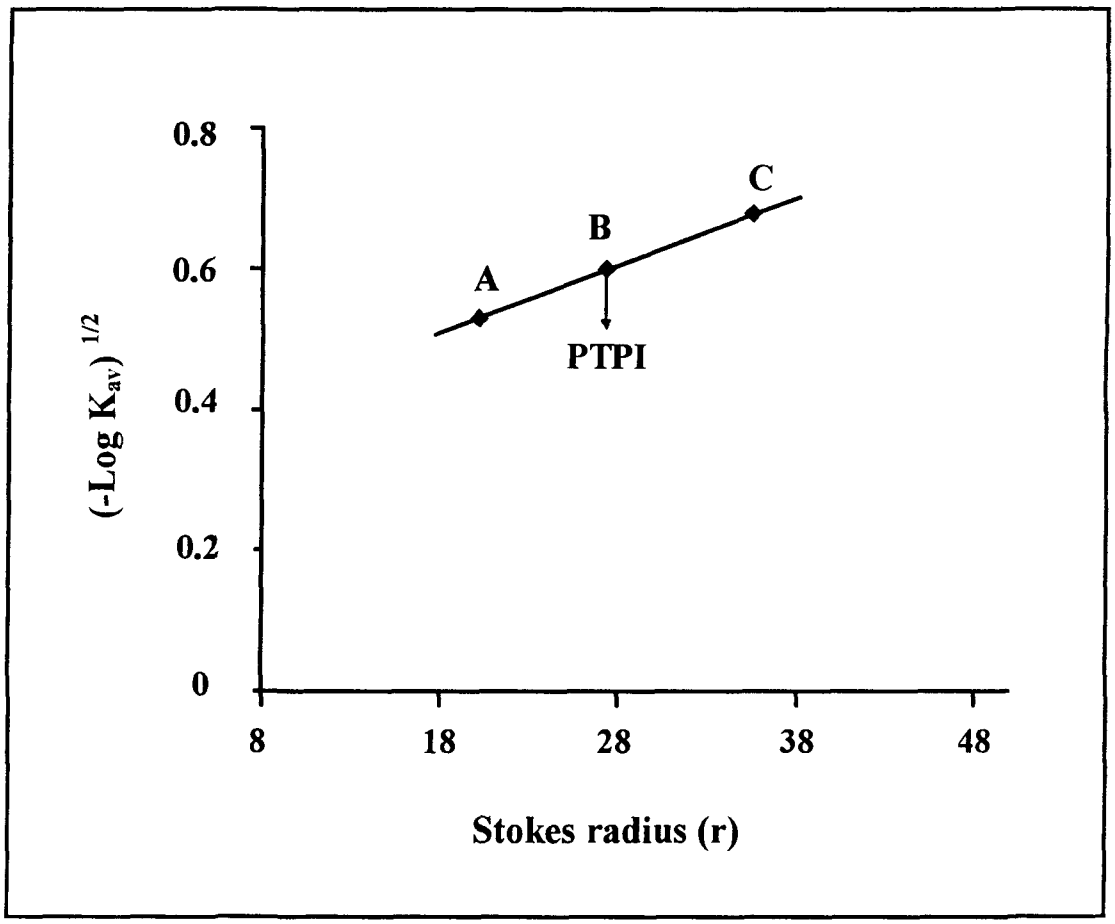
0.8
0.6
0.4
0.2
0
8
18
28
38
48
A
B
C
PTPI
(-Log K_{av}) $^{1/2}$
Stokes radius (r)

Carbohydrate content

Type 1 and type 2 cystatins, generally, lack carbohydrate content. Dissimilar to this PTPI was found to possess 2.32% carbohydrate content.

Sulphydryl group content

The sulphydryl groups in PTPI were titrated against DTNB. Colourless solution obtained indicated that no free sulphydryl groups are present in the purified inhibitor.

Effect of pH on activity of PTPI

Effect of pH on the thiol proteinase inhibitory activity of pancreatic thiol proteinase inhibitor was examined at various pH values. Fig. 18 shows that the inhibitor is stable in the pH range 3.0-10.0 and has maximum activity at pH 7.5.

Effect of temperature on activity of PTPI

Stability of PTPI was investigated as a function of temperature between 30 and 90°C in 50 mM sodium phosphate buffer pH 7.5, by means of inhibitory activity assay. PTPI remained maximally active within temperature range of 30-70°C [Fig. 19].

Temperature stability of PTPI

Goat PTPI was exposed to 90°C for varying time intervals, rapidly cooled and inhibitory activity determined by method of Kunitz [1947]. As illustrated in Fig. 20, PTPI retained approximately 40% of its activity till 120 min. The inhibitor was thus stable for 120 min at 90°C.

3.1.6 IMMUNOLOGICAL PROPERTIES

Antibody titre

The PTPI caused good immune response and the resulting antiserum had a titre of 25,118.86 as determined by direct binding ELISA in rabbit serum [Fig. 21].

Cross-reactivity

PTPI was immunogenic and induced antibody formation in rabbits. The antiserum raised against purified inhibitor showed cross reactivity with the inhibitor (indicated by single precipitin line on immunodiffusion plate) exhibiting immunogenic purity

Fig. 18 Effect of pH on activity of PTPI

50 μg of the inhibitor was incubated in 50 mM sodium acetate buffer, pH 3.0-6.0, sodium phosphate buffer, pH 7.0-8.0, tris-HCl buffer, pH 9.0, for 30 min at 37°C. After the incubation the pH of the mixture was neutralized and then 50 μg of activated papain was added and the mixture was further incubated for 60 min at 37°C. The following procedure was same as described in methods section for assaying the inhibitor using casein as substrate.

Fig. 19 Effect of temperature on PTPI

50 μg of the inhibitor was incubated in 50 mM sodium phosphate buffer, pH 7.5, at various temperatures for 30 min and then rapidly cooled. 50 μg of activated papain was added and kept for 60 min at 37°C. the remaining procedure for determining thiol proteinase inhibitory activity was same as described in methods section using casein as substrate.

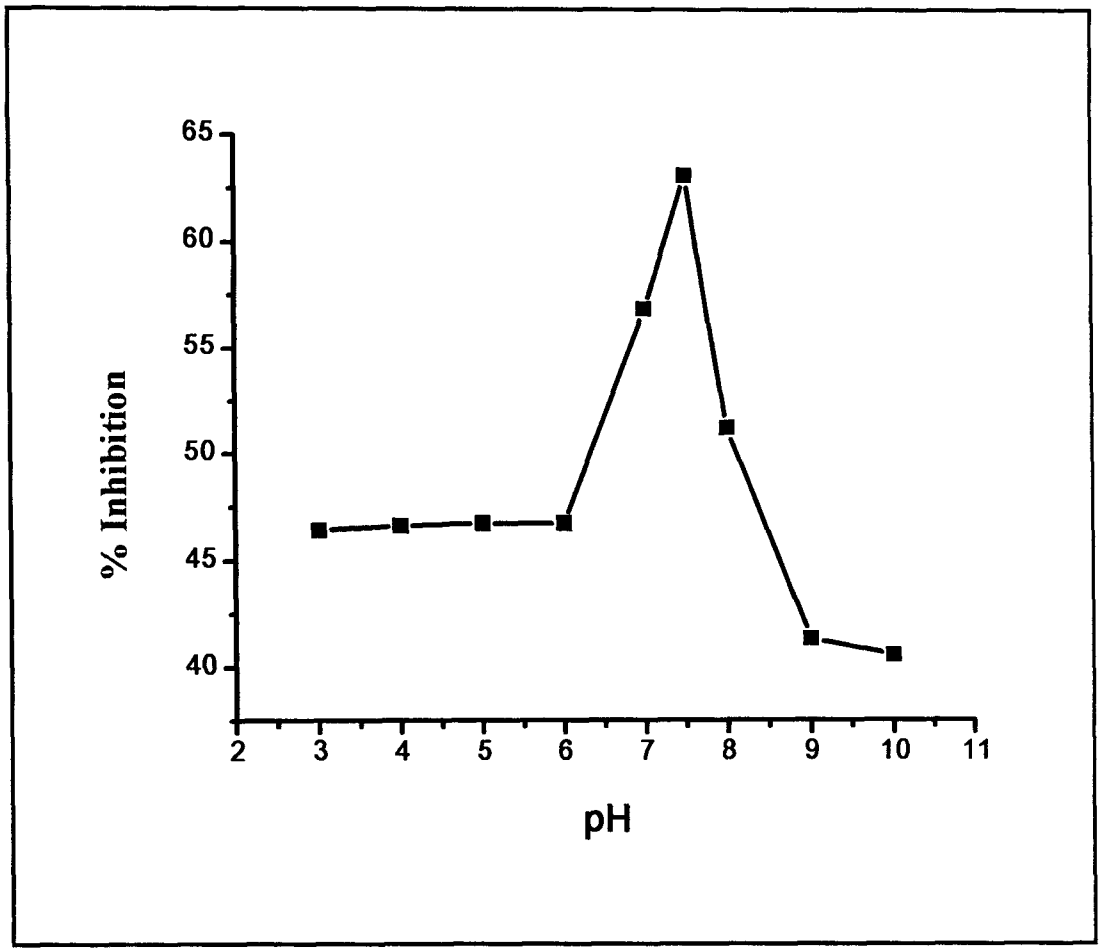
% Inhibition
65
60
55
50
45
40
2
3
4
5
6
7
8
9
10
11
pH

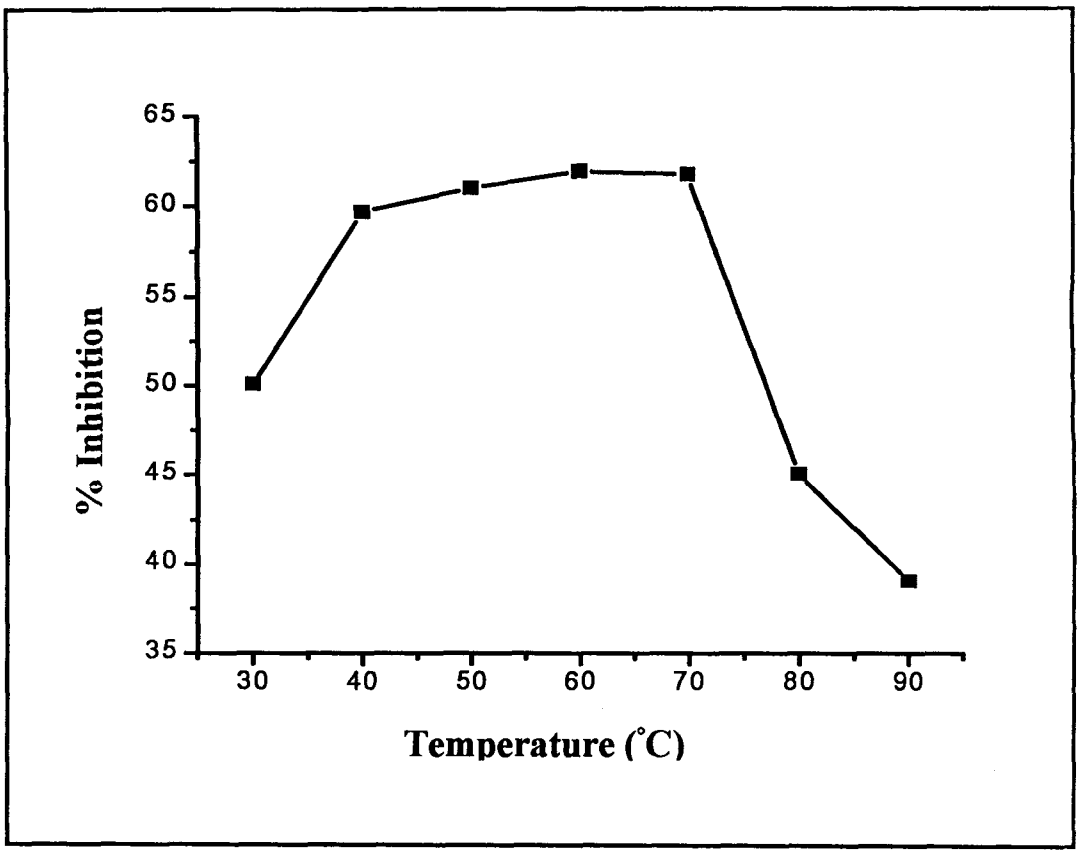
% Inhibition
65
60
55
50
45
40
35
30
40
50
60
70
80
90
Temperature (°C)

Fig. 20 Thermal stability of PTPI

50 μg of the inhibitor was incubated in 50 mM sodium phosphate buffer, pH 7.5, at 90°C for different time intervals, rapidly cooled. 50 μg of activated papain was added and incubated for 60 min at 37°C. Rest of the procedure was same as described in methods.

Fig. 21 Direct binding ELISA

Serially diluted antiserum and pre-immune serum were incubated with 0.5 μg/100 μl antigen. The procedure has been described in methods. The curve with hollow circles is for post-immunized sera, whereas the curve with solid circles is for pre-immunized sera.

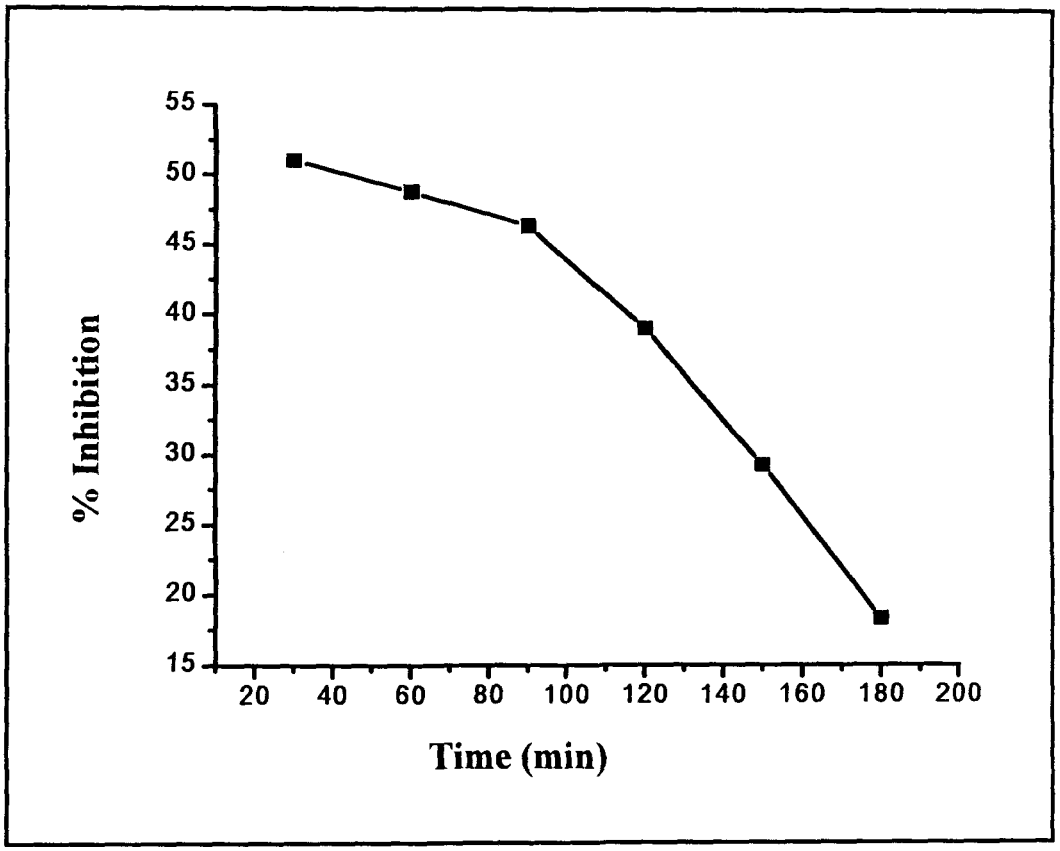
% Inhibition
55
50
45
40
35
30
25
20
15
20
40
60
80
100
120
140
160
180
200
Time (min)

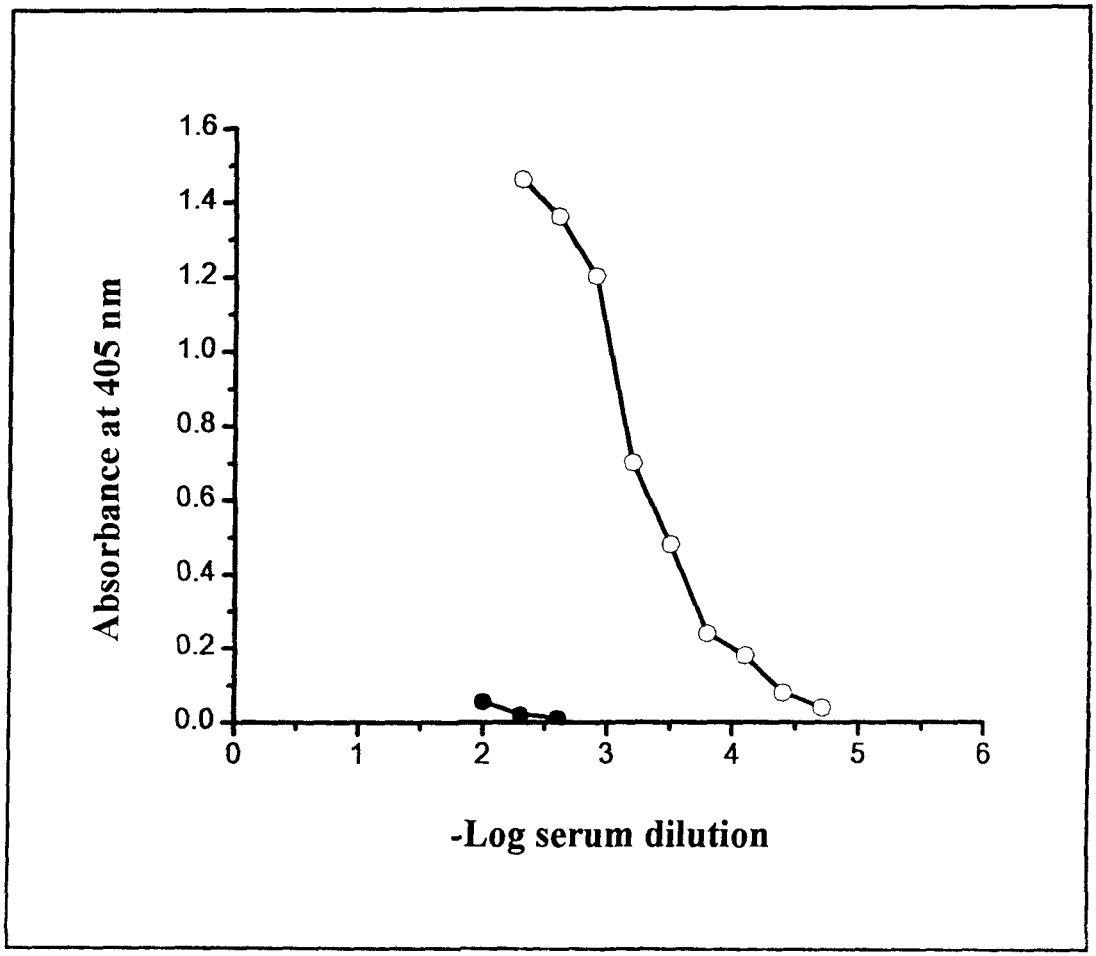
Absorbance at 405 nm
1.6
1.4
1.2
1.0
0.8
0.6
0.4
0.2
0.0
0
1
2
3
4
5
6
-Log serum dilution

and homogeneity of the inhibitor preparation [Fig. 22]. It exhibited no immunogenic identity with goat lung and brain cystatins isolated in our laboratory.

3.1.7 KINETIC PROPERTIES OF PTPI

Stoichiometry of Inhibition

The inhibition of proteinases was studied by varying their molar concentration at a fixed molar concentration of PTPI. The remaining activity of proteinase showed that as its concentration is increased from 0.01-0.06 μM it is progressively inhibited by 0.06 μM PTPI giving a stoichiometric ratio of 1:1, thus one molecule of PTPI inhibits one molecule of active proteinase. Same result was obtained for ficin and bromelain.

Inhibition of different proteinases

The inhibitory activity of PTPI towards thiol proteinases, papain, ficin and bromelain and serine proteinases, trypsin and chymotrypsin was examined using casein as substrate. PTPI inactivated papain and ficin very efficiently and bromelain to a slightly lesser extent. The order of inhibition was papain > ficin > bromelain. However it failed to inhibit bovine trypsin and chymotrypsin [Fig. 23].

Ki determination

Dissociation equilibrium constants (measured as Ki), for the binding of PTPI to plant cysteine proteinases papain, ficin and bromelain, were determined by monitoring the loss of enzyme activity and after lowering the respective inhibitor and proteinase concentration, which favour the dissociation of the complex. Ki values were determined using the steady state equation derived by Krupka and Laidler [1959],

$$\frac{[I]_o}{1-(V_i/V_o)} = Ki\left[\frac{1+[S]_o}{Km}\right]\left(\frac{V_i}{V_o}\right)+[E]_o$$

The increasing values of Ki (app) with an increase in the substrate concentration suggested a competitive mechanism of inhibition. The true Ki values were obtained from the replot of Ki (app) versus substrate concentration. The Ki values obtained for papain, ficin and bromelain are 5.88, 9.02 and 22.28 nM, respectively, implying the highest affinity of inhibitor for papain [Fig. 24-26: inset].

Fig. 22 Ouchterlony immunodiffusion

Anti-PTPI antiserum was raised in rabbits. For the immunodiffusion study, the antiserum was allowed to react with inhibitor (60 μg) on agarose plates as described in methods section. The central well contained the antiserum, whereas the surrounding three well contained purified PTPI.

Fig. 23 Inhibitory activity of PTPI with different proteinases

50 μg of thiol proteinases papain, ficin, bromelain and serine proteinases, trypsin and chymotrypsin were incubated with varying concentrations of PTPI (0-30 μg) for 30 min. The inhibitory activity of PTPI towards these proteinases was measured by using 2% casein as substrate.

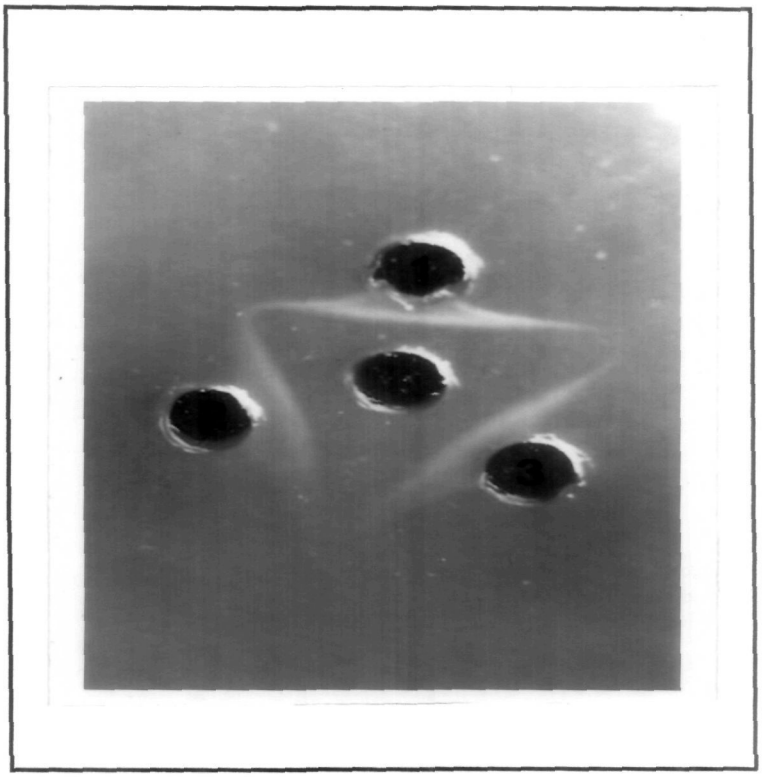

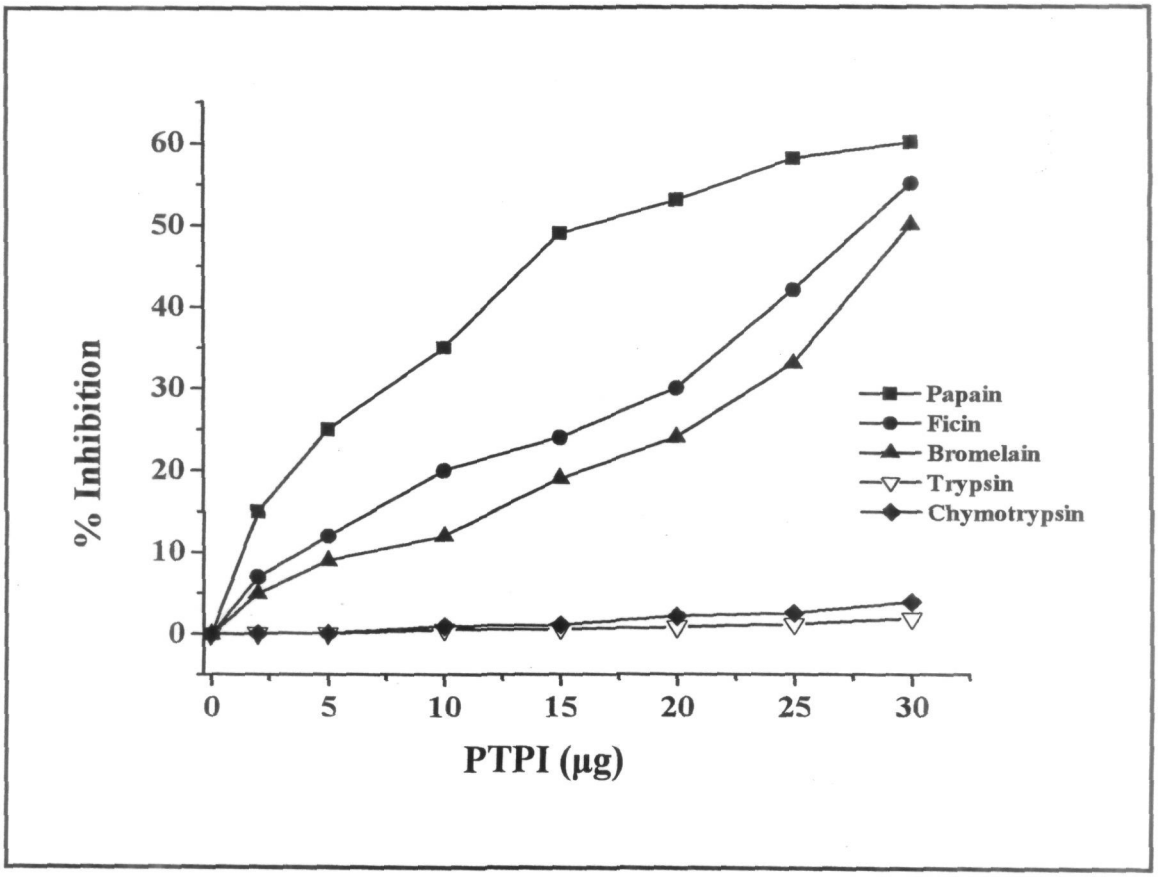
% Inhibition
PTPI (µg)
0
10
20
30
40
50
60
0
5
10
15
20
25
30
Papain
Ficin
Bromelain
Trypsin
Chymotrypsin

Fig. 24 **Determination of inhibition constant with (Ki) papain**

Papain was used at final concentration of 0.06 μM with increasing amounts of PTPI (0.06-0.24 μM) and measurements of residual activity were made as described in methods using casein as substrate. Four different substrate concentrations were used, i.e. 0.5 Km, 1 Km, 2 Km and 3 Km with Km = 2.4 mM. For the sake of clarity only the result obtained for [S] = 0.5 Km are shown. The inset shows the replot of experimental Ki (app) values versus [S]. Intercept on the ordinate give the true Ki.

Fig. 25 **Determination of inhibition constant (Ki) with ficin**

Ficin was used at final concentration of 0.06 μM with increasing amounts of PTPI (0.06-0.24 μM) and measurements of residual activity were made as described in methods using casein as substrate. Four different substrate concentrations were used, i.e. 0.5 Km, 1 Km, 2 Km and 3 Km with Km = 2.4 mM. For the sake of clarity only the result obtained for [S] = 0.5 Km are shown. The inset shows the replot of experimental Ki (app) values versus [S]. Intercept on the ordinate give the true Ki.

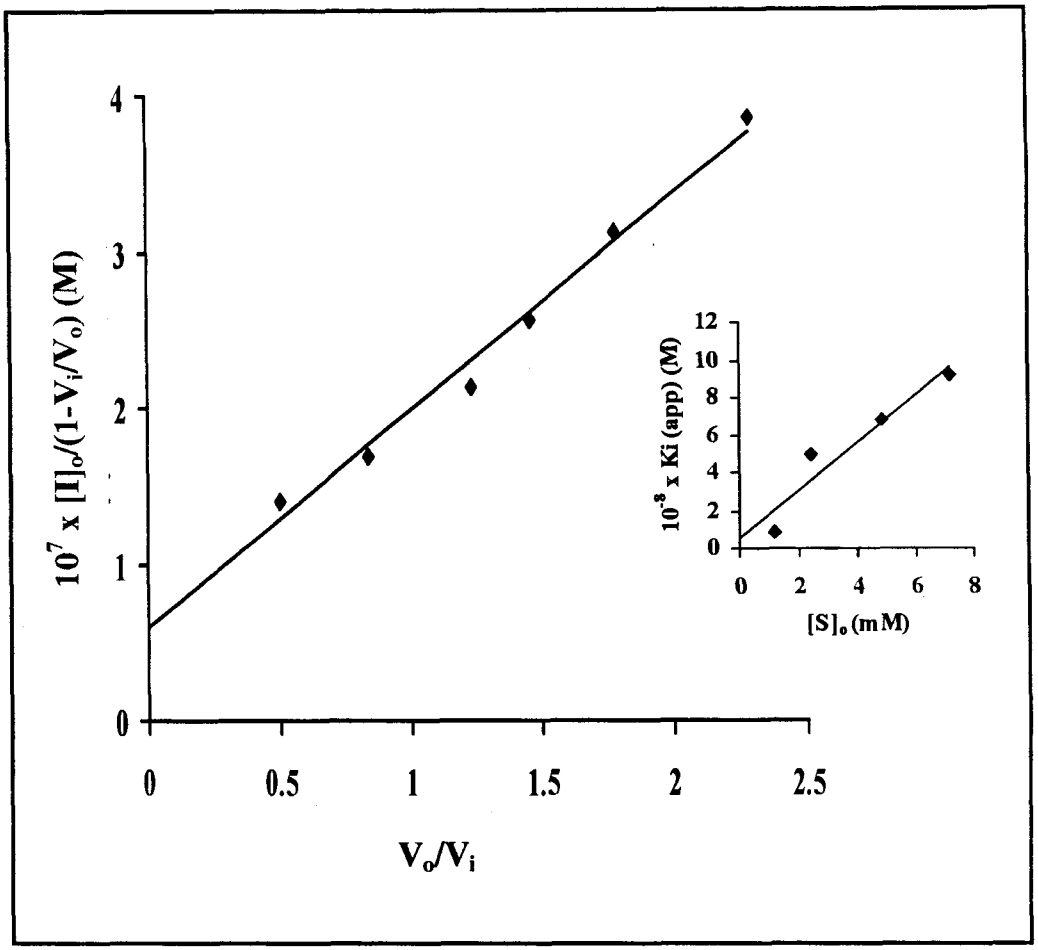
10^7 x $[I]_o/(1-V_i/V_o)$ (M)
V_o/V_i
10^{-8} x Ki (app) (M)
$[S]_o$ (mM)

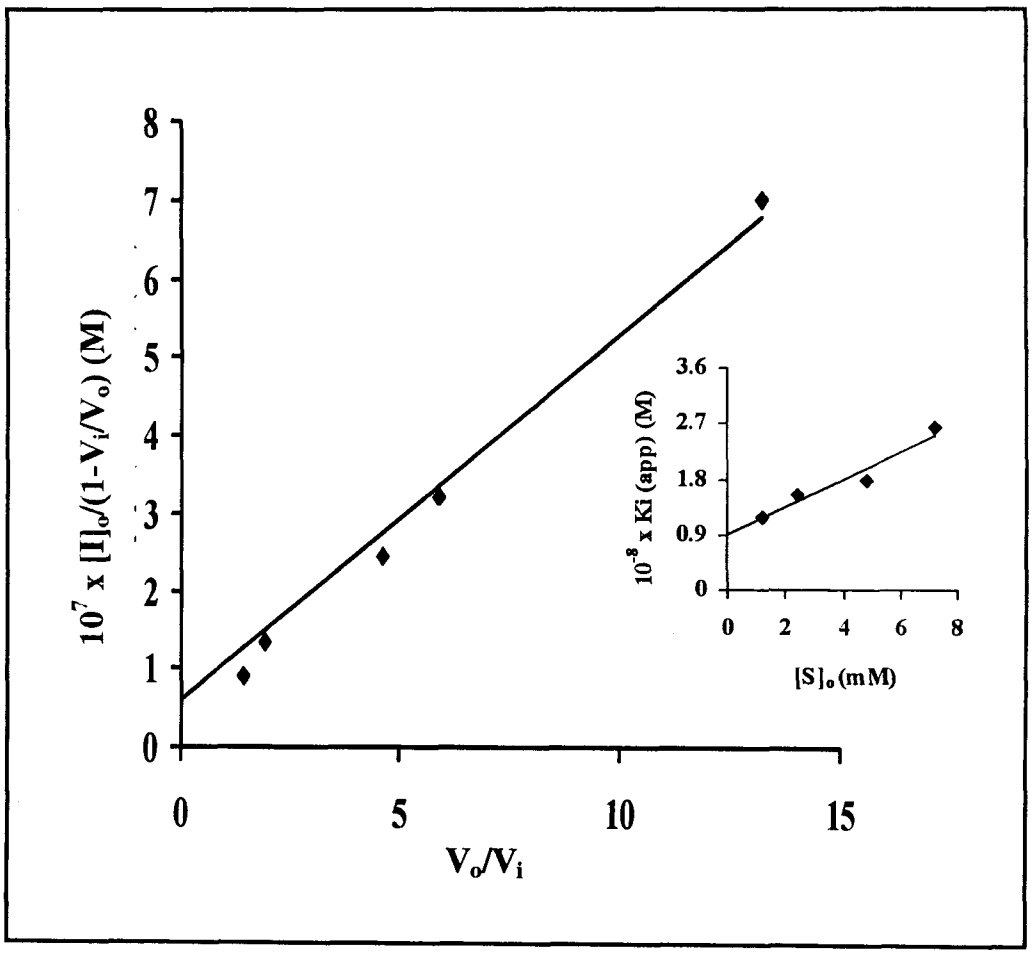
10^7 x $[I]_o/(1-V_i/V_o)$ (M)
V_o/V_i
10^{-8} x Ki (app) (M)
$[S]_o$ (mM)

Fig. 26 Determination of inhibition constant (Ki) with bromelain

Bromelain was used at final concentration of 0.06 μM with increasing amounts of PTPI (0.06-0.24 μM) and measurements of residual activity were made as described in methods using casein as substrate. Four different substrate concentrations were used, i.e. 0.5 Km, 1 Km, 2 Km and 3 Km with Km = 2.4 mM. For the sake of clarity only the result obtained for [S] = 0.5 Km are shown. The inset shows the replot of experimental Ki (app) values versus [S]. Intercept on the ordinate give the true Ki.

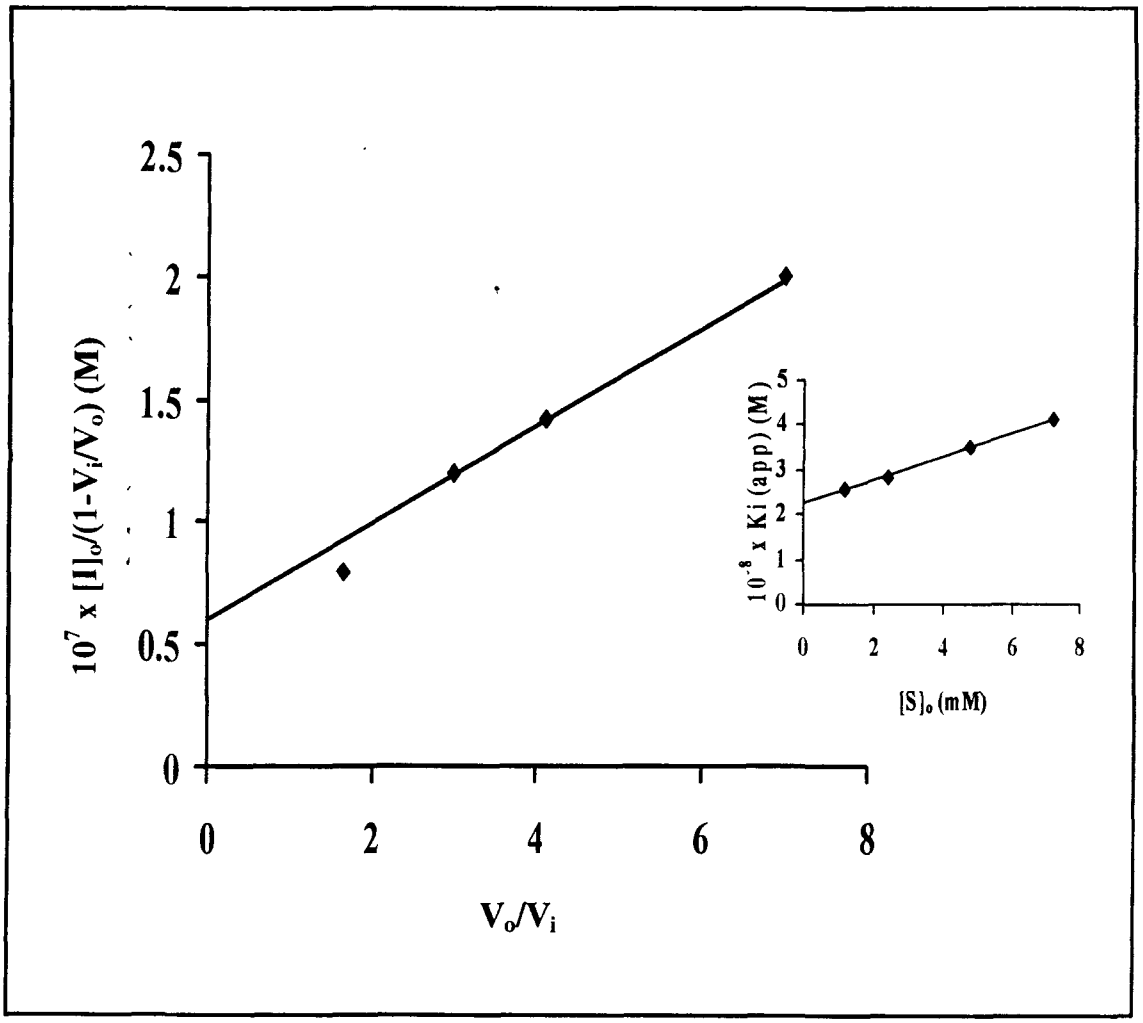
2.5
2
1.5
1
0.5
0
0
2
4
6
8
10^7 x [I]$_o$/(1-V_i/V_o) (M)
V_o/V_i
5
4
3
2
1
0
0
2
4
6
8
10^{-8} x Ki (app) (M)
[S]$_o$ (mM)

IC50 value

IC50 value is the concentration of the inhibitor at which 50% of the enzyme is inhibited. The IC50 values obtained with various thiol proteinases are summarized in table 7. The values obtained for the three proteinases, papain, ficin and bromelain, are 0.08, 0.078 and 0.154 μM, respectively, again suggesting greater affinity of the inhibitor for papaya proteinase.

Dissociation rate constant (K_{-1})

The conditions for the dissociation were taken such that the enzyme-inhibitor complex obeys first order kinetics during the initial part of the reaction. In this case the integrated form of the equation is given by,

$$\ln\left(\frac{[EI]}{[EI]_o}\right) = K_{-1}\, t$$

$$\log\left(\frac{[EI]}{[EI]_o}\right) = K_{-1}\, t / 2.303$$

Figures 27, 28 and 29 show the respective plots for papain, ficin and bromelain. The K_{-1} values obtained for papain, ficin and bromelain are 8.76×10^{-5}, 3.35×10^{-4} and 1.32×10^{-4} s^{-1}, respectively.

Association rate constant (K_{+1})

Association rate constants calculated from measured dissociation rate and dissociation equilibrium constants by the relation,

$$K_{+1} = \frac{K_{-1}}{Ki}$$

and hence the affinity of the inhibitor for proteinases is in the following order: papain (1.49×10^4 $M^{-1}s^{-1}$) > ficin (1.39×10^4 $M^{-1}s^{-1}$) > bromelain (5.94×10^3 $M^{-1}s^{-1}$).

Half life of the complex

The half life values of enzyme-inhibitor complexes were calculated using K_{-1} values by the equation,

$$t_{½} = \frac{0.693}{K_{-1}}$$

The calculated half-life values of papain-PTPI complex was 7.91×10^3 s, for

TABLE 7: KINETIC CONSTANTS OBTAINED ON INTERACTION OF PTPI WITH PROTEINASES – PAPAIN, FICIN AND BROMELAIN

Proteinase	Papain	Ficin	Bromelain
Ki (nM)	5.88±0.06	9.02±0.08	22.28±0.11
K_{+1} (M^{-1} s^{-1})	1.49±0.03x10^4	1.39±0.02x10^4	5.94±0.02x10^3
K_{-1} (s^{-1})	8.76±0.01x10^{-5}	3.35±0.02x10^{-4}	1.32±0.02x10^{-4}
Half life value (s)	7.91x10^3	5.51x10^3	5.23x10^3
IC50 (μM)	0.08	0.078	0.154

Results represent the mean ± SEM calculated from three independent experiments.

Fig. 27 **Determination of dissociation rate constant (K_{-1}) with papain**

Papain-PTPI complex (1μM) was preincubated for 30 min at 37°C before excess substrate was added to the mixture. Appearance of papain activity was recorded as a function of time. Inset shows plot of the data as described in methods.

Fig. 28 **Determination of dissociation rate constant (K_{-1}) with ficin**

Ficin-PTPI complex (1μM) was preincubated for 30 min at 37°C before excess substrate was added to the mixture. Appearance of papain activity was recorded as a function of time. Inset shows plot of the data as described in methods.

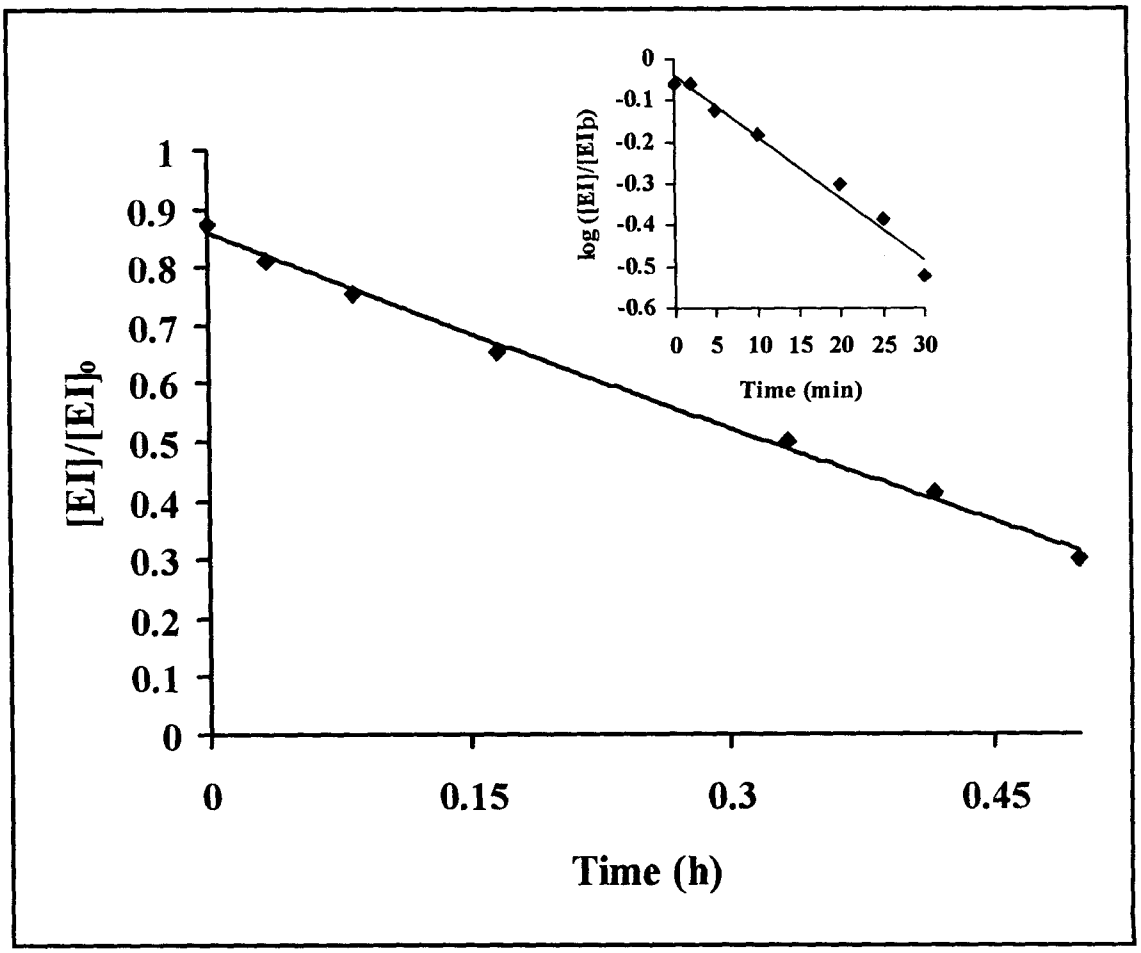
[EI]/[EI]o
1
0.9
0.8
0.7
0.6
0.5
0.4
0.3
0.2
0.1
0
0
0.15
0.3
0.45
Time (h)
log ([EI]/[EIb)
0
-0.1
-0.2
-0.3
-0.4
-0.5
-0.6
0 5 10 15 20 25 30
Time (min)

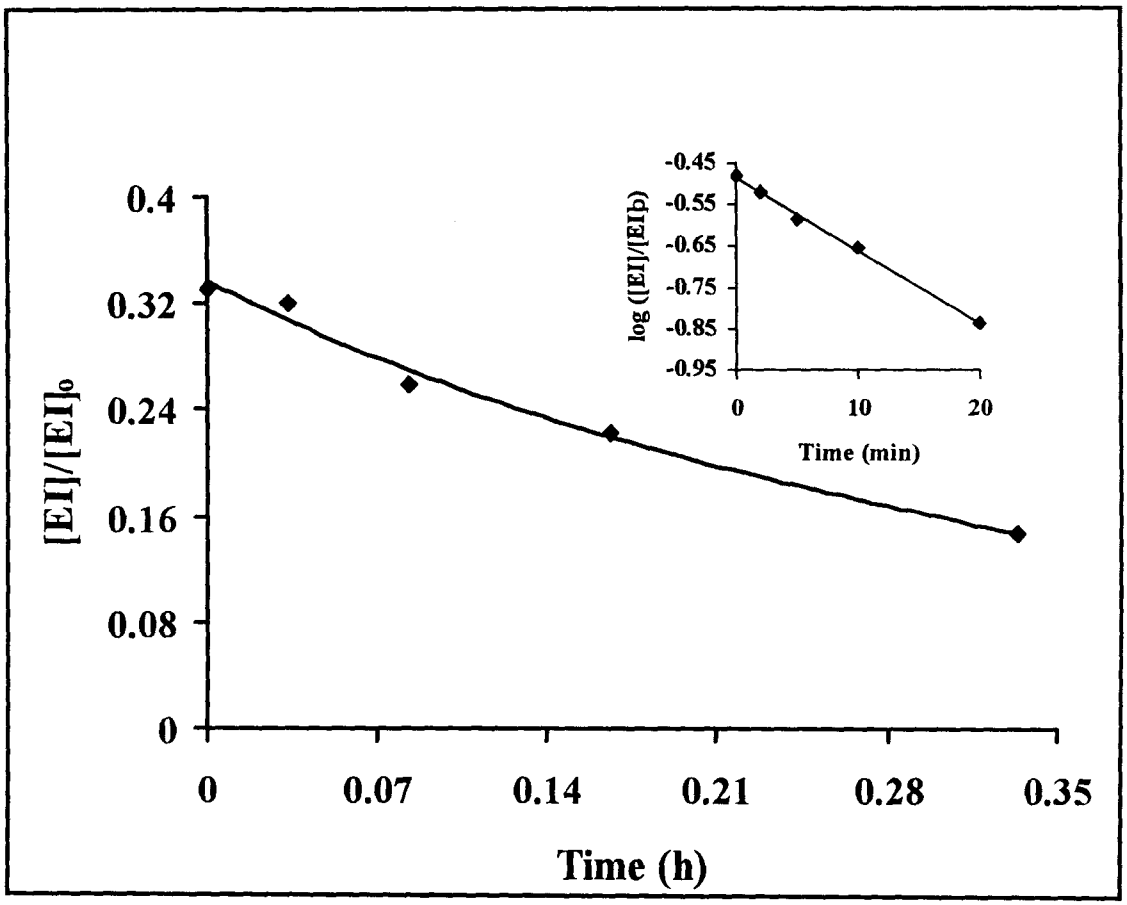
[EI]/[EI]o
0.4
0.32
0.24
0.16
0.08
0
0
0.07
0.14
0.21
0.28
0.35
Time (h)
log ([EI]/[EIb)
-0.45
-0.55
-0.65
-0.75
-0.85
-0.95
0
10
20
Time (min)

Fig. 29 Determination of dissociation rate constant (K_{-1}) with bromelain

Bromelain-PTPI complex (1μM) was preincubated for 30 min at 37°C before excess substrate was added to the mixture. Appearance of papain activity was recorded as a function of time. Inset shows plot of the data as described in methods.

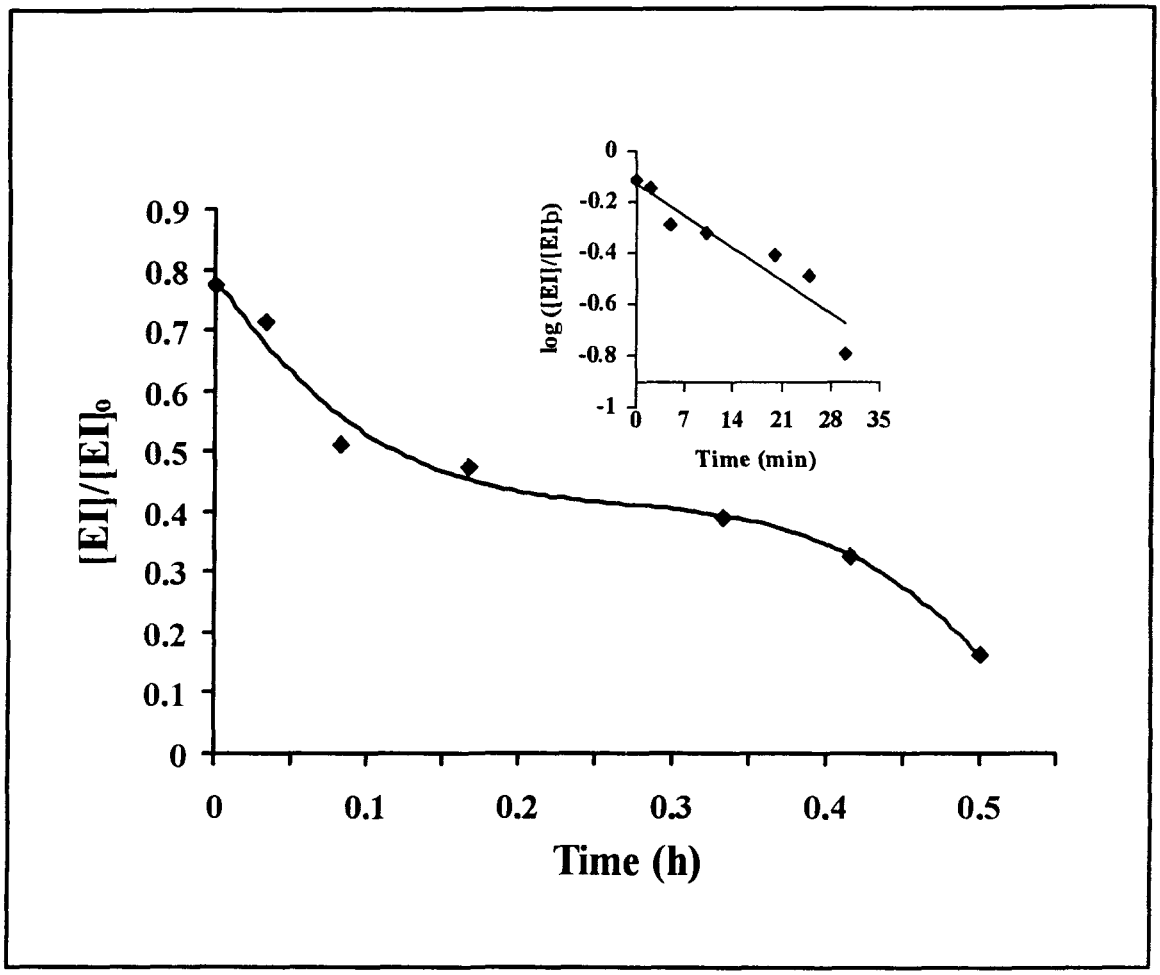
0.9
0.8
0.7
0.6
0.5
0.4
0.3
0.2
0.1
0
[EI]/[EI]o
0
0.1
0.2
0.3
0.4
0.5
Time (h)
0
-0.2
-0.4
-0.6
-0.8
-1
log ([EI]/[EI]o)
0
7
14
21
28
35
Time (min)

ficin-PTPI complex was 5.51 x 10^3 s and 5.23 x 10^3 s for bromelain-PTPI complex.

3.1.8 N-TERMINAL ANALYSIS

The N-terminal 24 amino acid residues of the heavier subunit (23.98 kDa) of PTPI were sequenced by the automated Edman degradation method. Table 8 shows the amino-terminal sequence of goat pancreatic thiol proteinase inhibitor and its sequence homology with other known mammalian cystatins. As in other cystatins, PTPI was found to possess a conserved glycine residue at 11^{th} position. Maximum sequence homology was observed with bovine skin cystatin C as compared to other cystatins like bovine parotid cystatin C, bovine colostrum cystatin C, human cystatin C, human stefin A & B, human placental cystatin and cystatin E.

HYDROPATHY PLOT

Using the sequence obtained from N-terminal analysis of PTPI, a hydropathy plot was made using the respective hydropathy indices [Kyte and Doolittle, 1982]. Among 24 residues sequenced, the stretch of 3–7, 7–11 and 15–19 residues has maximum hydropathy index suggesting that these residues might be present inside the hydrophobic core of the protein [Fig. 30].

3.1.9 SPECTRAL ANALYSES

Absorption spectrum

PTPI gave typical protein absorption with a maximum at 278 nm and a minimum at 250 nm. The ratio of the absorbance at 280/260 nm is 1.3 [Layne, 1957]. The millimolar absorption coefficient at 280 nm of PTPI is found to be 22.1 $mM^{-1}cm^{-1}$ by taking molecular weight value of 44,000. The interaction of inhibitor and papain at its stoichiometric ratio was studied at pH 7.5. Absorption difference spectrum of papain-PTPI complex showed peaks in the region of 245-255 nm, at 280 nm, negative peaks at around 290 nm and a shoulder at 260 nm [Fig. 31].

Fluorescence emission spectrum

After excitation at 280 nm, where phenol and indole groups absorb, the PTPI exhibits an emission spectrum with a maximum (λ_{max}) at 335 ± 1 nm which points to the non-polar tryptophyl side chains in the protein [Burstein et al., 1973].

TABLE 8: N-TERMINAL AMINO ACID SEQUENCE OF PTPI: A COMPARISON

Goat PTPI	**V**	**E**	V	**D**	D	A	**I**	V	V	**V**	**G**	Y	Y	**K**	**A**	**A**	Q	**V**	P	Y	Q	H	**A**	**H**
Human placental cystatin (8.33%)	Y	**E**	D	**D**	E	P	V	L	L	E	**G**	L	I	R	L	D	D	G	F	V	I	L	G	L
Human cystatin E (8.33%)	**V**	G	E	L	R	D	L	F	A	R	R	P	A	V	Q	K	A	A	Q	A	A	V	**A**	S
Bovine parotid cystatin C (12.5%)									L	L	**G**	G	L	M	E	**A**	D	**V**	M	E	E	G	G	Q
Human cystatin C (12.5%)	S	S	P	G	K	P	P	R	L	**V**	**G**	G	P	H	D	**A**	S	**V**	E	E	E	G	V	R
Bovine skin cystatin- C (20%)										L	**G**	G	L	H	E	**A**	D	**V**	N					
Bovine colostrum cystatin C (11.8%)								R	L	L	**G**	G	L	H	E	**A**	D	**V**	N	E	E	G	V	Q
Human stefin B (5.8%)							M	M	C	G	A	P	S	A	T	Q	P	A	T	A	E	T	Q	**H**
Human stefin A (5.8%)							M	I	P	G	**G**	L	S	E	**A**	M	P	A	T	P	E	I	Q	E
Human α_2 kininogen (14.3%)	**E**	-	S	Q	S	E	E	I	D	C	N	D	**K**	D										
Bovine α_2 kininogen (7.1%)	**E**	-	S	S	Q	-	E	I	D	C	N	D	P	Q	Q									
Sheep plasma LMW K1 (10%)	D	Q	H	K	S	E	**I**	A	Q	S														

The highly purified cystatin was transferred to PVDF membrane by Western blotting before doing amino acid analysis. Percent homology with other known cystatin N-terminal sequences is indicated in parenthesis.

Fig. 30 Hydropathy plot of the N-terminal residues of heavy subunit of PTPI

The hydropathy calculation was made according to the method of Kyte and Doolittle [1982] using already known hydropathy index of the 24 amino acid residues. A window size of 4 was selected for plot formation. The upper part of the graph shows the hydrophobic, and lower part hydrophilic regions.

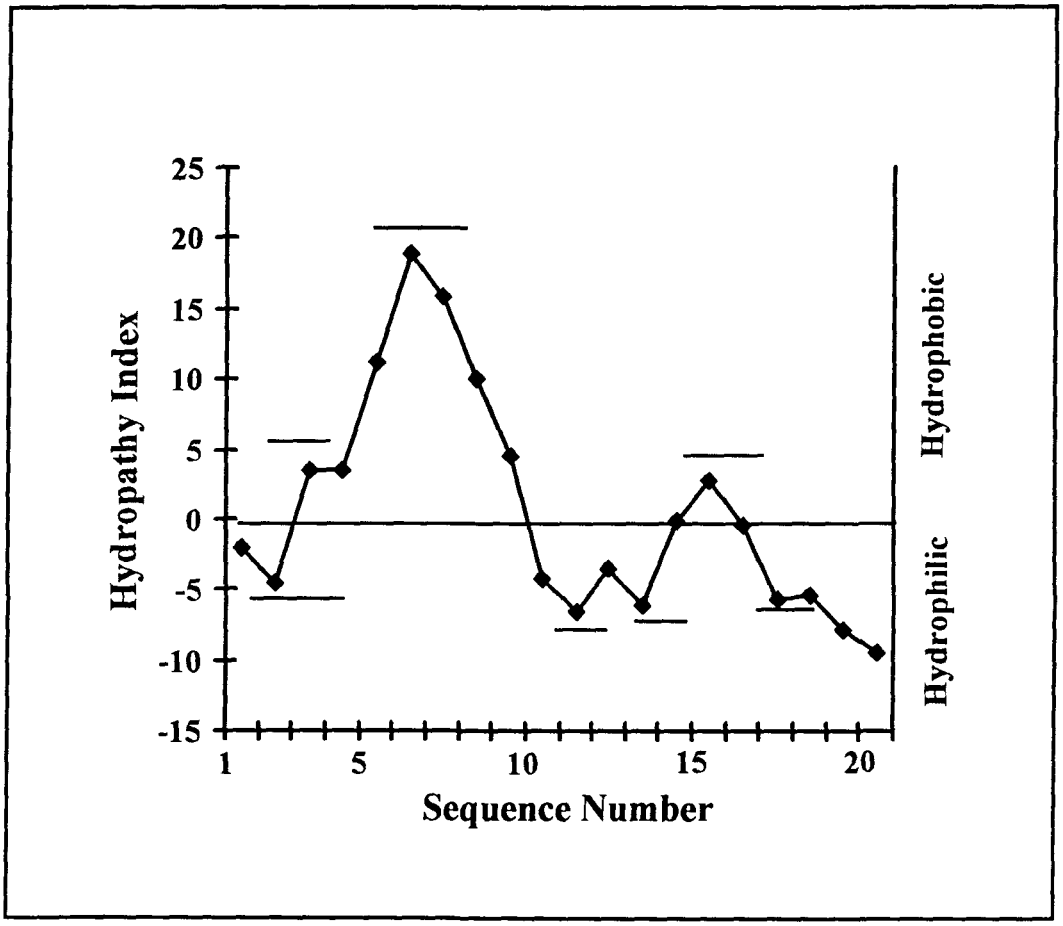
25
20
15
10
5
0
-5
-10
-15
Hydropathy Index
Hydrophobic
Hydrophilic
1
5
10
15
20
Sequence Number

The binding of PTPI to papain was accompanied by appreciable changes in fluorescence emission [Fig. 32]. There was a shift of fluorescence maximum to longer wavelength (from 335 to 345 nm) with considerable enhancement (+21.62%) of fluorescence intensity at λ_{max}.

Circular dichroism spectra of native PTPI and its complex with papain

The far-UV CD spectra of PTPI revealed α-helical structure of 17.18% [Fig. 33] [calculated using equation described by Chen et al., 1972]. Complexation of PTPI with papain resulted in complete loss of negative peaks and a strong positive peak is observed [Fig. 34]. Complex formation with papain abolished the native secondary structure and resulted in shifting of absorption maximum.

Fig. 31 UV-Absorption difference spectra measured for PTPI-papain complex

PTPI (2.66 μM) was incubated with activated papain for 30 min and an absorbance difference spectrum was calculated between 240 nm to 320 nm. PTPI and papain were in a molar ratio of 1:1.

Fig. 32 Fluorescence spectra of PTPI alone and PTPI in complex with papain

Fluorescence spectra of the inhibitor alone PTPI, papain and papain-PTPI complex was measured at excitation wavelength (λ_{ex}) of 280 nm and emission wavelength (λ_{em}) of 300-400 nm.The concentration of PTPI was 2 μM. The fluorescence of complex of PTPI with papain was measured at a molar ratio of 1:1. The slit width was 5 nm for excitation and 10 nm for emission beams.

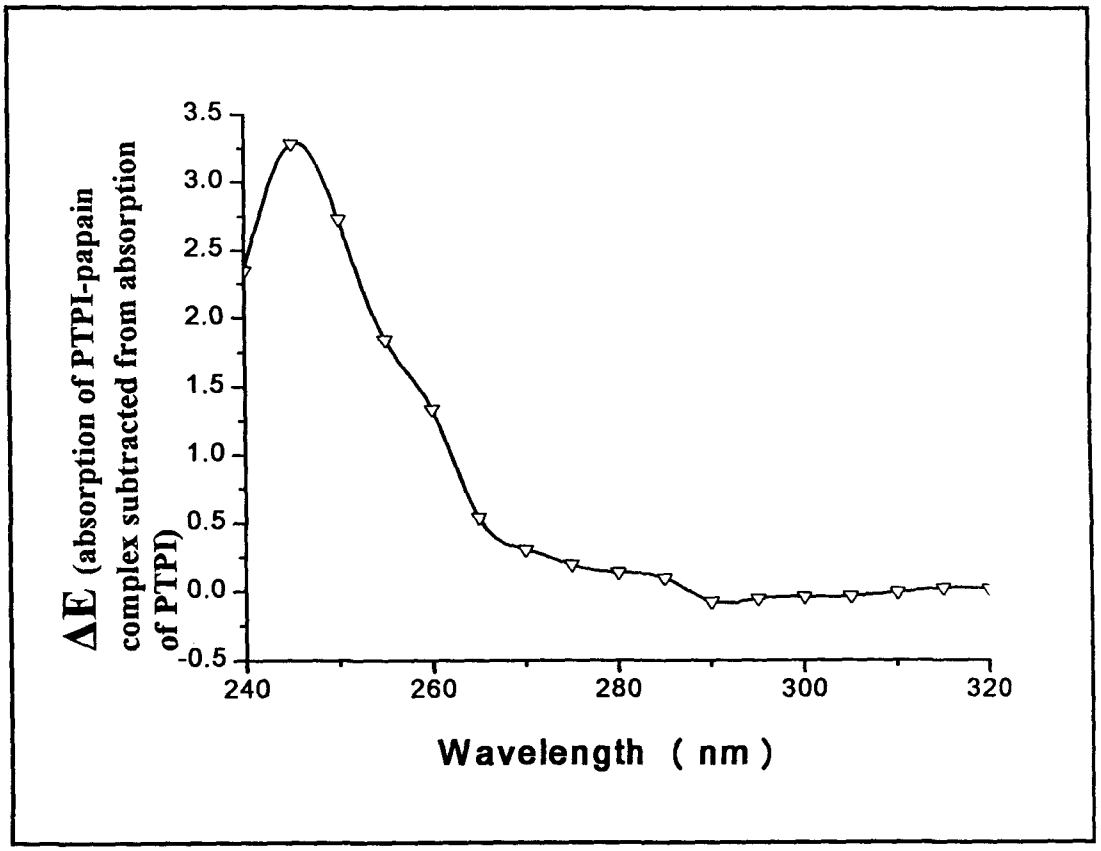
ΔE (absorption of PTPI-papain complex subtracted from absorption of PTPI)
3.5
3.0
2.5
2.0
1.5
1.0
0.5
0.0
-0.5
240
260
280
300
320
Wavelength (nm)

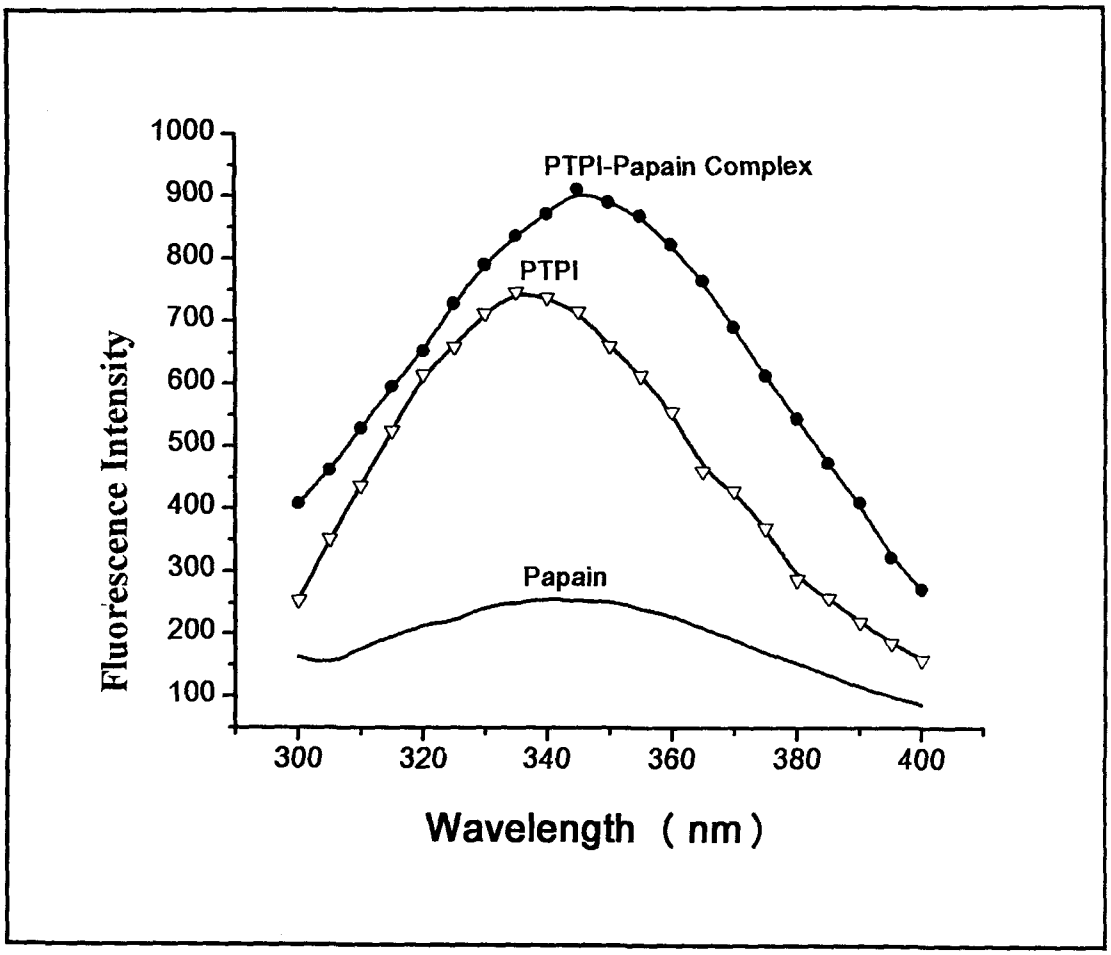
Fluorescence Intensity
1000
900
800
700
600
500
400
300
200
100
PTPI-Papain Complex
PTPI
Papain
300
320
340
360
380
400
Wavelength (nm)

Fig. 33 Far UV-CD spectra of native PTPI

The concentration of PTPI was 1.7 μM. Cells of 1mm path length were used. The buffer used was 50 mM sodium phosphate buffer, pH 7.5. Cells of 1 mm path length were used. The unit on the ordinate is mean residue ellipticity.

Fig. 34 Far UV-CD Spectra of PTPI in complex with papain

Far UV-CD spectra of native PTPI alone and papain-PTPI complex. The concentration of PTPI was 1.73 μM and PTPI and papain molar ratio was 1:1. The complex was obtained after incubation at 37°C for 30 minutes in 50 mM sodium phosphate buffer, pH 7.5. Cells of 1 mm path length were used. The unit on the ordinate is mean residue ellipticity.

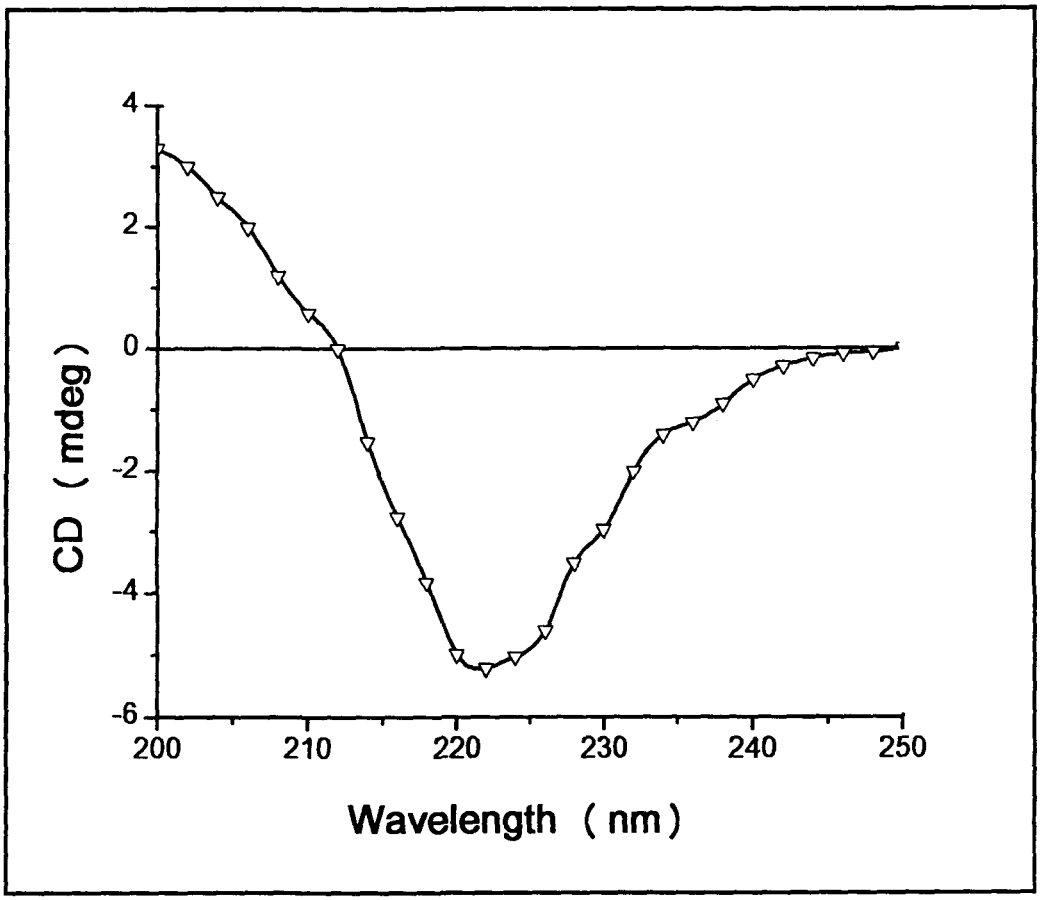
4
2
0
-2
-4
-6
CD (mdeg)
200
210
220
230
240
250
Wavelength (nm)

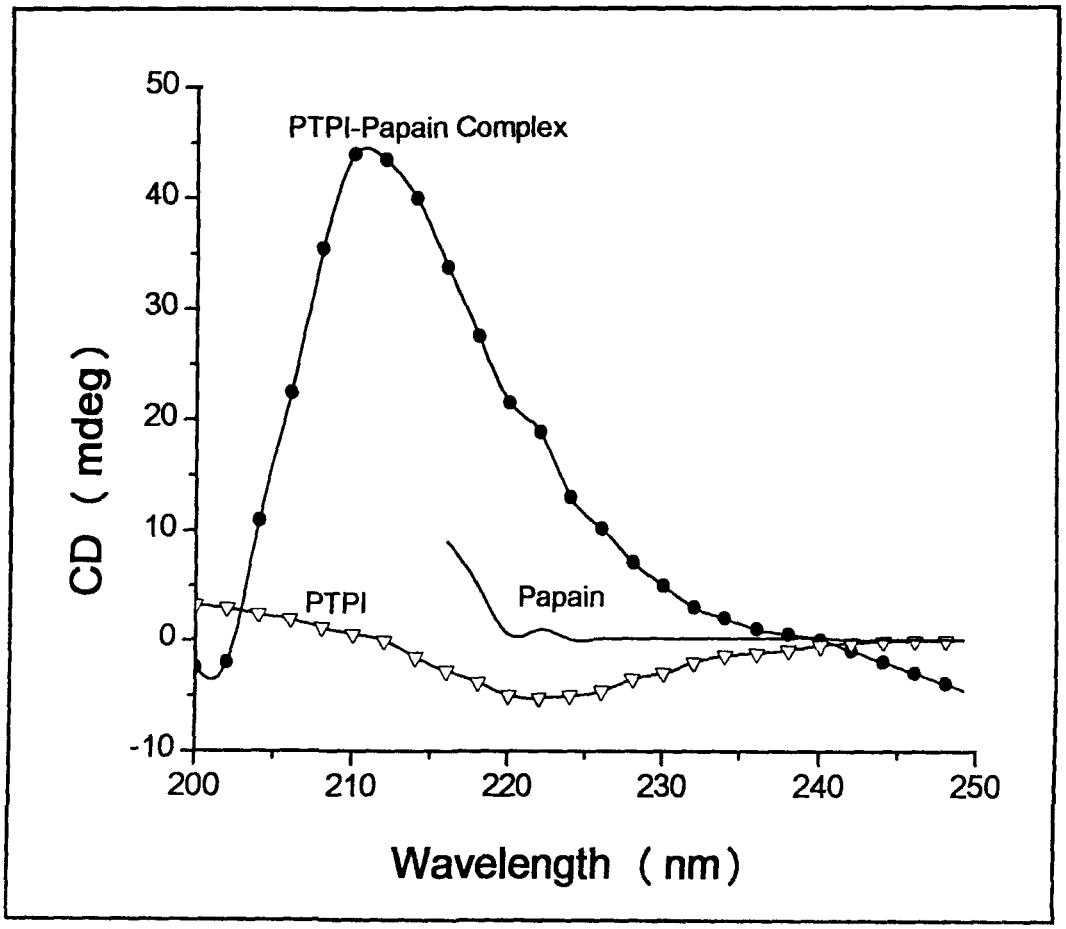
50
40
30
20
10
0
-10
CD (mdeg)
PTPI-Papain Complex
PTPI
Papain
200
210
220
230
240
250
Wavelength (nm)

Discussion

Chapter 1

DISCUSSION

Most of the evidences indicate that the proteolytic activity of both endogenous and exogenous cysteine proteinases is primarily regulated by a group of proteinase inhibitors belonging to the cystatin superfamily. These cysteine proteinase inhibitors (cystatins) are ubiquitous in organisms, ranging from bacteria to mammals. Cystatins are classified into three distinct families based on their sequence homology, presence of disulphide bonds and molecular mass [Abrahamson et al., 2003]. These inhibitors are of physiological importance because inhibition is achieved at physiological concentration of the inhibitor in a sufficiently short time with negligible dissociation of the complex [Beith, 1980]. TPIs (cystatins) are known to play important function in various pathophysiologic conditions [Turk et al., 2008; Shah and Bano, 2009] implying that cystatin functioning is pivotal for proper health maintenance.

Cystatins have been purified and characterized extensively from various mammalian sources like goat lung [Khan and Bano, 2009a], brain [Sumbul and Bano, 2006], human placenta [Rashid, et al. 2006a], goat kidney [Zehra et al., 2005], goat sheep plasma [Baba et al., 2005], human liver [Green et al., 1984] and human spleen [Jarvinen and Rinnie, 1982]. The presence of a thiol proteinase inhibitor in pancreas has been shown earlier [Ni et al., 1997] however; its isolation and physico-chemical characterization remained unattempted. Role of cathepsins in mediating exocrine and endocrine functions of pancreas has already been established (e.g. cathepsin B-conversion of trypsinogen to trypsin [Otto & Riesenkonig, 1975; Teich et al., 2002; Thrower et al., 2006], involvement of cathepsin B and H in the formation of insulin from proinsulin [Ansorge et al., 1977]). Recent literature implicates the role of calpains in insulin secretion and action [Sreenan et al., 2001; Kalbe et al., 2005]. Altered cysteine proteinase activity in pancreas is often correlated to deleterious consequences like onset or enhanced severity of pancreatitis [van Acker et al., 2002; Shikimi et al., 1987], diabetes [Weber et al., 2002; Sreenan et al.,2001] and tumors [Lorenzo et al., 2000]. However information about the regulation of cysteine proteinase activity by their proteinaceous inhibitors in pancreas is scarce.

In the present work, a thiol proteinase inhibitor (PTPI) was purified from goat pancreas by the method of Priyadarshini and Bano [2009]. The four step procedure involved alkaline treatment, acetone fractionation, ammonium sulphate fractionation and gel filtration chromatography. The procedure used provided a percent yield of

20.4 and fold purification of 500 [Table 6]. Purification of TPIs from other sources has been reported using affinity chromatography, chromatofocusing, gel filtration and ion exchange chromatography [Anastasi et al., 1983; Evans and Barrett, 1987; Khan and Bano, 2009a]. The purified inhibitor was found to be homogenous on the basis of charge and molecular weight as shown by native PAGE [Fig. 13]. In SDS-PAGE, both under reducing as well as non reducing conditions, PTPI gave two bands suggestive of presence two subunits [Fig. 14] held together by non covalent bonds.

The molecular weight of the isolated inhibitor ascertained from gel filtration chromatography on Sephacryl S 100 HR column [Fig. 15] was 43650 (~44000). Quite similar result was obtained in denaturing PAGE [Fig. 16b]. A slightly higher molecular weight obtained under reducing conditions (47194 compared to 43940 under non reducing conditions) is however, anomalous. The estimation of molecular weight on dodecyl sulphate gels is based on the hypothesis that all proteins bind fairly equal amount of detergents and that the complexes formed by protein and detergent adopt the same shape and conformation such that the electrophoretic mobility is function of the molecular weight and pore size of the gel. If a protein does not show such behaviour the molecular weight determination by this method becomes erroneous. Known examples of such proteins include polypeptide with unusual charge [Tung and Knight, 1971; Panyim and Chalkev, 1971], conformation [Bjork et al., 1972] or with unreduced disulphide bonds [Trayer et al., 1971] and glycoproteins [Mitchell et al., 1973]. The ambiguity of this method in case of PTPI could be that it deviates from the general behaviour of proteins in dodecyl sulphate solution. The SDS-PAGE was repeated thrice and same result was obtained.

Cystatins type 1 and type 2 have been classified on the basis of molecular weight and presence of disulphide bonds [Abrahamson et al., 2003]. Cystatins from tissues are usually small single subunit proteins with low molecular masses. Molecular masses of 11.4 kDa and 12 kDa have been reported for cysteine proteinase inhibitors isolated from human spleen [Jarvinen and Rinnie, 1982], 14 kDa-14.3 kDa for cystatins from bovine muscle [Zabari et al., 1993]. The molecular mass of PTPI is higher than those of stefins and cystatins (~11 kDa and 13 kDa, respectively) but lower than those of kininogens [~50 kDa-100 kDa] [Turk and Bode, 1991]. Low molecular mass of tissue cystatins is now contrasted with reports on high molecular mass. Ylonen et al. [1999] isolated and purified high molecular mass thiol proteinase inhibitors (of 43 kDa and ~52 kDa) from the skin of Atlantic salmon. Cystatins isolated from goat kidney were

reported to have a molecular mass of 67 kDa [Zehra et al., 2005]. A high molecular mass cystatin (of 70.8 kDa) has also been isolated from goat brain [Sumbul and Bano, 2006]. Recently, the work from our lab, has reported the purification of high molecular mass cystatins from goat lung [Khan and Bano, 2009a].

The purified inhibitor was characterized for its various hydrodynamic properties. Stokes radius of PTPI as deduced from its gel filtration behaviour was 27.3 Å. Diffusion coefficient of PTPI was found to be 7.87 x 10^{-7} cm^2 s^{-1}. The sedimentation coefficient of PTPI was calculated to be 3.83 s. The values of stokes radius and S_{max}/S ratio can be used to predict the shape of the protein molecule [Schurmann et al., 2001]. Globular proteins typically have S_{max}/S ratio of 1.2-1.3 (for example catalase and serum albumin have S_{max}/S of 1.20 and 1.29), and the ratio increases to 1.6-2.0 or more for elongated proteins [Erickson, 1982]. For PTPI S_{max}/S ratio was calculated to be 1.2. The values of stokes radius and S_{max}/S ratio for PTPI are in close agreement with those of ovalbumin, suggesting that PTPI is a globular in shape.

Generally, cystatins type 1 and type 2 isolated from tissues lack carbohydrates [Bode et al., 1988] whereas the presence of carbohydrates is a distinguishing property of type 3 cystatins, the kininogens [Ohkubo et al., 1984]. However, presence of carbohydrate has been reported in some tissue thiol proteinase inhibitors like cystatins E, F, M and those isolated from goat kidney and brain [Ni et al., 1997; 1998; Sotiropoulou et al., 1997; Zehra et al., 2005; Sumbul and Bano, 2006]. PTPI contains 2.32% carbohydrates and has no thiol group. Analysis of the influence of pH on activity of PTPI reveals that the inhibitor remains fairly active in the pH range of 3.0-10.0 [Fig. 18]. PTPI also exhibited stability in a wide temperature range of 30-70°C [Fig. 19] and remained active upto 120 min when heated to 90°C [Fig. 20]. High stability of the purified inhibitor in broad temperature and pH ranges is consistently found in other cystatins like goat lung cystatins [Khan and Bano, 2009a], goat brain cystatins [Sumbul and Bano, 2006], human placental cystatin [Rashid et al., 2006a], goat kidney cystatins [Zehra et al., 2005], stefin A and B [Zerovnik et al., 1997], etc.

The PTPI or pancreatic cystatin gave a good immune response with an antibody titre of 25,118.86 as determined by direct binding ELISA in rabbit serum [Fig. 21]. The antibodies raised against purified inhibitor gave a reaction of identity with the inhibitor as indicated by a single precipitin line on immunodiffusion suggesting that the isolated PTPI is pure. Experiments also showed that the antiserum had no immunogenic identity with goat brain and lung cystatins purified in our lab. This

indicates that the epitopes of goat pancreatic thiol proteinase inhibitor are different from goat brain and lung thiol proteinase inhibitors. The purified inhibitor was found to be specific for cysteine proteinases since no activity against aspartic (pepsin) and serine proteinases (trypsin and chymotrypsin) was detected. This has been reported for many other cystatins along with the thiol proteinase inhibitor isoforms purified from human spleen [Jarvinen and Rinnie, 1982], and other goat cystatins [Khan and Bano, 2009a; Sumbul and Bano, 2006; Zehra et al., 2005]. The stoichiometry of binding of purified cystatin to papain, ficin and bromelain was 1:1. This value shows that PTPI is a tight binding inhibitor of these proteinases and essentially all enzyme molecules are able to bind to the inhibitor. Anastasi et al. [1983] have also reported equimolar complexes of cystatin with cysteine proteinase. Abrahamson et al. [1987b] also reported the rapid formation of 1:1 complex between cystatin C and papain. There are other reports also demonstrating similar binding of thiol proteinase inhibitors with papain like that of the recombinant human cystatin C [Bjork et al., 1994], recombinant bovine cystatin C [Olsson et al., 1999], recombinant stefin A [Nicklin and Barrett, 1984]. Members of cystatin superfamily also show different binding stoichiometries with papain. The high molecular weight kininogens from human and sheep plasma as well as low molecular weight kininogens from the latter show 1:2 stoichiometry of interaction with papain [Baba et al., 2005; Turk et al., 1996b].

The IC50 values of the PTPI obtained for papain, ficin and bromelain were 0.08, 0.078 and 0.154 μM, respectively [Table 7]. Lower IC50 value suggests a greater affinity of the inhibitor towards the enzyme. The values obtained for PTPI indicate its greater affinity towards papain then for ficin and bromelain. Katunuma and Kominami [1985] have found IC50 value for the inhibitor isolated from rat liver as 0.16 μg for papain, 0.46 μg for ficin, 4.2 μg and 0.14 μg for cathepsin B and H, respectively.

Accurate Ki values were determined by working at lower enzyme concentrations and using equations derived by Krupka and Laidler [1959] and Henderson [1972]. Ki values were calculated from the slope of the curve obtained for the inhibition of caseinolytic activity of papain, ficin and bromelain. PTPI is a strong inhibitor of thiol proteinases as indicated by their Ki values. The data shows that PTPI inhibited papain, ficin and bromelain with Ki values of 5.88, 9.02 and 22.28 nM, respectively, under conditions of routine assay system [Table 7, Fig. 24-26]. Thus, of the enzymes studied,

PTPI binds most tightly to papain. These values are in good comparison with other thiol proteinase inhibitors. Sumbul and Bano [2006] obtained Ki values of 1.87×10^{-8} M and 3.125×10^{-8} M, for inhibition of papain by goat brain cystatins. Quite similar values were obtained for goat kidney cystatins [Zehra et al., 2005]. Human placental cystatin also gave a Ki value of 5.5×10^{-8} M for papain as reported by Rashid et al. [2006a]. Ki values of nanomolar range have been documented for cathepsin B, H and L with cystatin A [Barrett et al., 1984], cystatin C [Machleidt et al., 1986], cystatin D [Balbin et al., 1994]. Studies of the kinetics of binding of chicken cystatin to several cysteine proteinases have shown that these reactions are best described by the simple reversible bimolecular mechanism:

$$P + I \underset{K_{-1}}{\overset{K_{+1}}{\rightleftharpoons}} PI$$

Where P is the proteinase, I represents inhibitor and PI their complex [Björk and Ylinenjärvi, 1990; Henderson, 1972]. The same conclusion is strongly indicated by studies with PTPI in this work. The linear increase in the observed pseudo-first order rate constant for cysteine proteinases studied with PTPI concentration is consistent with a simple reversible bimolecular reaction mechanism [Nicklin and Barrett, 1984]. Moreover, the increasing value of Ki with an increase in substrate concentration suggests the inhibition to be competitive as reported earlier by Li et al., [2000] and by Nicklin and Barrett [1984] for inhibition of human cathepsin B by chicken cystatin. Latter obtained Ki (app) values of 1.85 and 3.68 nM with the substrate concentration of 0.05 and 0.39 mM, respectively. Possibly, all cystatins of family II, and perhaps also those of other families, interact with the target enzymes in same general manner. Association constant obtained for papain-PTPI interaction was 1.49×10^{4} $M^{-1}s^{-1}$. In general, proteinases having low Ki also have high K_{+1} and low K_{-1} values suggesting the stability of the enzyme inhibitor complex and rapidity of its formation. Our data is in accordance with this, thereby suggesting that the interaction of PTPI with papain is rapid and stable. The association rate constants obtained for ficin and bromelain were 1.39×10^{4} $M^{-1}s^{-1}$ and 5.94×10^{3} $M^{-1}s^{-1}$, respectively. Thus, reiterating the order of affinity as, papain > ficin > bromelain. The Ki and rate constants for association of the inhibitor with papain and ficin are also comparable with the values measured for chicken cystatin [Bjork et al., 1989], human cystatin C and bovine cystatin C [Bjork et al., 1994] and cystatin D [Balbin et al., 1994] for their interactions with various cysteine proteinases (papain, ficin and cathepsins B, H and L).

The dissociation constant (K_{-1}) values for the enzyme-inhibitor complex was determined by displacement procedure, in which the inhibitor released from the complex was trapped by excess substrate (casein) with increase in time. The amount of enzyme released from the complex was monitored by continuous measurement of enzyme activity. The respective K_{-1} values obtained for papain, ficin and bromelain are 8.76×10^{-5}, 3.35×10^{-4} and 1.32×10^{-4} s^{-1}, respectively [Fig. 27-29, Table 7]. The values of K_{-1} obtained in the present work are comparable to K_{-1} values obtained for chicken cystatin, 5×10^{-5} s^{-1} with papain [Nicklin and Barrett, 1984]. The published data on rate constants for other goat cystatins [Khan and Bano, 2009a; Sumbul and Bano, 2006; Zehra et al., 2005] is in similitude with our results. This resemblance in inhibitory mechanism of cystatins isolated from goat earlier reflects the species similarities. The above data gives comprehensive information about the kinetics of inhibition of purified thiol proteinase inhibitor with papain, ficin and bromelain and the overall comparison showed that PTPI inhibits papain more effectively compared to other two proteinases.

The N-terminal 24 amino acid residues of the heavier subunit (23.98 kDa) were sequenced, and some interesting results were obtained. As in other cystatins [Table 8], PTPI possesses a conserved glycine residue at 11^{th} position rather than the conserved position 9 in various species [Brzin et al., 1984]. Maximum sequence homology was observed with bovine skin cystatin C (20%) [Cimerman et al., 1996]. Fair sequence homology of PTPI was also observed with bovine parotid cystatin C (12.5%), bovine colostrum cystatin C (11.8%), and human cystatin C (12.5%) [Cimerman et al., 1996], sheep plasma LMW K1 [Baba et al., 2005], placental cystatin [Rashid et al., 2006a] and cystatin E [Ni et al., 1997]. Using sequence of these N-terminal amino acid residues, a hydropathy plot was made using the respective hydropathy indices [Kyte and Doolittle, 1982]. Among 24 residues sequenced, the stretch of 3-7, 7-11 and 15-19 residues has maximum hydropathy index suggesting that these residues might be present inside the hydrophobic core of the protein [Fig. 30].

The absence of disulphide bonds is a unique character of type 1 cystatin family members. Molecular masses of type 1 and 2 cystatin families range in 11 kDa to 13 kDa [Turk and Bode, 1991]. Presence of carbohydrates is however limited only to kininogens, with few exceptions found for members of type 2 cystatin family. PTPI is devoid of any disulphide linkage, has high molecular mass (44 kDa) and bears sequence similarities to both stefins and cystatins [Table 8]. Studies on kinetics of

inhibition as well as on biophysical interaction of PTPI with thiol proteinases shows that it bears resemblances with other members of type 2 cystatin family. Based on this the purified inhibitor can be regarded as a variant of type 1 and type 2 cystatin families. This is not unusual as there is growing list of proteins possessing some structural and functional motifs of cystatin superfamily, but bearing substantial differences causing them to be classified as variants of cystatin superfamily.

The interaction between papain and PTPI was studied using various spectroscopic techniques. The complex spectroscopic changes (observed in UV-difference spectrum of PTPI-papain complex) [Fig. 31] accompanying the binding of PTPI with papain indicate that the environment of several aromatic residues in the proteins has been perturbed upon interaction. Peak at 280 nm is indicative of changes around tyrosine residues [Donovan, 1969; 1973a; 1973b]. The shoulder around 260 nm may be partly due to phenylalanine and may also contain contribution from aromatic residues [Donovan, 1973a]. The changes at 290 nm suggest that aromatic amino acid residues are involved in binding with papain, like tryptophan. Such results are consistent with earlier reported results for interaction of low and high molecular weight kininogens, human placental cystatin, goat brain cystatin and rat cystatin with papain [Baba et al., 2005; Rashid et al., 2004; Sumbul & Bano, 2006; Takeda et al., 1983].

Fluorescence studies showed that complexation of PTPI with papain resulted in changes in intensity and shape of the emission spectrum. The maxima of cystatin shifted from 335 nm to 345 nm for the PTPI-papain complex which was accompanied by an increase in the fluorescence intensity. The largest increase of intensity was observed between 330-345 nm [Fig. 32] indicating that these changes arise predominantly from perturbations around tryptophan residues, either by exposure of tryptophan residues to the solvent or may originate from local interactions affecting chromophoric groups of the two proteins.

A CD spectrum in the far UV region depicts the contributions of the secondary structure of the protein [Jirgensons, 1970]. The α-helical structure of the protein in the far UV region is characterized by negative peaks at 208-210 nm, at 222 nm and a positive peak between 190-192 nm [Jirgensons, 1970; Chen et al., 1972]. PTPI has an α-helical content of 17.18%. The α helical content was calculated from the ellipticity values at 222 nm using equation given by Chen et al. [1972]. The CD spectra of PTPI (α helical content 17.18%) resembled that of cystatin A (with a low α helical content ~15%) [Stubbs et al., 1990; Pol et al., 1995]. This type of structure has also been

reported for chicken cystatin which has an α helical content of about 20% [Schwabe et al., 1984].

The goat pancreatic cystatin loses its native structure on formation of complex with papain [Fig. 34]. Far UV-CD spectra of the inhibitor-papain complex showed intense positive peak and complete loss of any negative peaks, characteristic of random coil structure [Ramasarma et al., 1994]. However, earlier studies for the interaction of chicken cystatin, human cystatin C and cystatin A with several proteinases reported no appreciable conformational adaptation of either protein [Pol et al., 1995; Lindahl et al., 1992; Takeda et al., 1983]. The positive ellipticity of PTPI-papain complex observed in the present case is in similitude with reports of Rashid et al., [2004] and Baba et al., [2005]. This feature of PTPI-papain interaction is comparable to that of serine proteinase inhibitors with target enzymes involving conformational change [Luthy et al., 1973; Quast et al., 1974; Olson and Shore, 1982].

The results indicate that the UV absorption, fluorescence emission and far UV CD changes are more due to conformational changes in proteins rather than any local interaction affecting the chromophoric groups of the two constituent proteins of the complex. The positive ellipticity observed for PI (proteinase-inhibitor) complex in far UV CD region further confirms that cystatin and papain both lose their native structures on formation of complex. The conformation of this complex resembles neither of the constituent proteins, rather indicates attainment of random coil structure due to this interaction. The kinetic studies also suggest formation of tight complex on interaction of inhibitor with papain.

PTPI is a good partner of other reported goat tissue cystatins in terms of its physical properties. Also, the pH and heat stability, interaction with papain, affinities towards other proteinases and N-terminal sequence analysis of the purified PTPI are quite similar to other cystatins; but differences in terms of its molecular mass, subunit structure, sulphydryl groups, and carbohydrate content from other tissue cystatins imply different routes of biosynthesis, different in vivo distribution and suggest a variety of physiological functions. It is interesting to speculate on the physiological role of this endogenous proteinase inhibitor. It seems likely that this endogenous inhibitor would at least serve a protective function against inappropriate proteolysis both with in the cell and outside the cell.

Chapter 2

Denaturing action of guanidine hydrochloride and urea towards pancreatic thiol proteinase inhibitor

3.2 RESULTS

The possibility of measuring the conformational stability of proteins with precision is important to resolve the protein folding problem, to define the structural characteristics of the proteins for studying their structure and function through mutational analysis and to applied research.

With this view, a systematic investigation on the effect of increasing concentration of guanidine hydrochloride (GdnHCl) and urea on the functional and structural parameters of pancreatic thiol proteinase inhibitor (PTPI) was performed using the following methods:

(1) Enzyme catalytic activity, to indicate the disruption of active site regions.

(2) Red shift of wavelength of the maximum fluorescence emission (λ_{max}), to monitor global structural changes induced by the denaturant.

(3) Ellipticity at 222 nm in the CD spectrum, to detect the secondary structural changes induced by GdnHCl and urea.

(4) ANS- binding to detect the appearance of hydrophobic patches in the enzyme molecule during unfolding.

Time dependent changes in the structural parameters and enzymatic activity of PTPI at increasing GdnHCl and urea concentrations were monitored to standardize the incubation time required for achieving equilibrium under these conditions. Under all of the conditions studied, the changes occurred within maximum of 2 h with no further alteration upto 12 h (data not shown). These observations demonstrated that an incubation time of 2 h is sufficient for achieving equilibrium under any condition of denaturant studied.

3.2.1 CHANGES IN MOLECULAR PROPERTIES OF PTPI ASSOCIATED WITH GdnHCl INDUCED UNFOLDING

Effect of GdnHCl on papain inhibitory activity of PTPI

Enzyme activity can be regarded as the most sensitive probe for studying protein unfolding and refolding as it reflects subtle readjustments at the active site, allowing very small conformational variations of an enzyme structure to be detected. Fig. 35 shows the effect of increasing concentration of GdnHCl on the papain inhibitory activity of PTPI. The inhibitor was incubated with increasing GdnHCl concentration

Fig. 35 Effect of increasing GdnHCl concentration on the activity of PTPI

Native PTPI (1 μM) was incubated with increasing concentration of GdnHCl (0-6 M) for 2 h at room temperature. PTPI was assayed for loss of antiproteinase activity by caseinolytic assay of Kunitz [1947]. Values are Mean ± SEM of four independent determinations.

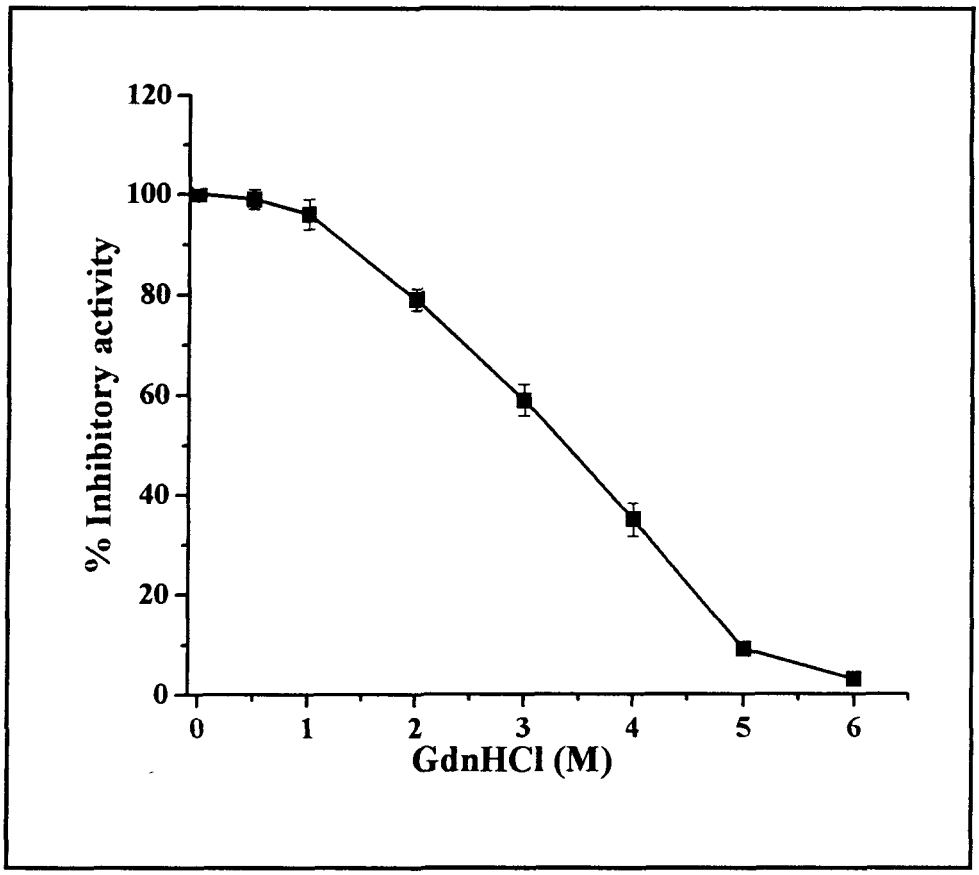
% Inhibitory activity
120
100
80
60
40
20
0
0
1
2
3
4
5
6
GdnHCl (M)

in 50 mM sodium phosphate buffer, pH 7.5 and its thiol proteinase inhibitory activity was monitored by the method of Kunitz [1947]. The activity of native PTPI was taken as 100. A sigmoidal dependence of enzymatic activity on GdnHCl concentration was observed. No significant effect of the denaturant on enzymatic activity of native PTPI was observed upto 1 M GdnHCl. Approximately, 20% loss of the papain inhibitory activity of PTPI occurred at 2 M GdnHCl. At 4 M GdnHCl concentration only 35% of the native enzyme activity was left. PTPI was found to be almost completely inactivated beyond 4 M GdnHCl.

Effect on spectroscopic properties of PTPI in the presence of GdnHCl

Optical spectroscopic studies on PTPI in the presence of increasing GdnHCl concentrations were performed to study the effect of denaturant on its structural properties.

Fluorescence spectra of PTPI in the presence of GdnHCl

The spectral parameters of fluorescence emission spectra such as position, shape and intensity are dependent on the electronic and dynamic properties of the chromophore environment; hence steady-state fluorescence has been extensively used to obtain information on the structural and dynamic properties of protein [Prajapati et al., 1998]. Fluorescence measurements were performed by using a 280 nm excitation wavelength in order to detect the contribution of both tryptophan and tyrosine residues. This choice is advantageous in having fluorescence signals that reflect the global conformational changes of the tertiary structure, rather than local modifications.

The modification of the microenvironment of aromatic residues of PTPI due to denaturant has been monitored by studying changes in the intensity and wavelength of emission maxima (λ_{max}) as a function of denaturant concentration. Fig. 36 illustrates changes in fluorescence emission intensity and λ_{max} (inset) of PTPI with increasing GdnHCl concentration (0-6 M). The wavelength of maximum emission (λ_{max}) is a robust signal for measuring the unfolding of proteins. The fluorescence emission spectrum of native PTPI shows a maximum of 335 nm that shifts to 350 nm in 6 M GdnHCl [Fig. 36 inset]. Prominent but a gradual red shift was observable only at concentrations beyond 3 M GdnHCl. There was little or no effect on the fluorescence intensity till 1 M GdnHCl. 2-4 M GdnHCl caused an increase in the emission intensity. Further, increment of denaturant concentration to 5 and 6 M, quenched the

Fig. 36 Intrinsic fluorescence analysis of PTPI on interaction with various concentrations of GdnHCl

The concentration of PTPI was 1 μM. PTPI was preincubated for 2 h at 25°C in 50 mM sodium phosphate buffer (pH 7.5) containing the increasing concentration of GdnHCl (0-6 M). Fluorescence was measured at an excitation wavelength of 280 nm and emission range of 300-400 nm with slitwidth of 5 nm. The inset shows changes in wavelength of maximum emission with increasing concentration of GdnHCl.

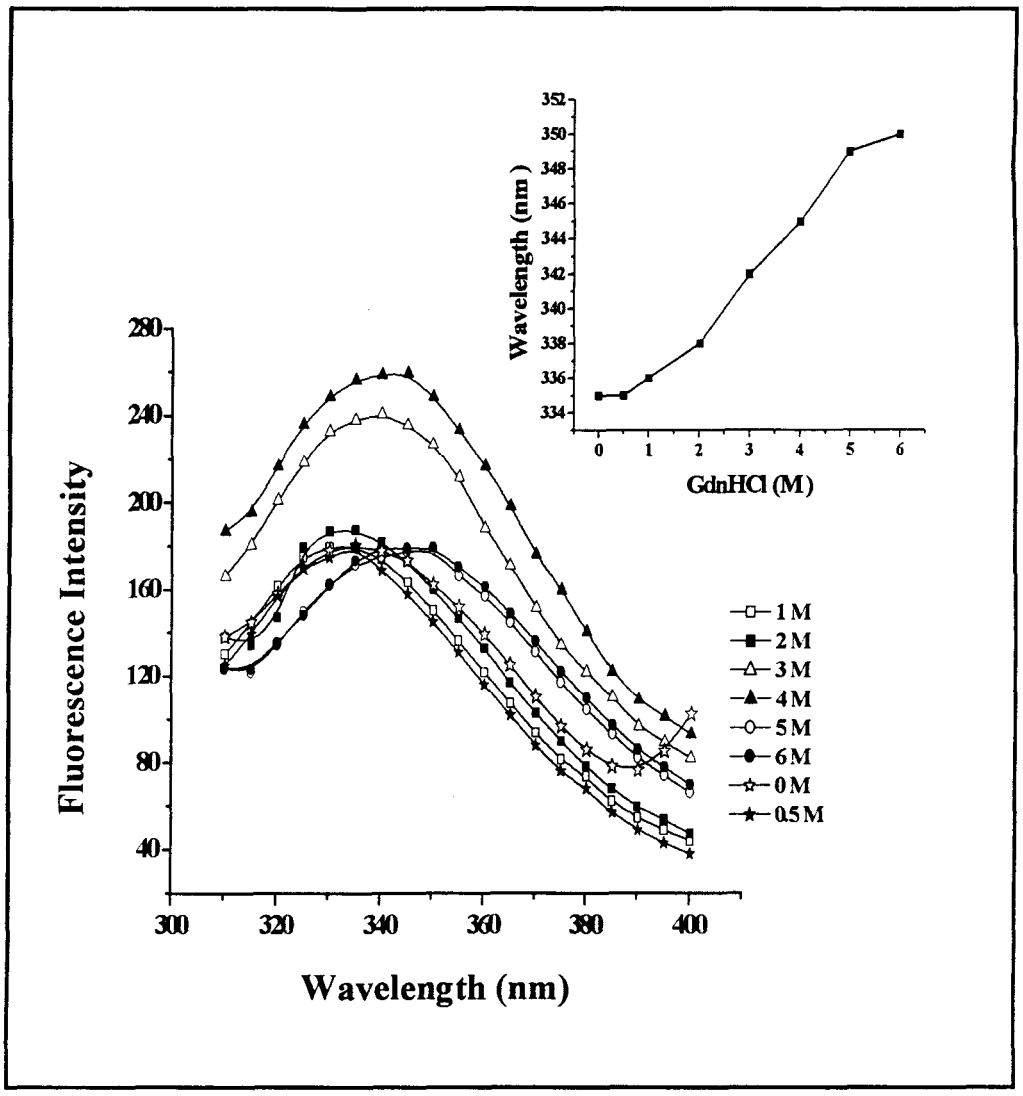
Fluorescence Intensity
Wavelength (nm)
280
240
200
160
120
80
40
300
320
340
360
380
400
1 M
2 M
3 M
4 M
5 M
6 M
0 M
0.5 M
Wavelength (nm)
GdnHCl (M)
352
350
348
346
344
342
340
338
336
334
0
1
2
3
4
5
6

fluorescence intensity below native. This effect has also been documented for GdnHCl mediated alteration in fluorescence emission of other multimeric proteins like alcohol dehydrogenase [Sacchetta et al., 2001], glutamate dehydrogenase [Ruiz et al., 2003], β-nerve growth factor [Timm & Neet, 1992]. It is well known that fluorescence spectra of proteins with maxima around 335 nm are characteristic of tryptophan residues well buried in the hydrophobic core, whereas fluorescence spectra with maximum around 350 nm are characteristic of tryptophan residues exposed to the aqueous solvent [Lakowicz, 1983]. Thus, treatment of PTPI with higher concentrations of GdnHCl results in exposure of the buried tryptophan moieties present in native inhibitor to the solvent. Also, decrease in emission intensity at high denaturant concentration may result from quenching of the tryptophan fluorescence by aqueous solvent. Such a situation can happen only when the denaturant induces unfolding of PTPI.

Secondary structure of PTPI in GdnHCl solutions

Far UV-CD studies on GdnHCl induced unfolding of PTPI were carried out to study the effect of GdnHCl on the secondary structure of the inhibitor. The CD observed below 230 nm is due to the peptide amide chromophore [Johnson, 1985] and can be used to estimate the content of secondary structure. In the far UV region, the CD spectrum of native PTPI shows the presence of fair amount of α-helical conformation [Priyadarshini and Bano, 2009]. It was found to possess 17.2% of α-helical content determined by the method of Chen et al. [1972]. Fig. 37 summarizes the effect of GdnHCl on secondary structure of PTPI. Upto 1 M GdnHCl, in similitude to activity and fluorescence results, minute effects are seen on mean residue ellipticity (MRE) at 222 nm. Beyond 4 M GdnHCl a complete loss of signal was observed. These observations suggest that treatment of PTPI with higher GdnHCl concentration results in complete unfolding of the inhibitor.

Midpoint of denaturation transition (Cm) in the presence of GdnHCl

The midpoint of chemical denaturation transition of proteins, abbreviated as Cm, can be defined as the concentration of the denaturant, at which 50% of the transition is complete, that is where $f_d = f_n$, fraction of denatured protein molecules is equal to fraction of native species.

Transition curves were constructed from various parameters determined in GdnHCl

Fig. 37 Secondary structure analysis of PTPI in the presence of GdnHCl

The figure shows changes in far UV CD spectra of PTPI denatured in increasing concentrations of GdnHCl (0-6 M). The conditions were same as for figure 3 except that the concentration of PTPI was 1.73 μM. The inset shows changes in MRE at 222 nm with increasing concentration of GdnHCl.

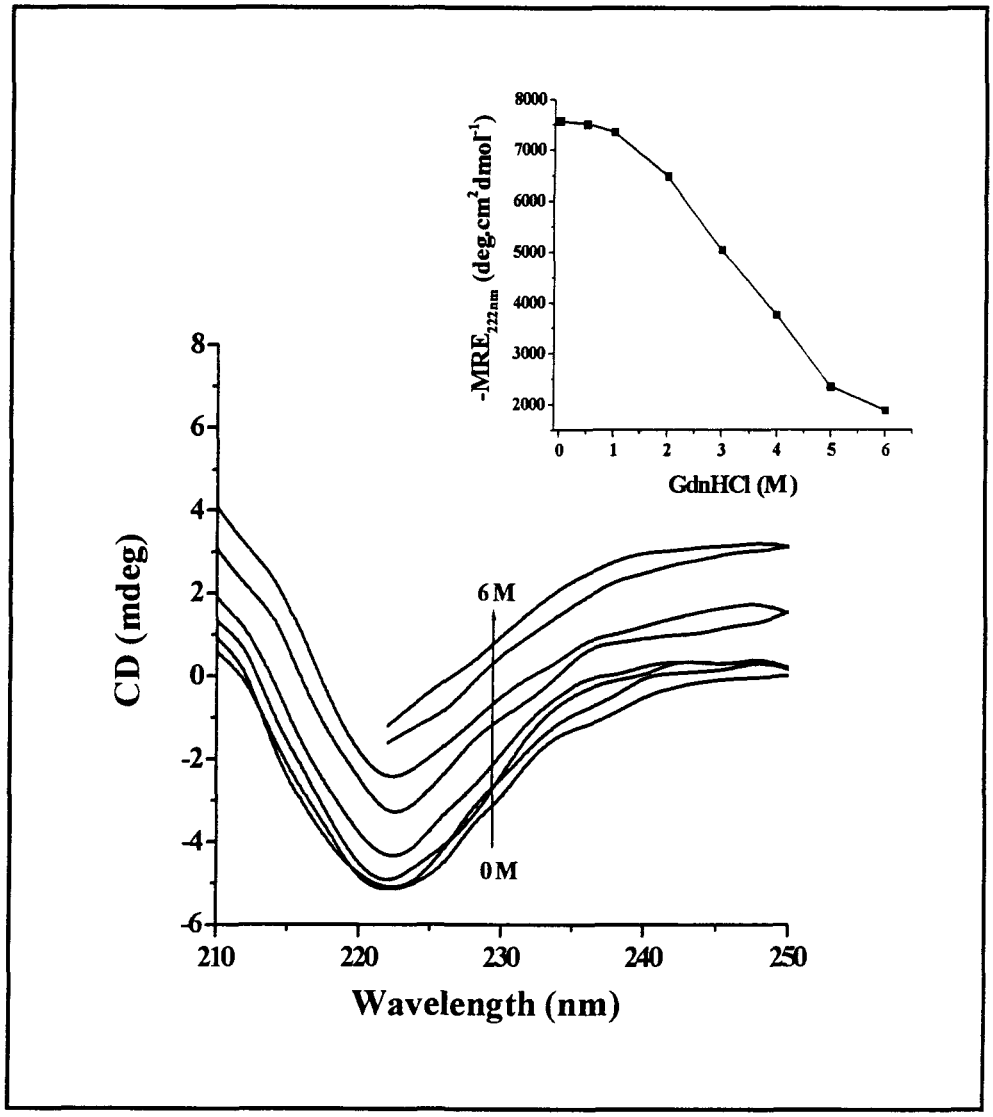
8000
7000
6000
5000
4000
3000
2000
-MRE222nm (deg.cm2dmol-1)
0
1
2
3
4
5
6
GdnHCl (M)
8
6
4
2
0
-2
-4
-6
CD (mdeg)
6 M
0 M
210
220
230
240
250
Wavelength (nm)

denaturation of PTPI. The results are depicted in Fig. 38. Cm determined from the equilibrium transition curve derived from activity data [Fig. 38a] was 3.2 M GdnHCl. Cm is a function of protein concentration in dimer coupled systems [Timm & Neet, 1992]. To analyze if the dissociation of dimeric PTPI and inactivation are coupled denaturation curves were constructed over a range in PTPI concentration (0.1, 1 and 10 μM). A concentration dependent shift in the midpoint of transition was observed, consistent with two-state model of denaturation [Fig. 38a]. Fig. 38b shows the normalized transition curve of changes in λ_{max} of PTPI as a function of GdnHCl concentration. The midpoint of transition (Cm) was again determined to be 3.2 M. Cm deduced from the normalized transition curve of MRE $_{222\ nm}$ [Fig. 38c] was also 3.2 M. Changes in the molecular properties of PTPI such as enzymatic activity, $MRE_{222\ nm}$, λ_{max} with increasing GdnHCl concentration reveal a monophasic sigmoidal dependence, with coincidental profiles [Fig. 38d], characteristic of cooperative unfolding, suggesting a two state model for denaturation of the inhibitor.

3.2.2 CHANGES IN MOLECULAR PROPERTIES OF PTPI ASSOCIATED WITH UREA INDUCED UNFOLDING

Although urea and GdnHCl are believed to have similar modes of action [Nandi & Robinson, 1984], GdnHCl is a monovalent salt that has both ionic and chaotropic effects [Mayr and Schmid, 1993; Makhatadze et al., 1998; Myers et al., 1995], whereas urea has only chaotropic effects. Thus, urea is an ideal control agent for distinguishing between the ionic and chaotropic effects of GdnHCl.

Urea induced changes in structural and functional properties of PTPI were studied by changes in papain inhibitory activity, fluorescence emission intensity and λ_{max} of emission and $MRE_{222\ nm}$ with increasing urea concentration.

Effect of urea on papain inhibitory activity of PTPI

PTPI was incubated with increasing concentration of urea in 50 mM sodium phosphate buffer (pH 7.5). Its thiol proteinase inhibitory activity was determined at each concentration of the denaturant using casein as substrate, by the method of Kunitz [1947]. Activity of native PTPI was taken to be 100. Fig. 39 shows that urea concentration lower than 1 M did not substantially affect the activity. 20% of activity was lost at 2 M urea concentration. At 4 M urea concentration 40% loss of

Fig. 38 Changes in functional and structural properties of PTPI in the presence of GdnHCl

The figure shows normalized transition curves for GdnHCl induced unfolding of PTPI as obtained from

(a) enzymatic activity

(b) wavelength of maximum emission

(c) MRE at 222 nm

(d) shows the coincidence of transition curves, (a), (b) and (c).

Panel (a) also shows the protein concentration dependence of PTPI denaturation. Inhibitory activity of PTPI was monitored at different concentrations, 0.1 μM -○-, 1 μM -□-, 10 μM -Δ- of the native protein each incubated with increasing concentrations of GdnHCl. Fraction of unfolded protein was calculated at each concentration as explained in methods section.

(a)

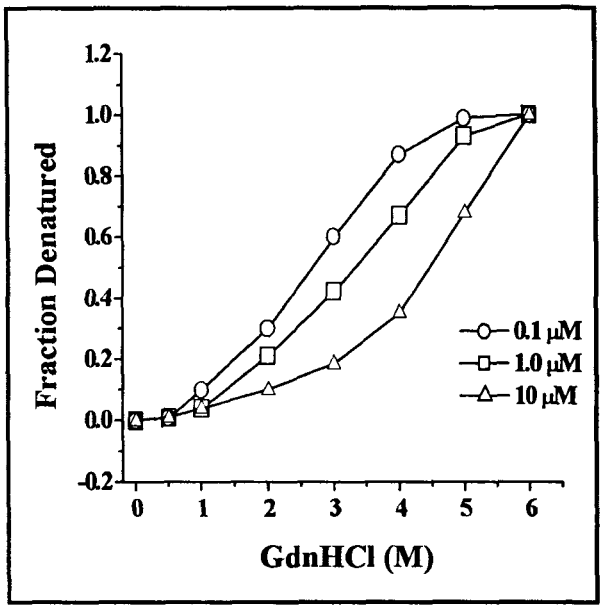
Fraction Denatured
GdnHCl (M)
0.1 μM
1.0 μM
10 μM

(b)

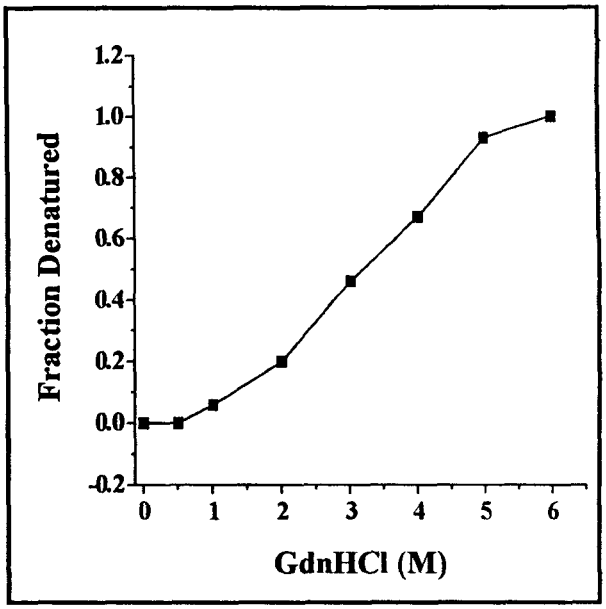
Fraction Denatured
GdnHCl (M)

(c)

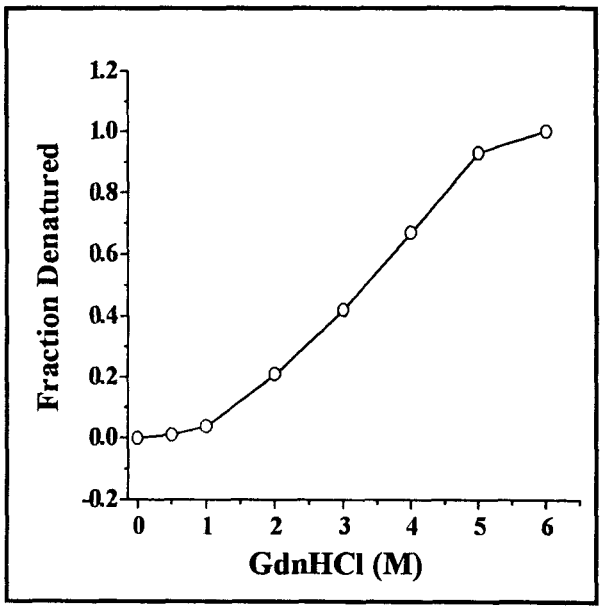
Fraction Denatured
GdnHCl (M)

(d)

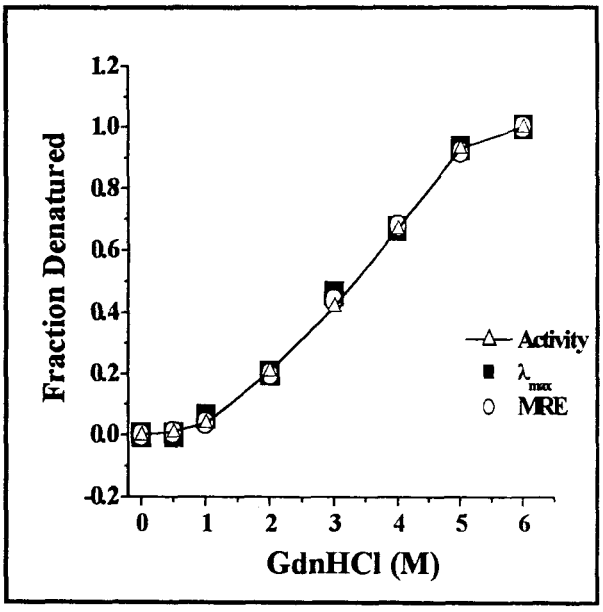
Fraction Denatured
GdnHCl (M)
Activity
λmax
MRE

Fig. 39 Effect of increasing urea concentration on activity of PTPI

Native PTPI (1 μM) was incubated with increasing concentration of urea (0-9 M) for 2 h at room temperature. PTPI was assayed for loss of antiproteinase activity by caseinolytic assay of Kunitz [1947]. Values are Mean ± SEM of four independent determinations.

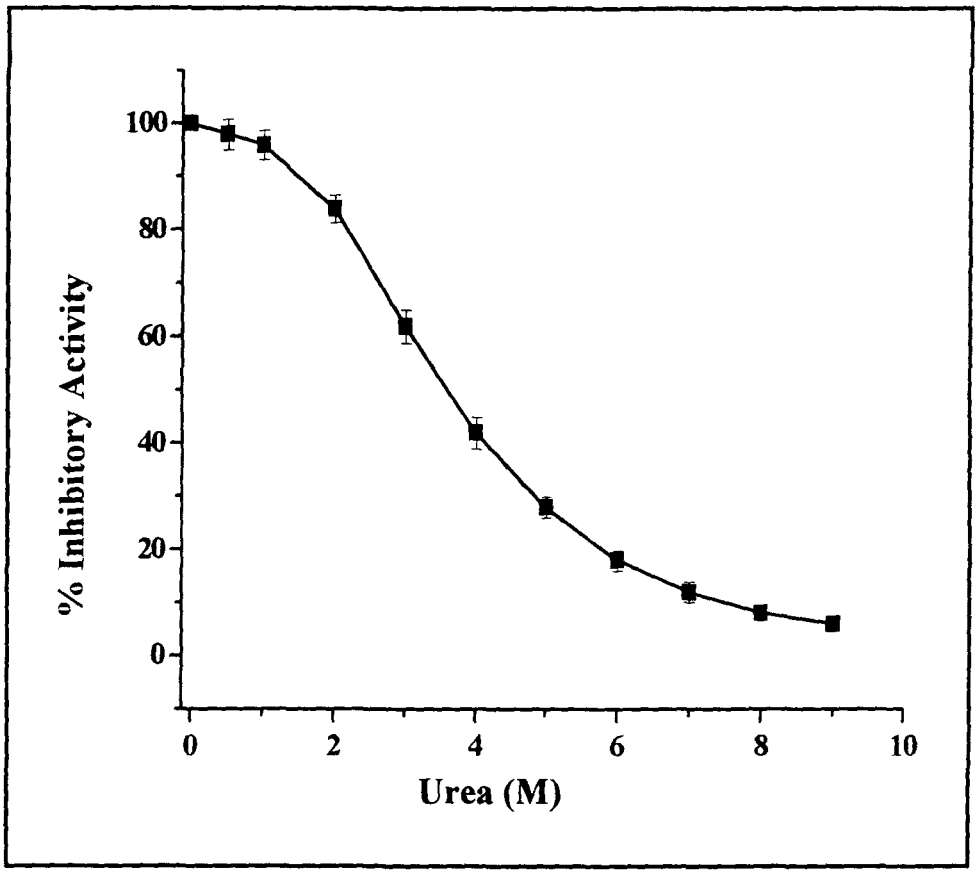
% Inhibitory Activity
100
80
60
40
20
0
0
2
4
6
8
10
Urea (M)

activity was obtained and only 18% of native PTPI papain inhibitory activity was observed at 6 M urea. Beyond this concentration the inhibitor was barely active.

Effect of urea on spectroscopic properties of PTPI

Fluorescence spectra of PTPI in the presence of urea

Intrinsic fluorescence emission spectra of native and unfolded proteins in the presence of increasing urea concentration are shown in Fig. 40. An increase in fluorescence emission of native PTPI without any shift in emission λ_{max} was observed till 2 M urea. Fluorescence emission enhancement was again noticed at 6 M urea, preceded by a plateau (at 4 and 5 M urea). A sharp increase in emission intensity was observed beyond 8 M urea with a marked red shift of λ_{max} to 350 nm which indicates that treatment of PTPI with high concentrations of urea leads to unfolding of the inhibitor. The maximum value of λ_{max} obtained for both denaturants was same.

Secondary structure of PTPI in urea solutions

Far UV-CD spectroscopy was used to monitor changes in secondary structure of PTPI upon urea induced unfolding. Incubation of PTPI in urea solutions results both in changes the shape of CD spectra and in urea-concentration dependent loss in ellipticity [Fig. 41]. Upon denaturation the negative CD below 230 nm diminishes significantly, consistent with the loss of ordered secondary structure that should accompany protein unfolding. At urea concentrations above 5 M, there is complete loss of negative peaks. A sigmoidal dependence of decrease in $MRE_{222\ nm}$ with increasing urea concentrations was observed with no change in the value observed for the native inhibitor upto 1 M urea.

Midpoint of denaturation transition (Cm) in presence of urea

As in GdnHCl-denaturation, Cm (the concentration at which 50% of the protein molecules exist in the unfolded state) was determined for urea denaturation also from the data derived on various parameters studied. Fig. 42a depicts the normalized transition curve for the loss of enzymatic activity in response to urea. The Cm value deduced from the curve was 3.6 M. No dependence of Cm on protein concentration was detected. It may be that inactivation and dimer dissociation in case of urea denaturation of PTPI are not coupled or as has been explained in the case of

Fig. 40 Intrinsic fluorescence analysis of PTPI on interaction with various concentrations of urea

The concentration of PTPI was 1 μM. PTPI was preincubated for 2 h at 25°C in 50 mM sodium phosphate buffer (pH 7.5) containing the increasing concentration of urea (0-9 M). Fluorescence was measured at an excitation wavelength of 280 nm and emission range of 300-400 nm with slit width of 5 nm. The inset shows changes in wavelength of maximum emission with increasing concentration of urea.

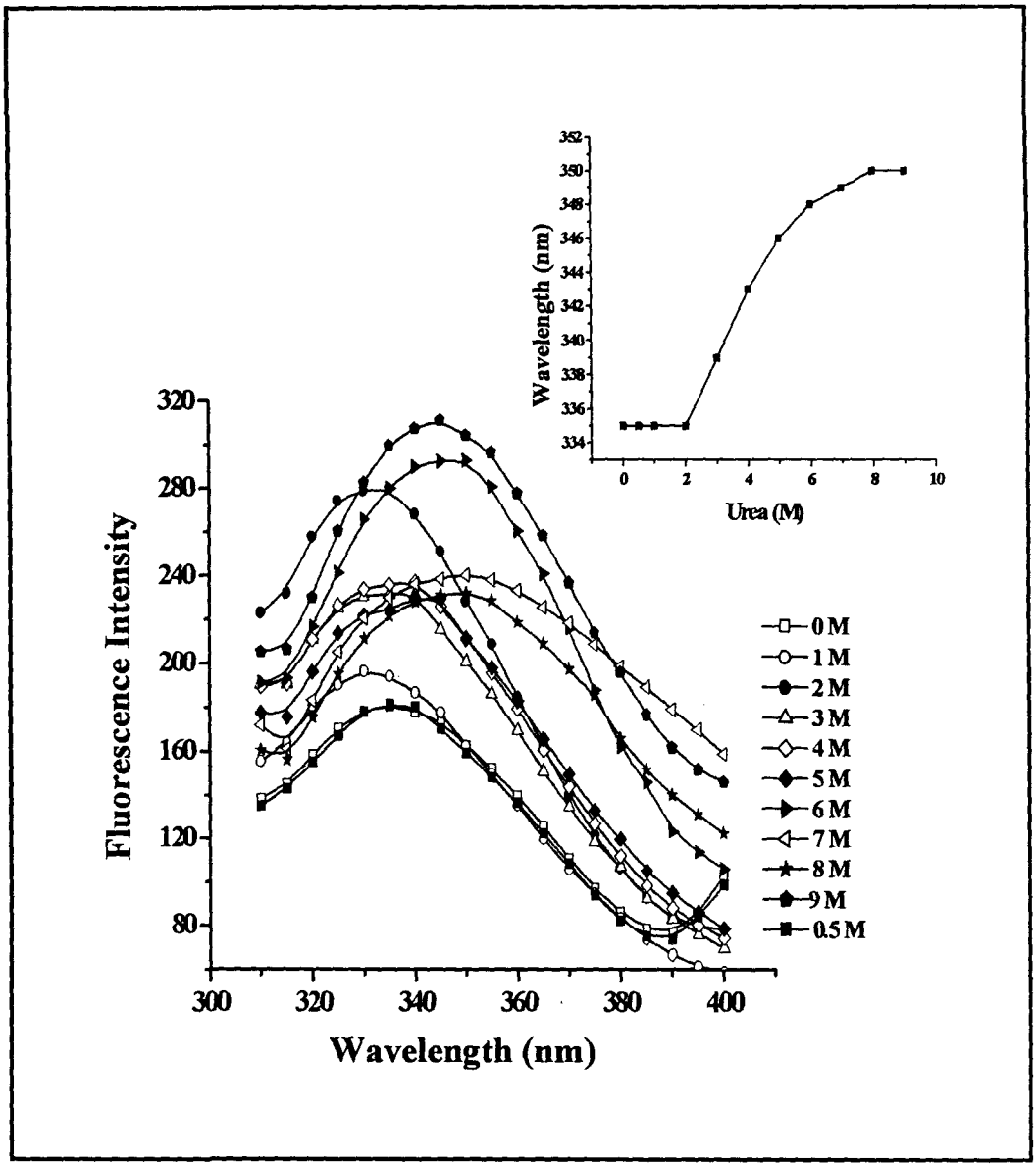
Fluorescence Intensity
Wavelength (nm)
320
280
240
200
160
120
80
300
320
340
360
380
400
0 M
1 M
2 M
3 M
4 M
5 M
6 M
7 M
8 M
9 M
0.5 M
Wavelength (nm)
Urea (M)
352
350
348
346
344
342
340
338
336
334
0
2
4
6
8
10

Fig. 41 Secondary structure analysis of PTPI in the presence of urea

The figure shows changes in far UV CD spectra of PTPI denatured in increasing concentrations of urea (0-9 M). The conditions were same as for figure 3 except that the concentration of PTPI was 1.73 μM. The inset shows changes in MRE at 222 nm with increasing concentration of urea.

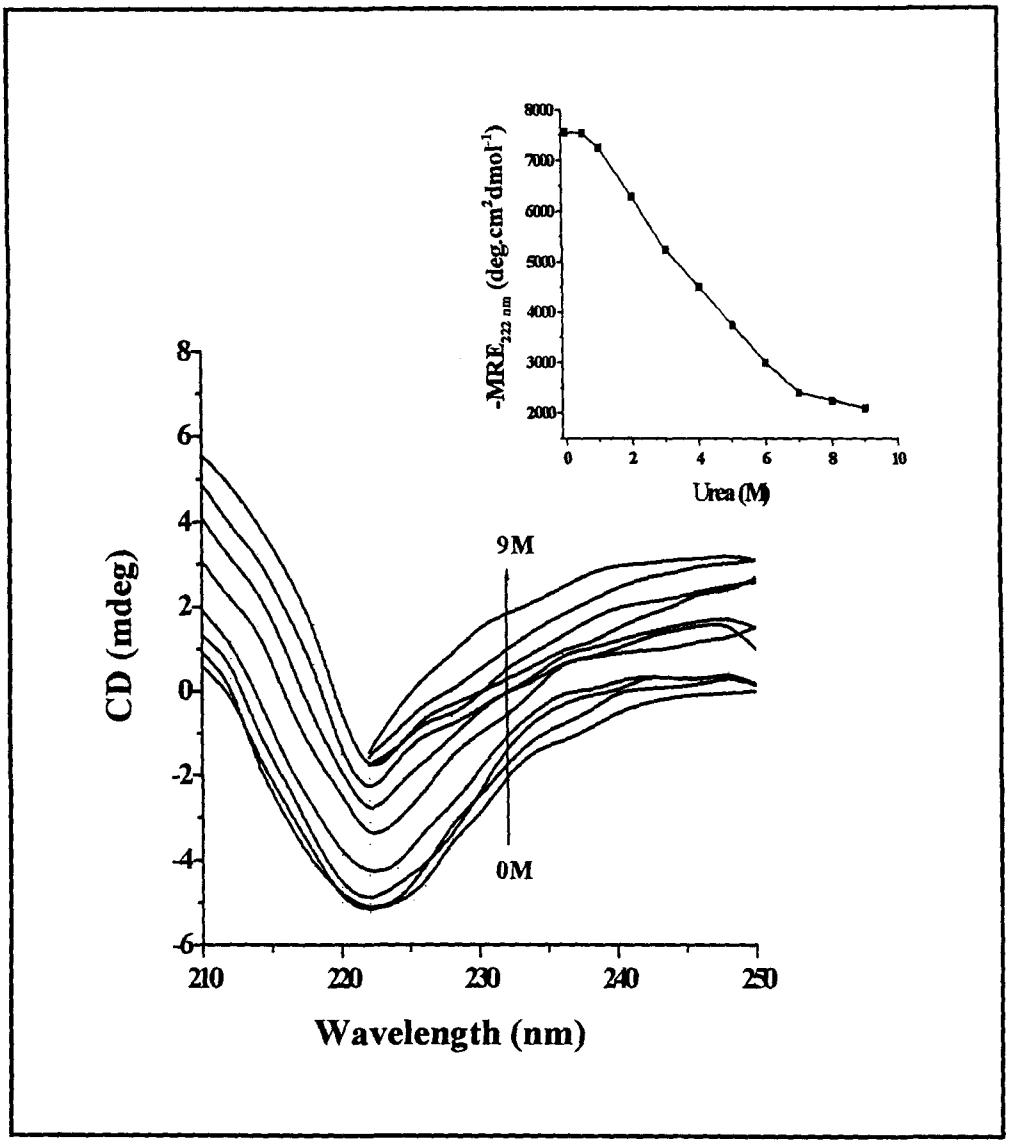
8000
7000
6000
5000
4000
3000
2000
-MRE222 nm (deg.cm2dmol-1)
0
2
4
6
8
10
Urea (M)
8
6
4
2
0
-2
-4
-6
CD (mdeg)
9M
0M
210
220
230
240
250
Wavelength (nm)

Fig. 42 Changes in functional and structural properties of PTPI in presence of urea

The figure shows normalized transition curves for urea induced unfolding of PTPI as obtained from

(a) enzymatic activity

(b) wavelength of maximum emission

(c) MRE at 222 nm

(d) shows the coincidence of transition curves, (a), (b) and (c).

Fraction of unfolded protein was calculated at each concentration as explained in methods section.

(a)

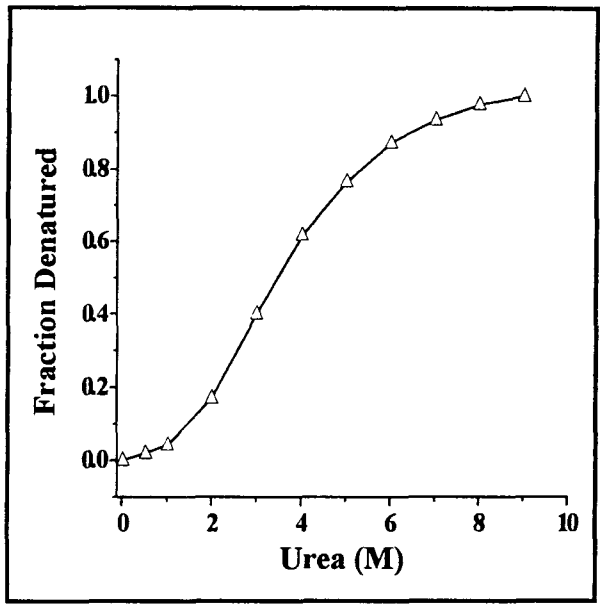
Fraction Denatured
1.0
0.8
0.6
0.4
0.2
0.0
0
2
4
6
8
10
Urea (M)

(b)

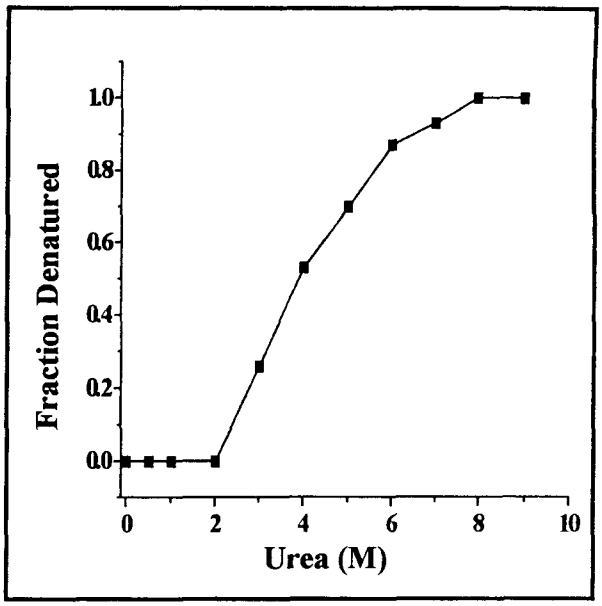
Fraction Denatured
1.0
0.8
0.6
0.4
0.2
0.0
0
2
4
6
8
10
Urea (M)

(c)

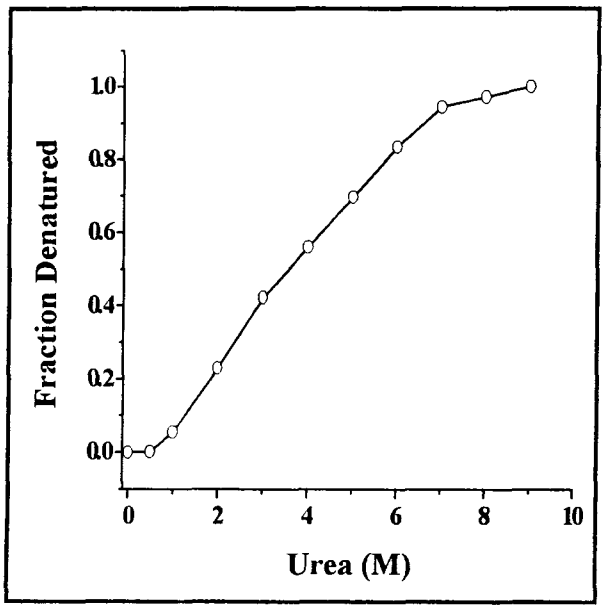
Fraction Denatured
1.0
0.8
0.6
0.4
0.2
0.0
0
2
4
6
8
10
Urea (M)

(d)

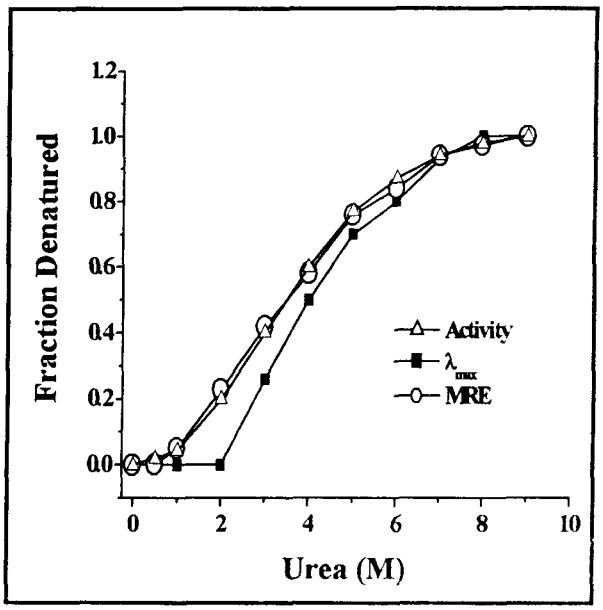
Fraction Denatured
1.2
1.0
0.8
0.6
0.4
0.2
0.0
0
2
4
6
8
10
Urea (M)
Activity
λmax
MRE

denaturation of the dimeric myosin rod, the equilibrium constants are likely to be very sensitive to denaturant concentration such that the effect of protein concentration is overshadowed [Nozais and Bechet, 1993]. The midpoint of λ_{max} transition curve was determined to be 4 M [Fig. 42b]. The Cm value deduced from $MRE_{222\ nm}$ transition curve was 3.6 M urea [Fig. 42c].

The urea denaturation profiles of PTPI as studied by monitoring the changes in inhibitory activity, fluorescence emission maximum and $MRE_{222\ nm}$ at increasing urea concentrations are non-coincident [Fig. 42d]. The inactivation of the inhibitor and loss of secondary structure can be seen as concomitant events. However, the modification (or substantial loss) in tertiary structure seems to occur at higher urea concentration since the midpoint of λ_{max} transition curve is located around 4 M [Fig. 42c].

3.2.3 ANS FLUORESCENCE

ANS has been widely used as a sensitive reporter of apolar regions in proteins and as a probe for protein non-native, partially unfolded conformations [Semisotnov et al., 1991; Stryer, 1965; Ptitsyn, 1995]. Such intermediates are characterized by the presence of solvent exposed hydrophobic clusters. The binding of ANS to apolar region of proteins results in a significant enhancement of ANS fluorescence intensity and in a pronounced blue-shift of λ_{max} [Semisotnov et al., 1991]. For ANS in the presence of native PTPI, significant fluorescence intensity with emission λ_{max} at 505 nm was observed indicating the hydrophobic interaction between ANS and native PTPI that may be present due to the presence of some exposed hydrophobic patches in native PTPI. Reports with native proteins interacting considerably with ANS are present. Bovine liver catalase binds to ANS in native state [Prakash et al., 2002] so does cytoplasmic creatine kinase [Couthon et al., 1995].

To check if any non-native intermediate is present in unfolding of PTPI by GdnHCl and urea, ANS binding to denatured PTPI at increasing concentrations of the denaturants was analyzed. Denatured protein samples were incubated with 50 molar excess of ANS and fluorescence was monitored. In GdnHCl denaturation there was absence of any notable binding of ANS to GdnHCl-treated PTPI. ANS emission intensity slightly decreased during urea denaturation indicating disruption of native PTPI structure. Also no appreciable changes were detected in ANS emission λ_{max} in both the cases, suggestive of no increase in apolar surface exposure during the process

[Fig. 43]. Similar results have been reported for creatine kinase. ANS binding fluorescence data for creatine kinase denaturation in 6 M urea and 3 M GdnHCl showed no hydrophobic surface exposure [Huang et al., 2001].

3.2.4 RENATURATION OF PTPI AFTER GdnHCl- AND UREA-INDUCED DENATURATION

For studying the renaturation of GdnHCl- and urea- treated PTPI, refolding studies were performed. PTPI was incubated with increasing concentrations of GdnHCl (0-6 M) or urea (0-9 M) for 2 h. For performing refolding studies, these samples were then diluted to 50-fold in 50 mM sodium phosphate buffer (pH 7.5). The extent of renaturation was monitored by the recovery of inhibitory activity and fluorescence properties; at regular intervals till 24 h. Table 9 depicts the properties of refolded PTPI. Regain of inhibitory activity of PTPI was taken to be the main criterion for refolding as the fully active enzyme under these conditions is the manifestation of active site being present in proper (native) conformation. The inhibitor did not regain its papain inhibitory activity on urea denaturation. In case of GdnHCl induced denaturation only 10% of the native activity was observed even at low denaturant concentrations. Also, as seen in table 9 at all time intervals, both in urea and GdnHCl mediated denaturation (at all denaturant concentrations) the inhibitor refolded to a species having significantly different spectroscopic properties, λ_{max} of which was within the range of 325-330 nm, instead of 335 nm (for native PTPI). Upon incubation with ANS, the refolded species obtained both in case of urea and GdnHCl, did not alter the emission spectra of the dye, in intensity or in λ_{max}.

Fig. 43 ANS fluorescence of PTPI at various concentrations of GdnHCl and urea

The figure shows dependence of fluorescence emission of ANS bound to PTPI on the denaturant concentration. No significant change in the fluorescence intensity (at 505 nm) is observed at any concentration of GdnHCl. In presence of urea, fluorescence intensity continuously decreases.

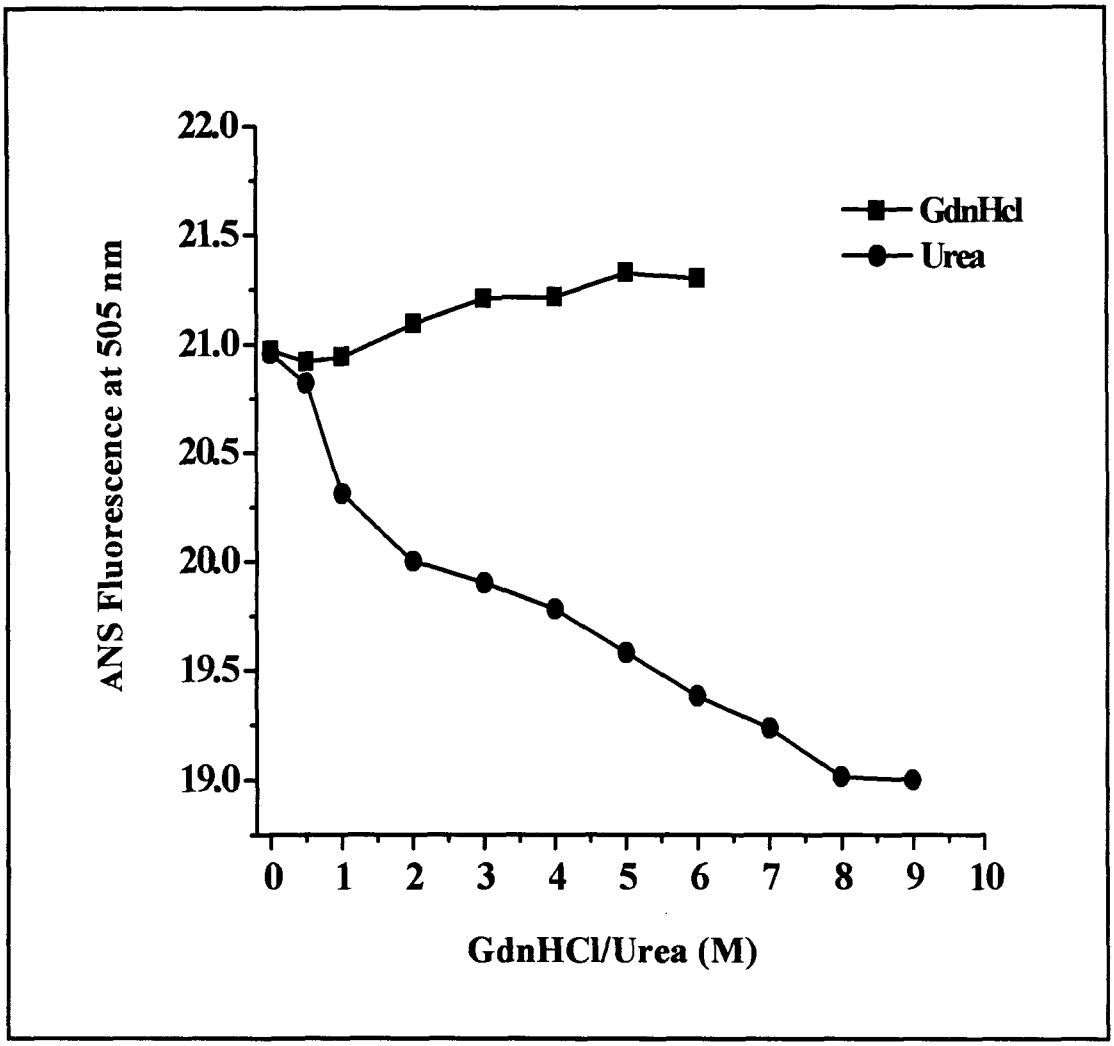
22.0
21.5
21.0
20.5
20.0
19.5
19.0
ANS Fluorescence at 505 nm
0
1
2
3
4
5
6
7
8
9
10
GdnHCl/Urea (M)
GdnHcl
Urea

TABLE 9: FLUORESCENCE EMISSION MAXIMA AND PAPAIN INHIBITORY ACTIVITY DURING REFOLDING OF PTPI AT VARIOUS TIME INTERVALS AFTER 50 FOLD DILUTION OF DENATURED SAMPLES

Denaturant	Papain inhibitory activity (%)[a]			
	2 h	**4 h**	**8 h**	**24 h**
GdnHCl	10	11	ND	ND
	Fluorescence emission maximum (nm)			
	2 h	**4 h**	**8 h**	**24 h**
GdnHCl	325	330	330	320
Urea	325	332	328	327

[a] Activity of the refolded PTPI was determined by the method of Kunitz [1947]. The activity is expressed as percent of native PTPI activity which was taken to be 100%.
ND: None Detected.

Discussion

Chapter 2

DISCUSSION

The altered levels (or activities) of cysteine proteinases (cathepsins) has been established as a cause for rheumatoid arthritis, osteoarthritis and osteoporosis [Vasiljeva et al., 2007], neurological disorders [Nakanishi, 2003], pancreatitis [van Acker et al., 2002], cancer [Gocheva & Joyce, 2007], etc. This fact prompted an increase in the interest in the enzymes that regulate CP activity, in vivo. Such proteinaceous inhibitors of CPs, ubiquitously distributed in organisms as well as tissues, primarily belong to the cystatin superfamily. Modified expression or function of the members of cystatin superfamily marks predisposition to diverse pathological states [Turk et al., 2008]. Studies that delve into the structural and functional properties of these inhibitors in response to various externally imposed conditions thus intend to provide a good approximation of the conformational stabilities of these inhibitors.

An interplay of various physicochemical forces- like hydrophobic interactions, ionic interactions, disulfide bonds and other local as well as non-local interactions maintain the three dimensional structure of proteins. The conformational stability of the native protein is a function of external variables, such as, temperature, pH, ionic strength and solvent composition and can be measured by equilibrium unfolding studies using urea and guanidine hydrochloride (GdnHCl) [Pace, 1986]. CD measurements in the far-UV region, detecting changes in the secondary structure and steady-state fluorescence measurements, detecting changes in the tertiary structure, are complementary tools to investigate the conformational stability of globular proteins.

Equilibrium denaturation studies usually focus primarily on monomeric globular proteins. However, multidomain and oligomeric proteins remain relatively little explored [Jeanicke, 1991].

A number of investigations on unfolding have already been conducted for various members of cystatin superfamily [Khan & Bano, 2009; Rashid et al., 2005; Jankowska et al., 2004; Zerovnik et al., 1992; etc.]. On these lines, equilibrium denaturation of the purified cystatin, PTPI, was undertaken.

The unfolding of PTPI in GdnHCl and urea suggests different unfolding pathways. The two possible pathways in urea and GdnHCl are represented schematically in Fig. 44. In the figure dotted arrow in case of GdnHCl denaturation represents partial reversibility of the process, whereas in case of urea denaturation it represents the

uncertainty in presence and placement of intermediate states. Analysis of PTPI denaturation by fluorescence emission λ_{max}, $MRE_{222\ nm}$, and enzymatic activity measurements reveals a coincident transition, with Cm value of 3.2 M for GdnHCl denaturation. These results are consistent with two-state transition involving a folded dimer and unfolded monomer.

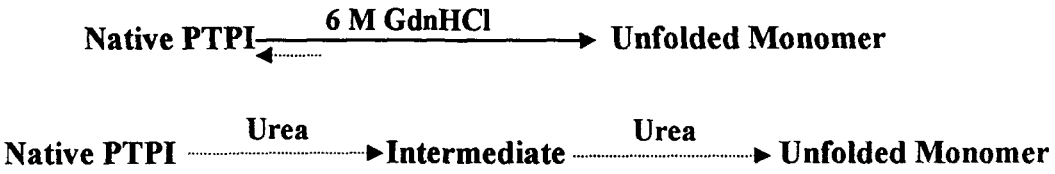

Fig. 44 Schematic diagram of GdnHCl- and urea- induced unfolding of PTPI

Equilibrium denaturation studies of the small dimeric globular proteins, f1 gene V protein [Liang & Terwilliger, 1991], P22 Arc repressor [Bowie and Sauer, 1989a], mouse-β-nerve growth factor [Timm & Neet, 1992], revealed that stable intermediates are not detected at equilibrium. The experimental data were consistent with a two-state model involving only the native dimer and denatured monomer. However, recent reports catalogue the presence of intermediates in denaturant induced unfolding of multimeric or large proteins [Garrido et al., 2005; Akhtar et al., 2002; Guo et al., 2004b; etc]. Two-state denaturation of dimeric proteins by GdnHCl has also been reported earlier [Timm & Neet, 1992].

Inactivation and loss of secondary structure appear to be concomitant events in urea denaturation [Fig. 42]. The midpoint of transition curves for ellipticity and inactivation by urea was 3.6 M. The midpoint value of the λ_{max} transition curve is shifted to a slightly higher concentration of urea (4 M). The non-coincidence of transition curves, as measured by probes that are sensitive to different levels of protein structure are consistent with a mechanism involving intermediate states [Kim & Baldwin, 1982]. The non-coincidence of the λ_{max} transition curve with those monitoring the changes in enzymic activity and ellipticity suggests the existence of intermediate states during urea denaturation. It may illustrate the unfolding of portions enclosing tryptophan residues. However, the intermediates are not clearly observed. As for example, no compact intermediate state possessing hydrophobic areas have been detected through ANS fluorescence. Intermediates in urea-induced unfolding of oligomeric enzymes have been documented for cytoplasmic creatine kinase [Couthon

et al., 1995], bovine liver catalase [Prakash et al., 2002], glucose dehydrogenase [Mendoza-Hernandez et al., 2000]. Creatine kinase denaturation by urea revealed presence of intermediate states adjudged by non-coincidence of the ellipticity curve with the curves presenting changes in enzymic activity, tertiary structure and molecular dimensions. However, intermediates were clearly observed in case of GdnHCl mediated creatine kinase unfolding [Couthon et al., 1995]. Presence of intermediate states in urea denaturation has also been documented for glucose dehydrogenase monitored easily by CD and fluorescence spectroscopy. Contrary to this, glucose oxidase was found to denture following a two-state model for urea [Akhtar et al., 2002].

Although monomeric, but high molecular mass goat lung cystatin are also known to denature in the presence of urea by following a multistep process [Khan and Bano, 2009b], suggesting the presence of aggregated/non-native intermediates in urea unfolding of high molecular mass proteins.

Refolding and reactivation of the denatured PTPI (both for urea- and GdnHCl-denaturation) was incomplete. The partially refolded PTPI gave maximum emission in range of 325-330 nm. Although close to the native enzyme and suggestive of a compact structure, its specific tertiary structure is quite different from the native PTPI, as no ANS binding was observed. This points to a disrupted native from. Activity gain was only 10% in case of GdnHCl, while in case of urea it remained undetected. This agrees with the generally recognised opinion that conformational integrity is important for maintaining the enzyme activity and the slight changes at the active site can lead to complete enzyme inactivation. In case of urea, it may point to large kinetic barrier for the unfolded monomer to reassociate into an active dimer. Or under in vivo conditions assisted folding might be taking place. Conditions for 100% recovery of active enzyme thus require optimization, in case of GdnHCl.

The data derived from these studies indicate that unfolding pathways in GdnHCl and urea are different. This is not surprising since the two denaturants interact with proteins in a different way. Apart from their hydrogen bond breaking effect, urea also acts on hydrophobic bonds [Kamoun, 1988] and ions arising from GdnHCl are known to modulate electrostatic interactions [Hagihara et al., 1994]. Urea is generally known to be about half as effective in protein unfolding and dissociation as GdnHCl [Pace, 1986]. This is suggestive of a '2-fold rule' [Mayers et al., 1995; Smith & Scholtz, 1996]. Multimeric proteins have higher ratio of [Cm (urea)/ Cm (GdnHCl)] [Akhtar et

al., 2002], which suggests that multimeric proteins are more susceptible to GdnHCl denaturation. Although, for proteins with non-two state transitions (as seen for urea induced denaturation in the present case) the Cm value may not be an accurate measure of the stability to the chaotrope, it does provide some indications for the differences in the interactions of the denaturant with different classes of proteins. The results of the present study show that PTPI is an exception to the '2-fold rule' of urea and GdnHCl denaturation. Fig. 38 and Fig. 42 present the results of denaturation of PTPI as monitored by the change in enzyme activity, $MRE_{222\ nm}$, and λ_{max} of fluorescence emission. The midpoint of transition for urea unfolding was 3.6 M (4 M from the λ_{max} curve), and that for GdnHCl was 3.2 M. Violation of '2-fold rule' for urea and GdnHCl denaturation has also been reported for the dimeric enzyme glucose oxidase [Akhtar et al., 2002]. This further points to significant contributions of both electrostatic and hydrophobic interactions in maintaining the active site and /or dimeric nature of the PTPI.

The results obtained in this study give an idea about the stability of PTPI and can be extrapolated to physiological conditions. Studying the behaviour and stability of proteins under denaturing conditions allows one to understand and quantify the forces that contribute to the conformational stability of protein in their aqueous environment [Pace, 1986]. Further the data on the stability of proteins can be used in algorithms to predict the structure or docking of proteins and to design new proteins with better activities and stabilising changes.

Chapter 3

In vitro fibrillation of pancreatic thiol proteinase inhibitor

3.3 RESULTS

Amyloid fibril formation is generally the result of the alteration of native conformation of proteins. The partially folded conformations are favoured by mutations or changes in pH and ionic strength [Pedersen et al., 2004]. Members of cystatin superfamily show predisposition for fibrillization. A number of reports are available on in vitro fibrillation of cystatins under experimentally exposed mild denaturational conditions, besides, cystatin C and stefin B fibrillation been incriminated in human cystatin C amyloid angiopathy (HCCAA) and progressive myoclonus epilepsy (EPM1), respectively [Turk et al., 2008].

The ability for rational design of conditions promoting amyloid formation with a wider range of proteins (than those so far identified in specific diseases) provides an opportunity to investigate in detail the mechanism of the underlying processes (in vivo) and hence to explore the factors that predispose individual sequences to form ordered aggregates under particular conditions. This could be an important factor in the development of strategies to combat amyloid formation/deposition.

On these footings, present study was designed to investigate the conditions under which the purified goat pancreatic thiol proteinase inhibitor fibrillates and to probe the inhibition or deaggregation of fibrils in the presence of divalent metal ions.

3.3.1 ACID DENATURATION OF PTPI

It has been well established that fibril formation requires appropriate physicochemical conditions, among which pH exerts a significant influence on the whole process of fibrillogenesis [Lai et al., 1996]. pH engendered deformation of proteins is common in biology. A number of proteins have been reported to exist as partially folded intermediates or as molten globules under acidic conditions [Rashid et al., 2006b; Kuwajima, 1989; Zerovnik et al., 1992; Ahmad and Khan, 2006; Brahma et al., 2005], a condition already emphasized as an important start point for amyloid aggregation. Thus to explore the existence of any non-native, partially unfolded intermediate under acidic conditions, PTPI was subjected to denaturation over a pH range of 1.0-7.0.

Fluorescence spectra of PTPI in the presence of varying pH

Acid induced unfolding of PTPI was followed by intrinsic fluorescence properties of the protein. PTPI incubated in buffers of different pH was excited at 280 nm to assess global conformational changes inflicted by pH. In its native state PTPI is

characterized by a peak at 335 nm (at pH 7.5) [Priyadarshini and Bano, 2009]. Till pH 5.0, no change is observed in λ_{max} of emission [Fig. 45a]. However, a 10 nm blue shift is observed at pH 3.0. Lowering the pH to 2.0 caused a red shift of 2 nm (compared to the state at pH 3.0) further followed by a red shift of 3 nm, at pH 1.0. On the other hand, as the pH is lowered from 7.0 to 1.0, fluorescence intensity is quenched [Fig. 45a]. This decrease in fluorescence intensity and a blue shift of 10 nm at pH 3.0 is indicative of burial of aromatic residues in the hydrophobic core of the protein and formation of a more compact structure. Red shift observed at pH 2.0 and 1.0 can be ascribed to slight unfolding of the structure.

Effect of pH on ANS spectrum of PTPI

In order to study the exposure of hydrophobic clusters of the PTPI during acid induced unfolding, effect of pH was followed by ANS fluorescence at 505 nm after exciting the ANS-protein complex at 380 nm [Fig. 45b]. Till pH 4.0, there was no appreciable increase in ANS binding. A sharp increase is noticeable at pH 3.0, reaching maximum at pH 1.0. Further, there was a shift in λ_{max} of ANS emission at pH 3.0, the λ_{max} of ANS-protein complex was blue shifted to 490 nm with no further change with pH reduction. These results show that at pH 3.0, small amount of hydrophobic clusters are present which bind ANS and also suggest the presence of large number of solvent accessible non-polar clusters in protein molecule at pH 1.0.

Perturbation of secondary structure of PTPI by pH

The effect of acid induced unfolding on secondary structure of PTPI was monitored by ellipticity measurements at 222 nm. The results are shown in Fig. 46. The ellipticity at 222 nm decreased markedly below pH 7.0, to a minimum value at around pH 3.0. A further decrease in pH below 3.0 resulted in a second transition corresponding to the formation of secondary structure which became maximum at pH 1.0. At pH 3.0, ~40% of secondary structure is lost. At pH 1.0, ~34% of secondary structure is regained and it is marked by the presence of 82% secondary structure. Thus it may be concluded that PTPI at pH 3.0 exists as a partially unfolded intermediate which has ~60% of residual secondary structure, but almost completely altered tertiary structure. PTPI at pH 1.0 exhibits more of molten globule like features with native like secondary structure contents, enhanced ability to bind ANS, however with tertiary contacts quite similar to native PTPI [Fig. 45a].

Fig. 45 pH dependence of intrinsic and ANS fluorescence properties of PTPI

(a) Figure shows variation in intrinsic fluorescence intensity at 335 nm and λ_{max} of emission of PTPI with pH. PTPI (1 μM) was incubated in 50 mM solutions of glycine/HCl (pH 2.0), sodium acetate (pH 3.0-5.0), sodium phosphate (pH 6.0-7.0) at room temperature for 4 h. The excitation wavelength was 280 nm and emission was recorded in range of 300-400 nm with a slit width of 5 nm.

(b) Figure shows variation in ANS fluorescence intensity at 505 nm and λ_{max} of emission of ANS-PTPI complex with pH. The samples were prepared as described above. The ANS to protein molar ratio was 1:50. ANS fluorescence was measured at an excitation wavelength of 380 nm in the emission range of 400-600 nm with a slit width of 5 nm.

(a)

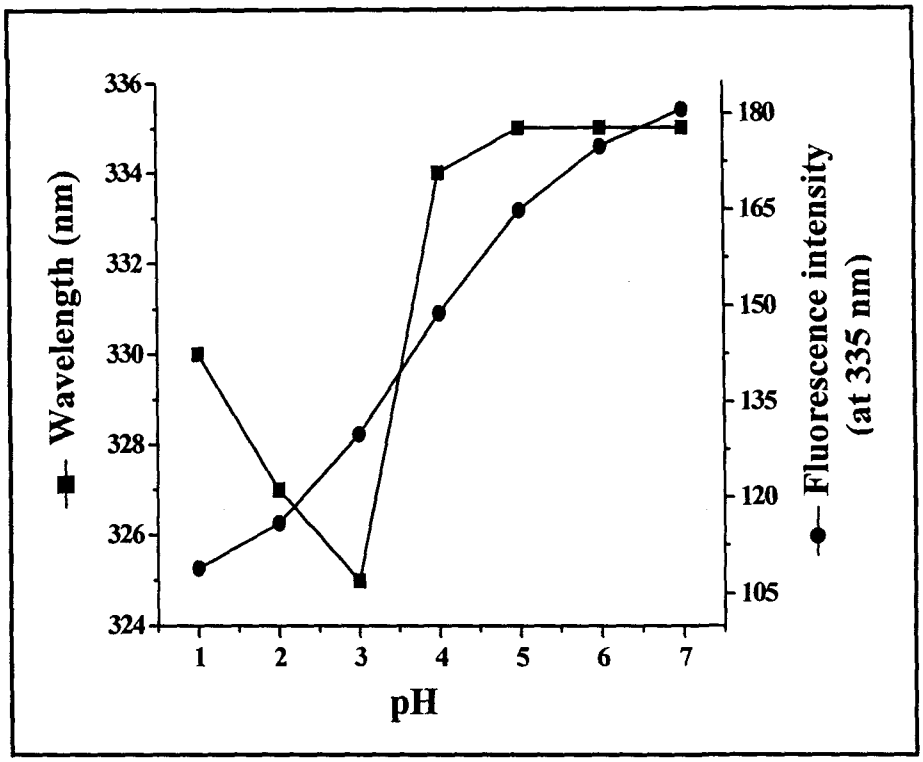
Wavelength (nm)
Fluorescence intensity (at 335 nm)
pH
336
334
332
330
328
326
324
180
165
150
135
120
105
1
2
3
4
5
6
7

(b)

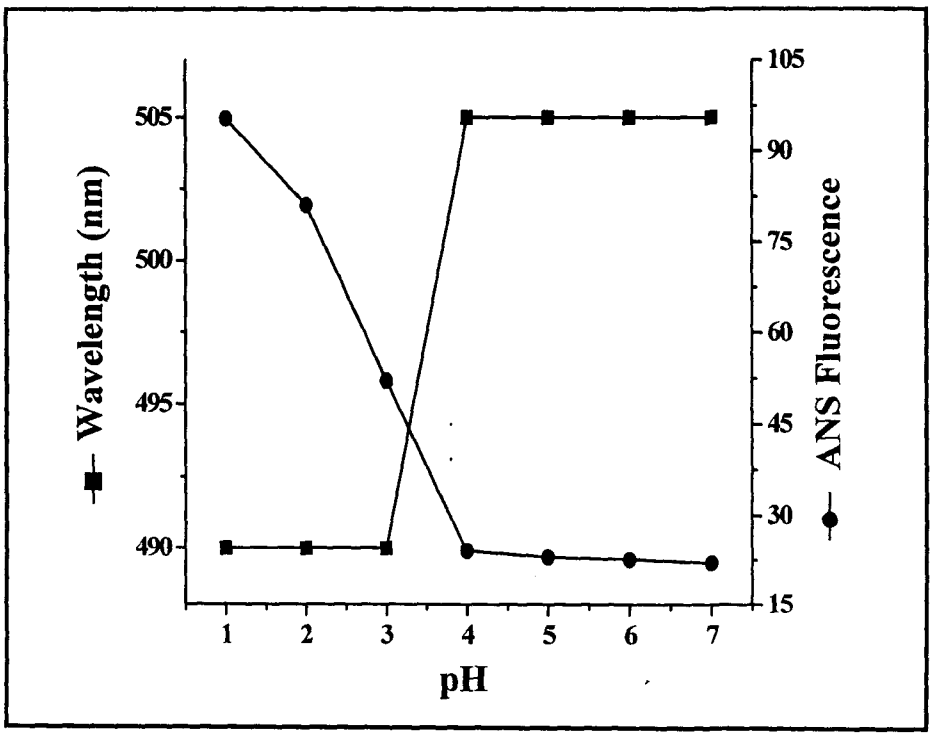
Wavelength (nm)
ANS Fluorescence
pH
505
500
495
490
105
90
75
60
45
30
15
1
2
3
4
5
6
7

Fig. 46 pH dependence of mean residue ellipticity (MRE) of PTPI at 222 nm

For far UV CD, 1.73 μM of PTPI was incubated in 50 mM solutions of glycine/HCl (pH 2.0), sodium acetate (pH 3.0-5.0), sodium phosphate (pH 6.0-7.0) at room temperature for 4 h. Cells of 1 mm pathlength were used.

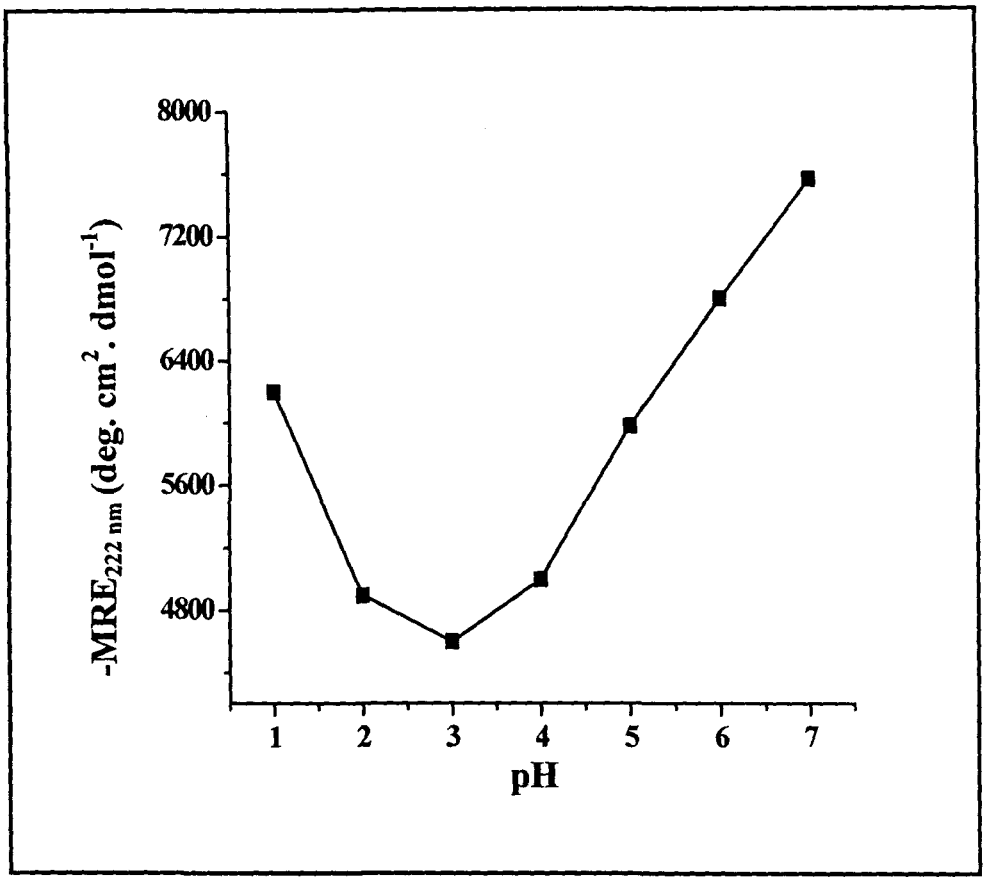
8000
7200
6400
5600
4800
-MRE222 nm (deg. cm2. dmol-1)
1
2
3
4
5
6
7
pH

3.3.2 EFFECT OF 2, 2, 2-TRIFLUOROETHANOL (TFE) ON ACIDIC pH INDUCED STATE OF PTPI

TFE has been used widely with other proteins to induce amyloid fibril formation [Zerovnik et al., 2007]. TFE has a double edged effect on proteins and peptides, on one hand, it can destroy the tertiary structure of proteins on the other hand, it can increase the α-helical structure of proteins and peptides via strengthening of the hydrogen bonds [Luo and Baldwin, 1998; 1997]. Effect of TFE on pH 3.0 state of PTPI was studied by means of intrinsic and extrinsic fluorescence and far UV CD.

Effect of TFE on the secondary structure of PTPI at pH 3.0

Fig. 47a shows changes in ellipticity at 222 nm of pH 3.0 state as a function of TFE concentration. As shown earlier approximately 40% loss in secondary structure at pH 3.0 occurred as compared to the native state at pH 7.5. Increase in concentration of TFE leads to increase in $MRE_{222\,nm}$ value. It is interesting to note that at 10% TFE the induced secondary structure reached almost the value for the native state. At higher TFE concentration denatured states with very high α-helical content were formed.

Native PTPI was also titrated with various concentrations of TFE. At all TFE concentrations accumulation of secondary structure was noticed with native PTPI transforming to an all-helical state beyond 10% TFE (data not shown).

Effect of TFE on intrinsic fluorescence of PTPI at pH 3.0

Since the pH 3.0 state of PTPI in presence of 10% (v/v) TFE shows native like secondary structure content it was of interest to study properties of pH 3.0 state in presence of TFE. Fig. 47b shows intrinsic emission spectra of PTPI at pH 7.5, pH 3.0 and pH 3.0 state in the presence of 10% (v/v) TFE. The emission spectrum of PTPI shows λ_{max} at 335 nm under native conditions. At pH 3.0, there was ~31% loss in fluorescence intensity and a change in λ_{max} to 325 nm suggesting internalization of tryptophan residues to a more hydrophobic environment [Haq et al., 2002]. At 10% (v/v) TFE concentration, there is ~17% increase in fluorescence intensity with further blue shift in λ_{max} to 323 nm, suggesting further internalization of tryptophan residues in the hydrophobic environment and creation of a more compact structure.

Fig. 47 Effect of TFE on PTPI at pH 3.0

(a) Figure shows the effect of increasing concentration of TFE (0-20%) on pH 3.0 state of PTPI as monitored by changes in MRE value at 222 nm. Cells of 1 mm pathlength were used.

(b) Intrinsic emission spectra of PTPI at pH 7.5, at pH 3.0 alone and in presence of 10% (v/v) TFE. The concentration of PTPI used was 1 μM. The excitation wavelength was 280 nm and emission was recorded in the range of 300-400 nm with a slit width of 5 nm.

(a)

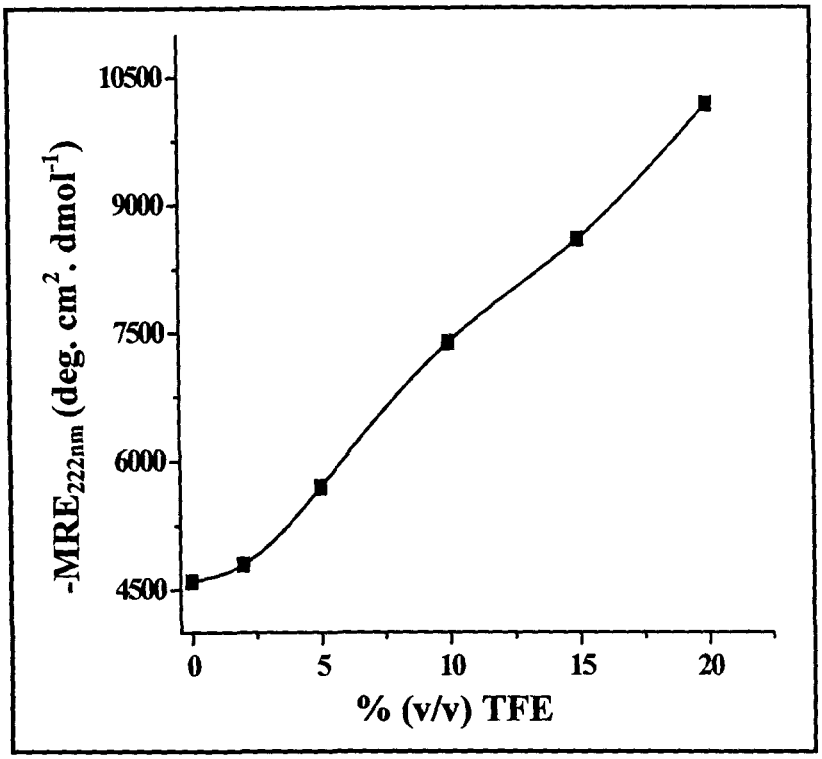
10500
9000
7500
6000
4500
-MRE222nm (deg. cm2. dmol-1)
0
5
10
15
20
% (v/v) TFE

(b)

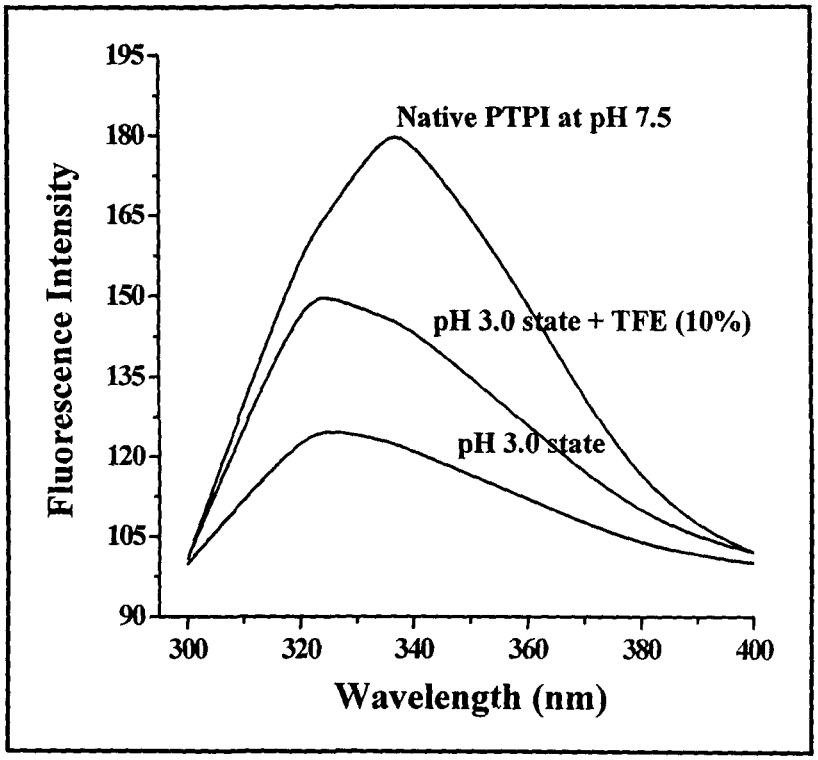
195
180
165
150
135
120
105
90
Fluorescence Intensity
Native PTPI at pH 7.5
pH 3.0 state + TFE (10%)
pH 3.0 state
300
320
340
360
380
400
Wavelength (nm)

Effect of TFE on ANS spectrum of PTPI at pH 3.0

Fluorescent hydrophobic probe ANS has higher affinity for the partially unfolded intermediates and molten globules than for the proteins in the native or fully unfolded state. Fig. 48a shows that ANS binds maximally to pH 3.0 state of PTPI in presence of 10% (v/v) TFE compared to minimal ANS binding to native PTPI. The emission maximum blue shifts to 485 nm in the presence of TFE as compared to those of pH 3.0 state (490 nm) and at pH 7.5 (505 nm), further suggesting that the protein is adopting an altered structure. Titration of the pH 3.0 state with increasing concentration of TFE as studied by ANS binding at 490 nm [Fig. 48b] indicates slight disruption of compact structure at 10% (v/v) TFE. However at higher TFE concentrations [15 and 20% (v/v)] the pH 3.0 state gets altered as there is decrease in exposed hydrophobic clusters available for ANS binding.

Similar studies were also conducted for acid induced pH 2.0 state and pH 1.0 state of PTPI. Unlike pH 3.0 state, no stabilized intermediates were observed. However, 10% (v/v) TFE was found to be predenaturational concentration in both the cases.

3.3.3 OPTIMAL pH AND TFE CONCENTRATION TO INDUCE PTPI AMYLOID FIBRIL GROWTH

Above results show that on decreasing the pH beyond 4.0 there is decrease in the dichroicity of PTPI at 222 nm and a blue shift of the λ_{max} of fluorescence emission. With further decrease in pH to 2.0 and 1.0 there are further alterations in conformation of the protein. As reported for many other proteins acidic conditions prevent complete unfolding of the protein molecule [Rashid et al., 2006b; Gupta et al., 2003; Artigues et al., 1994], and result in the formation of compact, non-native intermediates or molten globules. Acidic conditions render PTPI to adopt a partially unfolded conformation at pH 3.0 referred here as pH 3.0 state having substantial amount of secondary structure but devoid of native like tertiary state. At pH 1.0 more of a molten globule like intermediate is formed characterized by its compactness (compared to native state), persistence of secondary structure without well defined tertiary packing and a strong affinity for ANS as a consequence of the exposure of hydrophobic areas. TFE is known to induce α-helical states and to stabilize partially unfolded intermediates in proteins. PTPI at pH 3.0 gains native like secondary structure at 10% (v/v) TFE concentration and exhibits substantially exposed

Fig. 48 Fluorescence spectra of ANS bound to PTPI under different conditions

(a) Figure shows fluorescence emission spectra of ANS bound to PTPI at pH 7.5, at pH 3.0 alone and in presence of 10% (v/v) TFE.

(b) Figure shows the effect of increasing concentration of TFE on pH 3.0 state as monitored by changes in ANS binding at 490 nm.
The ANS to protein molar ratio was 1:50. ANS fluorescence was measured at an excitation wavelength of 380 nm in the emission range of 400-600 nm with a slit width of 5 nm.

(a)

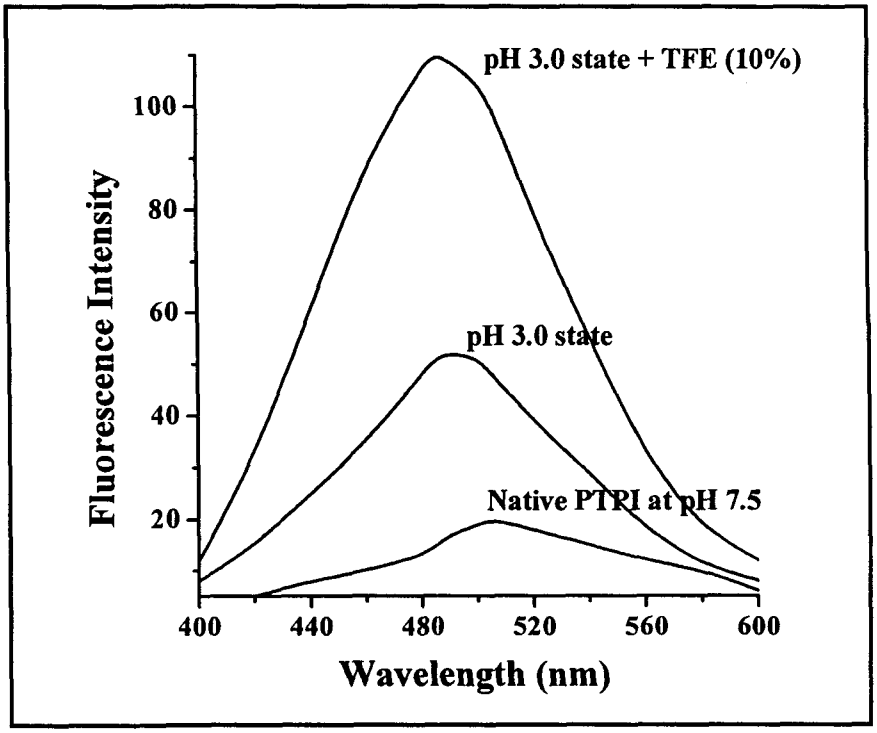
pH 3.0 state + TFE (10%)
pH 3.0 state
Native PTPI at pH 7.5
Fluorescence Intensity
100
80
60
40
20
400
440
480
520
560
600
Wavelength (nm)

(b)

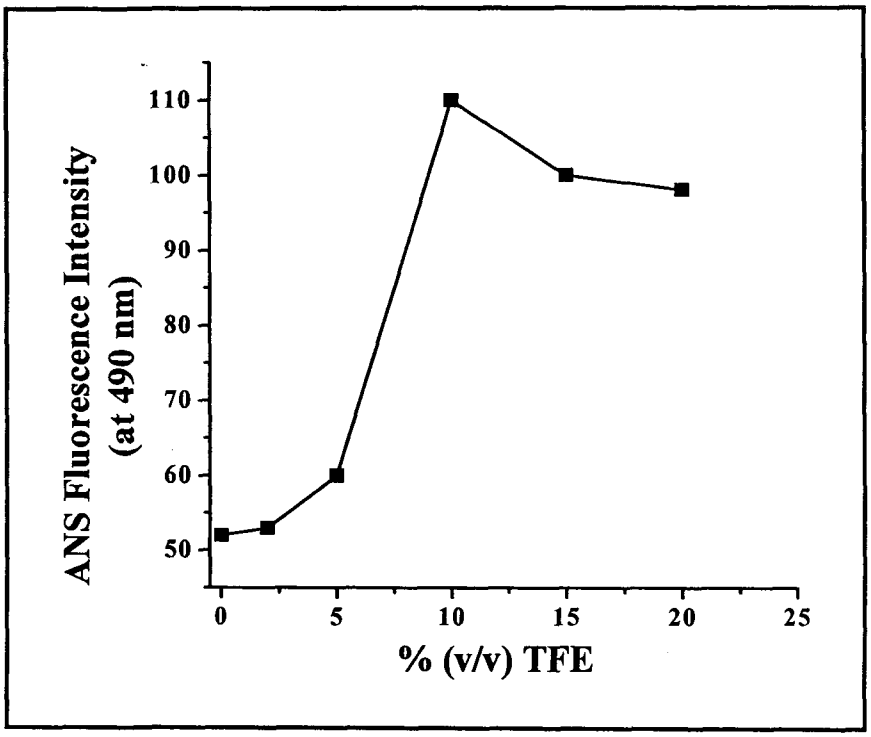
ANS Fluorescence Intensity
(at 490 nm)
110
100
90
80
70
60
50
0
5
10
15
20
25
% (v/v) TFE

hydrophobic patches (revealed by ANS binding). However, there is absence of native like tertiary fold. Beyond this concentration of TFE, denaturing states with very high α helical content were formed.

Based on these findings PTPI for amyloid growth was incubated in acidic medium, as it is known that TFE accelerates amyloid growth [Zerovnik et al., 2002a], 10% (v/v) TFE was added. Amyloid formation was followed by two standard procedures, thioflavin T (ThT) assay and transmission electron microscopy (TEM) [Nilsson, 2004], in the following six samples at regular time intervals,

PTPI at pH 1.0, 2.0 and at pH 3.0 and at these three pH in presence of 10% (v/v) TFE.

3.3.4 AMYLOID TYPE AGGREGATION/FIBRILLATION OF PTPI MONITORED BY ThT FLUORESCENCE

The enhancement in the fluorescence intensity of ThT upon binding to ordered protein aggregates is a rapid and sensitive method to show presence of fibrils. Free ThT has emission maximum at 450 nm. However, upon binding to fibrils the emission λ_{max} changes to 485 nm [Levine, 1999]. 50 μM PTPI was incubated at pH 2.0 and at pH 3.0, in presence of 0.15 M NaCl and 0.05% sodium azide. Changes in fluorescence emission of ThT were monitored at regular time intervals for both the samples. Results are depicted in Fig. 49a and 50a. The pH 2.0 sample, showed only ~5 fold enhancement in ThT fluorescence even after 55 days of incubation [Fig. 49a], suggesting a very lengthy lag phase. At pH 3.0 however, ~14 fold increment was observed within 5 days of incubation [Fig. 50a]. This indicates that at pH 3.0 the amyloid growth is rapid. PTPI samples incubated at neutral pH served as controls and showed no ThT binding. Results obtained for PTPI incubated at pH 1.0 were quite similar to those obtained for pH 3.0 sample. These results thus reveal that amyloid aggregates from PTPI form under acidic conditions and more readily at pH 3.0 and 1.0 than at pH 2.0.

Influence of TFE on amyloid aggregation of PTPI

To study the effect of TFE on the formation of aggregates of PTPI, 50 μM protein was incubated at pH 3.0 and at pH 2.0, with 0.15 M NaCl, 0.05 % sodium azide and 10% (v/v) TFE. Fig. 49b and 50b show the time course of the change of ThT fluorescence as the protein aggregates form at pH 2.0 and pH 3.0 in presence of 10%

(v/v) TFE. Typical fibrillation processes involve a lag phase followed by a relatively rapid elongation phase, which stabilizes at a plateau level when all the protein molecules have been incorporated into fibrils [Harper and Lansbury, 1997]. Whereas at pH 2.0 aggregates develop after a long lag phase and exhibit relatively less ThT fluorescence enhancement [observed at 55th day of incubation, Fig. 49a], in the presence of TFE the maximum ThT fluorescence is reached at 30th day of incubation with several fold increase in the intensity [Fig. 49b]. Similarly for the sample incubated at pH 3.0 in presence of TFE, amyloid aggregation started without a distinct lag phase with a profound fluorescent intensity enhancement [Fig. 50b]. The absence of lag phase suggests that amyloid aggregation of PTPI at pH 3.0 in presence of TFE, proceeds without a nucleation phase or the nucleus might have formed very rapidly (in the dead time of mixing). For PTPI incubated at pH 1.0, a rapid fibrillation was observed without any lag phase in presence of TFE. But ThT fluorescence intensity enhancement was lower to that obtained for pH 3.0.

3.3.5 TRANSMISSION ELECTRON MICROSCOPY IMAGES

Fibril formation was also followed by TEM. Fig. 51 shows TEM image of native dehydrated PTPI. No distinct fibril morphology is seen. Fig. 52 shows the TEM image of PTPI at pH 1.0 obtained after 15 days of incubation. Peculiar foliage like pattern is observed. Fig. 53 shows the TEM image obtained after one month of incubation of sample under similar conditions but at pH 2.0. It shows fibrils. Fig. 54 shows TEM image of PTPI at pH 3.0 in presence of 10% (v/v) TFE obtained after 15 days of incubation. Sharp fibril is observed.

3.3.6 EFFECT OF DIVALENT METAL IONS, Cu^{2+} AND Zn^{2+} ON PTPI FIBRILLATION

To date there is no potential cure to amyloidosis. Different effects of metal ions on amyloid aggregation have been documented. Fig. 55 shows the effect of Cu^{2+} and Zn^{2+} on ThT fluorescence of preformed fibrils. PTPI fibrils grown at pH 3.0 in the presence of 10% (v/v) TFE were used in the experiment. Just before the ThT assay metal solutions were added to the sample. Controls of each concentration of Cu^{2+} and Zn^{2+} were run to nullify the possibility of interaction with the dye. A concentration dependent decline in ThT fluorescence intensity at 485 nm was observed, about ~35%

Fig. 49 PTPI fibrillation at pH 2.0

(a) **Fluorescence emission spectra of Thioflavin T (ThT) dye in the presence of PTPI at pH 2.0**

Figure shows increase of ThT fluorescence on binding to the fibrils of PTPI obtained after 55 days of incubation. 50 μM protein was incubated at pH 2.0 at room temperature.

(b) **Time course of fibril growth of PTPI followed by ThT fluorescence at 485 nm at pH 2.0 and in presence of 10% (v/v) TFE**

50 μM PTPI was incubated at pH 2.0 alone and in presence of 10% (v/v) TFE. Excitation was at 440 nm and spectra were recorded from 455 to 600 nm with a slit width of 5 nm. For ThT assay 5 μM of incubated protein was used with a protein to ThT molar ratio of 1:6. The data were obtained after subtraction of the signal of the buffer containing ThT.

(a)

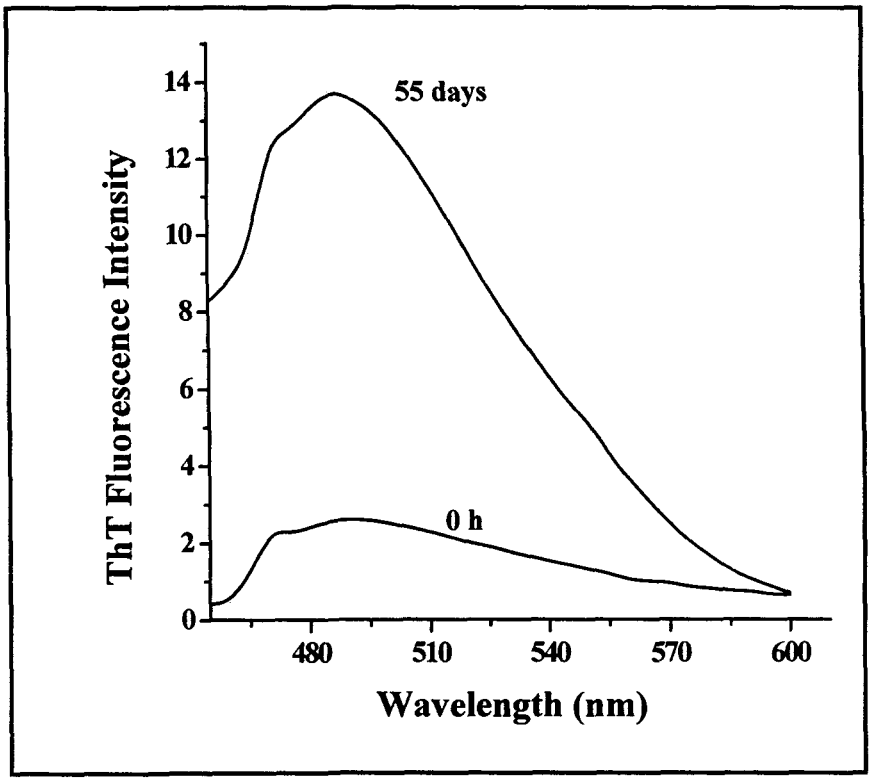
ThT Fluorescence Intensity
14
12
10
8
6
4
2
0
55 days
0 h
480
510
540
570
600
Wavelength (nm)

(b)

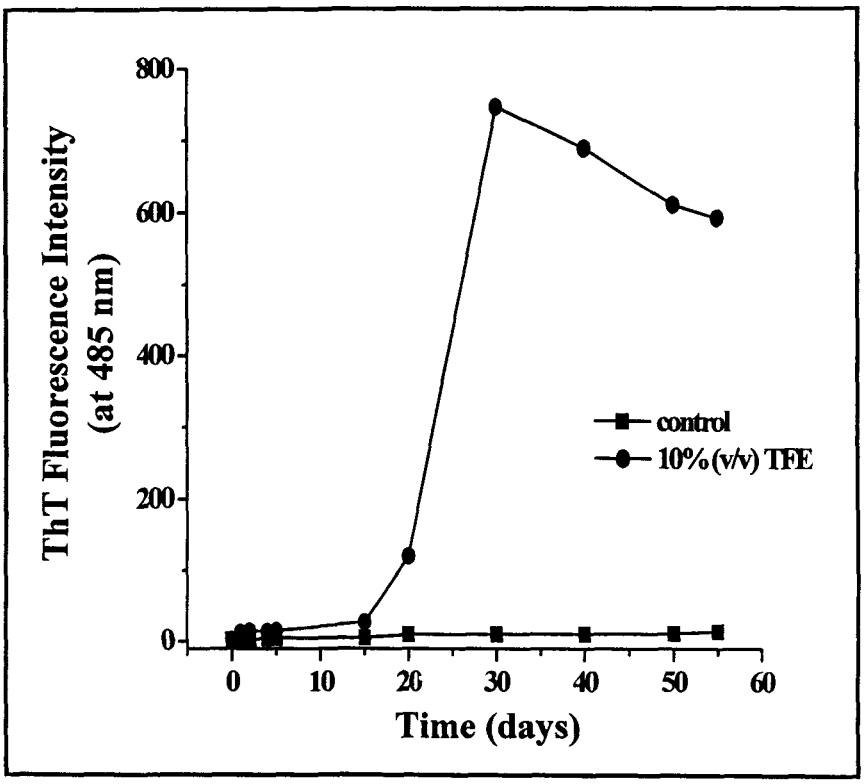
ThT Fluorescence Intensity
(at 485 nm)
800
600
400
200
0
control
10% (v/v) TFE
0
10
20
30
40
50
60
Time (days)

Fig. 50 PTPI fibrillation at pH 3.0

(a) Fluorescence emission spectra of Thioflavin T (ThT) dye in the presence of PTPI at pH 3.0

Figure shows increase of ThT fluorescence on binding to the fibrils of PTPI obtained after 5 days of incubation. 50 μM protein was incubated at pH 3.0 at room temperature.

(b) Time course of fibril growth of PTPI followed by ThT fluorescence at 485 nm at pH 3.0 and in presence of 10% (v/v) TFE

50 μM PTPI was incubated at pH 3.0 alone and in presence of 10% (v/v) TFE. Excitation was at 440 nm and spectra were recorded from 455 to 600 nm with a slit width of 5 nm. For ThT assay 5 μM of incubated protein was used with a protein to ThT molar ratio of 1:6. The data were obtained after subtraction of the signal of the buffer containing ThT.

(a)

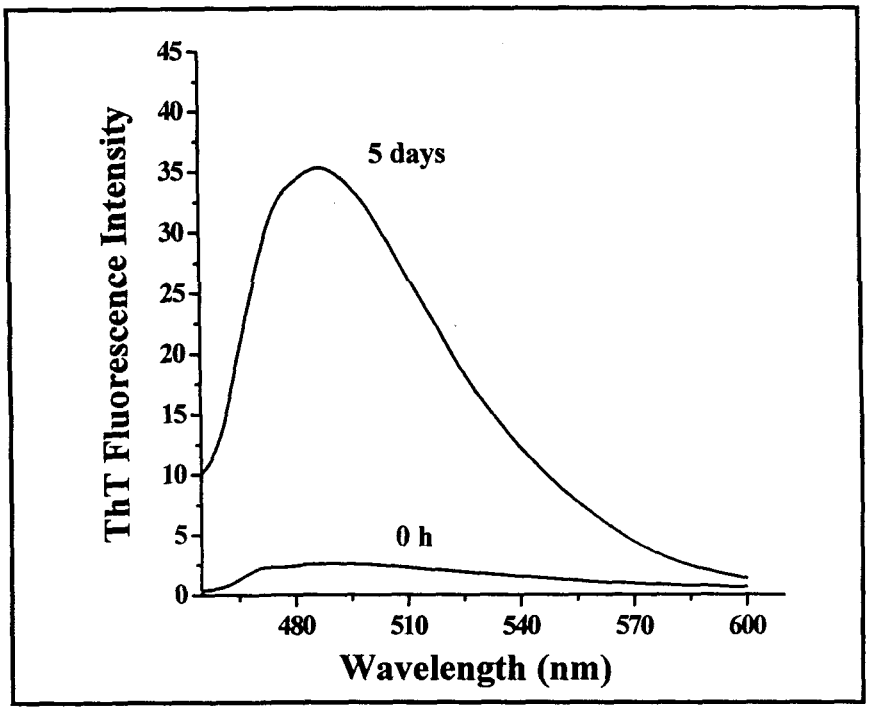
ThT Fluorescence Intensity
45
40
35
30
25
20
15
10
5
0
5 days
0 h
480
510
540
570
600
Wavelength (nm)

(b)

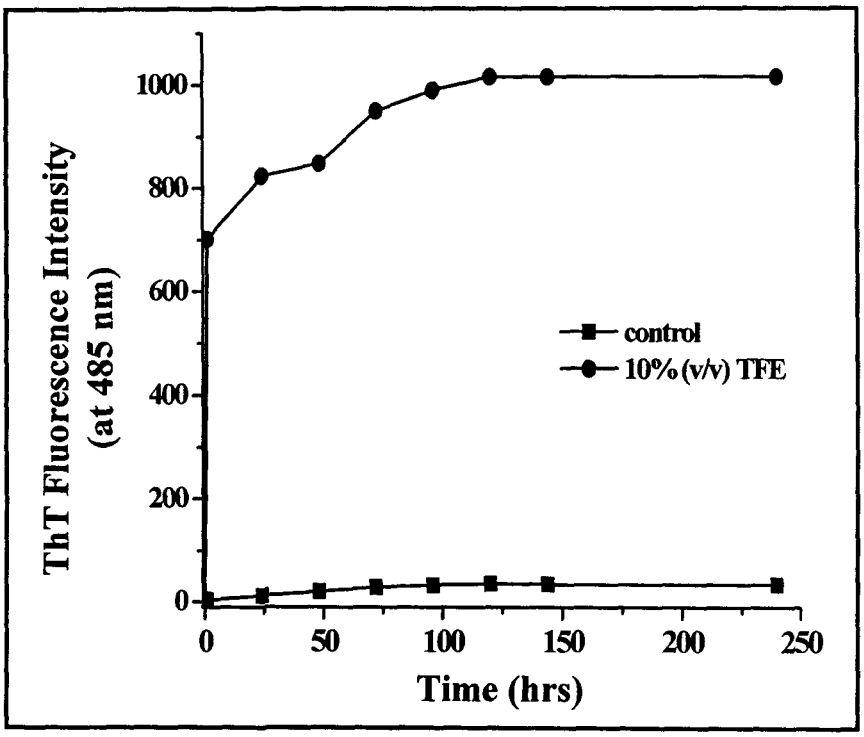
ThT Fluorescence Intensity
(at 485 nm)
1000
800
600
400
200
0
control
10% (v/v) TFE
0
50
100
150
200
250
Time (hrs)

Fig. 51 Electron micrograph of PTPI incubated under native conditions

Figure shows image obtained for native dehydrated PTPI. 50 μM of PTPI in 50 mM sodium phosphate buffer (pH 7.5) was used.

Fig. 52 Electron micrograph showing amyloid aggregation of PTPI incubated at pH 1.0

Figure shows image obtained for PTPI incubated at pH 1.0 in presence of 10% (v/v) TFE. Sample used was obtained after 15 days of incubation. Experimental details are provided in methods section.

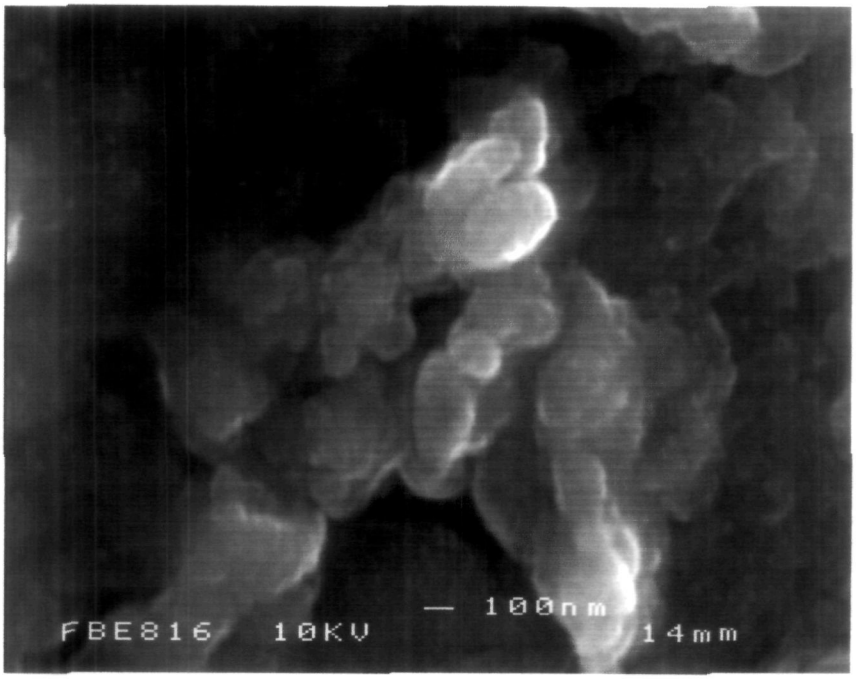
FBE816 10KV
100nm
14mm

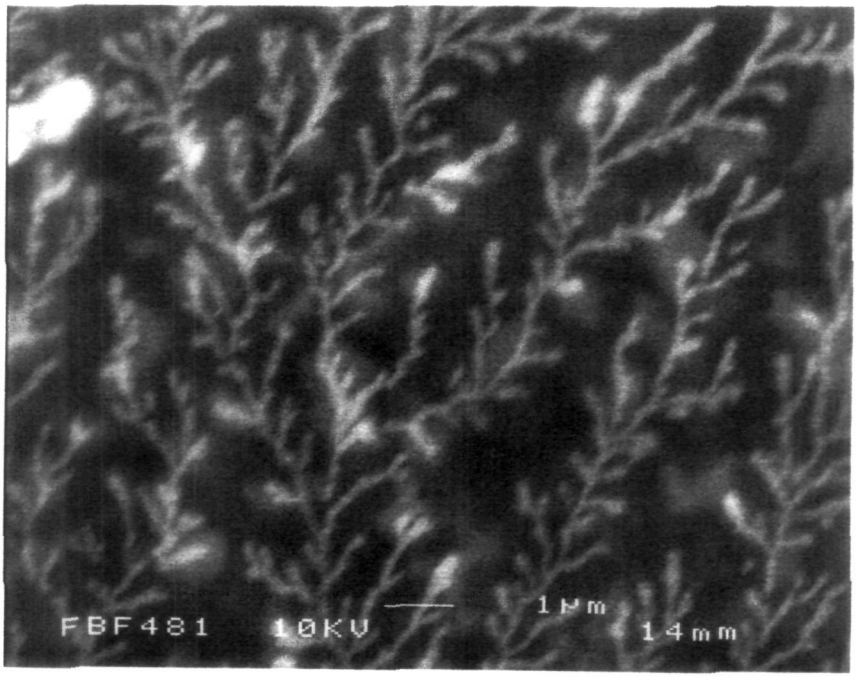
FBF481 10KV
1μm
14mm

Fig. 53 Electron micrographs showing amyloid aggregation of PTPI incubated at pH 2.0

Figure shows image obtained for PTPI (at different magnifications as shown by the size of bar lines) incubated at pH 2.0 (50 mM glycine/HCl) in presence of 10% (v/v) TFE. Sample used was obtained after 30 days of incubation. Experimental details are provided in methods section.


100µm
FBF464 10KV 14mm

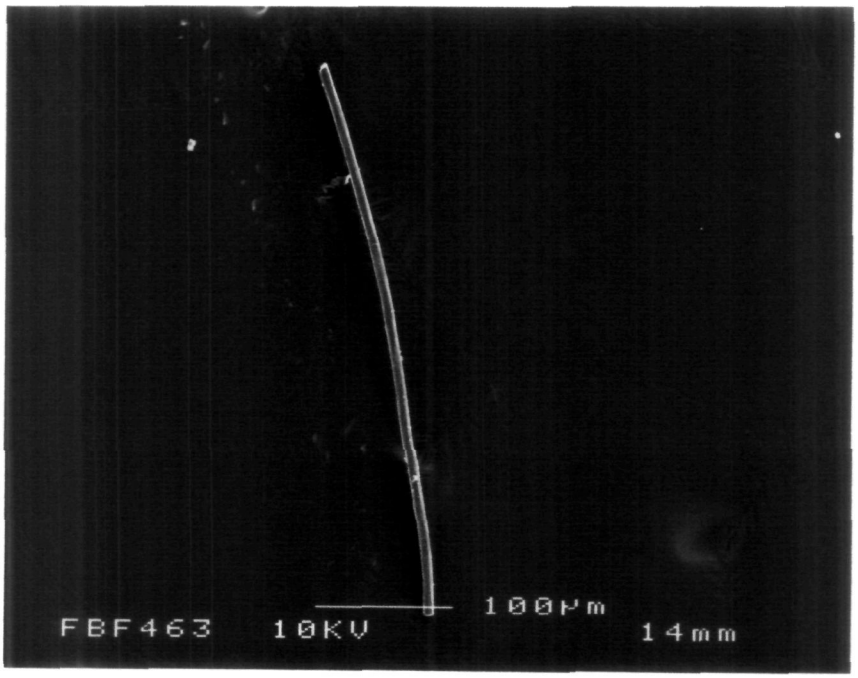
100µm
FBF463 10KV 14mm

Fig. 54 Electron micrographs showing amyloid aggregation of PTPI incubated at pH 3.0

Figure shows image obtained for PTPI (at different magnifications as shown by the size of bar lines) incubated at pH 3.0 (50 mM sodium acetate buffer) in presence of 10% (v/v) TFE. Sample used was obtained after 15 days of incubation. Experimental details are provided in methods section.

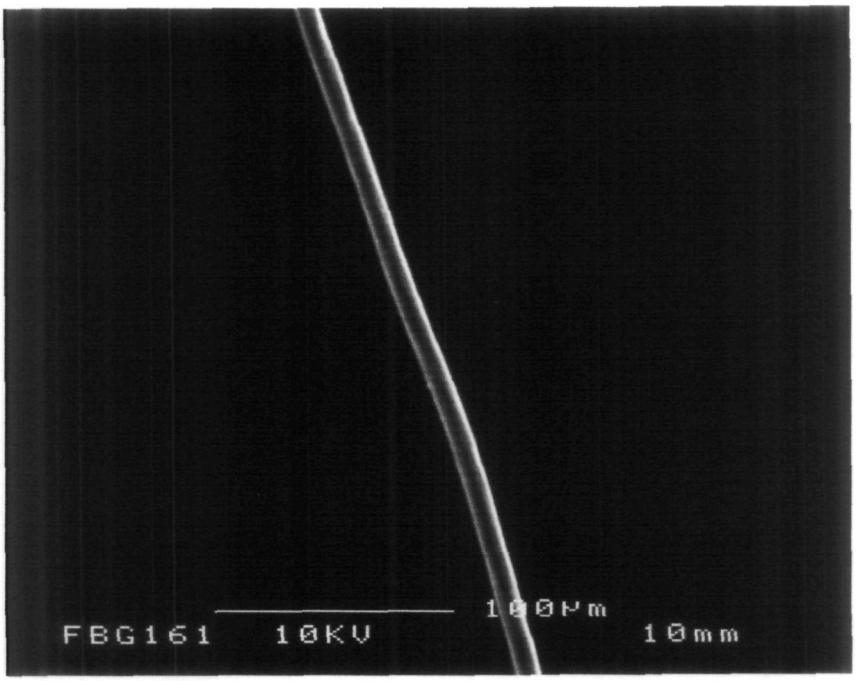
100μm
FBG161 10KV 10mm

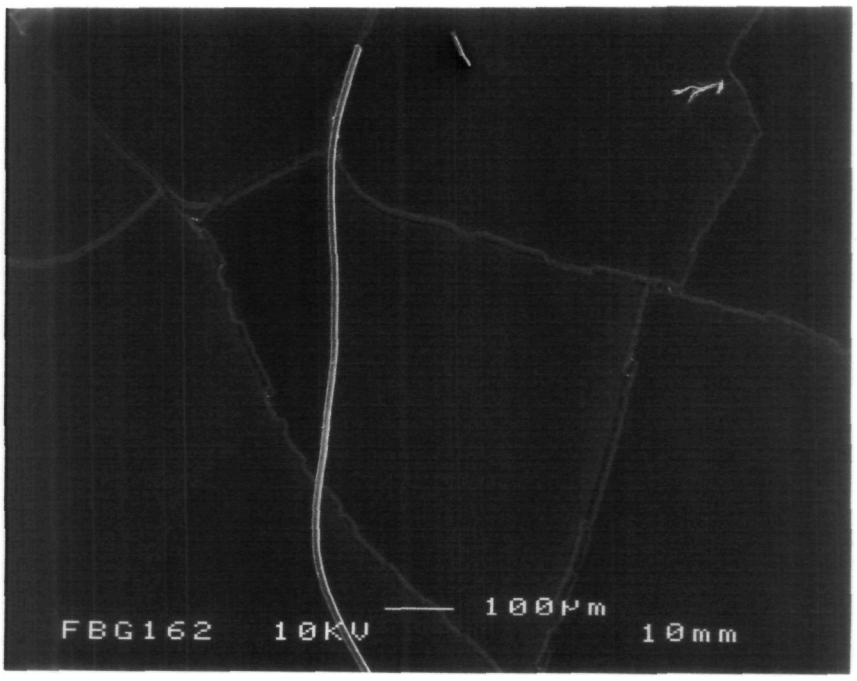
100μm
FBG162 10KV 10mm

decrease in intensity was observed at 10 μM Cu^{2+} ion concentration, which increased to ~42% at 20 μM culminating into 98% decline in ThT fluorescence at 50 μM Cu^{2+} ion concentration, beyond this concentration fluorescence intensity was too diminished for any discernible peak to be observed at 485 nm [Fig. 55a]. Similar effects were observed for Zn^{2+}. Minute decline (1-2%) in ThT fluorescence was observed till 6 μM Zn^{2+} ion concentration. At 10 μM Zn^{2+} ion concentration almost 97% of the intensity was quenched. Beyond this concentration no perceivable effect was seen [Fig. 55b].

When Cu^{2+} and Zn^{2+} were added at 50 μM and 10 μM concentration respectively, to 50 μM PTPI (pH 3.0, 10% (v/v) TFE) at the start of incubation, no ThT binding was observed, indicative of absence of any amyloid type aggregation in the presence of metal ions, suggesting Cu^{2+} and Zn^{2+} help in preventing amyloid formation.

Fig. 55 Inhibition of fibrillation of PTPI by Cu^{2+} and Zn^{2+} as probed by ThT fluorescence

(a) Figure shows inhibition of fibrillation as a function of Cu^{2+} concentration

(b) Figure shows inhibition of fibrillation as a function of Zn^{2+} concentration

For both the experiments 50 μM PTPI was incubated at pH 3.0 in presence of 10% (v/v) TFE. Metal solutions were added prior to ThT assay. Excitation was at 440 nm and spectra were recorded from 455 to 600 nm with a slit width of 5 nm. For ThT assay 5 μM of incubated protein was used with a protein to ThT molar ratio of 1:6. The data were obtained after subtraction of the signal of the buffer containing ThT.

(a)

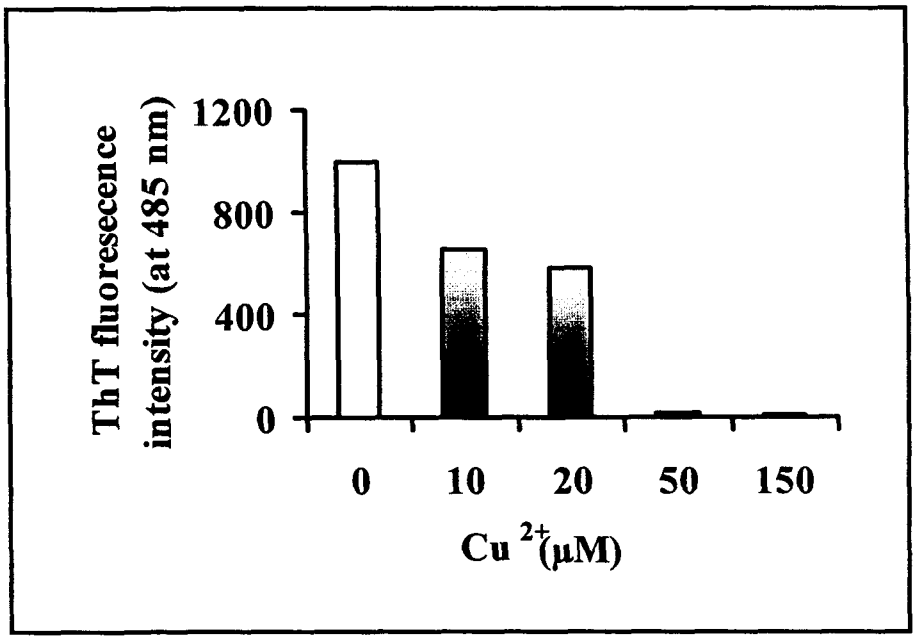
ThT fluoresecence intensity (at 485 nm)
1200
800
400
0
0
10
20
50
150
Cu 2+(μM)

(b)

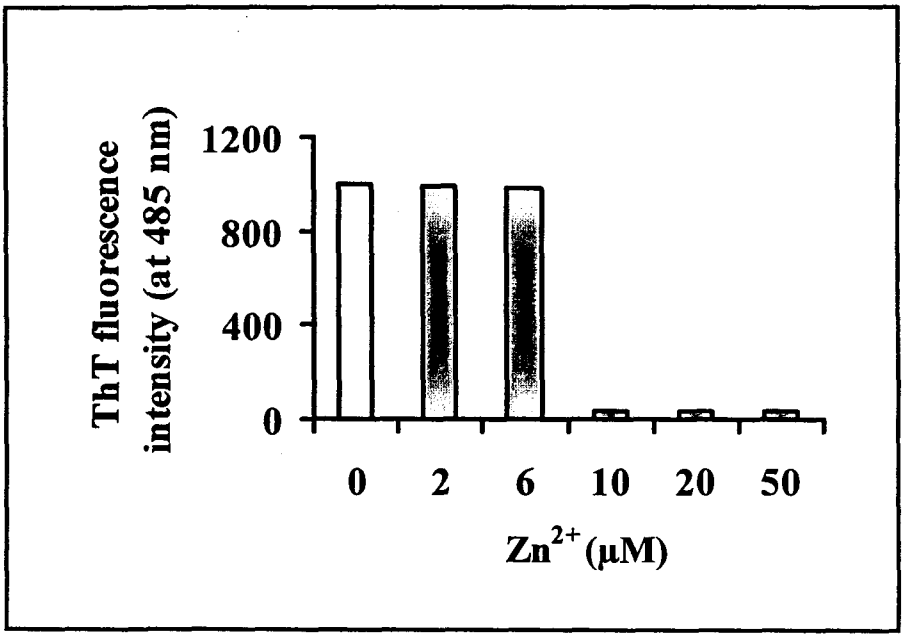
ThT fluorescence intensity (at 485 nm)
1200
800
400
0
0
2
6
10
20
50
Zn2+ (μM)

Discussion

Chapter 3

DISCUSSION

Cathepsin knockouts have demonstrated that cathepsins have specific and individual functions, which are very important for the normal functioning of the organism [Turk et al., 2001]. Among others they degrade the extracellular matrix, of importance in tumor progression and invasion [Gocheva and Joyce, 2007]. Accidentally escaped cathepsins from lysosomes are trapped by cystatins, their endogenous protein inhibitors. Cystatins comprise large family of thiol proteinase inhibitors. Members of cystatin superfamily have propensity to form fibrillar aggregates [Skerget et al., 2009]. Lately, various non-pathogenic proteins have been shown to form amyloid fibrils in vitro, such as acylphosphatase [Chiti et al., 1999], cold shock protein [Wilkins et al., 2000], hen lysozyme [Krebs et al., 2000], SH3 domain [Zurdo et al., 2001], cytochrome C [Pertinhez et al., 2001] and myoglobin [Fandrich et al., 2001], etc.

The aim of the present study was to define the requisite conditions for the in vitro fibrillation of pancreatic thiol proteinase inhibitor and thus test the generic ability of proteins to aggregate to β sheet rich fibrillar structures. The 'generic amyloid' hypothesis essentially states that the ability of proteins to form ordered fibrillar cross β-structures is inextricably linked to the nature of the protein backbone [Chiti et al., 1999; Dobson, 1999] and is independent of the structure of the native state. Thus, while some proteins obviously fibrillate more readily than others, it should be possible to find conditions that are sufficiently destabilizing for the native state to allow the protein to explore alternative conformations and lock on to the stable β-sheet aggregated state.

Exploring conditions for PTPI fibrillation

It is generally believed that globular proteins need to unfold, at least partially, to aggregate into amyloid or amyloid like fibrils [Chiti et al., 1999; Krebs et al., 2000; Fandrich et al., 2001; Rabzelj et al., 2005; Holm et al., 2007; Zerovnik et al., 2007]. Such a "conformational change hypothesis" is widely supported by a large body of experimental data. Proteins normally adopting a compact and well defined three-dimensional fold have a higher propensity to aggregate under conditions that promote their partial unfolding such as high temperature, high pressure, low pH or moderate conditions of organic solvents [Konno, 2001; Rabzelj et al., 2005; Soldi et al., 2005]. As noted for various proteins, amyloid formation by PTPI in vitro was achieved by

destabilizing the native state of the protein under conditions in which non-covalent interactions still remain favourable. PTPI when subjected to acid denaturation yields a 'partially unfolded intermediate', the pH 3.0 state and a molten globule like intermediate at pH 1.0 [Fig. 45 and 46]. From these results it can be inferred that the structure remaining at these low pH environments may not be residual native like structure that the acid unfolding has failed to disrupt, but rather newly formed organisations, and consequently with little resemblance to native structure [Buck et al., 1993].

PTPI at pH 3.0, 2.0 and 1.0 possess significant non-native secondary structure, which is likely to transform to amyloid aggregates and this tendency was judged by ThT fluorescence assay. PTPI incubated under these three acidic conditions tested positive for amyoid by Tht fluorescence assay. However, there were differences in ThT binding [Fig. 49a and Fig. 50a]. Distinct fibrillar states under different solution conditions have also been reported for stefin B [Zerovnik et al., 2007] where different type of fibrils originate from pH 4.8-native like and pH 3.3-molten globule like intermediate. Fibril growth has also been documented under (mild) acidic conditions for insulin [Ahmad et al., 2005], endostatin [He et al., 2006], acylphosphatase [Chiti et al., 1999], stefin B [Rabzelj et al., 2005] and stefin A and B [Jenko et al., 2004; Zerovnik et al., 2002b]. Rapid fibrillation was observed at pH 3.0 and 1.0 then at pH 2.0; suggesting that partially folded and native like molten globule states have a higher propensity to form aggregates [Fig. 49a and Fig. 50a]. This is supported by reports on fibrillation of bovine serum albumin [Holm et al., 2007].

It is a well known fact that 2, 2, 2-trifluoroethanol (TFE), a hydrogen bond promoting solvent has an accelerating effect on amyloid fibrillation. To find out the most appropriate concentration of TFE, required for PTPI fibril growth, influence of increasing concentration of TFE on pH 3.0 state of PTPI was studied. It was observed that at 10% (v/v) TFE, pH 3.0 state of PTPI gained sufficient amount of non-native secondary structure with increased amount of exposed non polar clusters whereas at higher concentrations of TFE, α-helical content was profoundly enhanced with decreased hydrophobic effect. Binary mixtures of water with alcohols like methanol, ethanol, or TFE have been shown to cause conformational transition of proteins into new stable conformational states with high α-helical content and disrupted tertiary and quaternary structure resembling that of molten globule intermediate [Polverino de Laureto et al., 2002]. Alcohols weaken non-local hydrophobic interactions while

enhancing local polar interactions (i.e. hydrogen bond) of proteins [Rashid et al., 2006b]. Alcohols induce significantly higher α-helical structures in partially or completely unfolded proteins as compared to those in folded proteins [Bhakuni, 1998]. Among various alcohols, TFE is often preferred because of its remarkable potential in stabilizing the α-helical structure [Gupta et al., 2003]. 10% (v/v) TFE was found to stabilize pH 3.0 state of PTPI drawing credence from previous reports. In this study, amyloid fibril growth was accelerated by addition of 10% (v/v) TFE to samples incubated at pH 2.0 as well as at pH 3.0 [Fig. 49b and 50b]. The lag observed initially for fibrillation at pH 2.0 was considerably reduced by addition of TFE and at pH 3.0 fibrillation initiated without any lag phase in presence of TFE. Quite similar results were obtained for sample incubated at pH 1.0. This suggests that pH 1.0 and pH 3.0 states of PTPI (in presence of TFE) have a higher tendency to aggregate and fibrillate. Enhancement of the rate of fibrillation by TFE has also been noted before. Stefin A and stefin B showed accelerated fibril growth in the presence of predenaturational TFE concentrations [Jenko et al., 2004; Rabzelj et al., 2005; Zerovnik et al., 2007]. This effect was also observed for fibrillation of acylphosphatase. Chiti et al. [1999] found that fibrillation of acylphosphatase proceeds at moderate concentration of trifluoroethanol. Chiti et al. [2001] reiterated similar effects of TFE, with HypF-N terminal domain. TFE was also found to promote fibrillation in case of endostatin [He et al., 2006].

Based on above discussion, possible mechanism of PTPI aggregation could be presented as,

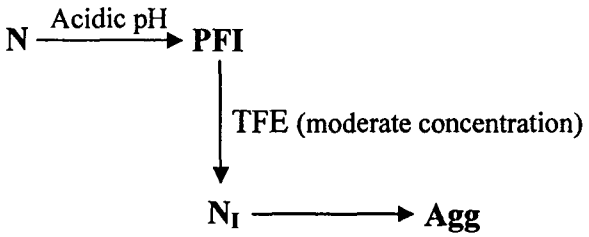

Fig. 56: Scheme for mechanism of PTPI aggregation, where N stands for native state, PFI for acid induced partially folded intermediate; N_I for TFE induced native like intermediate and Agg for amyloid aggregate.

The proposed mechanism shows that the protein may form fibrils from a partially folded intermediate stabilized by organic solvent TFE to a more native like structure, N_I. Thus it can be propounded that partially folded predenaturational intermediates

appear to be critical species in the fibrillation process. A probable explanation was offered by He et al. [2006] for the observation that destabilization of native fold and presence of non-native α-helix promotes fibrillation. They suggested that hydrophobic surface exposure and stability are two important factors controlling protein conformation. Unstable proteins with exposed hydrophobic surfaces result in molecular adhesion [Wodak and Janin, 2003]. In present case also PTPI at acidic pH [1.0, 2.0 and 3.0] was found to possess exposed non-polar clusters revealed by enhanced ANS binding [Fig. 45b]. In an environment that favors the conformational stability, α-helix would prevent the polypeptide chain from converting into fibril structure [Fandrich and Dobson, 2002]. Contrarily, under other conditions where mutagenesis or organic solvents reduce the stablitiy of the α-helical structure formed in proteins, the polypeptide is therefore ready to form fibrils. As for PTPI the α-helical structure revealed by far UV CD in Fig. 47a is not in the fully structured native conformation but is induced by TFE. This non-native α-helical structure of PTPI being unstable can easily transform to amyloid like aggregates [as shown by ThT fluorescence and TEM [Fig. 50b and 54]. Thus, unstable α-helix induced in proteins can facilitate fibril formation [He et al., 2006].

The fibrils obtained for PTPI incubated at pH 3.0 [Fig. 54, TEM image] were similar to classical straight needle-form structures characteristic of bona fide fibrils. Those obtained for PTPI incubated at pH 2.0, also exhibited fibrillar aggregates. However, peculiar foliage like pattern was obtained for PTPI incubated at pH 1.0. Distinct fibrillar patterns have also been shown for bovine serum albumin [Holm et al., 2007], endostatin [He et al., 2006], insulin [Grudzielanek et al., 2006] and β2 microglobulin [Hong et al., 2002]. This further suggests that PTPI is able to form different type of fibrils. It has already been noted that fibril morphologies differ depending upon solvent conditions [Zerovnik et al., 2007], which in the present case refer to differing pH.

Strategies against fibrillation of PTPI

A range of human disorders is associated with the extracellular deposition of insoluble protein aggregates of regular arrays of β sheet rich filaments or fibres of indefinite length, often coiled together in higher order structures [Frokjaer and Otzen, 2005; Dobson, 2003], example, Alzheimer's disease, prions disease, Huntington's and Parkinson's disease, type 2 diabetes etc. [Sambashivan and Eisenberg, 2006; Merlini

and Bellotti, 2003; Engel et al., 2008]. Because of the connection of amyloid fibrils to conformational diseases which are hitherto incurable, various compounds (natural and synthetic) are under experimentation for their efficacy in destabilizing and disaggregating amyloid fibrils or inhibiting the basic conformational change of the protein responsible for fibrillation. A number of compounds like curcumin, antibiotics, anticancer agents, nicotine etc. have been demonstrated to inhibit formation of fibrillar assemblies or are under trials [Zerovnik, 2002; Findies, 2000; Riviere et al., 2008].

Recent reports have shown that Cu^{2+} and Zn^{2+} retard the amyloid growth [Zerovnik et al., 2006; Raman et al., 2005]. These divalent metal ions were also used for inhibiting PTPI fibrillation and for disintegrating the formed fibrils. 50 μM Cu^{2+} and 10 μM Zn^{2+}, almost completely abolished ThT fluorescence enhancement. The same concentration when added to the PTPI sample prior to fibril induction, fibrillation seemed to be arrested. In this case, Cu^{2+} and Zn^{2+} may stabilize the protein, preventing the aggregation. In the former case, Cu^{2+} and Zn^{2+} salts might exert GdnHCl like action, disintegrating the ordered structure of fibrils.

Conclusively, these results sustain the generic hypothesis of amyloid fibrillation and outline the conditions necessary for PTPI fibrillization. The work also foreshadows the use of redox active metals like copper as therapeutic agents against amyloid formation. Lastly, it connects to the susceptibility of cystatin superfamily members for amyloid aggregation.

Chapter 4

Modification of pancreatic thiol proteinase inhibitor by reactive species:

1. Photosensitized riboflavin
2. Hydrogen peroxide
3. Hypochlorous acid
4. Nitric oxide

3.4 RESULTS

Pancreatic tissue exhibits particular sensitivity to oxidative stress, contributing to impaired functioning characteristic of diabetes, pancreatitis and fibrosis [Lenzen, 2008a]. Proteins offer the most potential targets of radical species and are usually rendered with compromised functions.

The purified protein, pancreatic thiol proteinase inhibitor (PTPI) was presumed to be equally sensitive (may be with somewhat enhanced susceptibility to reactive species, because of its host tissue). The experiments were thus focused to examine the effects of various reactive species on PTPI and also to investigate the potential of bioflavonoids quercetin (QE), caffeic acid (CA) and curcumin (Cur) to protect its damage against deleterious effects of the radicals by analyzing, papain inhibitory activity, along with intrinsic fluorescence and polyacrylamide gel electrophoresis behaviour of treated PTPI.

3.4.1A INTERACTION OF PTPI WITH PHOTOSENSITIZED RIBOFLAVIN

Riboflavin upon irradiation with fluorescent light generates reactive oxygen species like superoxide anion ($O_2^{\bullet-}$), singlet ($^1O_2$) and triplet oxygen ($^3O_2$), flavin radicals and substantial amounts of hydrogen peroxide [Husain et al., 2006].

Functional inactivation of PTPI by riboflavin

Effect of riboflavin on PTPI function was assessed by monitoring the changes in its antiproteolytic activity by caseinolytic assay of papain [Kunitz, 1947]. 1 μM PTPI was photo illuminated with increasing concentrations of riboflavin (5-50 μM) or with 40 μM riboflavin for various time intervals. The results obtained are summarized in Table 10. As shown in Table 10 (A) exposure of PTPI to increasing concentration of riboflavin, resulted in rapid decline of antiproteolytic activity (83% loss) towards papain, with half of the inactivation (56%) taking place at a concentration of riboflavin as low as 10 μM. Similarly, increase in length of exposure (0-60 min) of PTPI with riboflavin caused loss of inhibitory activity towards papain (Table 10 B), with more than 50% inhibition taking place after 30 min of incubation. To detect the ROS type involved in PTPI inactivation various free radical scavengers were used, Fig. 57 (A) illustrates the results obtained.

TABLE 10: LOSS OF ANTIPROTEOLYTIC ACTIVITY OF PTPI ON TREATMENT WITH PHOTOILLUMINATED RIBOFLAVIN AS A FUNCTION OF (A) CONCENTRATION OF RIBOFLAVIN AND (B) TIME OF INCUBATION

(A)

Riboflavin (μM)	0	5	10	20	30	40	50
% PTPI Activity[a]	100	61.08±2.2* (-39)	44.37±1.8* (-56)	33.51±1.6* (-66)	28.23±1.2* (-72)	20.48±1.3* (-80)	17.38±0.58* (-83)

(B)

Time of incubation (min)	0	10	20	30	40	50	60
% PTPI Activity[a]	100	85.76±3.8 (-14)	65.28±2.5* (-35)	27.16±2.3* (-73)	25.10±2.0* (-75)	22.12±1.3* (-78)	20.12±0.58* (-80)

PTPI (1μM) was incubated with increasing concentrations of riboflavin in light for 1 h or with 40 μM riboflavin for increasing intervals of time.
[a]PTPI was assayed for loss in antiproteolytic activity by caseinolytic method of Kunitz [1947]. The activity of native PTPI is taken to be 100.
Results are Mean±SEM for three or more separate experiments.
* Significantly different from native PTPI (control) at $p < 0.05$ by one way ANOVA.
Values in parentheses represent percent change from control.

Fig. 57 Effect of scavengers on riboflavin mediated inactivation of PTPI

(A) 1 μM PTPI was incubated with riboflavin (40 μM) alone or in presence of sodium azide/potassium iodide/thiourea/mannitol/sodium benzoate/uric acid/glucose (final concentration, 25 mM) or ascorbic acid (final concentration, 100 mM) for 30 min at room temperature under fluorescent light and assayed for antiproteolytic activity. None of the scavengers used had any effect on PTPI assay. Data are expressed as Mean ± SEM for four experiments. * $p < 0.05$ compared to PTPI+riboflavin alone.

(B) Native PTPI (1 μM) was incubated with riboflavin (40 μM) alone or in presence of curcumin (Cur □ , final concentration, 100 μM) or caffeic acid (CA □)/quercetin (QE□) (final concentration, 350 μM). Rest of the experimental conditions were same as above. Data are expressed as Mean ±SEM for four experiments. * $p < 0.05$ compared to PTPI+riboflavin alone.

(A)

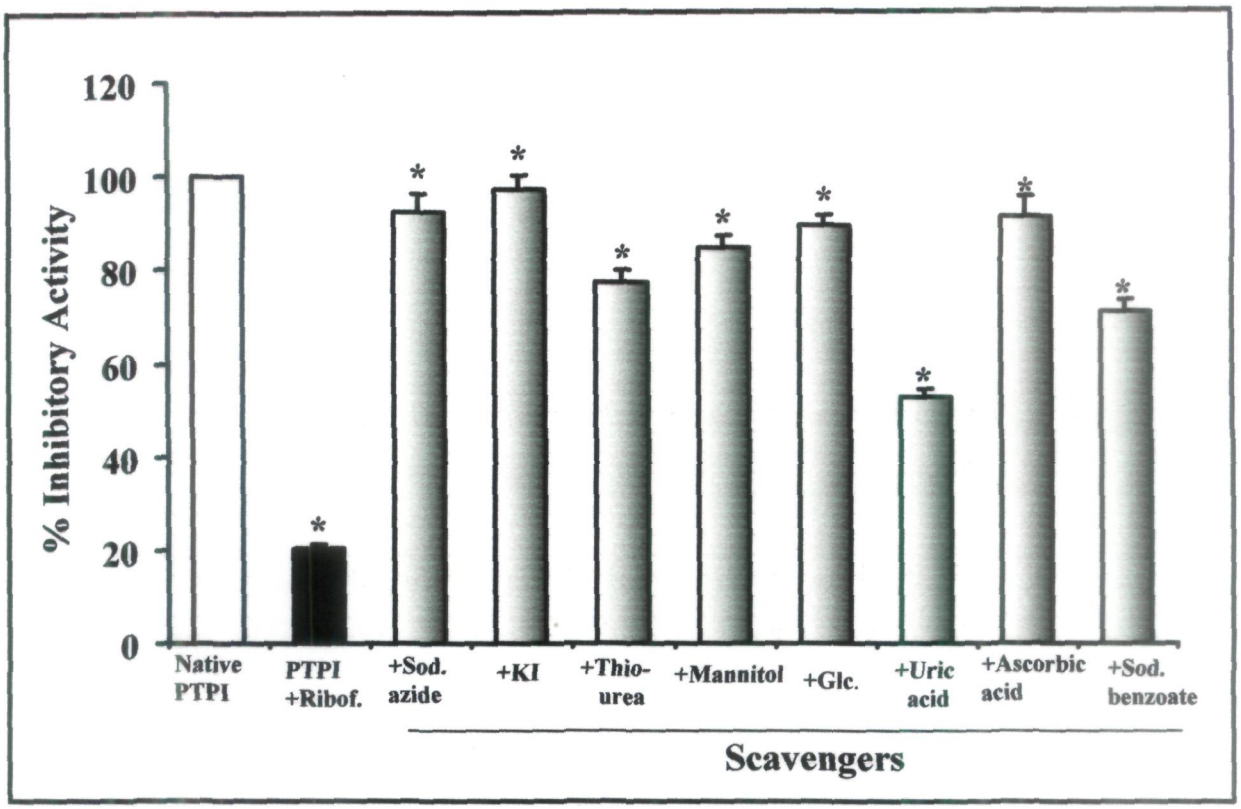
120
100
80
60
40
20
0
% Inhibitory Activity
Native PTPI
PTPI +Ribof.
+Sod. azide
+KI
+Thio-urea
+Mannitol
+Glc.
+Uric acid
+Ascorbic acid
+Sod. benzoate
Scavengers

(B)

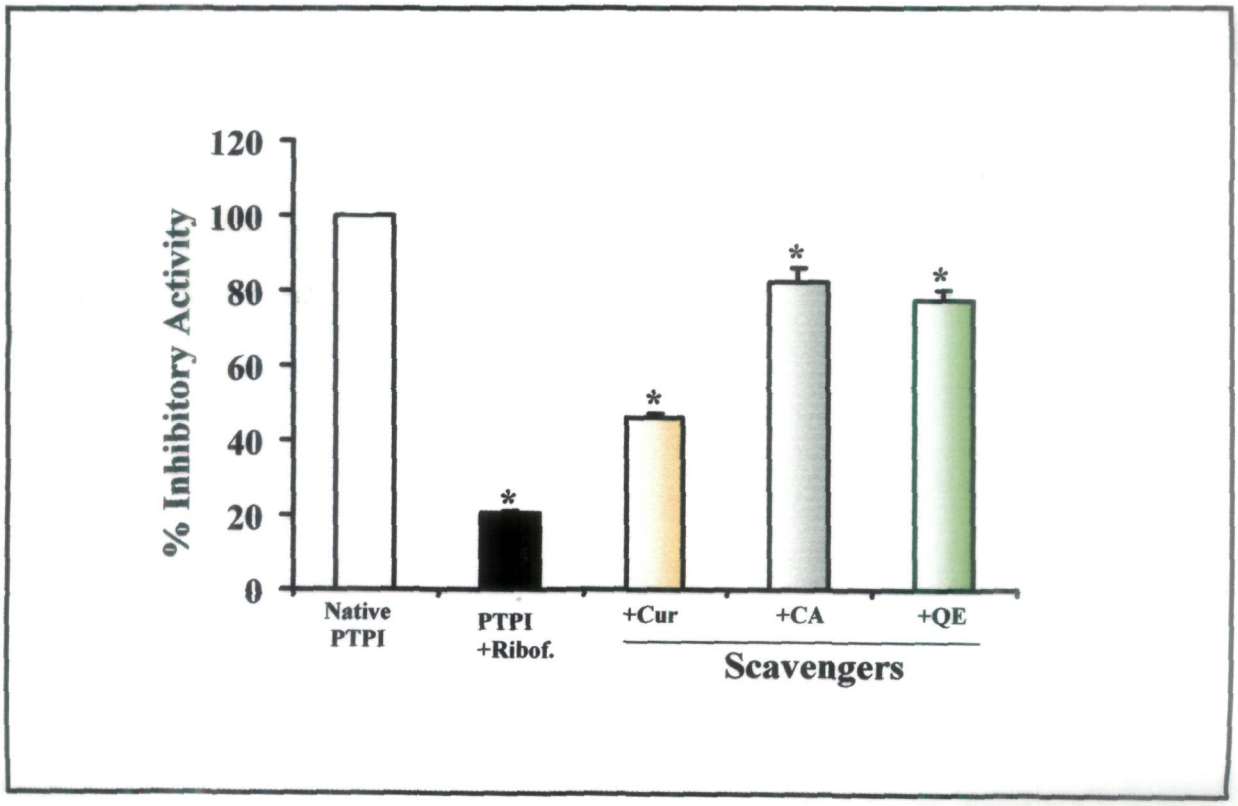
120
100
80
60
40
20
0
% Inhibitory Activity
Native PTPI
PTPI +Ribof.
+Cur
+CA
+QE
Scavengers

Maximum suppression of PTPI inactivation was caused by potassium iodide closely followed by sodium azide. Sodium azide is a scavenger of singlet oxygen and potassium iodide scavenges flavin triplet state. Sodium benzoate, mannitol and thiourea eliminate hydroxyl radicals [Khan and Khan, 2004; Martinez-Cayuela, 1995]. These hydroxyl radical scavengers also offered some protection explicating moderate role of these radicals in riboflavin mediated PTPI inactivation. Biological antioxidants such as uric acid, glucose and ascorbic acid were analysed for suppression of PTPI inactivation by riboflavin. Ascorbic acid was found to be most effective.

Structural modification of PTPI by riboflavin

The effects of various concentrations of photoilluminated riboflavin were also determined on the structure of PTPI. The samples incubated at increasing riboflavin concentrations (5-50 μM) were subjected to PAGE [Fig. 58]. At 5μM riboflavin concentration, a lighter intensity band was observed. At concentrations above that, till 30 μM, diffused bands were observed. At higher concentration, 40 and 50 μM, aggregation was observed with concomitant loss of native bands.

No aggregated products were observed in treated PTPI in presence of potassium iodide, sodium azide and ascorbic acid [Fig. 59]. Again propounding, flavin triplet and singlet state as main culprits for photodynamic modifications PTPI.

Treatment of PTPI with photo illuminated riboflavin drastically altered its intrinsic fluorescence properties. The fluorescence emission spectra of native PTPI gave an emission maximum at 335 nm when excited at 280 nm [Fig. 60] [Priyadarshini and Bano, 2009]. 1 μM PTPI photoilluminated with increasing concentration of riboflavin 5-50 μM was subjected to fluorescence spectroscopy to assess the effect on global conformation of protein, the samples were excited at 280 nm and emission range was 300-400 nm. Riboflavin treatment upto 10 μM did not induce any change in emission λ_{max} however ~ 44% decline in fluorescence intensity was precipitated. Beyond this concentration a blue shift of 5 nm (λ_{max} shifted to 330 nm compared to 335 nm for native) was observed with a profound decline (~75%) in fluorescence intensity [Fig. 60]. Effect of 40 μM riboflavin on intrinsic fluorescence of PTPI (1 μM) was also studied for various time periods (0-60 min). A time dependent gradual loss in fluorescence intensity with a similar blue shift was also observed after 20 min of incubation. To ascertain the effect of various scavengers in subjugating the detrimental consequences of the photodynamic action of riboflavin on structure of

Fig. 58 PAGE of native and riboflavin treated PTPI

Native PTPI (1 μM) was incubated with increasing riboflavin concentrations (5-50 μM) for 30 min under fluorescent light and subjected to non denaturing PAGE. Gels were silver stained.

Fig. 59 PAGE of PTPI exposed to riboflavin in presence of various scavengers

Native PTPI (1 μM) was incubated with 40 μM riboflavin in presence of various scavengers, sodium azide/potassium iodide (final concentration, 25 mM)/ascorbic acid (final concentration, 100 mM) or in presence of curcumin (Cur, final concentration, 100 μM) or caffeic acid (CA)/quercetin (QE) (final concentration, 350 μM) and subjected to non denaturing PAGE. The experimental conditions were same as defined for Fig. 58. Gels were silver stained.

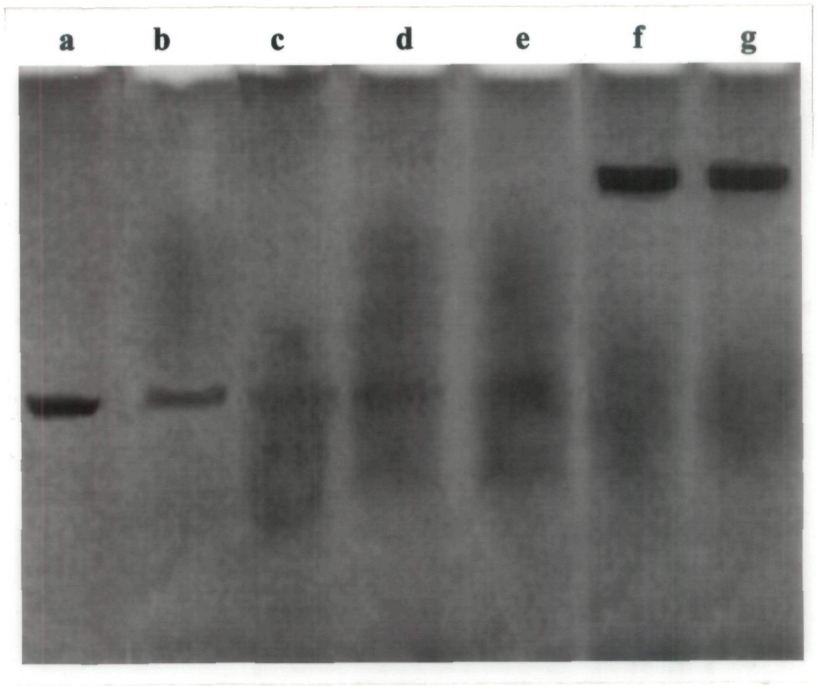

Lane	a	b	c	d	e	f	g
PTPI	+	+	+	+	+	+	+
Ribofavin (μM)	-	5	10	20	30	40	50

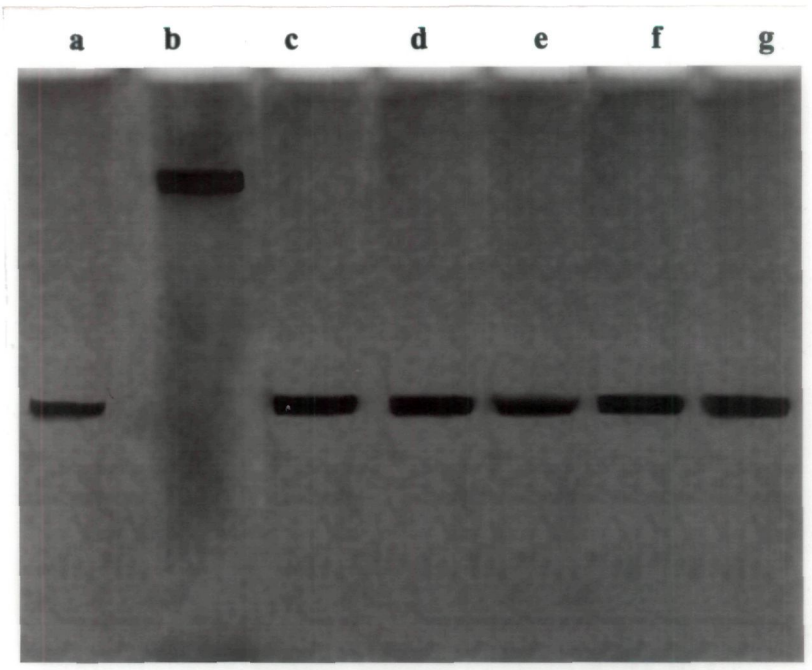

Lane	a	b	c	d	e	f	g
PTPI	+	+	+	+	+	+	+
Ribofavin (40 μM)	-	+	+	+	+	+	+
Scavenger	-	-	KI	Sod. azide	Ascorb -ic acid	CA	QE

Fig. 60 Intrinsic fluorescence analysis of PTPI treated with different concentrations of riboflavin

1 μM PTPI was incubated with increasing concentrations of riboflavin (5-50 μM) under fluorescent light for 30 min in a final reaction volume of 1 ml in 50 mM sodium phosphate (pH 7.5) at room temperature. The excitation wavelength was 280 nm and emission was recorded in range of 300-400 nm with a slit width of 5 nm. Trace 1 is native PTPI, or PTPI + riboflavin 5 μM (trace 2), 10 μM (trace 3), 20 μM (trace 4), 30 μM (trace 5), 40 μM (trace 6), 50 μM (trace 7).

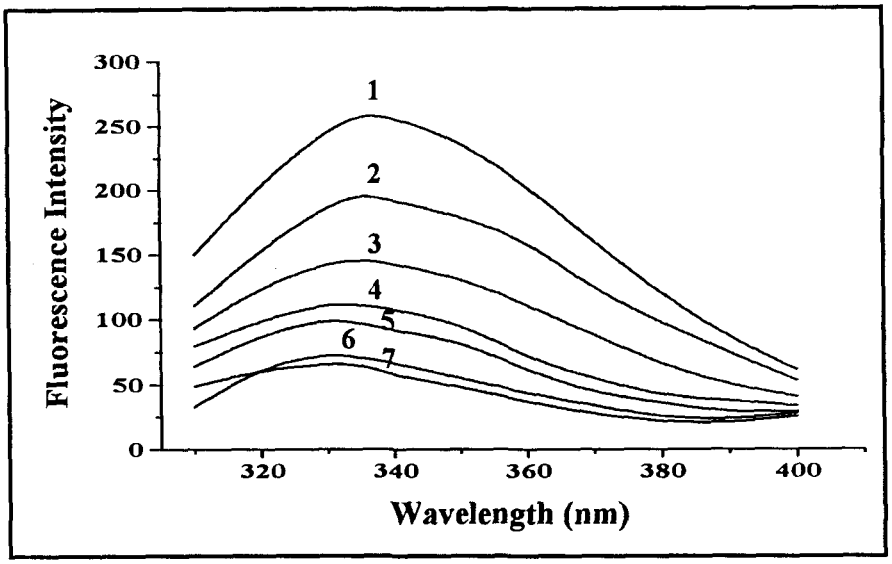

TABLE 11: RETENTION OF TRYPTOPHAN FLUORESCENCE IN THE PRESENCE OF DIFFERENT SCAVENGERS AND ANTIOXIDANTS

Condition 1 μM PTPI + 40 μM Riboflavin	% retention of tryptophan fluorescence
-	27.29
+ Sod. Benzoate	37.15
+ Mannitol	25.00
+ KI	77.17
+ Sod. Azide	77.60
+ Glucose	66.68
+ Ascorbic acid	76.35
+ Cur	59.15
+ CA	75.16
+ QE	66.70

Results are % retention of tryptophan fluorescence emission intensity (which is dependent upon but not synonymous with the number of tryptophan residues) measured at 280 nm excitation and 300-400 nm emission with a slit width of 5 nm. Experiment details are as described in methods section

PTPI, fluorescence spectra of treated PTPI in presence of scavengers was obtained and percent retention of tryptophan fluorescence was determined. The results are summarized in Table 11. Treated PTPI retained only 27% of native tryptophan fluorescence. Reaffirming the involvement of flavin triplet state and singlet oxygen in photodynamic modification of PTPI by riboflavin, maximum retention of tryptophan fluorescence (~78%) was seen in presence of potassium iodide and sodium azide. Mannitol and sodium benzoate exhibited <50% retention, implicating only faint involvement of hydroxyl radicals. Among biological antioxidants, ascorbic acid again showed maximum protection.

3.4.1B PROTECTIVE EFFECT OF BIOFLAVONOIDS

Curcumin (Cur), Caffeic acid (CA) and Quercetin (QE) against photodynamic modifications of PTPI

In quest of finding natural alternatives to scavengers, Cur, CA and QE were examined for their potency to revert/prevent any modification induced in PTPI by photosensitized riboflavin. Preliminary experiments were conducted to determine the most effective concentration of above three compounds. 350 μM CA and QE prevented loss of antiproteolytic activity of PTPI [Fig. 57B]. Aggregation of PTPI was also restrained by QE and CA [Fig. 59]. In presence of 350 μM CA, ~75% of tryptophan fluorescence was retained [Table 11]. QE afforded retention of tryptophan fluorescence to an extent similar to glucose. Cur (100 μM) however exerted only moderate preventive influence in all the features studied.

3.4.2A INTERACTION OF PTPI WITH HYDROGEN PEROXIDE (H_2O_2)

Hydroperoxides such as H_2O_2 and lipid hydroperoxides have been implicated as mediators of cellular injuries in a variety of clinical conditions including pancreatitis, cancer, etc. [Pryor et al., 2006]. Thus, deleterious effects of H_2O_2 and protective effects of polyphenols on PTPI were assessed.

Functional modification of PTPI by H_2O_2

H_2O_2 caused only modest inactivation of PTPI. Even at high concentrations of H_2O_2 (500 mM) only 50% of antiproteolytic activity of PTPI was compromised

[Table 12A]. To study the impact of H_2O_2 on activity of PTPI as a function of time, 1 μM PTPI was incubated with 250 mM H_2O_2 in dark for varying time periods (0-60 min) and activity of PTPI was determined [Kunitz, 1947]. A slow and gradual decline in activity was observed culminating to only a 50% loss [Table 12B]. The effect of various scavengers on H_2O_2 induced PTPI inactivation was studied. Sodium benzoate and thiourea did not show any protection. Mannitol offered 27% enhancement of the papain inhibitory activity of treated PTPI. Since manntiol, sodium benzoate and thiourea are specific hydroxyl scavengers, this suggests only partial involvement of these radicals in H_2O_2 mediated PTPI damage [Fig. 61]. Among biological antioxidants 25 mM glucose offered better protection than 100 mM ascorbic acid.

Structural modification of PTPI by H_2O_2

1 μM PTPI was exposed to (1-500 mM) H_2O_2 in dark for 30 min and the samples were analyzed by polyacrylamide gel electrophoresis. There was only a slight decline in band intensity as compared to the untreated PTPI, which was maximized at 500 mM H_2O_2. In parallel to modest inactivation of the inhibitor, the gross conformational status of PTPI remained largely unaffected even when exposed to high H_2O_2 concentration [Fig. 62]. In the presence of the scavenger mannitol and physiological antioxidant, glucose, the band intensity was retrieved to that of native PTPI [Fig. 63]. Gel results are presented for most conspicuous effects only.

The intrinsic fluorescence spectra of samples treated with various concentrations of H_2O_2 are depicted in Fig. 64. Complex changes were observed in contrast to the results of inactivation and PAGE. PTPI under native conditions gives fluorescence emission spectrum with maximum at 335 nm. Even at 1 mM H_2O_2, the emission λ_{max} suffered a red shift of 5 nm, with pronounced enhancement in intensity. No changes were noticeable till 50 mM H_2O_2 (spectra not shown). At higher concentrations fluorescence intensity decreased, reaching to that of native at 250 mM H_2O_2, while red shift to 340 nm was maintained. At 500 mM H_2O_2, λ_{max} suffered another red shift of 5 nm, reaching a value of 350 nm. When studied as a function of time, within 20 min, 250 mM H_2O_2 produced a red shift of 5 nm in λ_{max}. Within 60 min λ_{max} shifted to 350 nm from 335 nm for the native. Conclusively, H_2O_2 causes unfolding of PTPI. Keeping in view the complex alterations in fluorescence intensity of PTPI in presence of H_2O_2, regain of native λ_{max} of emission was chosen as a criterion to judge the effects of various scavengers on PTPI (1 μM) in presence of 250 mM H_2O_2.

TABLE 12: LOSS OF ANTIPROTEOLYTIC ACTIVITY OF PTPI ON TREATMENT WITH H_2O_2 AS A FUNCTION OF

(A) CONCENTRATION OF H_2O_2 AND

(B) TIME OF INCUBATION

(A)

H_2O_2 (mM)	0	1	10	50	100	250	500
% PTPI Activity[a]	100	97.00±3.8 (-3.0)	96.00±3.9 (-4.0)	83.00±3.9 (-17.0)	74.70±3.4 (-25.3)	66.40±2.1* (-33.6)	41.5±1.8* (-58.5)

(B)

Time of incubation (min)	0	10	20	30	40	50	60
% PTPI Activity[a]	100	92.12±3.8 (-8.0)	87.18±3.5 (-13)	68.10±2.3* (-32)	59.25±2.8* (-41)	50.18±2.3* (-50)	43.53±1.9* (-56)

PTPI (1μM) was incubated with increasing concentrations of H_2O_2 in dark for 1 h or with 250 mM H_2O_2 for increasing intervals of time.
[a]PTPI was assayed for loss in antiproteolytic activity by caseinolytic method of Kunitz [1947]. The activity of native PTPI is taken to be 100.
Results are Mean±SEM for three or more separate experiments.
* Significantly different from native PTPI (control) at $p < 0.05$ by one way ANOVA.
Values in parentheses represent percent change from control.

Fig. 61 Effect of scavengers on H_2O_2 mediated inactivation of PTPI

Native PTPI (1 μM) was incubated with H_2O_2 (250 mM) alone or in presence of mannitol/glucose (final concentration, 25 mM)/ascorbic acid (final concentration, 100 mM) or curcumin (Cur□ 100 μM)/ caffeic acid (CA □60 μM)/quercetin (QE □50 μM) for 30 min in a final reaction volume of 1 ml at room temperature in dark and was assayed for its antiproteolytic activity. None of the scavengers used had any effect on PTPI assay. Data are expressed as Mean ± SEM for four experiments. * $p < 0.05$ compared to PTPI+H_2O_2 alone.

Fig. 62 PAGE of native and H_2O_2 treated PTPI

Native PTPI (1 μM) was incubated with increasing H_2O_2 concentrations (1-500 mM) for 30 min in dark subjected to non denaturing PAGE. Gels were silver stained.

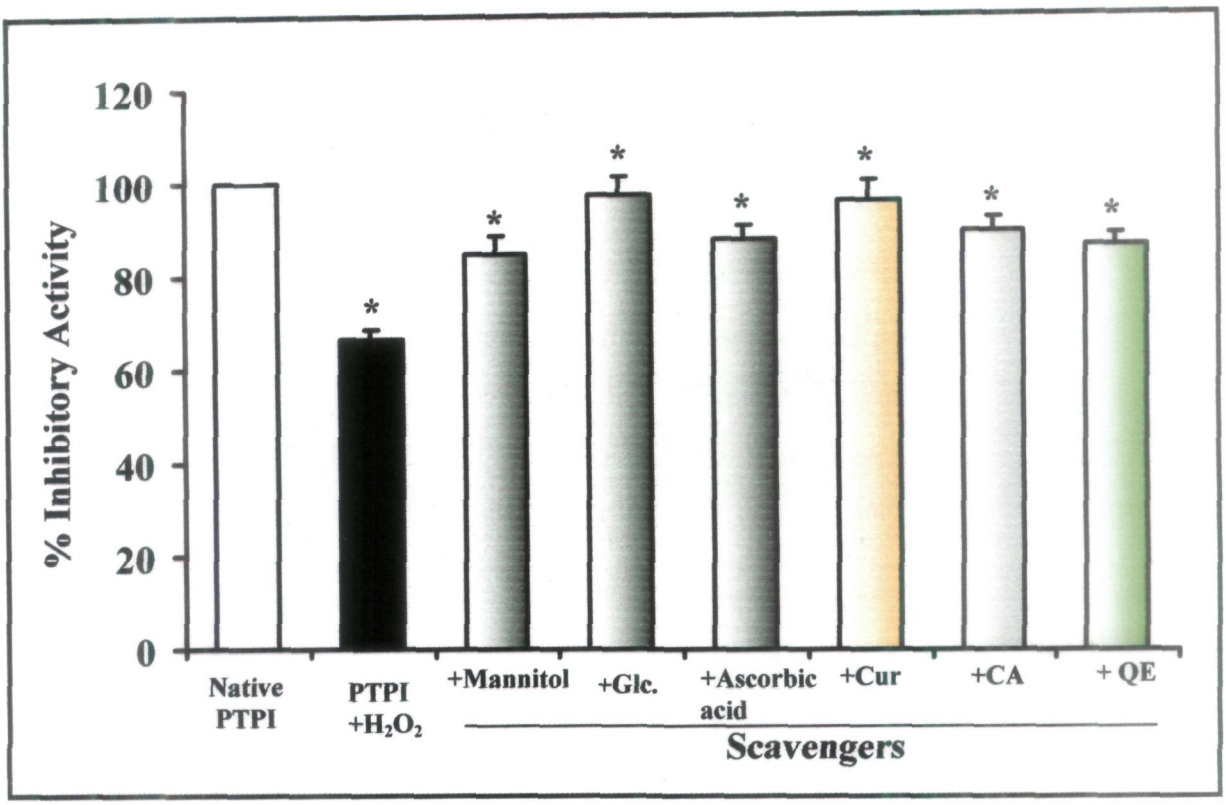

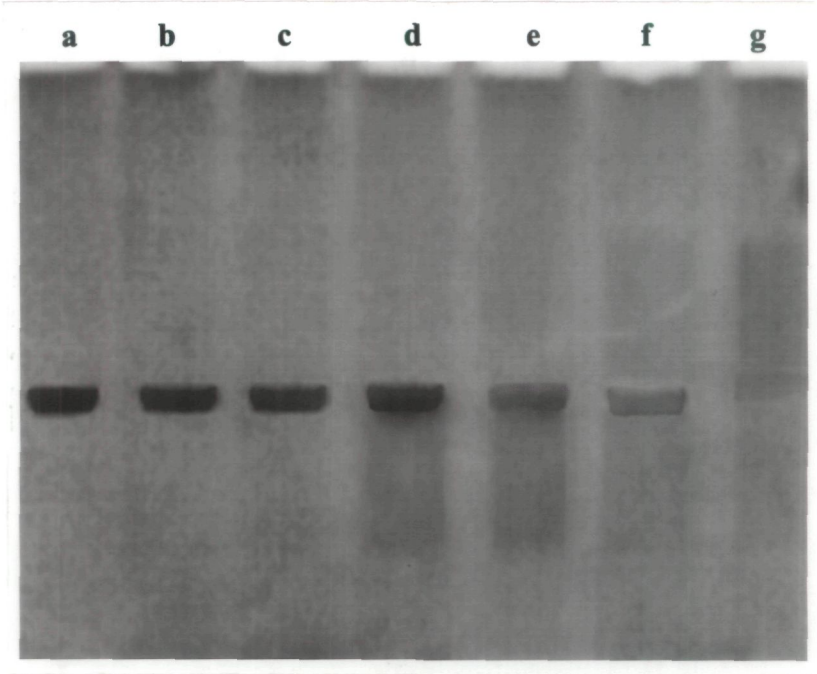

Lane	a	b	c	d	e	f	g
PTPI	+	+	+	+	+	+	+
H_2O_2 (mM)	-	1	10	50	100	250	500

Fig. 63 PAGE of PTPI exposed to H_2O_2 in presence of various scavengers

Native PTPI (1 μM) was incubated with 250 mM H_2O_2 in presence of various scavengers, mannitol/glucose (final concentration, 25 mM) or in presence of curcumin (Cur, final concentration, 100 μM) or caffeic acid (CA)/quercetin (QE) (final concentration, 60 and 50 μM, respectively) and subjected to non denaturing PAGE. The experimental conditions were same as defined for Fig. 61. Gels were silver stained.

Fig. 64 Intrinsic fluorescence analysis of PTPI treated with different concentrations of H_2O_2

1 μM PTPI was incubated with increasing concentrations of H_2O_2 in dark for 30 min in a final reaction volume of 1 ml in 50 mM sodium phosphate (pH 7.5) at room temperature. The excitation wavelength was 280 nm and emission was recorded in range of 300-400 nm with a slit width of 5 nm. Trace 1 is native PTPI. Trace 2 is PTPI treated with 1 mM H_2O_2. Trace 3 represents PTPI treated with 100 mM H_2O_2. Trace 4 and 5 are PTPI treated with 250 mM and 500 mM H_2O_2.

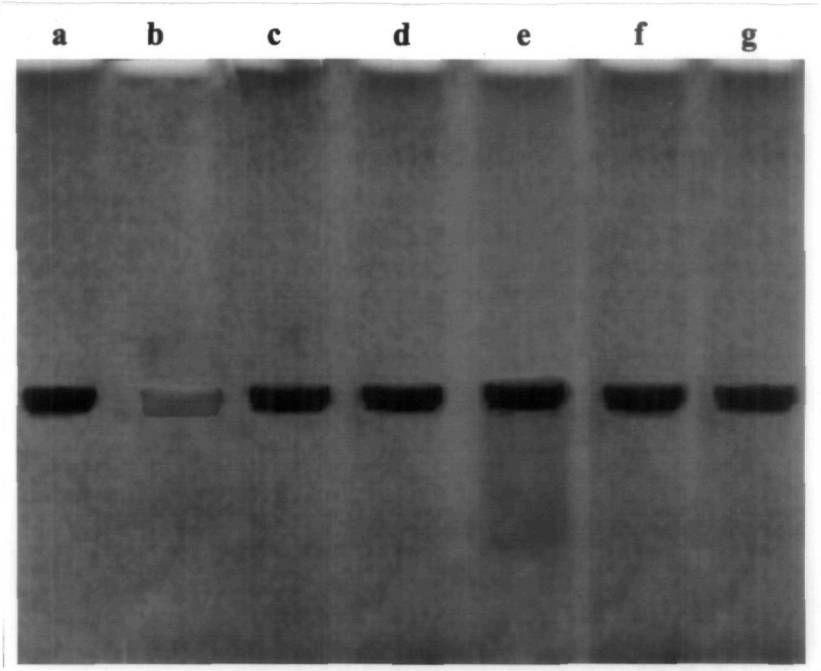

Lane	a	b	c	d	e	f	g
PTPI	+	+	+	+	+	+	+
H_2O_2 (mM)	-	+	+	+	+	+	+
Scavenger	-	-	Mann-itol	Gluco-se	Cur	CA	QE

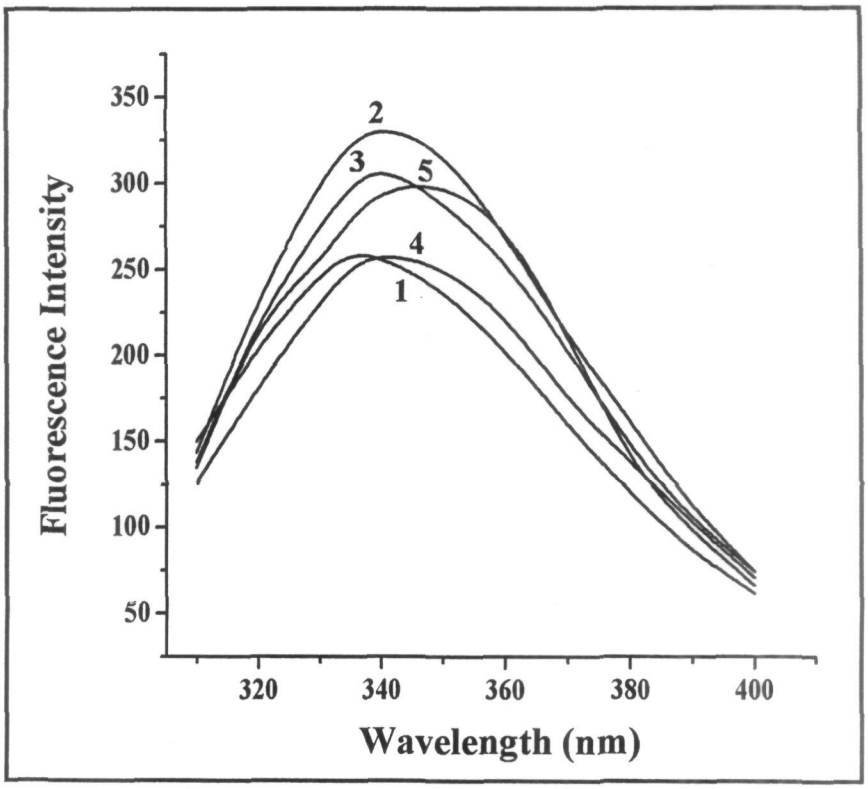

Thiourea and sodium benzoate did not show any impact. Glucose and ascorbic acid brought back the λ_{max} to 335 nm. Mannitol gave same effect however fluorescence intensity of the treated PTPI in its presence remained quenched below that of untreated PTPI.

3.4.2B PROTECTIVE EFFECT OF BIOFLAVONOIDS

Curcumin (Cur), caffeic acid (CA) and quercetin (QE) against H_2O_2 mediated modifications of PTPI

There is limited number of reports indicating direct subjugation of oxidative damage inflicted by H_2O_2 on proteins in vitro. Curcumin (Cur), caffeic acid (CA) and quercetin (QE) were probed for their suppressive effects against the adverse consequences of H_2O_2 on PTPI.

As shown in Fig. 61, among the three bioantioxidants, most substantial increment (45%) in the treated PTPI's inhibitory activity was brought about by 100 μM Cur, followed by a 35% enhancement spawned by 60 μM CA. QE (50 μM) showed a mediocre gain of 30% in activity. However, all of the three antioxidants, generated native like band pattern of PTPI even in the presence of 250 mM H_2O_2 [Fig. 63]. Intrinsic fluorescence properties of treated PTPI were also brought back to native in the presence of Cur, CA and QE.

3.4.3A INTERACTION OF PTPI WITH HYPOCHLOROUS ACID (HOCl)

Myeloperoxidase released by phagocytic cells at sites of inflammation, catalyzes the formation of potent chlorinating/oxidising agent hypochlorous acid from H_2O_2 and chloride ions. It is a recognized DNA and protein damaging agent [Jenner et al., 2002]. Effects of HOCl on function and structure of the purified inhibitor were analyzed.

Functional modification of PTPI by HOCl

The exposure of 1 μM PTPI to varying HOCl concentrations resulted in a dramatic change in its antiproteolytic potential. At concentration as low as 0.5 μM, HOCl incited 34% loss in activity of PTPI. At equimolar concentrations with the inhibitor, 60% PTPI activity was compromised. The inhibitor was barely active at 5 μM HOCl (~90% loss in activity). Beyond which no papain inhibitory activity was detected

[Table 13]. Since in vivo many physiological antioxidants will be present together with PTPI, the protective effect of two, namely glucose and ascorbic acid was studied [Fig. 65]. The HOCl mediated loss in activity, was diminished in the presence of ascorbic acid and glucose, with ascorbic acid exerting a better protection.

Structural modification of PTPI by HOCl

1 μM PTPI was incubated with increasing concentrations of HOCl. The samples were analyzed for impact on structural integrity of PTPI employing PAGE. As shown in Fig. 66, significant loss of the parent protein band was observed even at HOCl: PTPI ratio of 0.5:1. There was a progressive increase in fragmentation of the inhibitor (as assessed by the loss of parent protein band) at higher ratios with complete loss of any staining material at HOCl: PTPI ratio of 10:1. Physiological antioxidants glucose and ascorbic acid were expected to protect PTPI fragmentation. Fig. 67 illustrates the result obtained. 25 mM glucose and 100 mM ascorbic acid afforded significant protection.

The intrinsic fluorescence properties of PTPI were also adversely affected. As shown in Fig. 68 fluorescence intensity declined with increase in HOCl concentration. No fluorescence was observed beyond 5 μM HOCl. Interestingly, emission λ_{max} remained unaffected at all concentrations of HOCl. The protective effects of glucose and ascorbic acid were observed in retaining tryptophan fluorescence (~40% and ~45%, respectively) even in the presence of 5 μM HOCl.

3.4.3B PROTECTIVE EFFECT OF BIOFLAVONOIDS

Curcumin (Cur), caffeic acid (CA) and quercetin (QE) against HOCl mediated modifications of PTPI

Flavonoids have been extensively studied for their antioxidant properties against various free radicals. However, their effect on hypochlorous acid mediated damage is less known. Thus, present work was also aimed at exploring the potential of Cur, CA and QE against hypochlorite inflicted damage. As depicted in Fig. 65, 100 μM each of CA, Cur and QE, diminished the extent of loss of PTPI activity by several times causing the papain inhibitory potential of PTPI to remain close to that of native. Similar protection was also noticed in PAGE [Fig. 67]. All three antioxidants subjugated structural damage of PTPI caused by HOCl. Tryptophan fluorescence, lost

TABLE 13: LOSS OF ANTIPROTEOLYTIC ACTIVITY OF PTPI ON TREATMENT WITH HOCl AS A FUNCTION OF CONCENTRATION OF HOCl

HOCl (μM)	0	0.5	1.0	2.5	3.0	5.0	10
% PTPI Activity[a]	100	66.40±2.8* (-33.6)	39.84±1.1* (-60.16)	22.34±0.82* (-78.0)	17.93±0.68* (-82.07)	9.21±0.13* (-90.04)	-

PTPI (1μM) was incubated with increasing concentrations of HOCl for 30 min.
[a]PTPI was assayed for loss in antiproteolytic activity by caseinolytic method of Kunitz [1947]. The activity of native PTPI is taken to be 100. Results are Mean±SEM for three or more separate experiments.
* Significantly different from native PTPI (control) at $p < 0.05$ by one way ANOVA.
Values in parentheses represent percent change from control.

Fig. 65 Effect of scavengers on HOCl mediated inactivation of PTPI

Native PTPI (1 μM) was incubated with HOCl (5 μM) alone or in presence of glucose (final concentration, 25 mM)/ascorbic acid (final concentration, 100 mM) or curcumin (Cur □)/ caffeic acid (CA □)/quercetin (QE □) (final concentration, 100 μM, respectively) for 30 min in a final reaction volume of 1 ml at room temperature and was assayed for its antiproteolytic activity. None of the scavengers used had any effect on PTPI assay. Data are expressed as mean ± SEM for four experiments. * $p < 0.05$ compared to PTPI+HOCl alone.

Fig. 66 PAGE of native and HOCl treated PTPI

Native PTPI (1 μM) was incubated with increasing HOCl concentrations (0.5-10 μM) for 30 min followed by the addition of 100 μM GSH to quench residual oxidants and subjected to non denaturing PAGE. Gels were silver stained.

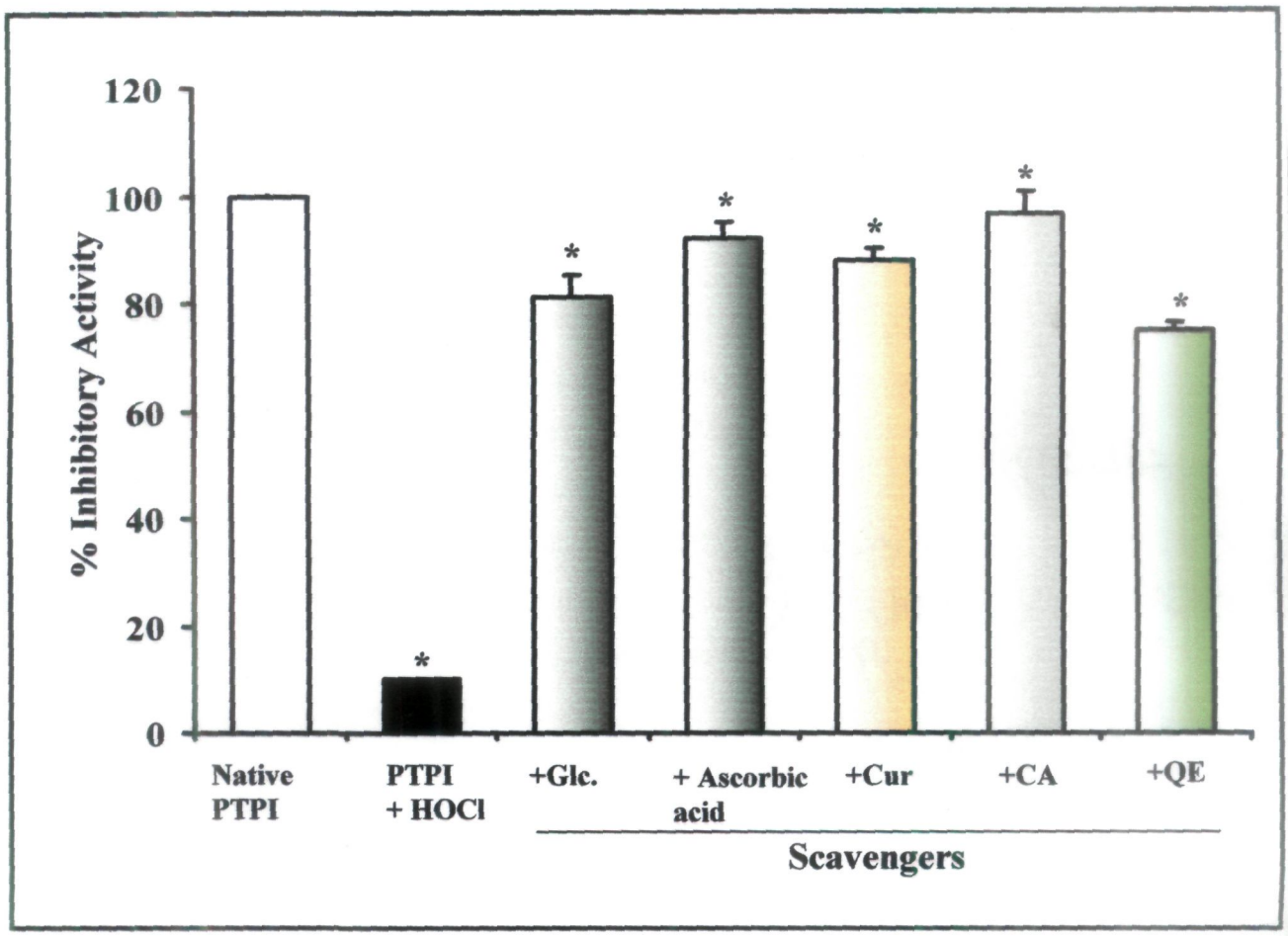

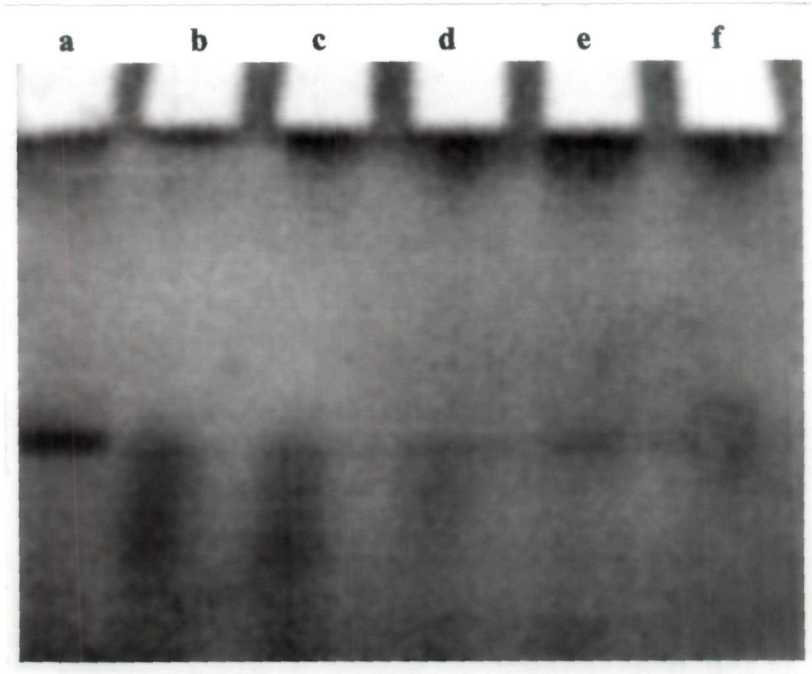

Lane	a	b	c	d	e	f
PTPI	+	+	+	+	+	+
HOCl (μM)	-	0.5	1	3	5	10

Fig. 67 PAGE of PTPI exposed to HOCl in presence of various scavengers

Native PTPI (1 μM) was incubated with 5 μM HOCl in presence of scavengers, glucose (final concentration, 25 mM) or ascorbic acid (final concentration, 100 mM) or in presence of curcumin (Cur)/caffeic acid (CA)/quercetin (QE) (final concentration, 100 μM) followed by the addition of 100 μM GSH to quench residual oxidants and subjected to non denaturing PAGE. The experimental conditions were same as defined for Fig. 66. Gels were silver stained.

Fig. 68 Intrinsic fluorescence analysis of PTPI treated with different concentrations of HOCl

1 μM PTPI was incubated with increasing concentrations of HOCl for 30 min in a final reaction volume of 1 ml in 50 mM sodium phosphate (pH 7.5) at room temperature. The reaction was stopped by adding 100 μM GSH. The excitation wavelength was 280 nm and emission was recorded in range of 300-400 nm with a slit width of 5 nm. Trace 1 is native PTPI, or PTPI + HOCl 0.5 μM (trace 2), 1 μM (trace 3), 3 μM (trace 4), 5 μM (trace 5).

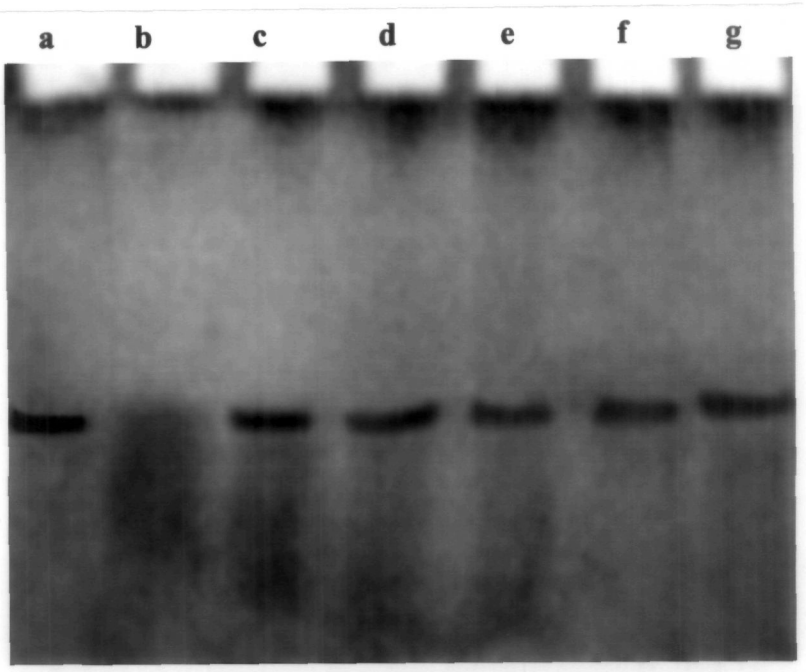

Lane	a	b	c	d	e	f	g
PTPI	+	+	+	+	+	+	+
HOCl (5 μM)	-	+	+	+	+	+	+
Scavenger	-	-	Glucose	Ascorbic acid	Cur	CA	QE

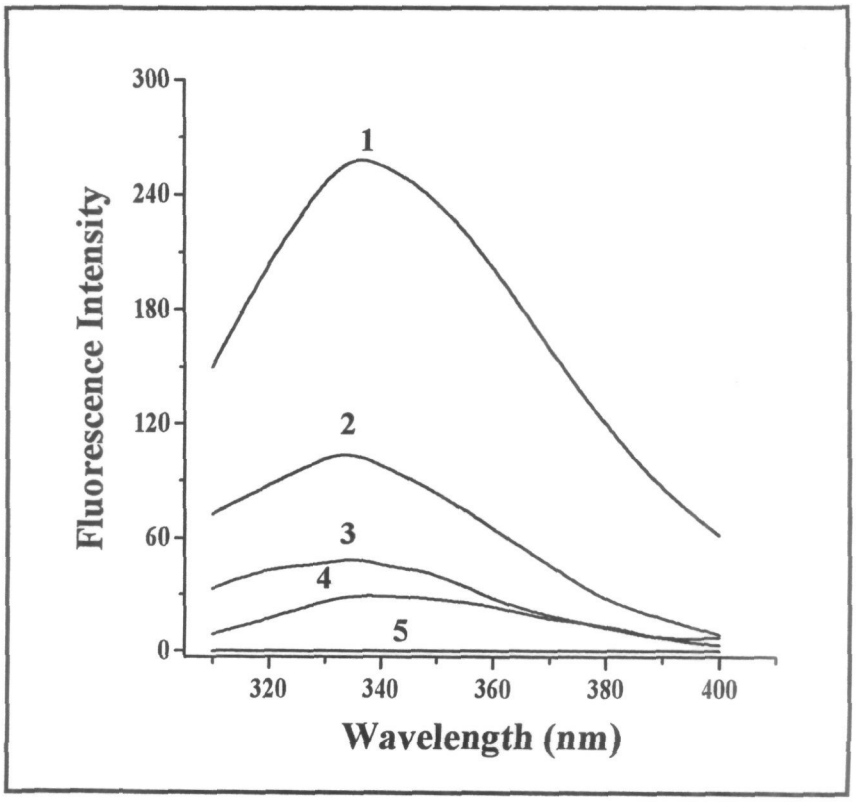

to 5 μM HOCl was ~99% retrieved [Fig. 69]. Percent retention of tryptophan fluorescence was ~71% and ~44% in presence of Cur and QE, respectively.

3.4.4A INTERACTION OF PTPI WITH NITRIC OXIDE (NO)

It is widely accepted that enhanced NO formation [and subsequent generation of complex cocktail of cytotoxic and oxidant reactive nitrogen species] contributes to oxidative and nitrosative stress in a variety of pancreatic and cardiovascular pathologies [Lenzen, 2008a; Denicola and Radi, 2005]. Thus, studies were undertaken to study the effects of NO on function and structure of purified pancreatic thiol proteinase inhibitor (PTPI). Also Cur, CA and QE were analyzed for their efficacies in ameliorating the detrimental effects of NO on PTPI.

Generation of NO

Sodium nitroprusside (SNP) was used as a selective NO donor. SNP in aqueous solution at physiological pH spontaneously generates NO, which interacts with oxygen to produce nitrite ion which can be estimated using Griess reagent. Incubation of solutions of SNP in phosphate buffered saline at 25°C resulted in linear time-dependent nitrite production.

Functional modification of PTPI by NO

1 μM PTPI was incubated with increasing concentrations of SNP (0.05 to 10 mM) for 30 min and its papain inhibitory activity was determined by caseinolytic assay of papain [Kunitz, 1947]. The functional loss of PTPI inhibitory activity was proportional to SNP concentration [Table 14]. Approximately 37% loss in activity was incurred by 0.05 mM SNP. At 1 mM SNP, a significant decline (72%) of native PTPI activity was observed with complete loss at 10 mM SNP concentration. Time dependent loss in PTPI activity was also monitored. PTPI (1 μM) was incubated with 0.05 mM SNP, and activity was determined for varying time intervals (0-180 min). There was a gradual decrease in inhibitory activity till 45 min. A sharp decline (60%) was observed after 60 min of incubation, 94% at 150 min, with no activity detected after 180 min of incubation.

Structural modification of PTPI by NO

Effect of NO on structural integrity of PTPI was examined by PAGE. No major

Fig. 69 Intrinsic fluorescence analysis of PTPI treated with HOCl in presence of natural antioxidants

1 μM PTPI was incubated with 5 μM HOCl in presence of curcumin (Cur)/caffeic acid (CA)/quercetin (QE) (final concentration, 100 μM) for 30 min in a final reaction volume of 1 ml in 50 mM sodium phosphate (pH 7.5) at room temperature. The reaction was stopped by adding 100 μM GSH. The excitation wavelength was 280 nm and emission was recorded in range of 300-400 nm with a slit width of 5 nm.

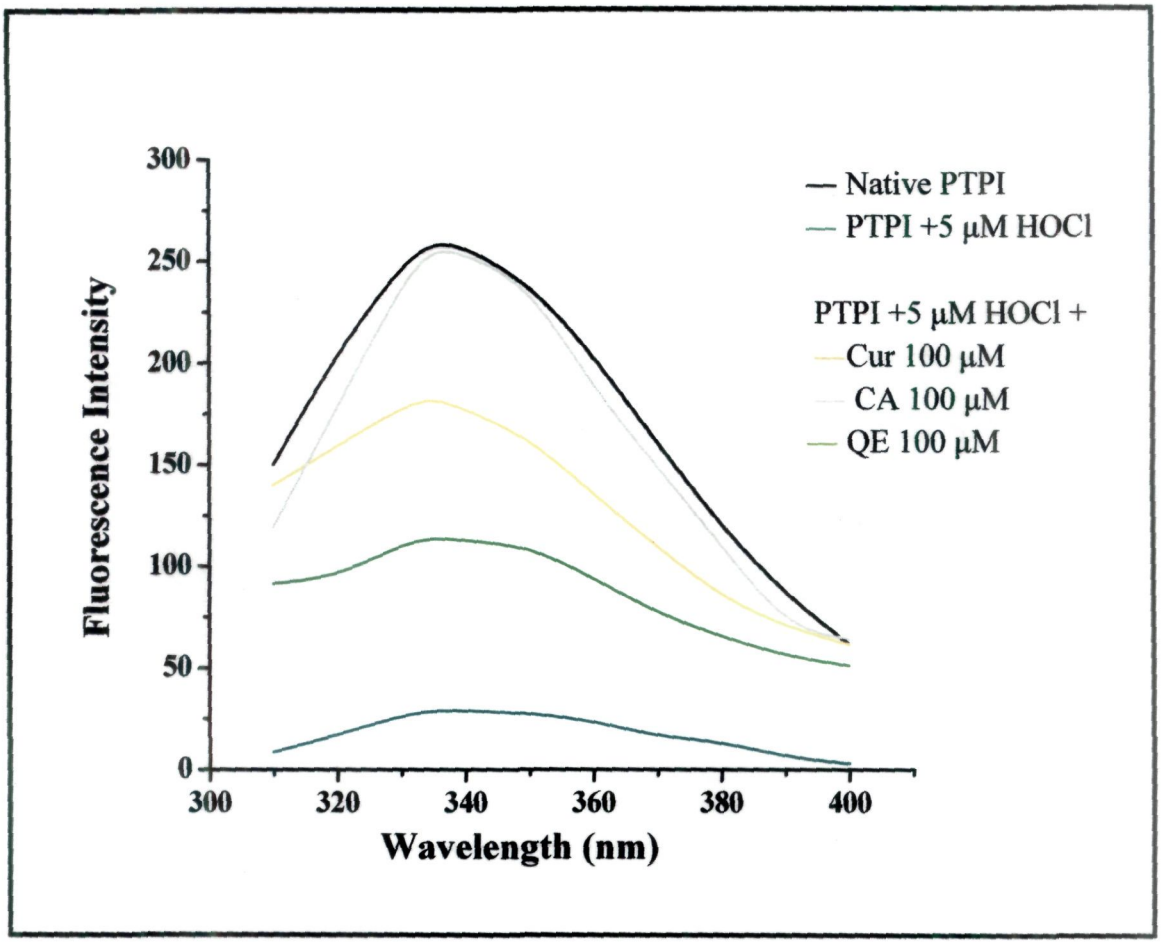
Fluorescence Intensity
300
250
200
150
100
50
0
300
320
340
360
380
400
Wavelength (nm)
Native PTPI
PTPI +5 μM HOCl
PTPI +5 μM HOCl +
Cur 100 μM
CA 100 μM
QE 100 μM

TABLE 14: LOSS OF ANTIPROTEOLYTIC ACTIVITY OF PTPI ON TREATMENT WITH SNP AS A FUNCTION OF (A) CONCENTRATION OF SNP AND (B) TIME OF INCUBATION

(A)

SNP (mM)	0	0.05	1.0	10
% PTPI Activity[a]	100	62.75±2.4* (-37.30)	28.00±0.92* (-72.0)	-

(B)

Time of incubation (min)	0	15	30	45	60	90	120	150	180
%PTPI Activity[a]	100	87.27±3.8 (-13.0)	65.42±3.1* (-35.0)	61.09±2.7* (-39.0)	40.13±1.5* (-60.0)	28.61±0.72* (-71.4)	12.10±0.56* (-88.0)	6.12±0.09* (-94)	-

PTPI (1μM) was incubated with increasing concentrations of SNP for 30 min or with 0.05 mM SNP for increasing intervals of time.
[a]PTPI was assayed for loss in antiproteolytic activity by caseinolytic method of Kunitz [1947]. The activity of native PTPI is taken to be 100.
Results are Mean±SEM for three or more separate experiments.
* Significantly different from native PTPI (control) at $p < 0.05$ by one way ANOVA.
Values in parentheses represent percent change from control.

modifications were observed. The parent band pattern was conserved at all concentrations except that band intensity was slightly increased [Fig. 70].

The modifications of amino acid residues of PTPI consequential to NO exposure were analyzed by intrinsic fluorescence spectroscopy by monitoring the changes in intensity and λ_{max}. The results are summarized in Fig. 71. Fluorescence intensity was considerably quenched at 0.05 mM SNP with a 5 nm red shift (from 335 nm for untreated PTPI to 340 nm). A further increase in concentration of SNP to 1 mM, quenched the intensity to 77.4% with another 5 nm red shift (to 350 nm). At 10 mM SNP, fluorescence was completely quenched. Conclusively, NO lead to quenching of fluorescence coupled to 15 nm red shift in λ_{max}.

When analyzed as a function of time, the decrease in fluorescence intensity was triggered within 15 min of incubation and culminated to ~71% decline at 180 min of incubation. The red shift of 15 nm precipitated within 60 min of incubation.

3.4.4B PROTECTIVE EFFECT OF BIOFLAVONOIDS

Curcumin (Cur), caffeic acid (CA) and quercetin (QE) against NO mediated modifications of PTPI

A great deal of evidence has amassed pointing to reactive nitrogen species (RNS) as the main contributors to nitrosative stress in a variety of pathologies. Therefore, targeting NO (and NO congeners) either directly by scavengers or indirectly by inhibitors of its downstream targets are exciting therapeutic strategies. In this respect, plant polyphenols offer to be attractive candidates. Present study was undertaken to examine the anti-nitrosative efficacies of CA, QE and Cur in reclamation of the NO induced modifications of PTPI.

For these studies, 1 μM PTPI was incubated with 1 mM SNP and the samples were analyzed by caseinolytic assay of papain [Kunitz, 1947] and fluorescence spectroscopy. NO mediated a decline in activity (72% loss, Table 14). 20 μM Cur prompted restoration of lost activity near to native [Fig. 72].

80 μM each of QE and CA inhibited the loss to a similar extent. These bioflavonoids were also analyzed for their potency to restore the structural changes induced by NO on PTPI. As shown in Fig. 73 all the three natural antioxidants negated the loss in tryptophan fluorescence and retrieved the native like fluorescence pattern in treated PTPI. Maximum protection was offered by CA and Cur.

Fig. 70 PAGE of native and SNP treated PTPI

Native PTPI (1 μM) was incubated with increasing SNP concentrations 0.05,1 and 10 mM, for 30 min and subjected to non denaturing PAGE. Gels were silver stained.

Fig. 71 Intrinsic fluorescence analysis of PTPI treated with different concentrations of SNP

1 μM PTPI was incubated with increasing concentrations of SNP for 30 min in a final reaction volume of 1 ml in 50 mM sodium phosphate (pH 7.5) at room temperature. The excitation wavelength was 280 nm and emission was recorded in range of 300-400 nm with a slit width of 5 nm. Trace 1 is native PTPI. Trace 2 is 0.05 mM, trace 3 is 1 mM and trace 4 is 10 mM SNP treated PTPI.

Lane	a	b	c	d
PTPI	+	+	+	+
SNP (mM)	-	0.05	1	10

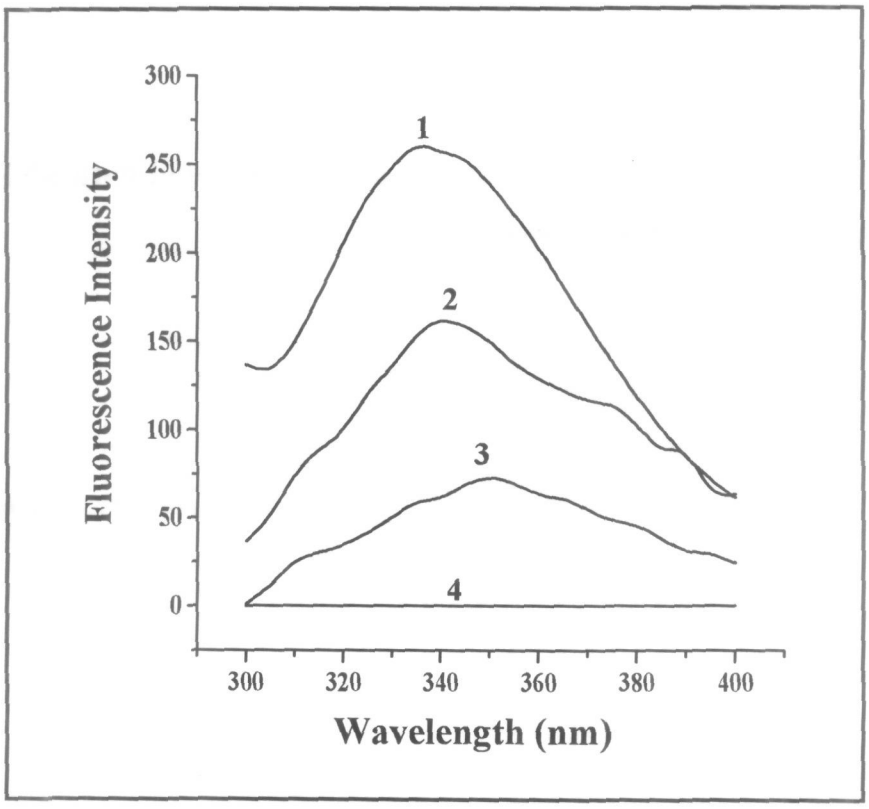

Fig. 72 Effect of natural antioxidants on SNP mediated inactivation of PTPI

Native PTPI (1 μM) was incubated with SNP (1 mM) alone or in presence of curcumin (Cur □)/ caffeic acid (CA □)/quercetin (QE □) (final concentration, 20 μM for Cur and 80 μM for CA and QE) for 30 min in a final reaction volume of 1 ml at room temperature and was assayed for its antiproteolytic activity. None of the scavengers used had any effect on PTPI assay. Data are expressed as Mean ± SEM for four experiments. * $p < 0.05$ compared to PTPI+SNP alone.

Fig. 73 Intrinsic fluorescence analysis of PTPI treated with SNP in presence of natural antioxidants

1 μM PTPI was incubated with 1 mM SNP in presence of curcumin (Cur)/caffeic acid (CA)/quercetin (QE) (final concentration, 20 μM for Cur, 80 μM for CA and QE) for 30 min in a final reaction volume of 1 ml in 50 mM sodium phosphate (pH 7.5) at room temperature. The excitation wavelength was 280 nm and emission was recorded in range of 300-400 nm with a slit width of 5 nm.

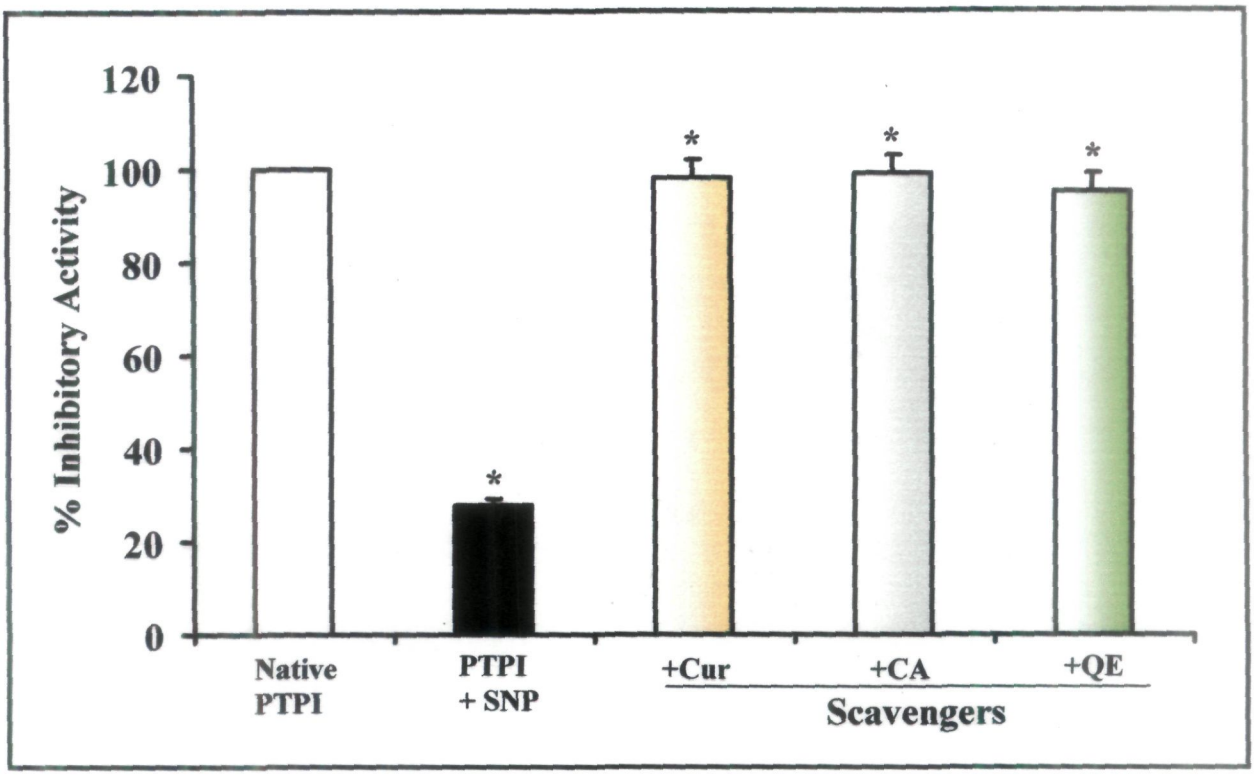
120
100
80
60
40
20
0
% Inhibitory Activity
*
*
*
*
Native PTPI
PTPI + SNP
+Cur
+CA
+QE
Scavengers

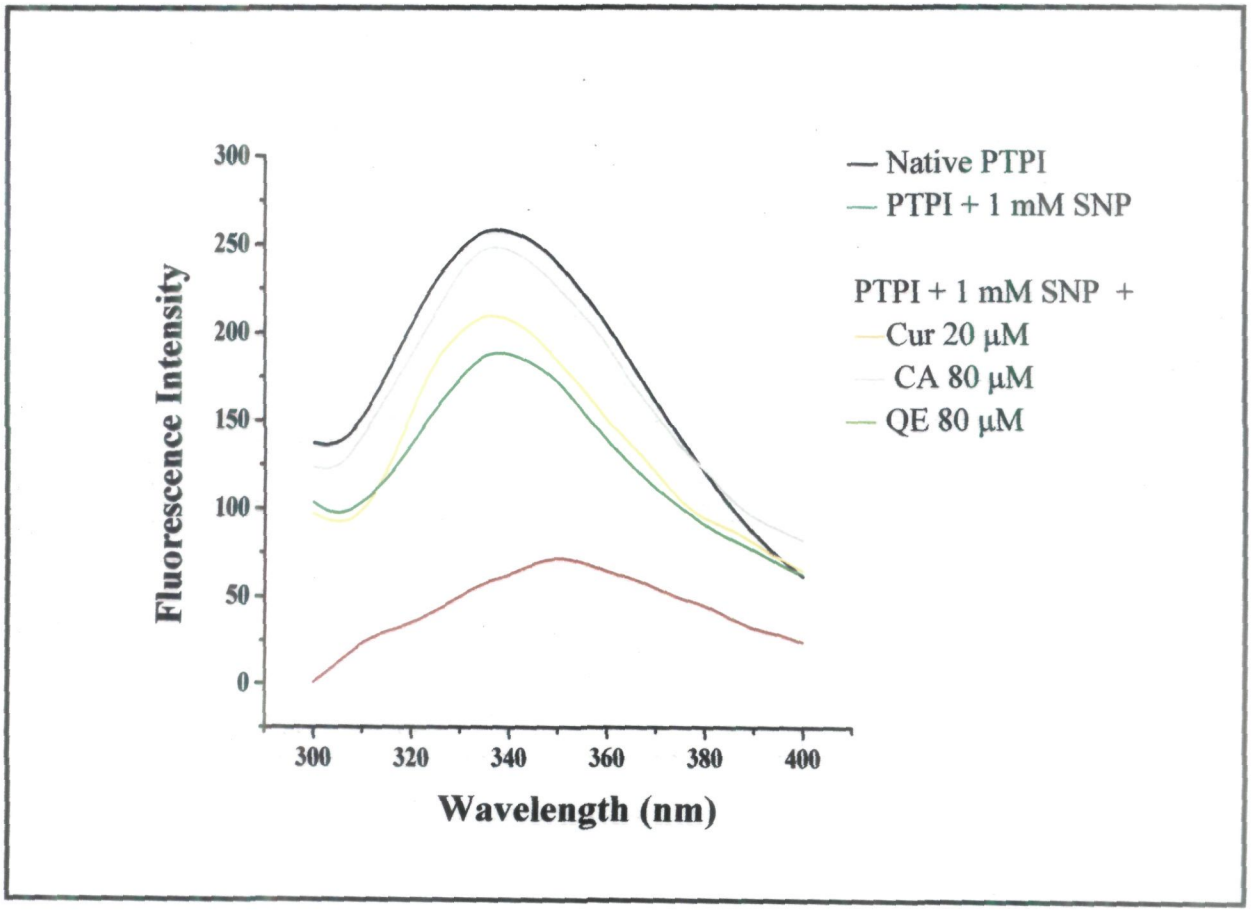
300
250
200
150
100
50
0
Fluorescence Intensity
300
320
340
360
380
400
Wavelength (nm)
— Native PTPI
— PTPI + 1 mM SNP
PTPI + 1 mM SNP +
— Cur 20 μM
— CA 80 μM
— QE 80 μM

Discussion

Chapter 4

DISCUSSION

Reactive species (ROS/RNS) like superoxide anions, hydroxyl radicals, hydrogen peroxide, and nitric oxide are the intermediates of regular pathway of aerobic metabolism and processes. These reactive species generated from normal metabolism or exogenous insults lead to peroxidation of membrane lipids and damage to cellular macromolecules like DNA and proteins. Aerobic organisms synthesize enzymes devoted to the prevention and repair of oxidative damage and extreme genetic deficiency in either of these two defences can lead to inviability in aerobic environments. The uncontrolled oxidative stress initiates a series of harmful biochemical events associated with diverse pathological processes [Droge, 2002].

There are numerous indications that ROS/RNS play significant role in various pancreatic pathologies including diabetes and its secondary complications like retinopathy, nephropathy and neuropathy, in chronic and acute pancreatitis and in pancreatic stellate cell fibrosis [Chvanov et al., 2005; Pacher et al., 2005; Lenzen, 2008a]. Interestingly, pancreas has been found to be exceptionally liable to oxidative and nitrosative damage as a consequence of its feeble antioxidant defence [Lenzen, 2008a, Neuschwander-Tetri et al., 1997].

Pancreatic thiol proteinases, cathepsin B, H and calpains are involved in activation of zymogen and insulin secretion and action [Thrower et al., 2006; Sreenan et al., 2001]. Their activity is primarily regulated by thiol proteinase inhibitors. In traumatic processes usually the balance between the lysosomal proteinases released by macrophages and neutrophils and their endogenous inhibitors is disturbed. This imbalance may originate from various reasons one of which may be inactivation by radical species viz. H_2O_2, HOCl, ROS, NO (and RNS).

The present work was thus outlined to deduce the effect of exposure of purified PTPI, in vitro, to photoilluminated riboflavin (mimicking the biological subjection to oxygen radicals [Tsai et al., 1985], non-radical oxidants H_2O_2 and HOCl and NO (generated from SNP), on its function and structure. The results evinced the susceptibility of PTPI to aforementioned reactive species and the modifications induced included altered molecular weight (aggregation or fragmentation), loss of fluorescence and inhibitory function.

Photosensitized riboflavin produces ROS [Husain et al., 2006] whose damaging effects have been documented in various proteins [Ali et al., 1991; Jazzar and Naseem,

1994; Husain et al., 2006; Hasan et al., 2006]. Among the various forms of ROS generated, singlet oxygen is of particular physiologic significance because of its selectively long life in aqueous solution, its ability to cross cell membrane barrier and high reactivity towards biomolecules [Joshi, 1998].

The results reveal the loss of PTPI function on exposure to photosensitized riboflavin. This bears similarity to sheep plasma high molecular weight kininogen (HMWK) [Baba et al., 2004], membrane proteins [Ali et al., 1991], BSA, invertase, lysozyme [Jazzar and Naseem, 1994] and trypsin [Husain et al., 2006; Hasan et al., 2006] damage caused by photosensitized riboflavin. Results obtained with specific ROS scavengers suggested that singlet oxygen and flavin triplet state were predominantly responsible for PTPI damage. Same results are reported for sheep HMWK and catalase [Baba et al., 2004; Gantchev and van Lier, 1995] showing that singlet oxygen and radical species can participate in photosensitizer-induced inactivation of enzymes. Riboflavin at higher concentration (40 and 50 μM) generated aggregate formation. This behaviour has also been reported earlier for sheep plasma HMWK [Baba et al., 2004] and goat brain cystatin [Sumbul and Bano, 2008]. Owing to the absence of free sulphydryls in purified PTPI [Priyadarshini and Bano, 2009] these aggregates might have formed due to the exposed hydrophobic patches. This is supported by the altered fluorescence of PTPI in presence of photoilluminated riboflavin (a 5 nm blue shift in λ_{max}, from 335 nm for native to 330 nm for the treated PTPI) and enhanced ANS binding to treated PTPI.

The reactive species like H_2O_2 and HOCl have been recognized as hallmark of inflammation [Martinez-Cayuela, 1995]. Macrophages and neutrophils reduce molecular oxygen to superoxide anion, as a part of host defence system to neutralize the invading pathogens [Marnett et al., 2003]. The superoxide produced is rapidly dismutated to hydrogen peroxide. Activated neutrophils release the enzyme myeloperoxidase that reacts with H_2O_2 and chloride ions present to form HOCl [Marnett et al., 2003], a reactive oxygen metabolite, that can modify amino acid residues, induce conformational changes in proteins and inactivate enzyme and enzyme inhibitors [Shechter et al., 1975; Wasil et al., 1987; Dean et al., 1997]. HOCl, a strong oxidant, is known to oxidize many important biomolecules such as DNA, proteins, enzymes and antiproteinases [Jerlich et al., 2000; Whiteman et al., 2003; Khan and Khan, 2004; Szuchman-Sapir et al., 2008].

The results reveal that PTPI, in the presence of HOCl lost its antiproteinase activity rapidly (within 30 min, 90% loss occurred at 5 μM HOCl). Inactivation of proteins like of α_2 M, by HOCl has been registered earlier [Khan and Khan, 2004]. Whiteman et al. [2003] reported a 90% loss in activity of isolated α_1 antiproteinase in presence of 7 μM HOCl. Protein inactivation by HOCl may occur through multiple mechanisms, like, oxidation of critical amino acid residues e.g. cysteine [Tyagi, 1991], methionine [Moreno and Pryor, 1992]; modification of tyrosines [Feste and Gan, 1981] as well as other residues [Whiteman, 1998]. PTPI inactivation may also be consequent to oxidation/ modification (chlorination) of residues crucial to its activity or due to diminished conformational integrity changing the active site region of the inhibitor.

H_2O_2 was found to be a modest inactivator of PTPI relative to HOCl (and other radicals studied). The treated inhibitor lost only 50% of its antiproteolytic activity even in presence of 500 mM H_2O_2 [Table 12A]. Use of scavengers reflected H_2O_2 as the damaging agent itself with only partial involvement of hydroxyl radicals. Non-radical (molecular reactions) driven damage of proteins (e.g. lens crystallins and α_2 M, in vitro) by H_2O_2 has been reported earlier [Khan and Khan, 2004; McNamara and Augusteyn, 1984]. The conformational status of H_2O_2-treated PTPI remained largely unchanged [Fig. 62]. Material with slightly higher mobility appeared at H_2O_2 concentration of 100 mM and above, with a little loss in the band intensity as compared to the parent protein band. Protein fragmentation by H_2O_2 has been shown for BSA by Hunt et al. [1988]. Correspondingly, significantly higher mobility material was observed for HOCl treated PTPI. Glucose and ascorbic acid lodged prevention of protein fragmentation [Fig. 66 and 67]. In case of H_2O_2, marked red shift of 15 nm was observed indicating change in the microenvironment of tryptophan residues towards polar [Fig. 64], and the loss of native folded state of PTPI. While in presence of HOCl, fluorescence of PTPI was quenched completely beyond 5 μM HOCl [Fig. 68] without any change in λ_{max}. In H_2O_2 mediated damage, the higher mobility material consists of fragmentation products, and the unfolding might have facilitated the protein fragmentation [Davies and Delsignore, 1987].

HOCl usually causes aggregation of proteins as has been shown for fibronectin [Vissers and Winterbourn, 1991], apolipoprotein A-I [Bergt et al., 2001], caprine α_2 M [Khan and Khan, 2004], ovalbumin [Olszowski et al., 1996], apohaemoglobin and apomyoglobin [Chapman et al., 2003]. Protein fragmentation by HOCl is substantiated from reports on serum albumin, Cu/Zn SOD, and glucose-6-phosphate

dehydrogenase [Hawkins and Davies, 1998; Ullrich et al., 1999; Auchere and Capeillere-Blandin, 2002]. HOCl reacts with amide groups of protein backbone and also with free amino groups of lysine residues of proteins yielding chloramines. These chloramines can than effectuate protein fragmentation. At low HOCl concentrations preferably lysines are modified limiting the rapid backbone fragmentation. Further, extent of fragmentation at low HOCl concentrations is defined by number of lysine residues in proteins [Hwakins and Davies, 1998]. The fluorescence profile of HOCl-treated PTPI reveals complete loss of intensity at concentrations above 5 μM without any change in λ_{max} of emission. There was a HOCl concentration dependent increase in higher mobility material when treated PTPI was subjected to PAGE [Fig. 66] with complete loss of any staining material at 10 μM HOCl. Separate bands were not discernible at any HOCl concentration. This suggests that HOCl even at very low concentrations (protein:HOCl ratio of 1:0.5) causes backbone fragmentation releasing smaller fragments which make up for the appearance of higher mobility material in PAGE. Upto protein:HOCl ratio of 1:5, though fragmentation was induced [Fig. 66], native PTPI might have existed in significant proportions defining the unaltered λ_{max}. Also, HOCl is prejudiced to modify tyrosine, phenylalanine (by chlorination), cysteine, methionine (by sulphoxidation and oxy-acid formation) than to oxidize tryptophan [Stadtman and Levine, 2003]. This might also explain the unaltered λ_{max} of PTPI mainly attributable to tryptophan.

NO is a highly reactive free radical gas, which can participate as a cytotoxic effector molecule and/or pathogenic mediator when produced at high rates by inflammatory stimuli induced nitric oxide synthase or over stimulation of constitutive forms of enzyme [Radi, 2004]. In contrast to the protective action of low levels of NO, its excess has injurious outcomes due to exacerbated oxidative damage [Pryor, 2006].

NO also caused extensive loss of PTPI function. Presumably NO enfeebled PTPI in quite a similar fashion as HOCl (by modification or damage of critical amino acid residues). A number of reports catalogue protein inactivation by NO through amino acid modification e.g. goat lung cystatin [Khan et al., 2009], catalase [Sigfrid et al., 2003; Brunelli et al., 2001] and cytochrome P450 [Wink et al., 1993] etc.

NO produced a red shift of 15 nm and PTPI was completely unfolded at higher concentration [Fig. 71]. Such effect has also been reported for goat lung cystatin [Khan et al., 2009]. There were no significant changes in the mobility of NO-treated PTPI when subjected to PAGE. However, increased band intensity was observed as

compared to native PTPI band. This may be due to increased reaction of NO-treated PTPI with silver stain reagent [Davies and Delsignore, 1987]. The drastic change in fluorescence profiles of NO-treated PTPI compared to unnoticeable conformational change on PAGE analysis can be supported to some extent by the initial association of oxidatively generated fragments of PTPI in a conformation similar to that of native protein [Dean et al., 1997]. Similar results were obtained for BSA damaged by hydroxyl radicals, in which initially only very small amount of molecules with changed size were detected [Hazell et al., 1994; Fisher and Stadtman, 1992].

DIETARY ANTIOXIDANTS AS STRATEGIES AGAINST FREE RADICAL DAMAGE

Many antioxidant defences, enzymatic (superoxide dismutase, catalase, glutathione peroxidase) and non-enzymatic (ascorbic acid, uric acid, glucose, glutathione, vitamin E) exist to maintain the balance between reactive species production and neutralization. However, they fail to provide complete protection against conditions of severe oxidative stress [Cesaratto et al., 2004]. Also the non enzymatic oxidants are relatively inefficient as high concentrations are required to prevent oxidative damage. This inefficiency is reinforced by the observation that protein derived radicals can be detected in plasma treated with low concentrations of HOCl even when endogenous antioxidants were present [Hawkins and Davies, 1998; Dean et al., 1997]. Besides, many synthetic antioxidants have shown toxic and/or mutagenic effects. These observations shifted the attention towards naturally occurring antioxidants.

Therefore, experiments were also designed to address these issues. Three plant components were chosen, whose protective effects in various pancreatic (and other organ) pathologies have already been registered, viz. Curcumin (Cur), Caffeic acid (CA) and Quercetin (QE) [Kanitkar et al., 2008; Jung et al., 2006; Kim et al., 2007]. These bioflavonoids are known for exerting pleiotropic health benefit through their antioxidant, anti-inflammatory, antimicrobial, anticancer, antidiabetic activities [Aggarwal et al., 2007; Takahama et al., 2009; Sreejayan and Rao, 1997].

Efficacy of these natural antioxidants against the detrimental effects of photosensotized riboflavin, H_2O_2, HOCl, and NO on PTPI, in vitro, was evaluated. Concentration dependent protective effect was observed for all the three, for all four

radical systems (results not shown). Only the most effective concentration of each, in every radical system is described.

Riboflavin mediated photodynamic damage of PTPI was considerably diminished by QE and CA. Cur provided only partial moderation. QE and CA (350 μM each) caused manifold enhancement in the activity of treated PTPI [Fig. 57B]. Aggregation (observed at 40 μM riboflavin) was also inhibited and tryptophan fluorescence retrieved back. However, Cur failed to show any preventive effects in the latter two cases. Major damage on PTPI by photoilluminated riboflavin was incurred by singlet oxygen and flavin triplet state. High concentration of phenolics has been shown to quench these two radical states [Cardoso et al., 2006]. Such effect was also provided by rutin, catechin and epigallocatechin gallate [Becker et al., 2005].

Direct mitigation of H_2O_2 toxicity in in vitro assay systems finds rare documentation. In the present study, PTPI inactivation (though modest), unfolding and loss in conformational integrity, induced by H_2O_2 was alleviated by 100 μM Cur, 60 μM CA and 50 μM QE. This concurs with the study of Nakayama [1994] in which CA and QE suppressed the H_2O_2 induced cytotoxicity in biological assay systems. In general ROS scavenging on the whole has been shown by Cur [Huang et al., 1988].

HOCl reduced PTPI's antipapain potential, and altered its structural integrity, presumably causing fragmentation and modification of constituent amino acid residues. CA (100 μM) effectuated almost complete reversal of the HOCl damage, followed closely by Cur (100 μM). QE exhibited slightly diminished protection. Diminution of hypochlorite induced damage on human serum albumin by flavonoids has been reported by Firuzi et al. [2004].

In the three radical systems studied, physiological antioxidants like ascorbic acid, glucose etc. were also employed but corresponding protection was attainable at millimolar concentrations corroborating the potency of natural antioxidants.

NO imposed deleterious effects on PTPI function and structure were ameliorated by these natural antioxidants. Cur, an established NO scavenger; completely reverted NO induced PTPI inactivation at 20 μM. 30-50 μM Cur was shown to be potent NO scavenger by Sreejayan and Rao [1997]; Onoda and Inano [2000]; Chan et al. [2005] and Sumanont et al. [2004]. This is also reinforced by the recent study of Khan et al. [2009], showing Cur to prevent NO mediated structural and functional damage of goat lung cystatin. Quite similar effect was shown by CA (80 μM). This is in conjunction with the works of Jung et al. [2006]; Gulcin [2006]; Olmos et al. [2008];

Chung et al. [2006]. 80 μM QE also protected against the NO induced damage. The results draw support from earlier reports [Lapidot et al., 2002; Hirota et al., 2005]. Structural alterations engendered by NO in PTPI were also diminished markedly by the three natural antioxidants.

These results are important as Cur, QE and CA,

a) come out to be potential scavengers of radical sinks viz. NO and HOCl.
b) provide alternate therapeutic strategies against free radical damage.
c) are effortlessly consumed by large proportion of human population and pose lesser or no side effects.

Chapter 5

Drug-PTPI interaction: Effect of pancreatitis causing and antidiabetic agents

3.5 RESULTS

The present set of experiments was devised to investigate the effects of sodium valproate (an antiepileptic drug causing pancreatitis), glimepiride (an antidiabetic drug of sulphonylurea class) and metformin hydrochloride (an antidiabetic drug, of biguanide class) on structure and function of PTPI.

3.5.1 INTERACTION OF PTPI WITH SODIUM VALPROATE

Association of valproate [Werlin and Fish, 2006] and cathepsin mediated trypsinogen activation with pancreatitis provoked the interest in probing the effects of valproate on PTPI, as thiol proteinase inhibitors (cystatins) are prime endogenous regulators of cathepsin activity.

The concentration of sodium valproate (VPA) used in the experiments was well within the therapeutic range [Werlin and Fish, 2006]. Fig. 74 depicts the effect of VPA on PTPI activity. 2 μM PTPI was incubated with increasing concentrations of the drug (2-20 μM) in 50 mM sodium phosphate buffer pH 7.5 at room temperature for 30 min and its papain inhibitory activity was determined by caseinolytic assay [Kunitz, 1947]. The activity of native PTPI was taken to be 100%. As shown in the figure, ~50% loss in PTPI activity occurred at 2 μM VPA concentration. 67% loss precipitated at 4 μM and at 10 μM only 20% activity was left. Beyond 10 μM the inhibitor was barely active.

Fluorescence and UV-vis absorption spectroscopy are powerful tools for the study of the reactivities of chemical and biological systems since it allows non-intrusive measurements of substances in low concentrations under physiological conditions. 2 μM PTPI treated with increasing concentrations of the drug (2-20 μM) was analyzed spectroscopically by above mentioned techniques. The excitation wavelength was chosen to be 280 nm to assess changes induced in global conformation of the inhibitor on interaction with the drug. The emission range was from 300-500 nm. As in Fig. 75, only mild changes were induced on PTPI. At 2μM drug concentration, ~20% decline in fluorescence intensity was observed. The intensity was slightly enhanced than native at 4 μM VPA. In presence of 6 μM drug, the fluorescence intensity was considerably increased (~40% above native). Between 8-15 μM VPA the intensity was again quenched although remaining faintly higher than the native. At 20 μM VPA concentration, the emission intensity increased 65% above untreated PTPI. However,

Fig. 74 Effect of Sodium valproate complexation on activity of PTPI

Native PTPI (2 μM) was incubated with increasing concentrations of sodium valproate (VPA) (2-20 μM) for 30 min at room temperature. PTPI was assayed for loss of antiproteinase activity by papain caseinolytic assay of Kunitz [1947]. Values are Mean ± SEM for four independent determinations. *Significantly different from native PTPI (control) at $p< 0.05$ by one way ANOVA.

Fig. 75 Intrinsic fluorescence analysis of PTPI on interaction with various concentrations of Sodium valproate (VPA)

The concentration of PTPI was 2 μM. PTPI was preincubated for 30 min at room temperature in 50 mM sodium phosphate buffer (pH 7.5) containing increasing concentration of VPA (2-20 μM). Fluorescence was measured at an excitation wavelength of 280 nm and emission range of 300-400 nm with slit width of 5 nm.

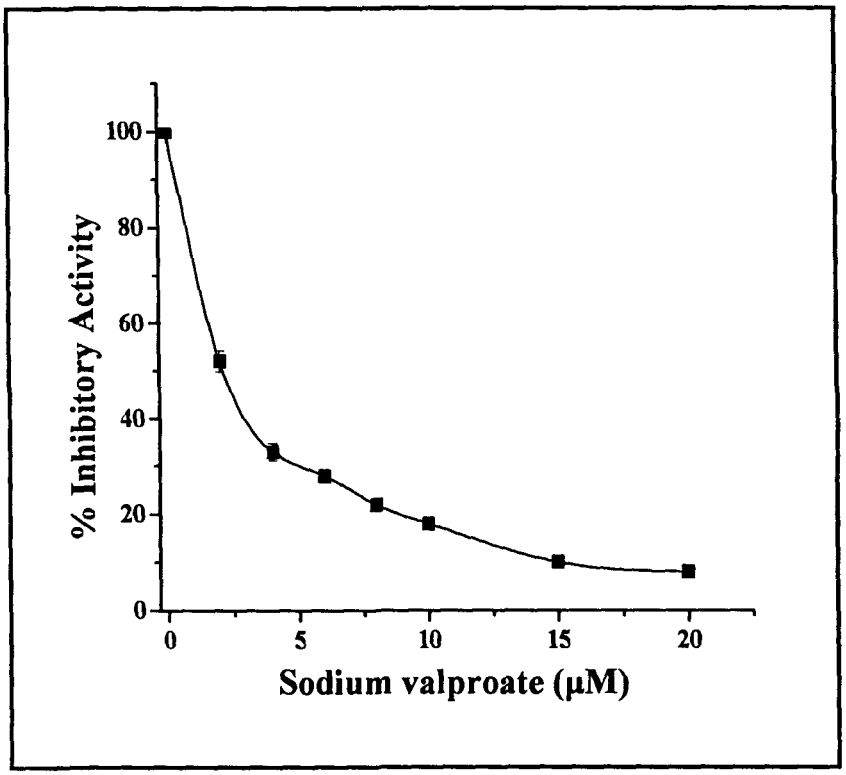
% Inhibitory Activity
100
80
60
40
20
0
0
5
10
15
20
Sodium valproate (μM)

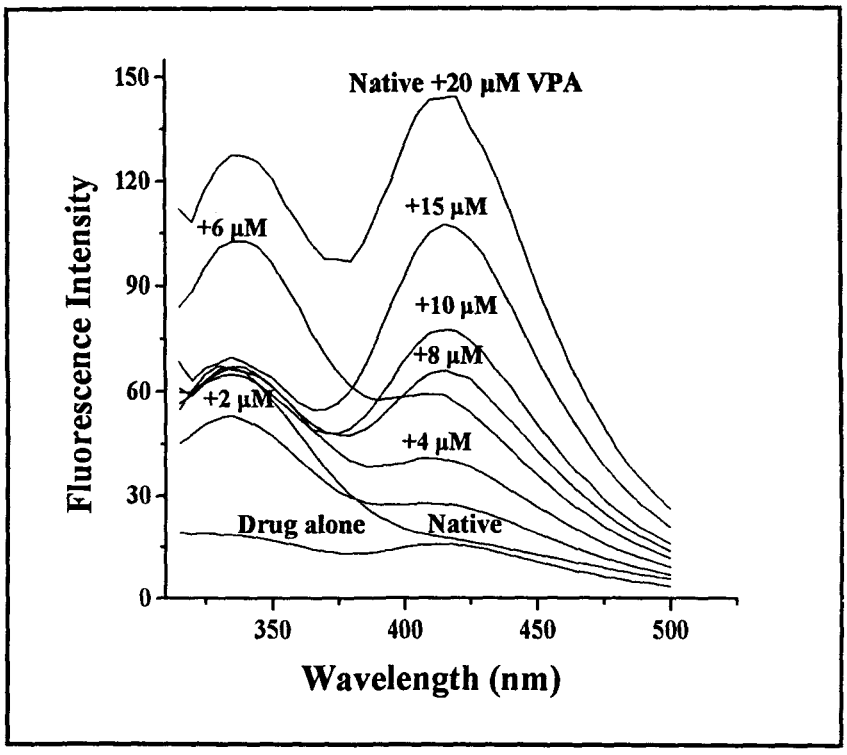
Fluorescence Intensity
150
120
90
60
30
0
Native +20 μM VPA
+15 μM
+6 μM
+10 μM
+8 μM
+2 μM
+4 μM
Drug alone
Native
350
400
450
500
Wavelength (nm)

at all the drug concentrations, wavelength of maximum emission (λ_{max}) remained unaltered. The UV-vis absorption difference spectra were computed at all the drug concentrations. However, profound changes were noted only for those obtained at 2, 6 and 20 μM VPA [Fig. 76]. The difference spectra obtained for PTPI interacted with 2 μM VPA, shows two distinct positive peaks at 230 nm and 285 nm. In the difference spectra obtained at 6 and 20 μM VPA, broad shoulders were observed at 260 nm and maxima at 255 and 295 nm. Besides, intense negative peaks were noticeable at 210 and 215 nm. On subjection to polyacrylamide gel electrophoresis, the gross conformation of PTPI at all VPA concentrations was found to be unaffected (results not shown).

3.5.2 INTERACTION OF PTPI WITH GLIMEPIRIDE

Glimepiride is an antidiabetic drug belonging to the sulphonylurea class. One of the adverse impacts of glimepiride therapy is the production of ROS in pancreatic cells [Sawada et al., 2008]. Thus the effect of therapeutic concentrations of glimepiride on PTPI activity and structure were examined. 2 μM PTPI was incubated with increasing concentrations of the drug (2-40 μM) in 50 mM sodium phosphate buffer pH 7.5 at room temperature for 30 min and its inhibitory activity was determined by caseinolytic assay of papain [Kunitz, 1947]. The activity of native PTPI was taken as 100%. On interaction with 2 μM glimepiride, 10% loss of PTPI activity was noticed [Fig. 77]. At 5 μM drug concentration 50% of inhibitor's activity was compromised. With no significant change in activity of PTPI till 35 μM glimepiride, a drastic decline (85%) was noticed at 40 μM drug concentration and the inhibitor retained only 15% of its original papain inhibition potential.

Effect of glimepiride on the structure of the inhibitor was analyzed by intrinsic fluorescence. The spectra were obtained by exciting the protein at 280 nm and the emission range was 300-500 nm. As shown in Fig. 78 the tertiary structure of the inhibitor remained more or less uninfluenced by the drug with only a little increment in fluorescence till 30 μM concentration. At 35 μM glimepiride, the intensity was slightly quenched below untreated PTPI. However at 40 μM glimepiride, pronounced enhancement in fluorescence intensity was observed. Similar to VPA, no change in λ_{max} was registered. When analyzed by UV-vis spectroscopy, corresponding to fluorescence results no significant changes were observed except at 40 μM glimepiride concentration. The difference spectra obtained at 40 μM drug

Fig. 76 UV-Absorption difference spectra measured for PTPI-VPA complexes

PTPI (2 μM) was incubated with VPA (2-20 μM) for 30 min and absorbance difference spectrum was calculated between 200 nm to 320 nm. Results are shown for complexes obtained at 2, 6 and 20 μM VPA.

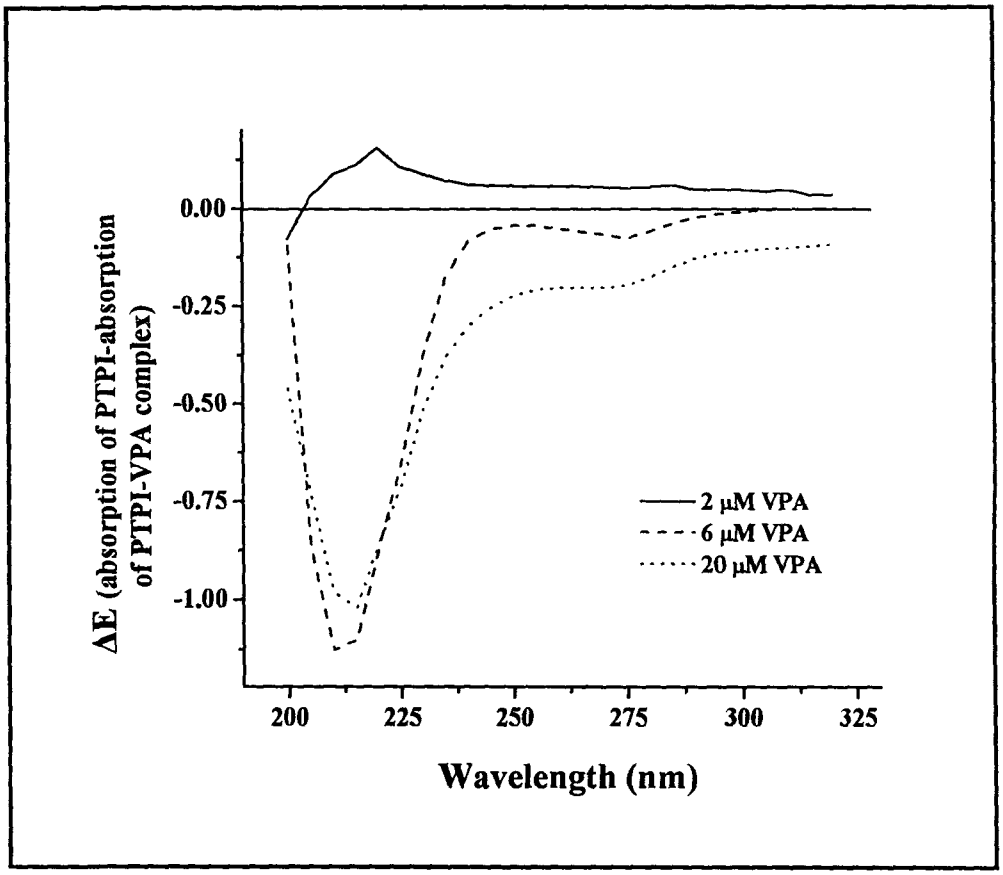
ΔE (absorption of PTPI-absorption of PTPI-VPA complex)
0.00
-0.25
-0.50
-0.75
-1.00
200
225
250
275
300
325
Wavelength (nm)
2 μM VPA
6 μM VPA
20 μM VPA

Fig. 77 Effect of glimepiride complexation on activity of PTPI

Native PTPI (2 μM) was incubated with increasing concentration of glimepiride (2-40 μM) for 30 min at room temperature. PTPI was assayed for loss of antiproteinase activity by papain caseinolytic assay of Kunitz [1947]. Values are Mean ± SEM for four independent determinations.
*Significantly different from native PTPI (control) at $p < 0.05$ by one way ANOVA.

Fig. 78 Intrinsic fluorescence analysis of PTPI on interaction with various concentrations of glimepiride

The concentration of PTPI was 2 μM. PTPI was preincubated for 30 min at room temperature in 50 mM sodium phosphate buffer (pH 7.5) containing the increasing concentration of glimepiride (2-40 μM). Fluorescence was measured at an excitation wavelength of 280 nm and emission range of 300-400 nm with slitwidth of 5 nm.

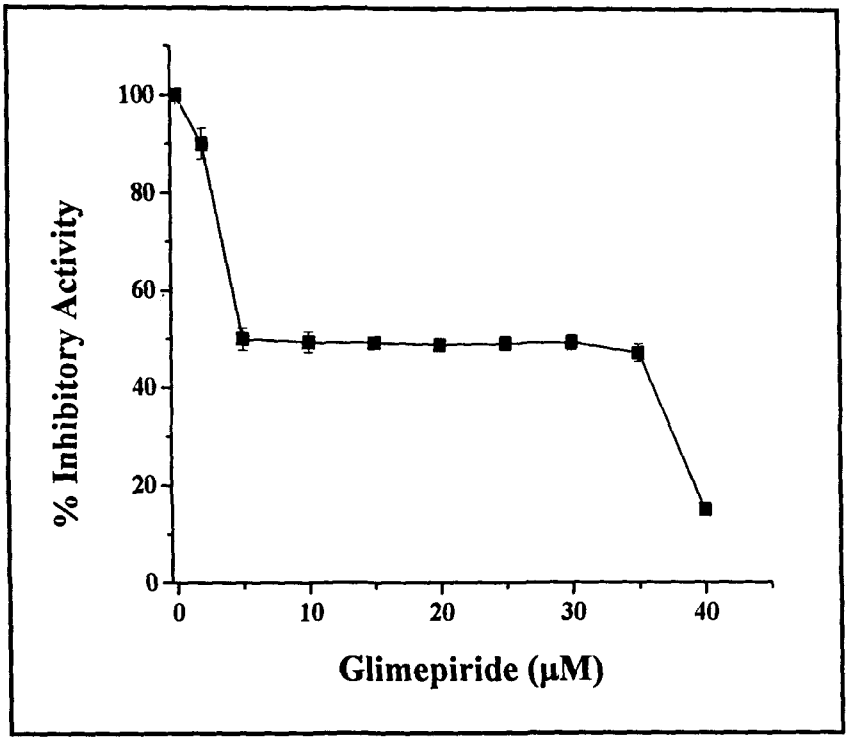
% Inhibitory Activity
100
80
60
40
20
0
0
10
20
30
40
Glimepiride (μM)

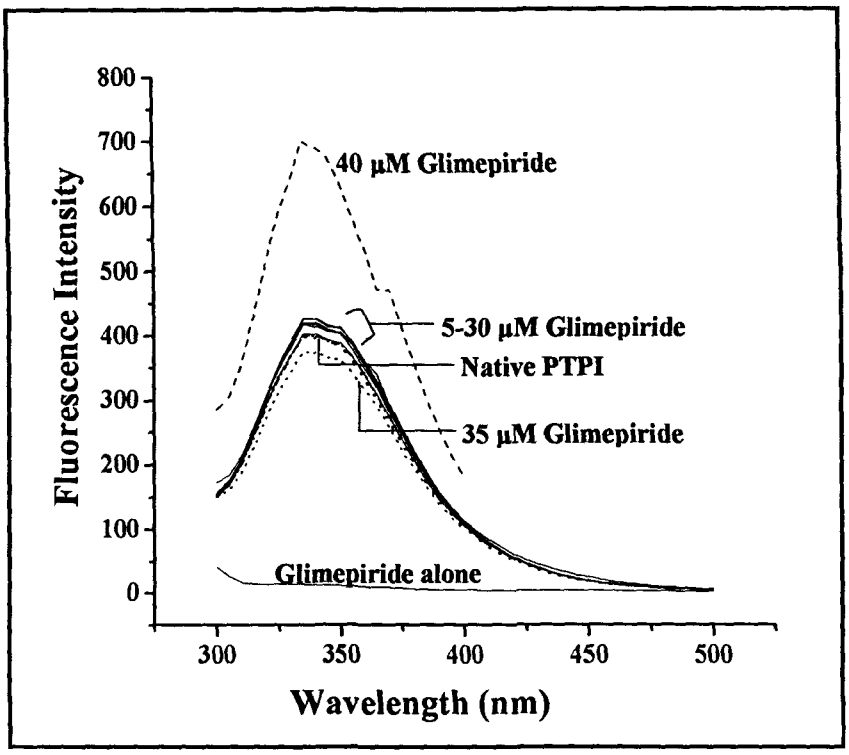
Fluorescence Intensity
800
700
600
500
400
300
200
100
0
40 μM Glimepiride
5-30 μM Glimepiride
Native PTPI
35 μM Glimepiride
Glimepiride alone
300
350
400
450
500
Wavelength (nm)

concentration is shown in Fig. 79. An intense negative peak was observed at 220 nm, a broad shoulder at 260 nm and a small negative peak at 280 nm. The difference spectra obtained at all other glimepiride concentrations showed small peaks in the region of 210-230 nm only. No changes were evidenced in the conformation of PTPI in the presence of drug in PAGE (results not shown).

3.5.3 INTERACTION OF PTPI WITH METFORMIN HYDROCHLORIDE

Another antidiabetic drug, metformin hydrochloride the only representative of the biguanide class, was also analyzed for its interaction with PTPI. 2 μM PTPI was incubated with increasing concentrations of the drug (2-12 μM) in 50 mM sodium phosphate buffer pH 7.5 at room temperature for 30 min. The effect of drug on antiproteolyitc potential of PTPI was determined by inhibition of caseinolytic activity of papain [Kunitz, 1947]. The activity of native PTPI was taken to be 100%. There was a gradual decline in PTPI activity with increasing drug concentration culminating to a 60% loss at 12 μM metformin hydrochloride. Progressive decline of ~20% each in activity of PTPI was observed at 2 μM and 4 μM concentrations of the drug, respectively. Further magnitude of decline was relatively smaller with increasing drug concentration. In contrast to sodium valproate and glimepiride, even at 12 μM metformin hydrochloride the inhibitor retained 40% of its antiproteolytic potential [Fig. 80].

The impact of drug interaction on structure of PTPI was also explored by fluorescence and UV-vis spectroscopy. PTPI treated in similar manner as for the activity measurements was subjected to fluorescence spectroscopic analysis. Fig. 81 illustrates the results obtained. λ_{max} of emission remained unaltered at all drug concentrations. There was little increment in fluorescence intensity in comparison to untreated PTPI. In a similar fashion, on subjection to UV-vis spectroscopy and PAGE no significant changes were observed on PTPI (results not shown).

Fig. 79 UV-Absorption difference spectra measured for PTPI-glimepiride complexes

PTPI (2 μM) was incubated with glimepiride (2-40 μM) for 30 min and absorbance difference spectrum was calculated between 200 nm to 320 nm. Results are shown for complex obtained at 40 μM glimepiride.

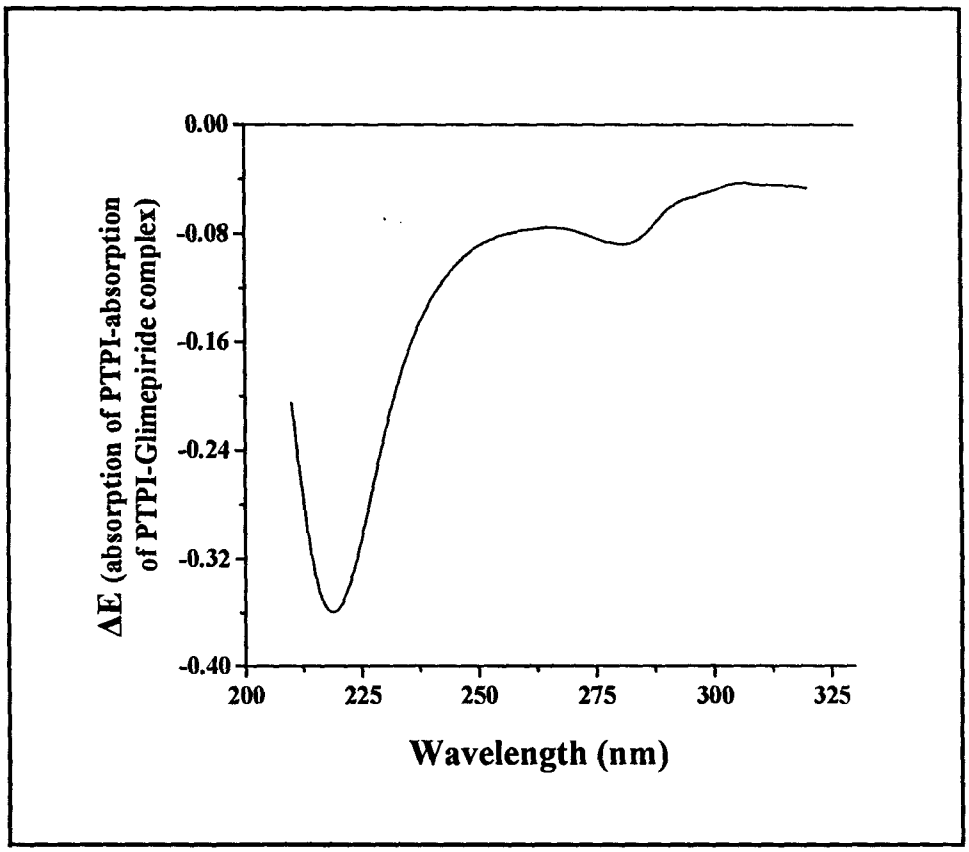
0.00
-0.08
-0.16
-0.24
-0.32
-0.40
200
225
250
275
300
325
ΔE (absorption of PTPI-absorption of PTPI-Glimepiride complex)
Wavelength (nm)

Fig. 80 Effect of metformin hydrochloride complexation on activity of PTPI

Native PTPI (2 μM) was incubated with increasing concentration of metformin hydrochloride (2-12 μM) for 30 min at room temperature. PTPI was assayed for loss of antiproteinase activity by caseinolytic assay of Kunitz [1947]. Values are Mean ± SEM for four independent determinations. *Significantly different from native PTPI (control) at $p < 0.05$ by one way ANOVA.

Fig. 81 Intrinsic fluorescence analysis of PTPI on interaction with various concentrations of metformin hydrochloride

The concentration of PTPI was 2 μM. PTPI was incubated for 30 min at room temperature in 50 mM sodium phosphate buffer (pH 7.5) containing the increasing concentration of metformin (2-12 μM). Fluorescence was measured at an excitation wavelength of 280 nm and emission range of 300-400 nm with slitwidth of 5 nm.

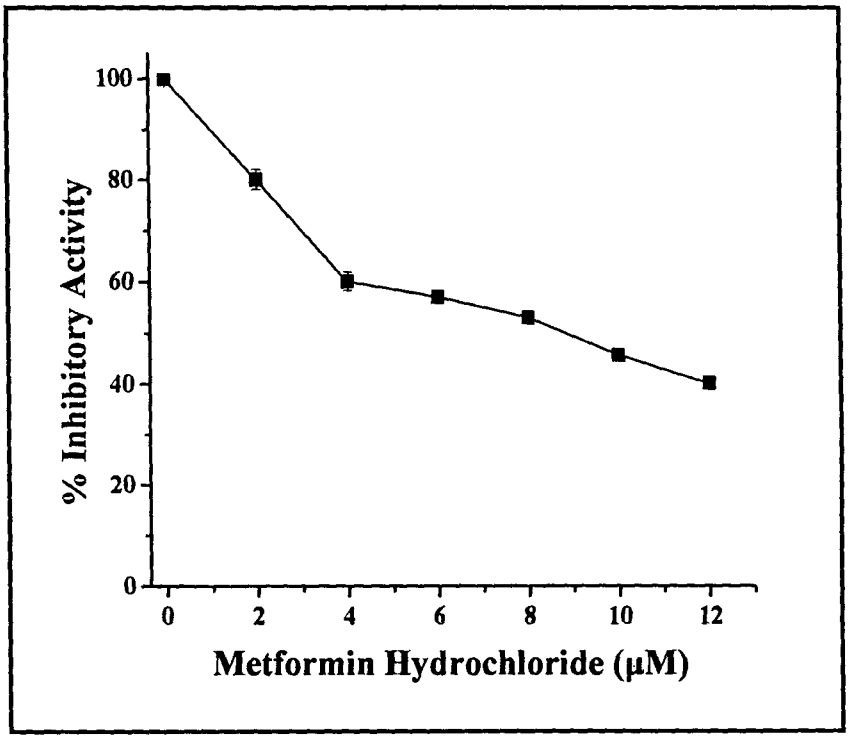
% Inhibitory Activity
100
80
60
40
20
0
0
2
4
6
8
10
12
Metformin Hydrochloride (μM)

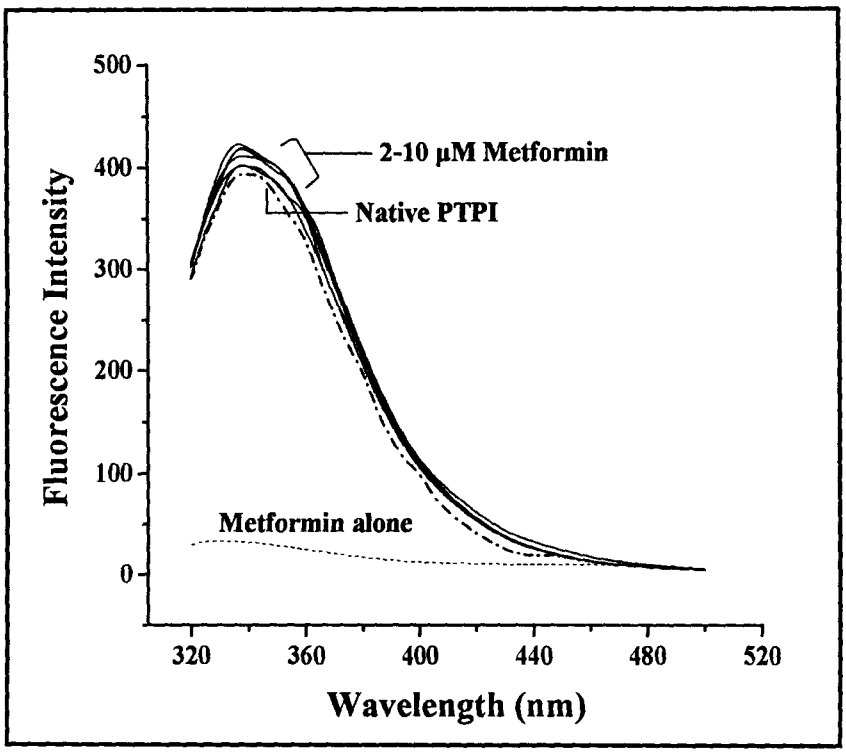
Fluorescence Intensity
500
400
300
200
100
0
2-10 μM Metformin
Native PTPI
Metformin alone
320
360
400
440
480
520
Wavelength (nm)

3.5.4 INTERACTION OF PTPI WITH INSULIN

Insulin is released from pancreas in response to body glucose levels indirectly regulating protein, carbohydrate and lipid metabolism and acting as a switch between carbohydrate and lipid metabolism. Improper insulin production causes diabetes mellitus/hyperinsulinism. Since, the introduction of insulin in the 1920s as a treatment for diabetes [Banting and Best, 1990], it is considered to be the most effective treatment for Type 1 and Type 2 diabetes.

Antihyperglycemic agent, proteinic in nature, recombinant insulin's interaction with PTPI was also investigated. 2 μM PTPI was incubated with monocomponent Huminsulin R, in inhibitor to insulin ratios of 1:1-1:10 in 50 mM sodium phosphate buffer pH 7.5 at room temperature for 30 min. The treated PTPI samples were subjected to fluorescence, UV-vis and CD spectroscopy (in the far UV region); to assess changes in the structure of PTPI induced upon complexation with Huminsulin R. The results of fluorescence are shown in Fig. 82. The insulin showed maximum emission at 304 nm and PTPI alone gave a λ_{max} of 335 nm [Priyadarshini and Bano, 2009]. At 1:1 molar ratio of PTPI to insulin, the λ_{max} was red shifted to 345 nm, with considerable enhancement in fluorescence intensity, with respect to PTPI or insulin alone. At a molar ratio of 1:2 of PTPI to insulin, 2 peaks were observed, one specific for insulin at 304 nm and other at 340 nm. At molar ratios lower than 1:1, λ_{max} of 345 nm was observed.

UV absorbance spectra of PTPI, insulin and their complexes are shown in Fig. 83. PTPI and insulin like other proteins showed peaks in regions of 200-210 nm and 278-280 nm. On complexation profound changes were introduced. At 1:1 molar ratio all peaks were abolished with a broad plateau in the range of 200-300 nm, with considerably enhanced absorbance. At 1:2 ratio the peak at 275 nm of lone proteins was shifted to 260 nm. At ratios, 1:4 to 1:10, the peak was again red shifted to 273-275 nm with considerable increment in absorbance.

To examine the effect of complexation on secondary structure of PTPI, the complexes were subjected to CD spectroscopy in the far UV region. For CD experiments, following molar ratios of PTPI:insulin were used, 1:05, 1:0.25, 1:0.5, 1:1 and 1:2. The spectrum of PTPI alone is characterized by a minimum at 222 nm [Priyadarshini and Bano, 2009]. Insulin gave two negative minima at 210 and 222 nm [Fig. 84]. On complexation a gradual increase in ellipticity at 222 nm was observed.

Fig. 82 Intrinsic fluorescence analysis of PTPI on interaction with various concentrations of insulin

The concentration of PTPI was 2 μM. PTPI was incubated for 30 min at room temperature in 50 mM sodium phosphate buffer (pH 7.5) with insulin in various molar ratios of PTPI to insulin (1:1 to 1:10). Fluorescence was measured at an excitation wavelength of 280 nm and emission range of 300-400 nm with slitwidth of 5 nm.

Fig. 83 Absorption spectra of PTPI-insulin complexes

The concentration of PTPI was 2 μM. PTPI was incubated for 30 min at room temperature in 50 mM sodium phosphate buffer (pH 7.5) with insulin in various molar ratios of PTPI to insulin (1:1 to 1:10). Absorbance was taken from 200 to 320 nm.

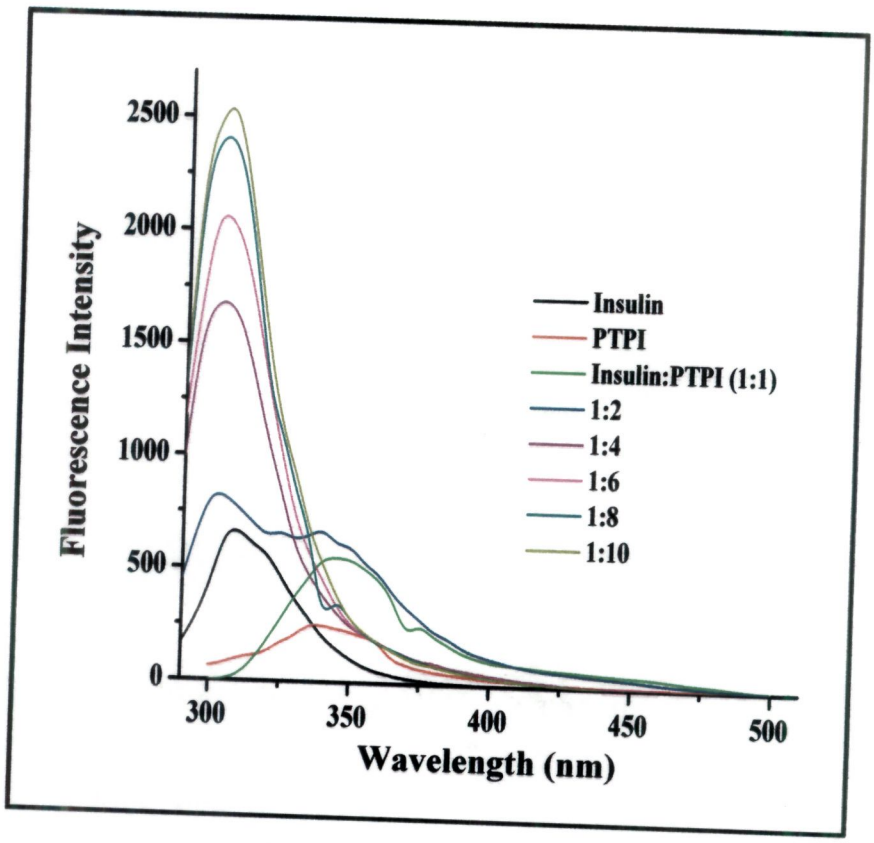
Fluorescence Intensity
2500
2000
1500
1000
500
0
300
350
400
450
500
Wavelength (nm)
Insulin
PTPI
Insulin:PTPI (1:1)
1:2
1:4
1:6
1:8
1:10

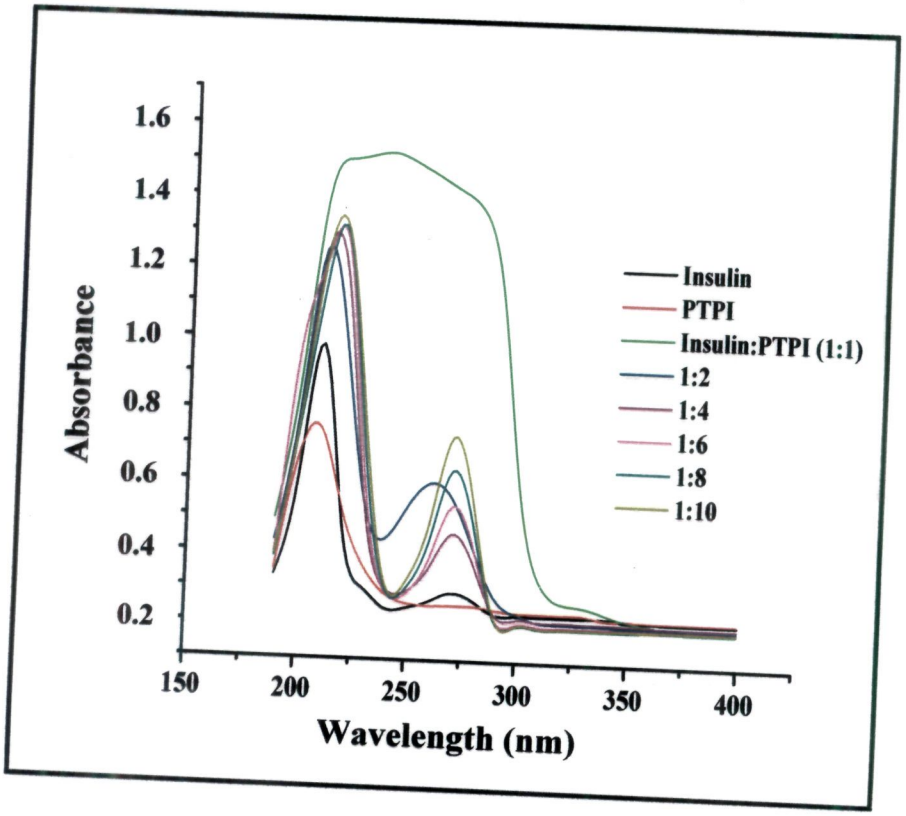
Absorbance
1.6
1.4
1.2
1.0
0.8
0.6
0.4
0.2
150
200
250
300
350
400
Wavelength (nm)
Insulin
PTPI
Insulin:PTPI (1:1)
1:2
1:4
1:6
1:8
1:10

Fig. 84 Far UV-CD Spectra of PTPI in complex with insulin

Far UV-CD spectra of PTPI and insulin alone and insulin-PTPI complexes. The concentration of PTPI was 1.73 μM and PTPI and insulin molar ratios were 1:0.05 to 1:2. The complexes were obtained after incubation at room temperature for 30 minutes in 50 mM sodium phosphate buffer, pH 7.5. Cells of 1 mm path length were used. The unit on the ordinate is mean residue ellipticity.

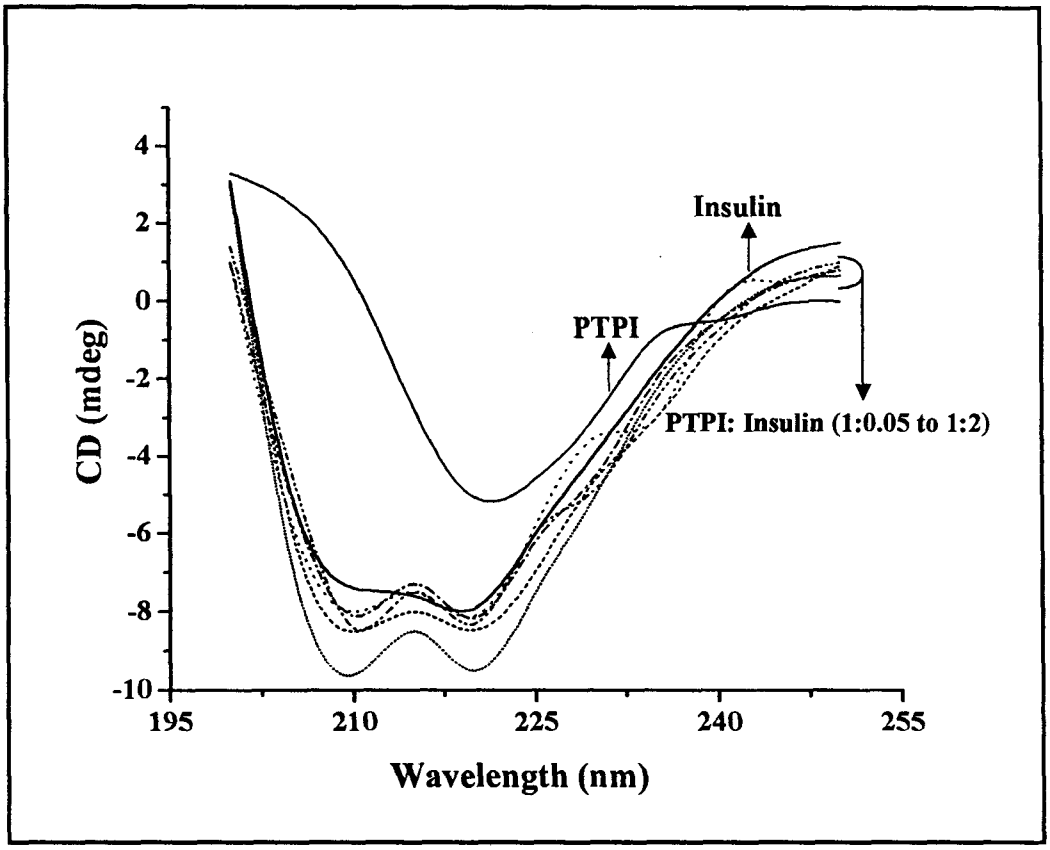
CD (mdeg)
4
2
0
-2
-4
-6
-8
-10
195
210
225
240
255
Wavelength (nm)
Insulin
PTPI
PTPI: Insulin (1:0.05 to 1:2)

Discussion

Chapter 5

DISCUSSION

Proteins are complex macromolecules that can adopt a large number of slightly different conformations within their native state, called conformational substrates. Even small structural differences between these substrates can lead to drastic changes in functional parameters. In addition, the marginal stability of the native conformation is delicate balance of various interactions in proteins (van der Waals, electrostatic, hydrogen bonds and disulphide bridges) [Sneppen and Zocchi, 2005] which is affected by pH, temperature or addition of small molecules such as substrates, coenzymes, inhibitors and activators that bind especially to the native state and alters this fragile equilibrium. In this regard, many drugs exert their activity by interaction with proteins.

Drug accumulation at off-target sites in body, lead to unintended off-target adverse reactions [Taniguchi et al., 2007; Scheiber et al., 2008] and drug/ligand induced protein structure conformational alterations [Takeda et al., 1988] are prime problems complicating drug medical therapy.

Numerous drugs have been implicated in the etiology of acute pancreatitis (referred to as drug induced pancreatitis), but reports unravelling its mechanism are sparse [Dhir et al., 2007]. Use of valproic acid (an antiepileptic agent) is associated with an elevated risk estimate for acute pancreatitis besides being incriminated as a potentially fatal hepatotoxic and teratogenic agent [Norgaard et al., 2006; Werlin and Fish, 2006]. Generally, no relationship between the occurrence of pancreatitis and duration of sodium valproate therapy, dosage, serum level, and the use of other anticonvulsants has been found [Werlin and Fish, 2006].

Commonly prescribed antidiabetic drugs are sulfonylureas (glimepiride) and biguanides (metformin), the former act by increasing the insulin release from the β cells of the pancreas and insulin sensitivity in peripheral cells and the latter by decreasing hepatic glucose production and increasing peripheral glucose uptake and use. Sulphonylureas are considered to cause β cell apoptosis, induce nitric oxide generation and reactive species production [Ansar and Ansari, 2006; Sawada et al., 2008]. Synthetic insulin is another commonly prescribed hypoglycemic agent.

Almost all the specific drugs have some side or adverse effects. Thus, study aimed at investigating the effects of above four drugs on purified goat pancreatic thiol proteinase inhibitor. Inclination for this study sprouted up as PTPI is shown to have

anti thiol proteinase activity. Cathepsin mediated trypsinogen activation is one of the initiator points of acute pancreatitis [Thrower et al., 2006; van Acker et al., 2002]. Also, insulin degradation is mediated probably by lysosomes [Sandberg and Borg, 2006]. Thiol proteinase inhibitors /cystatins serve as the main endogenous regulators of lysosomal cathepsins [Turk et al., 2008].

To assess the effect of interaction of these drugs on functional integrity of PTPI, the purified inhibitor was incubated with increasing concentrations of VPA/ glimepriride/ metfromin hydrochloride and its antiproteolytic potential was determined. Estimation of protein activity provides a sensitive means to monitor the effect of ligands on the protein as even minute changes in active site region can considerably affect the protein function. VPA diminished the activity of PTPI with almost complete inactivation of the inhibitor at higher concentration [Fig. 74] within a short span of time. Glimepiride induced inhibitor inactivation was less drastic. Considerable activity (~50%) was retained by PTPI till 30 μM drug concentration. Even at maximum concentration of the drug (40 μM) PTPI possessed 15% activity [Fig. 77]. Metformin hydrochloride was milder in inflicting inactivation on PTPI [Fig. 80]. Drug induced inactivation (functional derangement) of proteins has been reported earlier like horse liver alcohol dehydrogenase (ADH) activity was affected differentially by various drugs. Few like barbital, caffeine and diazepam exerted no effect, chlorpromazine, sulpiride, morphine etc. reduced the activity and phenytoin enhanced ADH activity [Roig et al., 1991]. Absence of any major drug induced conformational change in PTPI structure (as discussed later), suggest that inactivation of the inhibitor may be related to subtle changes in the conformation at the active site region induced by the drugs. Similar ligand binding induced functional changes have been shown for isocitrate dehydrogenase [Serry and Farrell Jr., 1990].

Intrinsic fluorescence of proteins provides considerable information about protein structure and dynamics and has been used extensively to study protein folding and association reactions [Lakowicz, 2006]. Various measurable parameters of fluorescence viz. quenching, enhancement of intensity, spectral shift etc. are used for interpretation of related structure-dynamics in proteins [Lakowicz, 2006]. In the present study, fluorescence spectroscopic measurements were undertaken to gain insight into the interaction and complexation of VPA, glimepiride, metformin hydrochloride and insulin with PTPI [Figs. 75, 78, 81 and 82]. In the presence of all these drugs, fluorescence intensity increased (though not profoundly) except for 2 μM

VPA and 35 μM glimepiride. Such a kind of change has been documented earlier. Interaction of ligands (phytohormones, cytokinins, abscisic and gibberellic acids) with wheat germ agglutinin resulted in ~60% increase in fluorescence intensity of native protein [Bogoeva et al., 2004]. Fluorescence enhancement of α1 antitrypsin on interaction with heparin and glucose has also been reported [Finotti and de Laureto, 1997]. Except for PTPI-insulin complexation, no shift in λ_{max} was noted. A 10 nm red shift was observed on formation of equimolar complex of insulin and PTPI, indicating exposure of aromatic residues to the solvent caused by conformational rearrangement of the two proteins [Monsellier and Bedouelle, 2005; Vivian and Callis, 2001]. When PTPI-insulin ratio was 1:2, there was a blue shift of 5 nm, suggestive of a change in environment of tryptophan residues to non polar.

Absorption spectral measurements of PTPI in the presence of drugs provided information related to their interaction. Difference spectra were computed by subtracting the absorption of PTPI-drug complex from the absorption of PTPI alone, for VPA/ glimepiride-PTPI complexes [Fig. 76 and 79]. The intense negative peaks at 210 and 215 nm observed for PTPI-VPA complexes obtained at 6 and 20 μM VPA concentrations, respectively may contain contributions from phenylalanine and histidine residues [Donovan, 1969]. The broad shoulders observed at 260 nm are also due to phenylalanine and may contain contribution form tryptophan [Donovan, 1969]. The peaks observed at 255 and 295 nm indicate the involvement of aromatic residues in interaction. A negative peak noticeable at 275 nm in difference spectra obtained at 6 μM VPA, suggest changes around tyrosine residues [Donovan, 1973a]. For the difference spectra obtained at 2 μM VPA, positive peaks at 230 nm and 285 nm might have the contribution of mainly tryptophan and tyrosine residues [Donovan, 1973a]. The negative peak at 275 nm and the difference peak at 295 nm are characteristic of blue shifts of tryptophan and tyrosine absorption bands and are usually interpreted as arising from increased exposure of these aromatic groups to the solvent [Donovan, 1969]. Difference spectra of glimepiride-PTPI complex at 40 μM glimepriride concentration, showed broad shoulder at 260 nm and a small negative peak at 280 nm, indicative of involvement of phenylalanine and tyrosine in complexation process.

The interaction between insulin-PTPI was studied from UV-vis absorption spectral data. Complex spectroscopic changes were noticed. Equimolar complex of PTPI and insulin showed only a broad absorption band in the region of 200-300 nm, suggesting that the native structure of both the proteins is altered on complexation. The blue shift

observed for 1:2 molar ratio, indicates the changes in the environment of tyrosine residues towards hydrophobic. At higher ratios, shift of spectra towards longer wavelengths was observed. These evidences clearly indicated the interaction and some complex formation between insulin and PTPI [Cui et al., 2004; Hu et al., 2004]. Similar changes have also been shown for UV-vis absorption spectra of horse myoglobin on interaction with phenothiazines promazine and triflupromazine hydrochlorides [Cheema et al., 2008].

Alterations in secondary structure of PTPI on complexation with insulin were also analyzed by CD spectroscopy. Two negative absorbance peaks at 210 and 222 nm for insulin alone and at 222 nm for PTPI alone, are typical peaks of α helix [Fig. 84]. Slight enhancement in ellipticity at 222 nm was observed for all molar ratios of PTPI-insulin, suggesting that binding of insulin to PTPI increased the α helical content of PTPI. Such enhanced ellipticity has also been reported for binding of ferulic acid to cytochrome C [Yang et al., 2007].

When drugs bind to a globular protein, the intramolecular forces responsible for maintaining the secondary and tertiary structures can be altered, resulting in conformational change of the protein [Salvi et al., 2001]. Such conformational changes of varied magnitude have been reported [Guo et al., 2004a; Cheema et al., 2008; Ahmed-Ouameur et al., 2006]. Thus, the results indicate that the UV absorption and fluorescence emission changes on VPA, glimepiride and metformin hydrochloride mediated interaction, are due to minor conformational changes in PTPI and mainly arise from local interactions affecting the chromophoric groups of the protein. While in case of insulin-PTPI interaction, conformational rearrangement might have occurred.

Drug induced changes in enzyme activities as their adverse effects have been an area of continual scientific investigation [Priyamvada et al., 2008]. Limited number of reports is available on effects of drugs on purified tissue proteins which do not function as carriers but are putative targets of the drug induced side effects or whose structural and functional modifications aid in drug mediated damage or are critical for the off-target tissue. This study has tried to explore the effects of few drugs on purified pancreatic thiol proteinase inhibitor. The drugs chosen are either incriminated or prescribed in pancreatic pathologies and thiol proteinase inhibitors are prime regulators of lysosomal cathepsins [Bohley et al., 1978].

On complexation with VPA (a pancreatitis causing drug) PTPI activity was severely challenged suggesting cathepsin inactivation might be one of the factors in VPA induced pancreatitis. Glimepiride causes β cell apoptosis [Ansar and Ansari, 2006]. These antidiabetic agents are also known to cause nitric oxide and reactive oxygen species production in pancreas [Sawada et al., 2008]. PTPI function was also compromised on interaction with these two drugs though it was less severe with metformin. Functional insulin receptors are known to occur in pancreatic β cells. Studies have shown that exogenous insulin in the presence or absence of nonstimulatory concentrations of glucose evokes exocytosis mediated by the β cell insulin receptor. This autocrine action of insulin diminishes as the concentration of free insulin on cell surface decreases or receptors get blocked [Aspinwall et al., 1999]. Cystatin β has been found to be colocalized with cathepsin in insulin secretory granules in rat pancreas [Watanabe et al., 1988]. In the present work complexation with insulin increased the α helical content of PTPI. Thus it may be speculated that this increase in the native stability of the inhibitor on complexation with (exogenous) insulin, may allow more efficient regulation of cathepsin activity under diseased states and thus preventing insulin degradation.

The possible implications of these results would be on designing therapeutic agents managing VPA induced pancreatitis, understanding of non responsiveness to antidiabetic agents after a period and provide a clue to increase insulin potency.

Conclusion

[IV] CONCLUSION

The results obtained are important as,

1. Isolation and purification of thiol proteinase inhibitors from specific tissue types would provide an insight into the in vivo regulation of the target proteinases. Studies delving into proteinases-PTPI interaction would possibly be informative for design of pharmacologically active synthetic inhibitors against cysteine proteinase/inhibitor malfunctioning derived pancreatic disorders.

2. The conformational stability of the native proteins is a function of external variables, such as, temperature, pH, ionic strength and solvent composition. Studies that delve into the structural and functional properties of the proteins in response to various externally imposed conditions thus provide a good approximation of their conformational stabilities.

3. Evidence for PTPI's susceptibility to fibrillate under experimentally induced conditions suggests that damage instigated by thiol proteinase inhibitor generated fibrils can't be ruled out in various pancreatic disorders. Prevention of fibrillation by copper and zinc point to the emerging possibilities against formation amyloid fibrils.

4. With the known proclivity of pancreas towards oxidative damage and disturbed protease-inhibitor balance in the inflammatory processes, PTPI's vulnerability to oxidative/nitrosative stress was expected. However, the benefiting effects of flavonoids obtained in the data against radical/oxidant mediated damage suggest a positive role of natural antioxidant supplementation in slowing down severity of pancreatitis or free radical induced diabetic complications. These results are further consequential as they suggest alternate, cost effective and safe therapy against free radical induced damage.

5. Sodium valproate induced loss of function change in the inhibitor could provide a rationale for the off target tissue injury caused by the drugs and for the design of agents against such an injury. Action of glimepiride and metformin on inhibitor point towards the mechanism that might be responsible for islet cell damage and hence to non responsiveness to these drugs on prolonged intake. Also, as in case of insulin, such studies provide a clue for enhancing drug potency.

Bibliography

[V] BIBLIOGRAPHY

Aagaard A, Listwan P, Cowieson N, Huber T, Ravasi T, et al. *Struct (Camb)* 2005; **13**:309-317.

Abe M, Abe K, Kuroda M and Arai S. *Eur J Biochem* 1992; **209**:933-937.

Abrahamson M, Alvarez-Fernandez M and Nathanson CM. *Biochem Soc Symp* 2003; **70**:179-199.

Abrahamson M, Barrett AJ, Salvesen G and Grubb A. *J Biol Chem* 1986; **261**:11282-11289.

Abrahamson M, Grubb A, Olafsson I and Lundwall A. *FEBS Lett* 1987a; **216**:229-233.

Abrahamson M, Ritonja A, Brown MA, Grubb A, Machleidt W, et al. *J Biol Chem* 1987b; **262**:9688-9694.

Agarwala KL, Kawabata S, Hirata M, Miyagi M, Tsunasawa S, et al. *J Biochem Tokyo* 1996; **119**:85-94.

Aggarwal BB, Sundaram C, Malani N and Ichikawa H. *Adv Exp Med Biol* 2007; **595**:1-75.

Aggeli A, Nyrkova IA, Bell M, Harding R, Carrick L, et al. *Proc Natl Acad Sci USA* 2001; **98**:11857-11862.

Aghajanyan HG, Arzumanyan AM, Arutunyan AA and Akopyan TN. *Neurochem Res* 1988; **13**:721-727.

Aguiar JM, Franco OL, Rigden DJ, Bloch C Jr, Monteiro AC, et al. *Proteins* 2006; **63**:662-670.

Ahmad A, Uversky VN, Hong D and Fink AL. *J Biol Chem* 2005; **280**:42669-42675.

Ahmad B and Khan RH. *J Biochem* 2006; **140**:501-508.

Ahmed-Ouameur A, Diamantoglou S, Sedaghat-Herati MR, Nafisi S, Carpentier R, et al. *Cell Biochem Biophys* 2006; **45**:203-213.

Ahuja S, Ahuja-Jensen P, Johnson LE, Caffe AR, Abrahamson M, et al. *Invest Ophthalmol Vis Sci* 2008; **49**:1089-1096.

Akhtar MS, Ahmad A and Bhakuni V. *Biochemistry* 2002; **41**:3819-3827.

Alber T. *Annu Rev Biochem* 1989; **58**:765-798.

Ali N, Upreti RK, Srivastava LP, Misra RB, Joshi PC, et al. *Indian J Exp Biol* 1991; **29**:818-822.

Aliberti J, Viola JP, Vieira-de-Abreu A, Bozza PT, Sher A, et al. *J Immunol* 2003; **170**:5349-5353.

Alvarez-Fernandez M, Barrett AJ, Gerhartz B, Dando PM, Ni J, et al. *J Biol Chem* 1999; **274**:19195-19203.

Alvarez-Fernandez M, Liang YH, Abrahamson M and Su XD. *J Biol Chem* 2005; **280**: 18221-18228.

Al-Wakeel JS, Hammad D, Memon NA, Tarif N, Shah I, et al. *Saudi J Kidney Dis Transpl* 2009; **20**:227-231.

Anastasi A, Brown MA, Kembhavi AA, Nicklin MJH, Sayers CA, et al. *Biochem J* 1983; **211**:129-138.

Andersson NE, Rydengard V, Mörgelin M and Schmidtchen A. *J Biol Chem* 2005; **280**:34832- 34839.

Andreae WA. *Nature* 1955; **175**:859-860.

Andrews P. *Biochem J* 1964; **91**:222-233.

Ansar MM and Ansari M. *Nitric Oxide* 2006; **14**:39-44.

Ansorge S, Kirschke H and Friedrich K. *Acta Biol Med Ger* 1977; **36**:1723-1727.

Arai S, Matsumoto I, Emori Y and Abe K. *J Agric Food Chem* 2002; **50**:6612-6617.

Artigues A, Iriarte A and Martinez-Carrion M. *J Biol Chem* 1994; **269**:21990-21999.

Asboth B, Mayer Z and Polgar L. *FEBS Lett* 1988; **233**:339-341.

Aspinwall CA, Lakey JR and Kennedy RT. *J Biol Chem* 1999; **274**:6360-6365.

Assfalg-Machleidt I, Jochun M, Klaubert W, Inthorn D and Machleidt W. *Biol Chem Hoppe-Seyler* 1988; **369**:263-269.

Atwood CS, Moir RD, Huang X, Scarpa RC, Bacarra ME, et al. *J Biol Chem* 1998; **273**:12817-12826.

Auchere F and Capeillere-Blandin C. *Free Radic Res* 2002; **36**:1185-1198.

Auerswald EA, Nagler DK, Schulze AJ, Engh RA, Genenger G, et al. *Eur J Biochem* 1994; **224**:407-415.

Baba SP, Patel DK and Bano B. *Free Radic Res* 2004; **38**:393-403.

Baba SP, Zehra S and Bano B. *The Protein J* 2005; **24**: 95-102.

Babior BM. *Am J Med* 2000; **109**:33-44

Balbin M, Hall A, Grubb A, Mason RW, Lopez-Otin C, et al. *J Biol Chem* 1994; **269**:23156-23162.

Banting FG and Best CH. *J Lab Clin Med* 1990; **115**:254-272.

Barrett AJ, Davies ME and Grubb A. *Biochem Biophys Res Commun* 1984; **120**:631-636.

Barrett AJ, Fritz H, Grubb A, Isemura S, Jarvinen M, et al. *Biochem J* 1986; **236**:312.

Barrett AJ, Rawlings ND and O' Brien EA. *J Struct Biol* 2001; **134**:95-102.

Barrett AJ, Rawlings ND and Woessner JF Jr (editors). *Handbook of Proteolytic Enzymes* (2nd edn.). Amsterdam: Academic, 2004.

Barrett AJ, Rawlings ND, Davies ME, Machleidt W, Salvesen G, et al. In: *Proteinase inhibitors*, Barrett AJ and Salvesen G (editors). Amsterdam: Elsevier, 1986; pp 515-569.

Barrett AJ. *Methods Enzymol* 1981; **80**:771-778.

Baum J, Simons BE Jr, Unger RH and Madison LL. *Diabetes* 1962; **11**:371-374.

Becker EM, Cardoso DR and Skibsted LH. *Eur Food Res Technol* 2005; **221**:382-386.

Beck IT and Sinclair DG (editors). The Exocrine pancreas proceedings of symposium held at Queen's University, Kingston, Ontario, Canada, June 1969; Churchill, London, 1971.

Beith J. *Bull Eur Physiopathol Respir* 1980; **16** (suppl):183-195.

Bergt C, Marsche G, Panzenboeck U, Heinecke JW, Malle E, et al. *Eur J Biochem* 2001; **268**:3523-3531.

Bever CT and Garver DW. *J Neurol Sci* 1995; **131**:71-73.

Bhakuni V. *Arch Biochem Biophys* 1998; **357**:274-284.

Bjork I and Ylinenjarvi K. *Biochemistry* 1990; **29**:1770-1776.

Bjork I, Alriksson E and Ylinenjarvi K. *Biochemistry* 1989; **28**:1568-1573.

Bjork I, Pol E, Raub-Segall E, Abrahamson M, Anddrew R, et al. *Biochem J* 1994; **299**:219-225.

Bjork J, Peterson BA and Sjoquert J. *Eur J Biochem* 1972; **29**:579-584.

Blackburn MN and Noltmann EN. *Arch Biochem Biophys* 1981; **212**:162-169.

Blaise GA, Gauvin D, Gangal M and Authier S. *Toxicology* 2005; **208**:177-192.

Blank EMF, Henskens YM, Van't H, Veerman EC and Nieuw AV. *Biol chem* 1996; **377**:847-850.

Bode W, Engh R, Musil D, Thiele U, Huber R, et al. *EMBO J* 1988; 7:2593-2599.

Bogoeva VP, Radeva MA, Atanasova LY, Stoitsova SR and Boteva RN. *Biochim Biophys Acta* 2004;**1698**:213-218.

Bohley P, Kirschke H, Langer J, Riemann S, Wiederanders B, et al. In: *Protein turnover and lysosomal function*, Segal HL and Doyle D (editors). New York: Academic Press, 1978; pp 379-391.

Bowden CL and Singh V. *Acta Psychiatr Scand Suppl* 2005; **426**:13-20.

Bowie JU and Sauer RT. *Biochemistry* 1989a; **28**: 7139-7143.

Bowie JU and Sauer RT. *Proc Natl Acad Sci USA* 1989b; **86**:2152-2156.

Brahma A, Mandal C and Bhattacharyya D. *Biochim Biophys Acta* 2005; **1751**:159-169.

Brix K, Dunkhorst A, Mayer K and Jordans S. *Biochimie* 2008; **90**:194-207.

Brown DR, Qin K, Herms JW, Madlung A, Manson J, et al. *Nature* 1997; **390**:684-687.

Brown WM and Dziegielewska KM. *Protein Sci* 1997; **6**:5-12.

Brunelli L, Yermilov V and Beckman JS. *Free Radic Biol Med* 2001; **30**:709-714.

Brzin J and Kidric M. *Biotechnol Genet Eng Rev* 1995; **13**:420-467.

Brzin J, Kopitar M, Locnikar P and Turk V. *FEBS Lett* 1982; **138**:193-197.

Brzin J, Kopitar M, Turk V and Machleidt W. *Hoppe-Seylers Z Physiol Chem* 1983; **364**:1475-1480.

Brzin J, Popovic T, Turk V, Borchart U and Machleidt W. *Biochem Biophys Res Commun* 1984; **118**:103-109.

Brzin J, Rogelj B, Popovic T, Strukelj B and Ritonja A. *J Biol Chem* 2000; **275**: 20104-20109.

Bucciantini M, Calloni G, Chiti F, Formigli L, Nosi D, et al. *J Biol Chem* 2004; **279**:31374-31382.

Buck M, Radford SE and Dobson CM. *Biochemistry* 1993; **32**:669-678.

Buffa R, Capella C, Solcia E, Frigerio B and Said SI. *Histochemistry* 1977; **50**:217-227.

Buhling F, Fengler A, Brandt W, Welte T, Ansorge S, et al. *Adv Exp Med Biol* 2000; **477**:241-254.

Burstein EA, Vedenkina NS and Ivkova MN. *Photochem Photobiol* 1973; **18**:263-279.

Butler EA and Flynn FV. *J Clin Pathol* 1961; **14**:172-178.

Buttle DJ, Burnett D and Abrahamson M. *Scand J Clin Lab Invest* 1990; **50**:509-516.

Cardoso DR, Olsen K, Moller JK and Skibsted LH. *J Agric Food Chem* 2006; **54**:5630-5636.

Castro L, Eiserich JP, Sweeney S, Radi R, et al. *Arch Biochem Biophys* 2004; **421**:99-107.

Cejka J and Fleischmann LE. *Arch Biochem Biophys* 1973; **157**:168-176.

Ceru S, Kokalj SJ, Rabzelj S, Skarabot M, Gutierrez-Aguirre I, et al. *Amyloid* 2008; **15**:147-159.

Cesaratto L, Vascotto C, Calligaris S and Tell G. *Ann Hepatol* 2004; **3**:86-92.

Chan MM, Adapala NS and Fong D. *Parasitol Res* 2005; **96**:49-56.

Chapman AL, Winterbourn CC, Brennan SO, Jordan TW and Kettle AJ. *Biochem J* 2003; **375**:33-40.

Cheema MA, Taboada P, Barbosa S, Gutierrez-Pichel M, Castro E, et al. *Colloids Surf B Biointerfaces* 2008; **63**:217-228.

Chen MS, Johnson B, Wen L, Muthukrishnan S, Kramer KJ, et al. *Protein Expr Purif* 1992; **3**:41- 49.

Chen YH, Yang JT and Martinez H. *Biochemistry* 1972; **11**:4120-4131.

Cheng T, Hitomi K, van Vlijmen-Willems IMJJ, de Jongh GJ, Yamamoto K, et al. *J Biol Chem* 2006; **281**:15893-15899.

Chiti F, Bucciantini M, Capanni C, Taddei N, Dobson CM, et al. *Protein Sci* 2001; **10**:2541-2547.

Chiti F, Webster P, Taddei N, Clark A, Stefani M, et al. *Proc Natl Acad Sci USA* 1999; **96**:3590-3594.

Choi EH, Kim JT, Kim JH, Kim SY, Song EY, et al. *Clin Chim Acta* 2009; **406**:45-51.

Choi SJ, Reddy SV and Devlin RD. *Cell Death Differ* 1994; **6**:1028-1042.

Chung MJ, Walker PA and Hogstrand C. *Aquat Toxicol* 2006; **80**:321-328.

Chung YB and Yang HJ. *Korean J Parasitol* 2008; **46**:183-186.

Chvanov M, Petersen OH and Tepikin A. *Philos Trans R Soc Lond B Biol Sci* 2005; **360**:2273-2284.

Cimerman N, Ksorok MD, Korant BD, Turk B and Turk V, et al. *Biol Chem Hoppe-Seyler* 1996; **377**:19-23.

Cobianchi L, Fornoni A, Pileggi A, Molano RD, Sanabria NY, et al. *Cell Transplant* 2008; **17**:559-566.

Colle A, Guinet R, Leclercq M and Manuel Y. *Clin Chim Acta* 1976; **67**:93-97.

Collins AR and Grubb A. *Oral Microbial immunol* 1998; **13**:59-61.

Cornwall GA and Hsia N. *Mol Cell Endocrinol* 2003; **200**:1-8.

Coskun O, Kanter M, Korkmaz A and Oter S. *Pharmacol Res* 2005; **51**:117-123.

Couthon F, Clottes E, Ebel C and Vial C. *Eur J Biochem* 1995; **234**:160-170.

Cox JL. *Front Biosci* 2009; **14**:463-474.

Crawford C. *Biochem J* 1987; **248**:589-594.

Cui FL, Fan J, Li JP and Hu ZD. *Bioorg Med Chem* 2004; **12**:151-157.

Davies KJ and Delsignore ME. *J Biol Chem* 1987; **262**:9908-9913.

Davies KJ, Delsignore ME and Lin SW. *J Biol Chem* 1987a; **262**:9902-9907.

Davies KJ, Lin SW and Pacifici RE. *J Biol Chem* 1987b; **262**:9914-9920.

Dawson TM, Dawson VL and Snyder SH. *Ann Neurol* 1992; **32**:297-311.

De Felice FG, Vieira MN, Meirelles MN, Morozova-Roche LA, Dobson CM, et al. *FASEB J* 2004; **18**:1099-1101.

Dean RT, Fu S, Stocker R and Davies MJ. *Biochem J* 1997; **324**:1-18.

Del Guerra S, Marselli L, Lupi R, Boggi U, Mosca F, et al. *J Diabetes Complications* 2005; **19**:60-64.

DeLa Cadena RA and Colman RW. *Trends Pharmacol Sci* 1991; **12**:272-275.

Delbridge ML and Kelly LE. *FEBS Lett* 1990; **274**:141-145.

Denicola A and Radi R. *Toxicology* 2005; **208**:273-288.

Denicola A, Batthyány C, Lissi E, Freeman BA, Rubbo H, et al. *J Biol Chem* 2002 ; **277**:932-936.

Devasagayam TP, Tilak JC, Boloor KK, Sane KS, Ghaskadbi SS, et al. *J Assoc Physicians India* 2004; **52**:794-804.

Dhillon N, Aggarwal BB, Newman RA, Wolff RA, Kunnumakkara AB, et al. *Clin Cancer Res* 2008; **14**:4491-4499.

Dhir R, Brown DK and Olden KW. *Drugs Today (Barc)* 2007; **43**:499-507.

Di Mascio P, Dewez B and Garcia CR. *Braz J Med Biol Res* 2000; **33**:11-17.

Ding TT and Harper JD. *Methods Enzymol* 1999; **309**:510-525.

Diop NN, Kidric M, Repellin A, Gareil M, d'Arcy-Lameta A, et al. *FEBS Lett* 2004; **577**:545-550.

Dobson CM. *Methods* 2004; **34**:4-14.

Dobson CM. *Nature* 2003; **426**:884-890.

Dobson CM. *Trends Biochem Sci* 1999; **24**:329-332.

Donovan JW. *J Biol Chem* 1969; **244**:1961-1967.

Donovan JW. *Methods Enzymol* 1973a; **27**:497-525.

Donovan JW. *Methods Enzymol* 1973b; **27**:525-548.

Droge W. *Physiol Rev* 2002; **82**:47-95.

Dubois M, Gilles MA, Hamilton JK, Rebers PA and Smith F. *Anal Chem* 1956; **28**:350-354.

Dziegielewska KM, Brown WM, Casey SJ, Christie DL, Foreman RC, et al. *J Biol Chem* 1990; **265**:4354-4357.

Dziegielewska KM, Mollgard K, Reynolds ML and Saunders NR. *Cell Tissue Res* 1987; **248**:33-41.

Dziegielewska KM and Brown WM. Molecular Biology Intelligence Unit, Landes RG Co., Texas, Int. Austin: Springer-Verlag, 1995.

Edman P and Begg G. *Eur J Biochem* 1967; **1**:80-91.

Eiserich JP, Hristova M, Cross CE, Jones AD, Freeman BA, et al. *Nature* 1998; **391**:393-397.

Ekiel I and Abrahamson M. *J Biol Chem* 1996; **271**:1314-1321.

Ekiel I, Abrahamson M, Fulton DB and Lindahl P. *J Mol Biol* 1997; **271**:266-271.

Ellman R. *Biochem Methods* 1959; **19**:446-451.

Elzanowski A, Barker WC, Hunt LT and Seibel-Ross E. *FEBS Lett* 1988; **227**:167-170.

Engel MFM, Khemte'mourian L, Kleijer CC, Meeldijk HJD, Jacobs J, et al. *Proc Natl Acad Sci USA* 2008; **105**:6033-6038.

Erickson HP. *Biophys J* 1982; **37**:96a.

Esnard F, Esnard A, Faucher D, Capony JP, Derancourt J, et al. *Biol Chem Hoppe Seyler* 1990; **371**:S161-S166.

Estrada S and Bjork I. *Protein Sci* 2000; **9**:2218-2224.

Estrada S, Pavlova A and Bjork I. *Biochemistry* 1999; **38**:7339-7345.

Evans HJ and Barrett AJ. *Biochem J* 1987; **246**:795-797.

Fandrich M and Dobson CM. *EMBO J* 2002; **21**:5682-5690.

Fandrich M, Fletcher MA and Dobson CM. *Nature* 2001; **410**:165-166.

Ferreira ST and De Felice FG. *FEBS Lett* 2001; **498**:129-134.

Feste A and Gan JC. *J Biol Chem* 1981; **256**:6374-6380.

Filipe P, Haigle J, Silva JN, Freitas J, Fernandes A, et al. *Eur J Biochem* 2004; **271**:1991-1999.

Filipek R, Rzychon M, Oleksy A, Gruca M, Dubin A, et al. *J Biol Chem* 2003; **278**: 40959-40966.

Findeis MA. *Biochim Biophys Acta* 2000; **1502**:76-84.

Finkelstadt JT. *Proc Soc Exp Biol Med* 1957; **95**:302-304.

Finotti P and de Laureto PP. *Arch Biochem Biophys* 1997; **347**:19-29.

Firuzi O, Mladenka P, Petrucci R, Marrosu G and Saso L. *J Pharm Pharmacol* 2004; **56**:801-807.

Fisher MT and Stadtman ER. *J Biol Chem* 1992; **267**:1872-1880.

Foghsgaard L, Wissing D, Mauch D, Lademann U, Bastholm L, et al. *J Cell Biol* 2001; **153**:999-1010.

Fossum K and Whitaker JR. *Arch Biochem Biophys* 1968; **125**:367-375.

Fraki JE. *Arch Dermatol Res* 1976; **255**:217-220.

Freiji JP, Abrahamson M, Olafsson I, Velasco G, Grubb A, et al. *J Biol Chem* 1991; **266**:20538-20543.

Fried LF. *Kidney Int* 2009; **75**:578-580.

Frokjaer S and Otzen DE. *Nat Rev Drug Delivery* 2005; **4**:298-306.

Gantchev TG and van Lier JE. *Photochem Photobiol* 1995; **62**:123-134.

Garrido F, Gasset M, Sanz-Aparicio J, Alfonso C and Pajares MA. *Biochem J* 2005; **391**:589-599.

Garrison WM. *Chem Rev* 1987; **87**:381-398.

Gerstner T, Büsing D, Bell N, Longin E, Kasper JM, et al. *J Gastroenterol* 2007; **42**:39-48.

Ghafourifar P and Cadenas E. *Trends Pharmacol Sci* 2005; **26**:190-195.

Ghafourifar P, Schenk U, Klein SD and Richter C. *J Biol Chem* 1999; **274**:31185-31188.

Gocheva V and Joyce JA. *Cell Cycle* 2007; **6**:60-64.

Gocheva V, Zeng W, Ke D, Klimstra D, Reinheckel T, et al. *Genes Dev* 2006; **20**:543-556.

Goldsbury CS, Cooper GJ, Goldie KN, Muller SA, Saafi EL, et al. *J Struct Biol* 1997; **119**:17-27.

Gotz J, Ittner LM and Lim YA. *Cell Mol Life Sci* 2009; **66**:1321-1325.

Gounaris AD, Brown MA and Barrett A J. *Biochem J* 1984; **218**:939-946.

Goyal L. *Cell* 2001; **104**:805-808.

Graf WD, Oleinik OE, Glauser TA, Maertens P, Eder DN, et al. *Neuropediatrics* 1998; **29**:195-201.

Grant SK, Deckman IC, Culp JS, Minnich MD, Brooks IS, et al. *Biochemistry* 1992; **31**:9491-9501.

Green GDJ, Kembhavi AA, Davies ME and Barrett AJ. *Biochem J* 1984; **218**: 939-946.

Green LC, Wagner DA, Glogowski J, Skipper PL, Wishnok JS, et al. *Anal Biochem* 1982; **126**:131-138.

Greenberger NJ, Toskes PP. *Acute and chronic pancreatitis.* Harrison's online. 2006; Available:www.accessmedicine.com

Grubb A, Lofberg H and Barrett AJ. *FEBS Lett* 1984; **170**:370-374.

Grudzielanek S and Smirnovas V and Winter R. *J Mol Biol* 2006; **356**:497-509.

Grzonka Z, Jankowska E, Kasprzykowski F, Kasprzykowska R, Lankiewicz L, et al. *Acta Biochim Pol* 2001; **48**:1-20.

Gulcin I. *Toxicology* 2006; **217**:213-220.

Guncar G, Klemencic I, Turk B, Turk V, Karaoglanovic-Carmona A, et al. *Structure* 2000; **8**:305-313.

Guncar G, Podobnik M, Pungercar J, Strukelj B, Turk V, et al. *Structure* 1998; **6**:51-61.

Guo M, Jian-Wei Z, Ping-Gui YI, Zhi-Cai S, Gui-Xiang H, et al. *Anal Sci* 2004a; **20**:465-470.

Guo Q, Zhao F, Guo Z and Wang X. *J Biochem* 2004b; **136**:49-56.

Gupta P, Khan RH and Saleemuddin M. *Arch Biochem Biophys* 2003; **413**:199-206.

Hagihara Y, Tan Y and Goto Y. *J Mol Biol* 1994; **237**:336-348.

Halangk W, Lerch MM, Brandt-Nedelev B, Roth W, Ruthenbuerger M, et al. *J Clin Invest* 2000; **106**:773-781

Halfon S, Ford J, Foster J, Dowling L, Lucian L, et al. *J Biol Chem* 1998; **273**:16400-16408.

Halliwell B and Gutteridge JMC. *Free Radicals in Biology and Medicine*, 4th edn, Clarendon Press, Oxford, 2007.

Hamil KG, Liu Q, Sivashanmugam P, Yenugu S, Soundararajan R, et al. *Endocrinology* 2002; **143**:2787-2796.

Hamilton G, Colbert JD, Schuettelkopf AW and Watts C. *EMBO J* 2008; **27**:499-508.

Hammer ND, Wang X, McGuffie BA and Chapman MR. *J Alzheimers Dis* 2008; **13**:407-419.

Haq SK, Rasheedi S and Khan RH. *Eur J Biochem* 2002; **269**:47-52.

Harper JD and Lansbury PT Jr. *Annu Rev Biochem* 1997; **66**:385-407.

Hasan N, Ali I and Naseem I. *Med Sci Monit* 2006; **12**:BR283-289.

Hawkins CL and Davies MJ. *Biochem J* 1998; **332**:617-625.

Hayashi H, Tokuda A and Udaka K. *J Exp Med* 1960; **112**:237-247.

Hazell LJ, van den Berg JJ and Stocker R. *Biochem J* 1994; **302**:297-304.

He Y, Zhou H, Tang H and Luo Y. *J Biol Chem* 2006; **281**:1048-1057.

Heitz P, Polak JM, Bloom SR and Pearse AG. *Gut* 1976; **17**:755-758.

Henderson PJF. *Biochem J* 1972; **127**:321-333.

Hertog MG and Hollman PC. *Eur J Clin Nutr* 1996; **50**:63-71.

Hirado M, Tsunasawa S, Sakiyama F, Niiobe M and Fujii S. *FEBS Lett* 1985; **186**:41-45.

Hirota S, Takahama U, Ly TN and Yamauchi R. *J Agric Food Chem* 2005; **53**:3265-3272.

Hochwald GM and Thorbecke GJ. *Proc Soc Exp Biol Med* 1962; **109**:91-95.

Holm NK, Jespersen SK, Thomassen LV, Wolff TY, Sehgal P, et al. *Biochim Biophys Acta* 2007; **1774**:1128-1138.

Hong DP, Gozu M, Hasegawa K, Naiki H and Goto Y. *J Biol Chem* 2002; **277**:21554-21560.

Hopsu-Havu VK, Joronen I, Jarvinen M and Rinne A. *Br J Dermatol* 1983a; **109**:77-85.

Hornby JA, Luo JK, Stevens JM, Wallace LA, Kaplan W, et al. *Biochemistry* 2000; **39**:12336-12344.

Hortscansky P, Christopeit T, Schroeckh V and Fandrich M. *Protein Sci* 2005; **14**:2915-2918.

Hu Yan-Jun, Liu YI, Wang Jia-Bo, Xiao Xiao-He and Qu Song-Sheng. *J Pharma Biomed* Analysis 2004; **36**:915-919.

Huang K, Park YD, Cao ZF and Zhou HM. *Biochim Biophys Acta* 2001; **1545**:305-313.

Huang MT, Smart RC, Wong CQ and Conney AH. *Cancer Res* 1988; **48**:5941-5946.

Huang Y and Wang KK. *Trends Mol Med* 2001; 7:355-362.

Hunt JV, Simpson JA and Dean RT. *Biochem J* 1988; **250**:87-93.

Husain E, Fatima RA, Ali IA and Naseem I. *Indian J Biochem Biophys* 2006; **43**:312-318.

Ischiropoulos H. *Biochem Biophys Res Commun* 2003; **305**:776-783.

Isemura S, Saitoh E, Ito S, Isemura M and Sanada K. *J Biochem* 1984b; **96**:1311-1314.

Isemura S, Saitoh E, Ito S, Sanada K and Minakata K. *J Biochem* 1991; **110**:648-654.

Isemura S, Saitoh E, Sanada K, Isemura M and Ito S. In: *Cysteine Proteinase and their inhibitors,* Turk V (editor). Berlin, Walter de Gruyter: 1986.

Isemura S, Saitoh E and Sanada K. *J Biochem* 1984a; **96**:489-498.

Jaenicke R and Lilie H. *Adv Protein Chem* 2000; **53**:329-401.

Jaenicke R. *Biochemistry* 1991; **30**:3147-3161.

Jaenicke R. *Pmg Biophys Mol Biol* 1987; **49**:117-237.

Jankowska E, Wiczk W and Grzonka Z. *Eur Biophys J* 2004; **33**:454-461.

Janowski R, Kozak M, Jankowska E, Grzonka Z, Grubb A, et al. *Nat Struct Biol* 2001; **8**:316-320.

Jarvinen M and Rinnie A. *Biochim Biophys Acta* 1982; **708**:210-217.

Jarvinen M. *J Invest Dermatol* 1978; **71**:114-118.

Jarvinen M, Rasanen O and Rinnie A. *J Invest Dermatol* 1978; **71**:119-121.

Jarvinen M. *Acta Chemica Scand* 1976; **B30**:933-940.

Jazzar MM and Naseem I. *Biochem Mol Biol Int* 1994; **34**:883-895.

Jenko Kokalj S, Guncar G, Stern I, Morgan G, Rabzelj S, et al. *J Mol Biol* 2007; **366**: 1569-1579.

Jenko S, Dolenc I, Guncar G, Dobersek A, Podobnik M, et al. *J Mol Biol* 2003; **326**:875-885.

Jenko S, Skarabot M, Kenig M, Guncar G, Musevic I, et al. *Proteins* 2004; **55**:417-425.

Jenner AM, Ruiz JE, Dunster C, Halliwell B, Mann GE, et al. *Arterioscler Thromb Vasc Biol* 2002; **22**:574-580.

Jensson O, Gudmundsson G, Arnason A, Blondal H, Petursdottir I, et al. *Acta Neurol Scand* 1987; **76**:102-114.

Jerlich A, Hammel M, Nigon F, Chapman MJ and Schaur RJ. *Eur J Biochem* 2000; **267**:4137-4143.

Jirgensons B. *Biochim Biophys Acta* 1970; **200**:9-17.

Joensuu T, Kuronen M, Alakurtti K, Tegelberg S, Hakala P, et al. *Eur J Hum Genet* 2007; **15**:185-193.

Johnson WC Jr. *Methods Biochem Anal* 1985; **31**:61-163.

Joshi PC. *Indian J Biochem Biophys* 1998; **35**:208-215.

Joshi PC. *Toxicol Lett* 1985; **26**:211-217.

Joyce JA, Baruch A, Chehade K, Meyer-Morse N, Giraudo E, et al. *Cancer Cell* 2004; **5**:443-453.

Jung UJ, Lee MK, Park YB, Jeon SM and Choi MS. *J Pharmacol Exp Ther* 2006; **318**:476-483.

Juranek I and Bezek S. *Gen Physiol Biophys* 2005; **24**:263-278.

Kalbe L, Leunda A, Sparre T, Meulemans C, Ahn MT, et al. *Br J Nutr* 2005 ; **93**:309-316.

Kamoun PP. *Trends Biochem Sci* 1988; **13**:424-425.

Kanitkar M, Gokhale K, Galande S and Bhonde RR. *Br J Pharmacol* 2008; **155**:702-713.

Kato T, Imatani T, Minaguchi K, Saitoh E and Okuda K. *Mol Immunol* 2002; **39**:423-430.

Kato T, Imatani T, Miura T, Minaguchi K, Saitoh E, et al. *Biol Chem* 2000; **381**:1143-1147.

Kato T, Ito T, Imatani T, Minaguchi K, Saitoh E and Okuda K. *Biol Chem* 2004; **385**:419-422.

Katunuma N and Kominami E. *Curr Topics Cell Regul* 1985; **27**:345-360.

Kawai Y and Arinze IJ. *Cancer Res* 2006; **66**:6563-6569.

Keilova H and TomasekV. *Coll Czech Chem Commun* 1975; **40**:218-224.

Kelly JW. *Curr Opin Struct Biol* 1998; **8**:101-106.

Keppler D. *Cancer Lett* 2006; **235**:159-176.

Keynes RG, Griffiths C and Garthwaite J. *Biochem J* 2003; **369**:399-406.

Khan MS and Bano B. *Biochemistry (Mosc)* 2009; **74**:781-788.

Khan MS and Bano B. *Int J Pept Res Ther* 2009; **15**:81-86.

Khan MS, Priyadarshini M and Bano B. *J Agric Food Chem* 2009; **57**:6055-6059.

Khan SA and Khan FH. *Biochim Biophys Acta* 2004; **1674**:139-148.

Khaznadji E, Collins P, Dalton JP, Bigot Y and Moire N. *Int J Parasitol* 2005; **35**:1115-1125.

Khurana R, Ionescu-Zanetti C, Pope M, Li J, Neilson L, et al. *Biophys J* 2003; **85**: 1135-1144.

Kim EK, Kwon KB, Song MY, Han MJ, Lee JH, et al. *Pancreas* 2007; **35**:e1-e9.

Kim PS and Baldwin RL. *Annu Rev Biochem* 1982; **51**:459-489.

Kim PS and Baldwin RL. *Annu Rev Biochem* 1990; **59**:631-660.

Klunk WE, Jacob RF and Mason RP. *Methods Enzymol* 1999; **309**:285-305.

Koide T, Foster D, Yoshitake S and Davie EW. *Biochemistry* 1986; **25**:2220-2225.

Koiwa H, Bressan RA and Hasegawa PM. *Trends Plant Sci* 1997; **21**:379-384.

Kominami E, Wakamatsu N and Katunuma N. *Biochem Biophys Res Commun* 1981; **99**:568-575.

Konno T. *Protein Sci* 2001; **10**:2093-2101.

Kopitar M, Brzin J, Zvonar T, Locnikar P, Kregar I, et al. *FEBS Lett* 1978; **91**:355-359.

Kopitar M, Stern F and Marks N. *Biochem Biophys Res Commun* 1983; **112**:1000-1006.

Kopitar-Jerala N. *FEBS Lett* 2006; **580**:6295-6301.

Kopitz C, Anton M, Gansbacher B and Kruger A. *Cancer Res* 2005; **65**:8608-8612.

Korolenko TA, Filatova TG, Cherkanova MS, Khalikova TA and Bravve Iiu. *Biomed Khim* 2008; **54**:210-217.

Koshizuka Y, Yamada T, Hoshi K, Ogasawara T, Chung UI, et al. *J Biol Chem* 2003; **278**:48259-48266.

Kostrouchova M, Kostrouch Z and Kostrouchova M. *Folia Biol (Praha)* 2007; **53**:37-49.

Kotsyfakis M, Karim S, Andersen JF, Mather TN and Ribeiro JMC. *J Biol Chem* 2007; **282**:29256-29263.

Kotsyfakis M, Sa-Nunes A, Francischetti IMB, Mather TN, Andersen JF, et al. *J Biol Chem* 2006; **281**:26298-26307.

Krebs MR, Bromley EH and Donald AM. *J Struct Biol* 2005; **149**:30-37.

Krebs MR, Wilkins DK, Chung EW, Pitkeathly MC, Chamberlain AK, et al. *J Mol Biol* 2000; **300**:541-549.

Krupka RM and Laidler KJ. *Can J Chem* 1959; **51**:1268-1271.

Kunitz M. *J Physiol.* 1947; **30**: 291-310.

Kuwajima K. *Proteins* 1989; **6**:87-103.

Kyte J and Doolittle RF. *J Mol Biol* 1982; **157**:105-132.

Lacy PE and Davies J. *Diabetes* 1957; **6**:354-357.

Laemmli UK. *Nature* 1970; **227**:680-685.

Lai Z, Colon W and Kelly JW. *Biochemistry* 1996; **35**:6470-6482.

Lakowicz JR. *Principles of Fluorescence Spectroscopy* 3rd ed., 2006; XXVI, 954: p 1255.

Lakowicz JR. *Principles of fluorescence Spectroscopy.* New York: Plenum Press, 1983.

Lalitha S, Shade RE, Murdock LM, Hasegawa PM, Bressan RA, et al. *J Agric Food Chem* 2005;**53**:1591-1597.

Langerholc T, Zavasnik-Bergant V, Turk B, Turk V, Abrahamson M, et al. *FEBS J* 2005; **272**:1535-1545.

Lashuel HA, Hartley DM, Balakhaneh D, Aggarwal A, Teichberg S, et al. *J Biol Chem* 2002; **277**:42881-42890.

Lapidot T, Walker MD and Kanner J. *J Agric Food Chem* 2002; **50**:7220-7225.

Laurent TC and Killander J. *J Chromatogr* 1964; **14**:317-330.

Layne E. *Methods Enzymol* 1957; **3**:447-455.

Lee C, Bongcam-Rudloff E, Sollner C, Jahnen-Dechent W and Claesson-Welsh L. *Front Biosci* 2009; **14**:2911-2922.

Lee MJ, Yu GR, Park SH, Cho BH, Ahn JS, et al. *Clin Cancer Res* 2008; **14**:1080-1089.

Lenarcic B and Bevec T. *Biol Chem* 1998; **379**:105-111.

Lenarcic B and Turk V. *J Biol Chem* 1999; **274**:563-566.

Lenarcic B, Krasovec M, Ritonja A, Olafsson I and Turk V. *FEBS Lett* 1991; **280**: 211-215.

Lenarcic B, Krizaj I, Zunec P and TurkV. *FEBS Lett* 1996; **395**:113-118.

Lenarcic B, Ritonja A, Strukelj B, Turk B and Turk V. *J Biol Chem* 1997; **272**:13899-13903.

Lenney JF, Tolan JR, Sugai WJ and Lee AG. *Eur J Biochem* 1979; **101**:153-161.

Lenzen S. *Biochem Soc Trans* 2008a; **36**:343-347.

Lenzen S. *Diabetologia* 2008b; **51**:216-226.

Leung L. *J Lab Clin Med* 1993; **121**:630-631.

Leung-Tack J, Tavera C, Gensac MC, Martinez J and Colle A. *Exp Cell Res* 1990; **188**:16-22.

LeVine H 3rd. *Methods Enzymol* 1999; **309**:274-284.

Liang H and Terwillger TC. *Biochemistry* 1991; **30**:2772-2782.

Li F, An M and Baynes TL. *Comp Biochem Physiol Part B:Biochem and Mol Biol* 2000; **125**:493-502.

Li S, Ao J and Chen X. *Mol Immunol* 2009; **46**:1638-1646.

Li W, Ding F, Zhang L, Liu Z, Wu Y, et al. *Clin Cancer Res* 2005; **11**:8753-8762.

Li Y, Friel PJ, Robinson MO, McLean DJ and Griswold MD. *Biol Reprod* 2002; **67**:1872-1880.

Lieuallen K, Pennacchio LA, Park M, Myers RM and Lennon GG. *Hum Mol Genet* 2001; **10**:1867-1871.

Lindahl P, Abrahamson M and Bjork I. *Biochem J* 1992; **128**:49-55.

Liu X, Miller MJ, Joshi MS, Sadowska-Krowicka H, Clark DA, et al. *J Biol Chem* 1998; **273**:18709-18713.

Liu Y, Gotte G, Libonati M and Eisenberg D. *Nat Struct Biol* 2001; **8**: 211-214.

Lofberg H, Grubb A, Davidsson J, Kjellander B, Stromblad LG, et al. *Acat Endocrinol* 1983; **104**:69-76.

Lofberg H, Grubb AO and Brun A. *Biomed Res* 1981; **2**:298-306.

Lofberg H, Grubb AO, Jornvau H, Moller CA, Stromblad LG, et al. *Acat Endocrinol* 1982; **100**:595-598.

Lomakin A, Chung DS, Benedek GB, Kirschner DA and Teplow DB. *Proc Natl Acad Sci USA* 1996; **93**:1125-1129.

Lorenzo K, Ton P, Clark JL, Coulibaly S, Mach L. *Cancer Res* 2000; **60**:4070-4076.

Lowry OH, Rosenbrough NJ, Farr AL and Randall RJ. *J Biol Chem* 1951; **193**:265-275.

Luo P and Baldwin RL. *Biochemistry* 1997; **36**:8413-8421.

Luo Y and Baldwin RL. *J Mol Biol* 1998; **279**:49-57.

Lutgens SP, Cleutjens KB, Daemen MJ and Heeneman S. *FASEB J* 2007; **21**:3029-3041.

Luthy JA, Praissman M, Finkentadt WR and Laskowski M Jr. *J Biol Chem* 1973;

248:1760-1771.

Machleidt W, Borchart U, Fritz H, Brzin J, Ritonja A, et al. *Hoppe Seylers Z Physiol Chem* 1983; **364**:1481-1486.

Machleidt W, Ritonja A, Popovic T, Kotnik M, Brzin J, et al. In:*Cysteine proteinases and their inhibitors*, Turk V (editor). Berlin: Walter de Gruyter. 1986; pp 3-18.

Machleidt W, Thiele U, Laber B, Assfalg-Machleidt I, Esterl A, et al. *FEBS Lett* 1989; **243**:234-238.

Makhatadze GI, Lopez MM, Richardson JM and Thomas ST. *Protein Sci* 1998; 7:689-697.

Manoury B, Hewitt EW and Morrice N. *Nature* 1998; **396**:695-699.

Marcocci L, Maguire JJ, Droy-Lefaix MT and Packer L. *Biochem Biophys Res Commun* 1994a; **201**:748-755.

Marnett LJ, Riggins JN and West JD. *J Clin Invest* 2003; **111**:583-593.

Martin JR, Craven CJ, Jerala R, Kroon-Zitko L, Zerovnik E, et al. *J Mol Biol* 1995; **246**:331-343.

Martin JR, Jerala R, Kroon-Zitko L, Zerovnik E, Turk V, et al. *Eur J Biochem* 1994; **225**:1181-1194.

Martinez M, Diaz-Mendoza M, Carrillo L and Diaz I. *FEBS Lett* 2007; **581**:2914-2918.

Martinez-Cayuela M. *Biochimie* 1995; 77:147-161.

Mason RW. *Arch Biochem Biophys* 1989; **273**:367-374.

Mayr LM and Schmid FX. *Biochemistry* 1993; **32**:7994-7998.

McGraw Hills Access medicine, The McGraw-Hill Companies, www.accessmedicine.com

McNamara M and Augusteyn RC. *Exp Eye Res* 1984; **38**:45-56.

Meghana K, Sanjeev G and Ramesh B. *Eur J Pharmacol* 2007; **577**:183-191.

Mei G, Rosato N, Silva N Jr, Rush R, Gratton E, et al. *Biochemistry* 1992; **31**:7224-7230.

Mendoza-Hernandez G, Minauro F and Rendon JL. *Biochim Biophys Acta* 2000; **1478**:221-231.

Merlini G and Bellotti V. *N Engl J Med* 2003; **349**:583-596.

MEROPS peptidase database (http://merops.sanger.ac.uk).

Mertens-Talcott SU and Percival SS. *Cancer Lett* 2005; **218**:141-151.

Mi W, Pawlik M, Sastre M, Jung SS, Radvinsky DS, et al. *Nat Genet* 2007; **39**:1440-1442.

Mihelic M and Turk D. *Biol Chem.* 2007; **388**:1123-1130.

Mihelic M, Teuscher C, Turk V and Turk D. *FEBS Lett* 2006; 580: 4195-4199.

Milla ME and Sauer RT. *Biochemistry* 1994; **33**:1125-1133.

Minakata K and Asano M. *Biol Chem Hoppe-Seyler* 1985; **366**:15-18.

Mitchell ED, Riquetti, Loring RH and Carraway KI. *Biochim Biophys Acta* 1973; **295**:314-322.

Mohamed MM and Sloane BF. *Nat Rev Cancer* 2006; **6**:764-775.

Moller CA, Lofberg H, Grubb AO, Olsson SO, Davies ME, et al. *Neuroendocrinol* 1985; **41**:400-404.

Moncada S, Palmer RM and Higgs EA. *Pharmacol Rev* 1991; **43**:109-142.

Monsellier E and Bedouelle H. *Protein Eng Des Sel* 2005; **18**:445-456.

Monteiro ACS, Abrahamson M, Lima APCA, Vannier-Santos MA and Scharfstein J. *J Cell Sci* 2001; **114**:3933-3942.

Moreno JJ and Pryor WA. *Chem Res Toxicol* 1992; **5**:425-4331.

Morgan GJ, Giannini S, Hounslow AM, Craven CJ, Zerovnik E, et al. *J Mol Biol* 2008; **375**:487-498.

Morris JC. *J Phys Chem* 1966; **70**:3798–3805.

Mu MM, Chakravortty D, Sugiyama T, Koide N, Takahashi K, et al. *J Endotoxin Res* 2001; 7:431-438.

Müller-Esterl W, Fritz H, Kellermann J, Lottspeich F, Machleidt W, et al. *FEBS Lett* 1985b; **191**:221-226.

Müller-Esterl W, Fritz H, Machleidt W, Ritonja A, Brzin J, et al. *FEBS Lett* 1985a; **182**:310-314.

Müller-Esterl W. *Semin Thromb Hemost* 1987; **13**:115-126.

Murachi T, Neurath H. *J Biol Chem* 1960; **235**:99-107.

Musil D, Zucic D, Turk D, Engh RA, Mayr I, et al. *EMBO J* 1991; **10**:2321-2330.

Myers JK, Pace CN and Scholtz JM. *Protein Sci* 1995; **4**:2138-2148.

Nakanishi H. *Ageing Res Rev* 2003; **2**:367-381.

Nakayama T. *Cancer Res* 1994; **54**:1991s-1993s.

Nandi PK and Robinson DR. *Biochemistry* 1984; **23**:6661-6668.

Nawa H, Kitamura N, Hirose T, Asai M, Inayama S, et al. *Proc Natl Acad Sci USA* 1983; **80**:90-94.

Neet KE and Timm DE. *Protein Sci* 1994; **4**:2167-2174.

Nesternko MV, Tilley M and Upton SJ. *J Biochem Biophys Methods* 1994; **28**:239-242.

Neuschwander-Tetri BA, Presti ME and Wells LD. *Pancreas* 1997; **14**:342-349.

Ni J, Abrahamson M, Zhang M, Alvarez-Fernandez M, Grubb A, et al. *J Biol Chem* 1997; **272**:10853-10858.

Ni J, Fernandez MA and Danielsson L. *J Biol Chem* 1998; **273**:24797-24804.

Nicklin MJH and Barrett AJ. *Biochem J* 1984; **223**:245-253.

Niederau C, Klonowski H, Schulz HU, Sarbia M, Luthen R, et al. *Free Radic Biol Med* 1996; **20**:877-886.

Nilsson MR. *Methods* 2004; **34**:151-160.

Nordberg J and Arner ES. *Free Radic Biol Med* 2001; **31**:1287-1312.

Nørgaard M, Jacobsen J, Ratanajamit C, Jepsen P, McLaughlin JK, et al. *Am J Ther* 2006; **13**:113-117.

Nozais M and Bechet JJ. *Eur J Biochem* 1993; **218**:1049-1055.

Novinec M, Grass RN, Stark WJ, Turk V, Baici A, et al. *J Biolm Chem.* 2007; **282**:7893–7902.

Nycander M and Bjork I. *Biochem J* 1990; **271**:281-284.

Nycander M, Estrada S, Mort JS, Abrahamson M and Bjork I. *FEBS Lett* 1998; **422**:61-62.

Ohkubo I, Kurachi K, Takasawa T, Shiokawa H and Sasaki M. *Biochemistry* 1984; **23**:5691-5697.

Oliva ML, Carmona AK, Andrade SS, Cotrin SS, Soares-Costa A, et al. *Biochem Biophys Res Commun* 2004; **320**:1082-1086.

Olmos A, Giner RM, Recio MC, Ríos JL, Gil-Benso R, et al. *Arch Biochem Biophys* 2008; **475**:66-71.

Olson ST and Shore JD. *Biol Chem* 1982; **257**:14891-14895.

Olsson S, Ek B and Bjork I. *Biochim Biophys Acta* 1999; **1432**:73-81.

Olszowski S, Olszowska E, Stelmaszynska T, Krawczyk A, Marcinkiewicz J, et al. *Acta Biochim Pol* 1996; **43**:661-672.

Onoda M and Inano H. *Nitric Oxide* 2000; **4**:505-515.

Oppert B, Morgan TD, Hartzer K, Lenarcic B, Galesa K, et al. *Comp. Biochem Physiol C Toxicol Pharmacol* 2003; **134**:481-490.

Orci L, Baetens D, Dubois MP and Rufener C. *Horm Metab Res* 1975; 7:400-402.

Otto K and Riesenkonig H. Biochim Biophys Acta 1975; **379**:462-475.

Ouchterlony O. *Acta Pathol Microbiol Scand* 1962; **26**:579-599.

Pace CN. *CRC Crit Rev Biochem* 1975; **3**:1-43.

Pace CN. *Methods Enzymol* 1986; **131**:266-280.

Pace CN. *Trends Biochem Sci* 1990; **15**:14-17.

Pacher P, Obrosova IG, Mabley JG and Szabó C. *Curr Med Chem* 2005; **12**:267-275.

Pakula AA and Sauer RT. *Proteins Struct Funct Genet* 1989; **5**:202-210.

Pallares I, Berenguer C, Aviles FX, Vendrell J and Ventura S. *BMC Struct Biol* 2007; 7:75.

Palsdottir A, Snorradottir AO and Thorsteinsson L. *Brain Pathol* 2006; **16**:55-59.

Panyim S and Chalklev R. *J Biol Chem* 1971; **246**:7557-7560.

Paraoan L, Gray D, Hiscott P, Garcia-Finana M, Lane B, et al. *Front Biosci* 2009; **14**:2504-2513.

Park YD, Jung JY, Kim DW, Kim WS, Hahn MJ, et al. *J Protein Chem* 2003; **22**:463-471.

Parker B, Ciocca D, Bidwell B, Gago F, Fanelli M, et al. *J Pathol* 2008; **214**:337-346.

Pavlova A and Bjork I. *Biochemistry* 2003; **42**:11326-11333.

Pavlova A, Krupa JC, Mort JS, Abrahamson M and Björk I. *FEBS Lett* 2000; **487**:156-160.

Pedersen JS, Christiansen G and Otzen DE. *J Mol Biol* 2004; **341**:575-588.

Pedersen KO. *Nature* 1944; **154**:575.

Pennacchio LA, Lehesjoki AE, Stone NE, Willour VL, Virtaneva K, et al. *Science* 1996; **271**:1731-1734.

Pertinhez TA, Bouchard M, Tomlinson EJ, Wain R, Ferguson SJ, et al. *FEBS Lett* 2001; **495**:184-186.

Peskin AV and Winterbourn CC. *Free Radic Biol Med* 2001; **30**:572-579.

Peterson EA and Sober HA. In: *Methods Enzymol*, Colowick SP and Kaplan NO (editors). New York:Academic Press, 1962; **5**:3.

Petty RD, Kerr KM, Murray GI, Nicolson MC, Rooney PH, et al. *J Clin Oncol* 2006; **24:**1729-1744.

Pluger EB, Boes M, Alfonso C, Schröter CJ, Kalbacher H, et al. *Eur J Immunol* 2002; **32**:467-476.

Pol E and Bjork I. *Protein Sci* 2001; **10**:1729-1738.

Pol E, Olsson SL, Estrada S, Prasthofer TW, and Bjork I. *Biochem J* 1995; **311**:275-282.

Polverino de Laureto P, Frare E, Gottardo R and Fontana A. *Proteins* 2002; **49**:385-397.

Pontremoli S, Melloni E, Salamino F, Sparatore B, Michetti M, et al. *Proc Natl Acad Sci USA* 1983; **80**:1261-1264.

Poulik MD, Shinnick CS and Smithies O. *Mol Immunol* 1981; **18**:569-572.

Prajapati S, Bhakuni V, Babu KR and Jain SK. *Eur J Biochem* 1998; **255**:178-184.

Prakash K, Prajapati S, Ahmad A, Jain SK and Bhakuni V. *Protein Sci* 2002; **11**:46-57.

Priyadarshini M and Bano B. *Amino Acids* 2009; 10.1007/s00726-009-0308-x.

Priyamvada S, Priyadarshini M, Arivarasu NA, Farooq N, Khan S, et al. *Prostaglandins Leukot Essent Fatty Acids* 2008; **78**:369-381.

Pryor WA, Houk KN, Foote CS, Fukuto JM, Ignarro LJ, et al. *Am J Physiol Regul Integr Comp Physiol* 2006; **291**:R491-511.

Ptitsyn OB. *Adv Protein Chem* 1995; **47**:83-229.

Punturieri A, Filippov S, Allen E, Caras I, Murray R, et al. *J Exp Med* 2000; **192**:789-99.

Quast U, Engel J, Heumann H, Krause G and Steffen E. *Biochemistry* 1974; **13**:2510-2520.

Rabzelj S, Turk V and Zerovnik E. *Protein Sci* 2005; **14**:2713-2722.

Rabzelj S, Viero G, Gutiérrez-Aguirre I, Turk V, Dalla Serra M, et al. *FEBS J* 2008; **275**:2455-2466.

Radi R. *Proc Natl Acad Sci USA* 2004; **101**:4003-4008.

Raman B, Ban T, Yamaguchi K, Sakai M, Kawai T, et al. *J Biol Chem* 2005; **280**: 16157-16162.

Ramasarma PR, Rao AGA and Rao D. *Biochim Biophys Acta* 1994; **1248**:35-42.

Rashid F, Sharma S and Bano B. *Placenta* 2006a; **2**:822-831.

Rashid F, Sharma S and Bano B. *Protein J* 2005; **24**:283-292.

Rashid F, Sharma S, Baig MA and Bano B. *Biochem Cell Biol* 2006b; **84**:126-134.

Rashid F, Baba SP, Sharma S and Bano B. *Protein Pept Lett* 2004; **11**:583-591.

Rau B, Poch B, Gansauge F, Bauer A, Nussler AK, et al. *Ann Surg* 2000; **231**:352-360.

Rawlings ND and Barrett AJ. *J Mol Evol* 1990; **30**:60-71.

Rawlings ND, Tolle DP and Barrett AJ. *Biochem J* 2004b; **378**:705-716.

Rawlings ND, Tolle DP and Barrett AJ. *Nucleic Acids Res* 2004a; **32**:D160-D164 (Database issue).

Ridnour LA, Thomas DD, Mancardi D, Espey MG, Miranda KM, et al. *Biol Chem* 2004; **385**:1-10.

Rinnie A, Alavaikko M, Jarvinen M, Martikinen J, Kartunen T, et al. *Virchows Arch Cell Pathol* 1983; **43**:121-126.

Rinnie A, Rasanen O, Jarvinen M, Dammert K, Kallioinen M, et al. *Acta Histochem* 1984; **74**:75-79.

Rinnie A, Jarvinen M and Rasanen O. *Acta Histochem* 1978; **63**:183-192.

Rivenbark AG and Coleman WB. *Front Biosci* 2009; **14**:453-462.

Riviere C, Richard T, Vitrac X, Merillon JM, Valls J, et al. *Bioorg Med Chem Lett* 2008; **18**:828-831.

Rochet JC and Lansbury PT Jr. *Curr Opin Struct Biol* 2000; **10**:60-68.

Rocken C, Stix B, Brömme D, Ansorge S, Roessner A, et al. *Am J Pathol* 2001; **158**:1029-1038.

Roig MG, Bello F, Burguillo FJ, Cachaza JM and Kennedy JF. *J Pharm Sci* 1991; **80**:267-270.

Rose RC, McCorrmick DB, Li TK, Lumeng L, Haddad JG Jr, et al. *Fed Proc* 1986; **45**:30-39.

Rossi A, Deveraux Q, Turk B and Sali A. *Biol Chem* 2004; **385**:363-372.

Ruiz JL, Ferrer J, Pire C, Llorca FI and Bonete MJ. *J Protein Chem* 2003; **22**:295-301.

Sabate R and Saupe SJ. *Biochem Biophys Res Commun* 2007; **360**:135-138.

Sacchetta P, Aceto A, Bucciarelli T, Dragani B, Santarone S, et al. *Eur J Biochem* 1993; **215**:741-745.

Sacchetta P, Di Rado R, Saliola M, Bozzi A, Falcone C, et al. *Biochim Biophys Acta* 2001; **1545**:238-244.

Salvesen G, Parkes C, Abrahamson M, Grubb A and Barrett AJ. *Biochem J* 1986a; **234**:429-434.

Salvesen G, Parkes C, Rawlings ND, Brown MA, Barrett AJ, et al. In: *Cysteine Proteinases and their Inhibitors*, Turk V (editor). Berlin and New York: Walter de Gruyter, 1986b; pp 413-428.

Salvi A, Carrupt P, Tillement J and Testa B. *Biochem Pharmacol* 2001; **61**:1237-1242.

Sambashivan S and Eisenberg D. *BioTech Int* 2006; **18**:6-10.

Sandberg M and Borg LA. *Biol Cell* 2006; **98**:307-315.

Sandoval M, Liu X, Mannick EE, Clark DA and Miller MJ. *Gastroenterol* 1997; **113**:1480-1488.

Sandstrom P, Brooke-Smith ME, Thomas AC, Grivell MB, Saccone GT, et al. *Pancreas* 2005; **30**:e10-e15.

Sawada F, Inoguchi T, Tsubouchi H, Sasaki S, Fujii M, et al. *Metabolism* 2008; **57**:1038-1045.

Saxena I and Tayyab S. *Cell Mol Life Sci* 1997; **53**:13-23.

Scharfstein J, Schmitz V, Svensjö E, Granato A and Monteiro AC. *Scand J Immunol* 2007; **66**:128-136.

Scheiber J, Chen B, Milik M, Sukuru SCK, Bender A, et al. *J Chem Inf Model* 2008;

10.1021/ci800344p.

Schierack P, Lucius R, Sonnenburg B, Schilling K and Hartmann S. *Infect Immun* 2003; **71**:2422-2429.

Schuttelkopf AW, Hamilton G, Watts C and van Aalten DMF. *J Biol Chem* 2006; **281**:16570-16575.

Schurmann G, Haspel J, Grumet M and Erickson HP. *Mol Cell Biol* 2001; **12**:1765-1773.

Schwabe C, Anastasi A, Crow H, McDonald JK and Barrett AJ. *Biochem J* 1984; **217**:813-817.

Seckler R and Jaenicke R. *FASEB J* 1992; **6**:2545-2552.

Seery VL and Farrell HM. *J Biol Chem* 1990; **265**:17644-17648.

Sekine T and Poulik MD. *Clin Chim Acta* 1982; **120**:225-235.

Semisotnov GV, Rodionova NA, Razgulyaev OI, Uversky VN, Gripas AF, et al. *Biopolymers* 1991; **31**:119-218.

Sen LC and Whitaker JR. *Arch Biochem Biophys* 1973; **158**:623-632.

Serpell LC, Sunde M, Benson MD, Tennent GA, Pepys MB, et al. *J Mol Biol* 2000b; **300**:1033-1039.

Serpell LC. *Biochim Biophys Acta* 2000a; **1502**:16-30.

Shah A and Bano B. *Int J Pept Res Ther* 2009; **15**:43-48.

Shechter Y, Burstein Y and Patchornik A. *Biochemistry* 1975; **14**:4497-4503.

Shikimi T, Yamamoto D and Handa M. *J Pharmacobiodyn* 1987; **10**:750-757.

Shimizu K. *J Gastroenterol* 2008; **43**:823-832.

Shoemaker K, Holloway JL, Whitmore TE, Maurer M and Feldhaus AL. *Gene* 2000; **245**:103-108.

Sies H. In: *Oxidative Stress*, Sies H (editor) Academic Press: London, 1985; pp1-8.

Sigfrid LA, Cunningham JM, Beeharry N, Lortz S, Tiedge M, et al. *J Mol Endocrinol* 2003; **31**:509-518.

Skerget K, Vilfan A, Pompe-Novak M, Turk V, Waltho JP, et al. *Proteins* 2009; **74**:425-436.

Smith JF, Knowles TP, Dobson CM, Macphee CE and Welland ME. *Proc Natl Acad Sci USA* 2006; **103**:15806-15811.

Smith JS and Scholtz JM. *Biochemistry* 1996; **35**:7292-7297.

Sneppen K, Zocchi G. *Physics in molecular biology*. Cambridge University Press, Cambridge, UK, 2005.

Sohar I, Laszlo A, Gaal K and Mechler F. *Biol Chem Hoppe-Seyler* 1988; **369**:277-284.

Sokol JP and Schiemann WP. *Mol Cancer Res* 2004; **2**:183-195.

Sokol JP, Neil JR, Schiemann BJ and Schiemann WP. *Breast Cancer Res* 2005; 7:R844-853.

Soldi G, Bemporad F, Torrassa S, Relini A, Ramazzotti M, et al. *Biophys J* 2005; **89**:4234-4244.

Sotiropoulou G, Anisowicz A and Sager R. *J Biol Chem* 1997; **272**:903-910.

Soto C. *FEBS Lett* 2001; **498**:204-207.

Spector R. *J Neurochem* 1980; **35**:202-209.

Sreejayan and Rao MN. *J Pharm Pharmacol* 1997; **49**:105-107.

Sreenan SK, Zhou YP, Otani K, Hansen PA, Currie KP, et al. *Diabetes* 2001; **50**:2013-2020.

Stadtman ER and Levine RL. *Amino Acids* 2003; **25**:207-218.

Staniforth RA, Giannini S, Higgins LD, Conroy MJ, Hounslow AM, et al. *EMBO J* 2001; **20**:4774-4781.

Steif C, Weber P, Hinz HJ, Flossdorf J, Cesareni G, et al. *Biochemistry* 1993; **32**:3867-3876.

Steinbeck MJ, Khan AU and Karnovsky MJ. *J Biol Chem* 1993; **268**:15649-15654.

Stoka V, Nycander M, Lenarcic B, Labriola C, Cazzulo JJ, et al. *FEBS Lett* 1995; **370**:101-104.

Stoka V, Turk B and Turk V. *IUBMB Life* 2005; **57**:347-353.

Stryer L. *J Mol Biol* 1965; **13**:482-495.

Stubbs MT, Laber B, Bode W, Huber R, Jerala R, et al. *EMBO J* 1990; **9**:1939-1948.

Sumanont Y, Murakami Y, Tohda M, Vajragupta O, Matsumoto K, et al. *Biol Pharm Bull* 2004; **27**:170-173.

Sumbul S and Bano B. *Neurochem Res* 2006; **31**:1327-1336.

Sumbul S and Bano B. *Protein Pept Lett* 2008; **15**:20-26.

Sun H, Li N, Wang X, Liu S, Chen T, et al. *Biochem Biophys Res Commun* 2003; **301**:176-182.

Sutton HG, Fusco A and Cornwall GA. *Endocrinology* 1999; **140**:2721-2732.

Sutton-Walsh HG, Whelly S and Cornwall GA. *J Androl* 2006; **27**:802-815.

Suzuki T and Natori S. *J Biol Chem* 1985; **260**:5115-5120.

Szuchman-Sapir AJ, Pattison DI, Ellis NA, Hawkins CL, Davies MJ, et al. *Free Radic Biol Med* 2008; **45**:789-798.

Takahama U, Hirota S and Kawagishi S. *Free Radic Res* 2009; **43**:250-261.

Takeda A, Kobayashi S and Samejima T. *J Biochem* 1983; **94**:811-820.

Takeda K, Wada A, Yamamoto K, Hachiya K and Batra PP. *J Colloid Interface Sci* 1988; **125**:307-313.

Tanford C. *Adv Protein Chem* 1968; **23**:121-282.

Tanford C. Physical Chemistry of Macromolecules. New York, John Wiley, 1961.

Taniguchi CM, Armstrong SR, Green LC, Goaln DE and Tashjian AH Jr. *Fundamental Principles of Pharmacology*. Wolters kluwer, Lippincott Williams and Wilkins. 2007; Chapter 5: pp 63-73.

Taupin P, Ray J, Fischer WH, Suhr ST, Hakansson K, et al. *Neuron* 2000; **28**:385-397.

Teich N, Bödeker H and Keim V. *BMC Gastroenterol* 2002; **2**:16-19.

Thrower EC, Villalvilla Diaz de APE, Kolodecik TR, and Gorelick FS. *Am J Physiol Gastrointest Liver Physiol* 2006; **290**:G894-G902.

Tien M, Berlett BS, Levine RL, Chock PB and Stadtman ER. *Proc Natl Acad Sci USA* 1999; **96**:7809-7814.

Timm DE, deHaseth PL and Neet KE. *Biochemistry* 1994; **33**:4667-4676.

Timm DE and Neet KE. *Protein Sci* 1992; **1**:236-244.

Tohonen V, Osterlund C and Nordqvist K. *Proc Natl Acad Sci USA* 1998; **95**:14208-14213.

Trabandt A, Gay RE, Fassbender HG and Gay S. *Arthritis Rheum* 1991; **34**:1444-1449.

Trayer HR, Nozaki Y, Reynolds JA and Tanford C. *J Biol Chem* 1971; **426**:4485-4488.

Trivedi CD and Pitchumoni CS. *J Clin Gastroenterol* 2005; **39**:709-16.

Tsai CS, Godin JR and Wand AJ. *Biochem J* 1985; **225**:203-208.

Tsai HT, Wang PH, Tee YT, Lin LY, Hsieh YS, et al. *Fertil Steril* 2009; **91**:549-555.

Tsui FW, Tsui HW, Mok S, Mlinaric I, Copeland NG, et al. *Genomics* 1993; **15**:507-514.

Tsushima H, Higashiyama K and Mine H. *Arch Dermatol Res* 1996; **288**:484-488.

Tumminello FM, Badalamenti G, Incorvaia L, Fulfaro F, D'Amico C, et al. *Med Oncol* 2009; **26**:10-15.

Tung JS and Knight Ca. *Biochem Biophys Res Commun* 1971; **43**:1117-1121.

Turk B and Stoka V. *FEBS Lett* 2007; **581**:2761-2767.

Turk B, Krizaj I, Kralj B, Dolenc I, Popovic T, et al. *J Biol Chem* 1993; **268**:7323-7329.

Turk B, Ritonja A, Bjork I, Stoka V, Dolenc I, et al. *FEBS Lett* 1995; **360**:101-105.

Turk B, Stoka V, Turk V, Johansson G, Cazzulo JJ and Bjork I. *FEBS Lett* 1996b; **391**:109-112.

Turk B, Turk D and Salvesen GS. *Curr Pharm Des* 2002; **8**:1623-1637.

Turk B, Turk D and Salvesen GS. *Medicinal Chem Rev Online* 2005; **2**:283-297.

Turk B, Turk D and Turk V. *Biochim Biophys Acta* 2000; **1477**:98-111.

Turk B, Turk V and Turk D. *Biol Chem* 1997; **378**:141-150.

Turk B. *Nat Rev Drug Discov* 2006; **5**:785-799.

Turk D, Janjic V, Stern I, Podobnik M, Lamba D, et al. *EMBO J* 2001; **20**: 6570-6582.

Turk V and Bode W. *FEBS Lett* 1991; **285**:213-219.

Turk V and Turk B. *Acta Chim Slov* 2008; **55**:727-738.

Turk V, Brzin J, Lenarcic B, Locnikar P, Popovic T, et al. In: *Intracellular Protein Catabolism*, V Alan R Liss Inc.: New York, 1985; pp 91-103.

Turk V, Brzin J, Longer M, Ritonja A, Eropkin M, et al. *Hoppe Seylers Z Physiol Chem* 1983; **364**:1487-1496.

Turk V, Kos J and Turk B. *Cancer Cell* 2004; **5**:409-410.

Turk V, Stoka V and Turk D. *Front Biosci* 2008; **13**:5406-5420.

Turk V, Turk B and Turk D. *EMBO J* 2001; **20**:4629-4633.

Turk V, Turk B, Guncar G, Turk D and Kos J. *Adv Enzyme Regul* 2002; **42**:285-303.

Turrens JF. *J Physiol* 2003; **552**:335-344.

Tyagi SC. *J Biol Chem* 1991; **266**:5279-5285.

Uchida K, Kato Y and Kawakishi S. *Biochem Biophys Res Commun* 1990; **169**:265-271.

Ullah MF and Khan MW. *Asian Pac J Cancer Prev* 2008; **9**:187-195.

Ullrich O, Reinheckel T, Sitte N and Grune T. *Free Radic Biol Med* 1999; **27**:487-492.

Urunuela A, Sevillano S, De la Mano AM, Manso MA, Orfao A, et al. *Biochim Biophys Acta* 2002; **1588**:159-164.

Utsunomiya T, Hara Y, Kataoka A, Morita M, Arakawa H, et al. *Clin Cancer Res* 2002; **8**:2591-2594.

Uversky VN, Li J and Fink AL. *J Biol Chem* 2001; **276**:10737-10744.

Valko M, Leibfritz D, Moncol J, Cronin MT, Mazur M, et al. *Int J Biochem Cell Biol* 2007; **39**:44-84.

van Acker GJ, Saluja AK, Bhagat L, Singh VP, Song AM, et al. *Am J Physiol Gastrointest Liver Physiol* 2002; **283**:G794-800.

Vasiljeva O, Papazoglou A, Kruger A, Brodoefel H, Korovin M, et al. *Cancer Res* 2006; **66**:5242-5250.

Vasiljeva O, Reinheckel T, Peters C, Turk D, Turk V, et al. *Curr Pharm Des* 2007; **13**:387-403.

Verdot L, Lalmanach G, Vercruysse V, Hoebeke J, Gauthier F, et al. *Eur J Biochem* 1999; **266**:1111-1117.

Verzijl N, DeGroot J, Oldehinkel E, Bank RA, Thorpe SR, et al. *Biochem J* 2000; **350**:381-387.

Vissers MC and Winterbourn CC. *Arch Biochem Biophys* 1991; **285**:53-59.

Vivian JT and Callis PR. *Biophys J* 2001; **80**:2093-2109.

Voller A, Bidwell DE and Bartlett A. *Bull World Health Organ* 1976; **53**:55-65.

von Horsten HH, Johnson SS, San Francisco SK, Hastert MC, Whelly SM, et al. *J Biol Chem* 2007; **282**:32912-32923.

Wadsworth TL and Koop DR. *Biochem Pharmacol* 1999; **57**:941-949.

Wahlbom M, Wang X, Lindstrom V, Carlemalm E, Jaskolski M, et al. *J Biol Chem* 2007; **282**:18318-18326.

Wasil M, Halliwell B, Hutchison DC and Baum H. *Biochem J* 1987; **243**:219-223.

Watanabe M, Watanabe T, Ishii Y, Matsuba H, Kimura S, et al. *J Histochem Cytochem* 1988; **36**:783-791.

Weber H, Hopp HH, Wagner AC, Noack T, Jonas L, et al. *Pancreas* 2002; **24**:63-74.

Weber K and Osborn M. *J Biol Chem* 1969; **244**:4406-4412.

Wei L, Berman Y, Castano EM, Cadene M, Beavis RC, et al. *J Biol Chem* 1998; **273**:11806-11814.

Wen ZM and Ye ST. *Asian Pacific J Allergy Immunol* 1993; **11**:13-18.

Werle B, Schanzenbacher U, Lah TT, Ebert E, Julke B, et al. *Oncol Rep* 2006; **16**:647-655.

Werlin SL and Fish DL. *Pediatrics* 2006; **118**:1660-1663.

Whiteman M, Rose P and Halliwell B. *Biochem Biophys Res Commun* 2003; **303**:1217-1224.

Whiteman M. PhD Thesis, University of London, 1998.

Wilkins BDK, Dobson CM and Gross M. *Eur J Biochem* 2000; **267**:2609-2616.

Wink DA, Darbyshire JF, Nims RW, Saavedra JE and Ford PC. *Chem Res Toxicol* 1993; **6**:23-27.

Winterbourn CC and Kettle AJ. *Free Radic Biol Med* 2000; **29**:403-409.

Wodak SJ and Janin J. *Adv Protein Chem* 2003; **61**:9-73.

Wolff SP and Dean RT. *Biochem J* 1986; **234**:399-403.

Wu J and Haard NF. *Comp Biochem Physiol C Toxicol Pharmacol* 2000; **127**:209-220.

Xiang Y, Nie DS, Wang J, Tan XJ, Deng Y, et al. *Acta Biochim Biophys Sin* (Shanghai) 2005; **37**:11-18.

Yan LJ and Sohal RS. *Curr Protoc Cell Biol* Chapter 7: Unit 7.9. Willey Interscience, 2002.

Yang F, Zhou BR, Zhang P, Zhao YF, Chen J, et al. *Chem Biol Interact* 2007; **170**:231-243.

Yang Y, Liu S, Qin Z, Cui Y, Qin Y, et al. *Mol Biol Rep* 2009; **36**:677-682.

Yao M and Bolen DW. *Biochemistry* 1995; **34**:3771-3781.

Ylonen A, Rinne A, Herttuainen J, Bogwald J, Jarvinen M and Kalkkinen N. *Eur J Biochem* 1999; **266**:1066-1072.

Zabari M, Berri M, Rouchon P, Zamora F, Tassy C, et al. *Biochimie* 1993; **75**:937-945.

Zaidi M, Troen B, Moonga BS and E Abe. *J Bone Miner Res* 2001; **16**:1747-1749.

Zavasnik-Bergant T. *Front Biosci* 2008; **13**:4625-4637.

Zeeuwen PL, Cheng T and Schalkwijk J. *J Invest Dermatol* 2009; **129**:1327-1338.

Zehra S, Shahid PB and Bano B. *Comp Biochem Physiol-Part B* 2005; **142**:361-368.

Zerovnik E, Cimermann N, Kos J, Turk V and Lohner K. *Biol Chem* 1997; **378**:1199-1203.

Zerovnik E, Jerala R, Kroon-Zitko L, Pain RH and Turk V. *J Biol Chem* 1992; **267**:9041-9046.

Zerovnik E, Pompe-Novak M, Skarabot M, Ravnikar M, Musevic I, et al. *Biochim Biophys Acta* 2002a; **1594**:1-5.

Zerovnik E, Skarabot M, Skerget K, Giannini S, Stoka V, et al. *Amyloid* 2007; **14**:237-247.

Zerovnik E, Skerget K, Tusek-Znidaric M, Loeschner C, Brazier MW, et al. *FEBS J* 2006; **273**:4250-4263.

Zerovnik E, Turk V and Waltho JP. *Biochem Soc Trans* 2002b; **30**:543-547.

Zerovnik E. *Eur J Biochem* 2002; **269**:3362-3371.

Zhang J, Shridhar R, Dai Q, Song J, Barlow SC, et al. *Cancer Res* 2004; **64**:6957-6964.

Zurdo J, Guijarro JI, Jimenez JL, Saibil HR and Dobson CM. *J Mol Biol* 2001; **311**:325-340.

Biography

List of Publications

1. **M Priyadarshini** and B Bano. Cystatin like thiol proteinase inhibitor from goat pancreas: purification and detailed biochemical characterization. *Amino Acids*, 2009; DOI 10.1007/ s00726-009-0308-x.

2. Md S Khan, **M Priyadarshini** and B Bano. Preventive effect of curcumin and quercetin against nitric oxide mediated modification of goat lung cystatin. *J Agric Food Chem*, 2009; 57(14):6055-6059.

3. S Priyamvada, **M Priyadarshini**, NA Arivarasu, N Farooq, S Khan, SA Khan, MW Khan and ANK Yusufi. Studies on the protective effect of dietary fish oil on gentamicin-induced nephrotoxicity and oxidative damage in rat kidney. *Prostaglandins Leukot Essent Fatty Acids*. 2008; 78(6):369-381.

4. M Kaleem, **M Priyadarshini**, Q U Ahmed, M Asif, B Bano. Beneficial effects of Annona squamosa extract in streptozotocin-induced diabetic rats. *Singapore Med J*, 2008; 49(10):1-5.

5. **M Priyadarshini**, Md S Khan, B Bano. Papain inhibition by pleural and pancreatic thiol proteinase inhibitors: a comparative study. *J Enz Inhibition Med Chem* (Communicated).

6. **M Priyadarshini**, Md S Khan, B Bano. Protective effect of dietary antioxidants against nitrosative damage of pancreatic thiol proteinase inhibitor. *Clin Chim Acta* (Communicated).

7. **M Priyadarshini**, Md S Khan, B Bano. Designing conditions for fibrillation of cystatin like caprine thiol proteinase inhibitor. (*Manuscript under preparation*)

8. **M Priyadarshini**, Md S Khan, R H Khan, B Bano. Dimeric pancreatic thiol proteinase inhibitor denaturation by urea and guanidine hydrochloride: different mechanisms of unfolding. (*Manuscript under preparation*)

Abstracts

1. **M Priyadarshini**, Md. S Khan, A. Shah, M. Atif, F. Amin, M. Faisal and B Bano. Effects of guanidine hydrochloride on the conformation and enzyme activity of goat pancreatic cystatin. In: *Souvenir cum abstract book*, International SFRR Satellite Symposium. Department of Biochemistry, Aligarh Muslim University, Aligarh (March 17-18, 2009).

2. Md. S Khan, **M Priyadarshini**, A. Shah, M. Atif, M. Faisal, F. Amin and B Bano. Preventive effect of curcumin and quercetin against nitruc oxide mediated modification of goat lung cystatin. In: *Souvenir cum abstract book*, International SFRR Satellite Symposium. Department of Biochemistry, Aligarh Muslim University, Aligarh (March 17-18, 2009).

3. F. Amin, **M Priyadarshini**, A. Shah, M. Atif, M. Faisal, A. A. Khan and S. J. Rizvi. Interaction of riboflavin with mammalian thiol protease inhibitor. In: *Souvenir cum abstract book*, International SFRR Satellite Symposium. Department of Biochemistry, Aligarh Muslim University, Aligarh (March 17-18, 2009).

4. A. Shah, **M Priyadarshini**, Md. S Khan, M. Atif, F. Amin, M. Faisal, and B Bano. Purification and characterization of liver cyctatin. In: *Souvenir cum abstract book*, International SFRR Satellite Symposium. Department of Biochemistry, Aligarh Muslim University, Aligarh (March 17-18, 2009).

5. Md. S Khan, S. Sumbul, **M Priyadarshini**, A. Shah, M. Atif, and B Bano. Comparative study of urea and Gdn HCl denaturation of goat lung cystatin. In: International Symposium on the Predictive, Preventive and Mechanistic Mutagenesis & XXXIII EMSI Annual Meeting. Department of Agricultural Micro Biology, Aligarh Muslim University, Aligarh (January 1-3, 2008).

6. Arivarasu NA, Priyamvada S, **Priyadarshini M**, Khan S, Khan MW, Khan SA and Mahmood R. Gastrointestinal toxicity in rats induced by a carcinogen : in vitro and in vivo. In: International Symposium on the Predictive, Preventive and Mechanistic Mutagenesis & XXXIII EMSI Annual Meeting. Department of Agricultural Micro Biology, Aligarh Muslim University, Aligarh (January 1-3, 2008).

7. **M Priyadarshini**, Md. S Khan, A. Shah, F. Amin, M. Atif and B Bano. Goat pancreas thiol protease inhibitor: purification and characterization. In: *Souvenir cum Abstracts*: National symposium on Recent Advances in Biochemistry and Allied Sciences. Department of Biochemistry, Aligarh Muslim University, Aligarh (March 25, 2008).

8. Md. S Khan, **M Priyadarshini**, A. Shah, M. Atif and B Bano. Denaturation of goat lung cystatin revealing an intermediate stage in the unfolding pathway. In: *Souvenir cum Abstracts*: National symposium on Recent Advances in Biochemistry and Allied Sciences. Department of Biochemistry, Aligarh Muslim University, Aligarh (March 25, 2008).

9. A. Shah, **M Priyadarshini**, Md. S Khan, M. Atif and B Bano. Purification and partial characterization of goat liver cystatin. In: *Souvenir cum Abstracts*: National symposium on Recent Advances in Biochemistry and Allied Sciences. Department of Biochemistry, Aligarh Muslim University, Aligarh (March 25, 2008).

10. M. Atif, S. Sumbul, **M Priyadarshini**, Md. S Khan, A. Shah and B Bano. Purification and partial characterization of cystatin from goat muscle. In: *Souvenir cum Abstracts*: National

symposium on Recent Advances in Biochemistry and Allied Sciences. Department of Biochemistry, Aligarh Muslim University, Aligarh (March 25, 2008).

11. **M Priyadarshini**, Md. S Khan, F. Amin and B Bano. Spectroscopic and kinetic characterization of goat pancreatic cystatin: interaction with activated papain. In: *Souvenir cum abstract book*, National symposium on advances in clinical biochemistry biomarkers, molecular diagnosis and quality assurances & Ist UPACBICON. Dept. of Biochemistry, F/o medicine, Jawaharlal Nehru Medical College, Aligarh Muslim University, Aligarh (November15-16, 2008).

12. A. Shah, **M Priyadarshini**, Md. S Khan, F. Amin, and B Bano. Clinically relevant cystatin: Purification and characterization from goat liver. In: *Souvenir cum abstract book*, National symposium on advances in clinical biochemistry biomarkers, molecular diagnosis and quality assurances & Ist UPACBICON. Dept. of Biochemistry, F/o medicine, Jawaharlal Nehru Medical College, Aligarh Muslim University, Aligarh (November15-16, 2008).

13. F. Amin, **M Priyadarshini**, M. Atif, M. Faisal, A. A. Khan, S. J. Rizvi and B Bano. Partial purification and characterization of cystatin from buffalo brain. In: *Souvenir cum abstract book*, National symposium on advances in clinical biochemistry biomarkers, molecular diagnosis and quality assurances & Ist UPACBICON. Dept. of Biochemistry, F/o medicine, Jawaharlal Nehru Medical College, Aligarh Muslim University, Aligarh (November15-16, 2008).

14. M. Atif, **M Priyadarshini**, Md. S Khan, A. Shah, F. Amin, M.F. Mustafa and B Bano. Purification and partial characterization of cystatin from goat muscle. In: *Souvenir cum abstract book*, National symposium on advances in clinical biochemistry biomarkers, molecular diagnosis and quality assurances & Ist UPACBICON. Dept. of Biochemistry, F/o medicine, Jawaharlal Nehru Medical College, Aligarh Muslim University, Aligarh (November15-16, 2008).

15. **M Priyadarshini**, S. Sumbul and B Bano. Purification and partial characterization of thiol protease inhibitor (cystatin) from goat liver. In: *Souvenir and Abstracts* Second J & K Science Congress organized by University of Kashmir (July 25-27, 2006).

16. Priyamvada S, Arivarasu NA, **Priyadarshini M**, Khan SA and Yusufi ANK. Efficacy of omega-3 and omega-6 fatty acids under gentamicin (GM) induced nephrotoxicity on rat kidney. In: *Souvenir and Abstracts* Second J & K Science Congress organized by University of Kashmir (July 25-27, 2006).

17. Md. S Khan, S. Sumbul, **M Priyadarshini** and B Bano. Purification and partial characterization of cystatin from goat muscle. In: *Souvenir and Abstracts* Second J & K Science Congress organized by University of Kashmir (July 25-27, 2006).

18. S. Sumbul, **M Priyadarshini** and B Bano. Purification and partial characterization of trypsin inhibitor from Cicer arietinum and composition analysis of Phaselus mungo and Cicer arietinum. In: *Souvenir and Abstracts* Second J & K Science Congress organized by University of Kashmir (July 25-27, 2006).

19. Md. S Khan, **M Priyadarshini** and B Bano. Isolation and spectroscopic studies of lung cystatins from Capra hircus. In: *75th Annual meeting of Society of Biological Chemists*, Jawaharlal Nehru University, New Delhi (December 8-11, 2006).

Amino Acids
DOI 10.1007/s00726-009-0308-x

ORIGINAL ARTICLE

Cystatin like thiol proteinase inhibitor from pancreas of *Capra hircus*: purification and detailed biochemical characterization

Medha Priyadarshini · Bilqees Bano

Received: 17 February 2009 / Accepted: 14 May 2009

Abstract A thiol proteinase inhibitor from *Capra hircus* (goat) pancreas (PTPI) isolated by ammonium sulphate precipitation (20–80%) and gel filtration chromatography on Sephacryl S-100HR, with 20.4% yield and 500-fold purification, gave molecular mass of 44 kDa determined by its electrophoretic and gel filtration behavior, respectively. The stokes radius, diffusion and sedimentation coefficients of PTPI were 27.3 Å, 7.87×10^{-7} cm^2 s^{-1} and 3.83 s, respectively. It was stable in pH range 3–10 and up to 70°C (critical temperature, $E_a = 21$ kJ mol^{-1}). Kinetic analysis revealed reversible and competitive mode of inhibition with PTPI showing the highest inhibitory efficiency against papain ($K_i = 5.88$ nM). The partial amino acid sequence analysis showed that it shared good homology with bovine parotid and skin cystatin C. PTPI possessed 17.18% α helical content assessed by CD spectroscopy. The hydropathy plot of first 24 residues suggested that most amino acids of this stretch might be in the hydrophobic core of the protein.

Keywords Goat pancreas cystatin · Kinetics of inhibition · Amino acid sequence · Mammalian cystatins · Characterization

Introduction

Proteolytic enzymes are essential for the survival of all kinds of organisms, and are encoded for by approximately 2% of all the genes (Barrett et al. 2001). Despite their vital functions, these proteases are potentially very damaging in living systems. Cells therefore have several distinct mechanisms to check their enormous hydrolytic potential, important among which are the interactions of the proteases with inhibitors. The major proteases of the lysosomal pathway of protein degradation, cathepsins, are naturally regulated by cystatins. Cystatins (thiol protease inhibitors, TPI), reversible competitive inhibitors of thiol dependent (cysteine) proteases, are widely distributed in animals and plants and are also reported in some lower eukaryotes. Generally, they are classified into three distinct families based on their sequence homology, presence of disulphide bonds and molecular mass (Abrahamson et al. 2003; Turk et al. 1997). Family I—the stefins (mammalian cystatin A and B and bovine stefin C) are cytosolic proteins of about 100-residue single chains, with no disulphide bonds or carbohydrates (Turk et al. 1997). Family II—the cystatins (chicken cystatin) are primarily extracellular and each has a single chain of about 120 amino acids with two disulphide bonds and no carbohydrates (Bode et al. 1988). Family III—the kininogens are blood plasma glycoproteins and have several cystatin like domains (Ohkubo et al. 1984).

Physiologically important cystatins are known to act as defensive agents against bacteria, viruses, and plant eating insects (Ylonen et al. 1999). They can also regulate cell death, antigen presentation and their expression is altered in malignant processes (Ylonen et al. 1999). Cystatins have been purified and characterized from various sources including goat kidney (Zehra et al. 2005), goat brain (Sumbul and Bano 2006), sheep plasma (Shahid et al. 2005), human placenta (Rashid et al. 2006), human spleen (Jarvinen and Rinnie 1982), human liver (Green et al. 1984), and amyloid fibrils (Cohen et al. 1983), etc. The present investigation aimed at understanding the functioning of thiol dependent protease inhibitors in pancreas, the

M. Priyadarshini · B. Bano (✉)
Department of Biochemistry, Faculty of Life Sciences,
Aligarh Muslim University, Aligarh 202002,
Uttar Pradesh, India
e-mail: bbilqees@gmail.com

Published online: 14 July 2009

JOURNAL OF AGRICULTURAL AND FOOD CHEMISTRY
ARTICLE

J. Agric. Food Chem. 2009, 57, 6055–6059 6055
DOI:10.1021/jf900356w

Preventive Effect of Curcumin and Quercetin against Nitric Oxide Mediated Modification of Goat Lung Cystatin

MOHD SHAHNAWAZ KHAN, MEDHA PRIYADARSHINI, AND BILQEES BANO*

Department of Biochemistry, Faculty of life sciences, A.M.U.Aligarh. U.P., India

Cysteine proteinase inhibitors are of prime physiologic importance inside the cells, controlling the activities of lysosomal cysteine proteases. The present work aimed to realize the effects of nitric oxide on the structure and function of goat lung cystatin (GLC) and to evaluate antinitrostative efficacy of curcumin and quercetin. Nitric oxide induced structural modifications were followed by fluorescence spectroscopy and PAGE and functional inactivation by monitoring the inhibition of caseinolytic activity of papain. Ten millimolar sodium nitroprusside (SNP) caused time dependent inactivation of GLC-I with complete functional loss precipitating at 180 min. Curcumin (50 μM) and quercetin (250 μM) opposed such loss in papain inhibitory activity of GLC-I. Loss in tertiary structure of GLC-I (fluorescence quenching and 15 nm red shift) was observed on SNP treatment. Inhibition of functional and structural SNP mediated damage of GLC-I by curcumin (50 μM) and quercetin (250 μM) reaffirms their NO scavenging potency.

KEYWORDS: NO; protease inhibitor; asthma; curcumin; quercetin

INTRODUCTION

Nitric oxide (NO) is an omnipresent intercellular messenger in all vertebrates, modulating blood flow (*1*), thrombosis (*2*) and neural activity (*3*). The production of nitric oxide is also important for nonspecific host defense, helping to kill tumors and intracellular pathogens. However, under pathophysiological conditions, NO has damaging effects. It is found to be involved in neural disorders involving oxidative stress such as Parkinson's disease (*4*), Alzheimer's disease (*5*), ischemia (*6*), Huntington's disease (*7*), amyotrophic lateral sclerosis (*8*) and multiple sclerosis (*9*). Excessive production of NO (a known mediator of inflammation) is correlated with nitrostative stress in tissues. Although NO$^{\bullet}$ is a free radical, it has selective reactivity and reacts predominantly with other paramagnetic species, including ferrous or ferric iron in heme proteins or iron−sulfur centers, and other radical species such as molecular oxygen (O_2), superoxide anion ($^{\bullet}O_2^-$) and lipid or protein radicals (*10*−*14*). Reaction of NO with $^{\bullet}O_2^-$ at a near diffusion limited rate yields peroxynitrite ($ONOO^-$), a powerful oxidizing species, to which many of the cytotoxic properties of NO$^{\bullet}$ have been attributed (*15*).

Lung diseases like cancer, emphysema and idiopathic pulmonary fibrosis are known to be caused by an imbalance between the activities of endogenous inhibitors and cysteine proteinases (cathepsins) (*16*). Cystatins, noncovalent competitive inhibitors of cysteine proteinases (cathepsins B, H, L and S) (*17*), are ubiquitously present in mammalian system. These inhibitors protect the cells from unwanted proteolysis which may otherwise cause a number of pathologies like purulent bronchitis (*18*), Rheumatoid arthritis (*19*), osteoporosis (*20*), Alzheimer's disease (*21*), metastasizing cancer (*22*) and microbial invasion (*23*).

NO is a thermodynamically unstable molecule and tends to react with other bio molecules especially proteins resulting in their oxidation, nitration and nitrosylation, with the concomitant effects on many cellular mechanisms. Increased ROS/RNS (NO$^{\bullet}$) levels are consequential to chronic/acute lung inflammation. A common factor in inflammation is that the equilibrium between lysosomal enzymes released by macrophages or neutrophilic granulocytes and their endogenous inhibitors in the extra cellular space is disturbed. This imbalance may originate from many reasons, one of which may be inactivation by ROS/RNS released by neutrophilic granulocytes during the process of inflammation.

Various researches have been undertaken to evaluate the potential benefits of complementary and alternatives medicines (botanicals, flavonoids, herbs, etc.) to oppose the toxicity associated with reactive species generated during various pathogenic states.

Curcumin (diferuloylmethane), the major coloring pigment present in the rhizomes of *Curcuma longa* (turmeric), is a spice widely used in Indian cooking and for medicinal purposes (*24*). Curcumin has been shown to possess many therapeutic properties including antioxidant (*25*), anti-inflammatory (*26*) and anticancer properties (*27*). It also protects DNA against singlet-oxygen-induced strand break (*28*), lipids from peroxidation (*29*) and oxyhemoglobin from nitrite induced oxidation (*30*).

Quercetin is the main flavonoid in the diet and is consumed as quercetin-3-rutinoside (in black tea about 40%), quercetin-4′-glucoside (45% in onions) and quercetin-3-glucoside (mainly in tea, apples and tomatoes) (*31*, *32*). Flavonoids exhibit several positive health aspects; they possess anticarcinogenic, antimutagenic, antioxidant, immune-stimulating and estrogen-active

*To whom correspondence should be addressed. Prof. Bilqees Bano. Mailing address: Department of Biochemistry Faculty of Life sciences A.M.U., Aligarh. 202002 U.P., India. Tel: +91-571-2700857. E-mail: banobilqees@gmail.com.

Published on Web 06/17/2009